

# **FEASIBILITY STUDY FOR LARGE UNDERGROUND CAVERNS AND AUXILIARY INFRASTRUCTURE FACILITIES OF THE LAGUNA PROJECT AT THE LSC (CANFRANC, HUESCA, SPAIN)**

REVISION 12<sup>th</sup> May 2010

## **REVISION 12<sup>TH</sup> MAY 2010**

### **INDEX**

<b>1. FOREWORD.....</b>	<b>1</b>	<b>3.1.5 Caverns for other uses .....</b>	<b>17</b>
<b>2. INTRODUCTION TO THE SITE.....</b>	<b>2</b>	<b>3.1.6 Summary.....</b>	<b>17</b>
<b>2.1 GENERAL FEATURES .....</b>	<b>3</b>	<b>3.2 EXCAVATION METHODS AND SUPPORT SYSTEMS OF SOME</b>	<b>19</b>
<b>2.2 SITE CHARACTERISATION .....</b>	<b>4</b>	<b>LARGE PERMANENT UNDERGROUND CAVERNS .....</b>	<b>19</b>
2.2.1 Climate .....	4	3.2.1 Super - KAMIOKANDE .....	19
2.2.2 Hydrography .....	5	3.2.2 Gjøvik Olympic Mountain Hall, Norway .....	21
2.2.3 Population .....	6	3.2.3 Power Plants.....	22
<b>2.3 EXISTING INFRASTRUCTURES.....</b>	<b>6</b>	<b>3.3 SUPPORT SYSTEMS ADOPTED IN SOME LARGE PERMANENT</b>	<b>23</b>
2.3.1 Roads and railways network.....	6	<b>UNDERGROUND CAVERNS .....</b>	<b>23</b>
2.3.2 Underground facilities .....	7	<b>3.4 REFERENCES.....</b>	<b>25</b>
<b>2.4 DETECTOR OPTIONS CONSIDERED FOR THE SITE .....</b>	<b>8</b>	<b>4. GEOLOGICAL FEATURES OF THE CANFRANC SITE .....</b>	<b>27</b>
2.4.1 Water Cherenkov technology (MEMPHYS).....	8	<b>4.1 INTRODUCTION.....</b>	<b>27</b>
2.4.2 Liquid Scintillator technology (LENA).....	10	<b>4.2 GEOLOGICAL FRAMEWORK .....</b>	<b>27</b>
2.4.3 Liquid Argon Technology (GLACIER) .....	10	<b>4.3 STRATIGRAPHY .....</b>	<b>29</b>
<b>2.5 ADVANTAGES OF THE SITE AND THE CONSIDERED LAYOUT</b>	<b>12</b>	4.3.1 Introduction .....	29
<b>3. OVERVIEW ON LARGE UNDEGROUND CAVERNS</b>	<b>13</b>	4.3.2 Lithologies .....	29
<b>3.1 PRECEDENTS OF LARGE UNDEGROUND CAVERNS.....</b>	<b>13</b>	<b>4.4 TECTONICS.....</b>	<b>31</b>
3.1.1 Caverns for physics experiments .....	13	4.4.1 Variscan Orogeny .....	31
3.1.2 Permanent mining caverns .....	15	4.4.2 Alpine Orogeny .....	32
3.1.3 Underground fuel storage facilities .....	15	<b>4.5 METAMORPHISM OF THE MATERIALS IN THE AXIAL ZONE...</b>	<b>32</b>
3.1.4 Power plant caverns .....	16	<b>4.6 GEOMORPHOLOGY.....</b>	<b>33</b>
		<b>4.7 HYDROGEOLOGY .....</b>	<b>33</b>
		<b>5. SEISMOLOGICAL PATTERNS OF THE CANFRANC AREA</b>	<b>35</b>
		<b>5.1 SEISMOTECTONIC STUDY .....</b>	<b>35</b>
		5.1.1 Introduction .....	35

5.1.2	Pyrenean Seismotectonic Zoning.....	36	7.1.4	Auxiliary caverns .....	80
5.1.3	Determinist Study.....	38	7.2	GEOMECHANICAL DESCRIPTION OF THE SITE .....	81
5.1.4	Probabilistic approach.....	45	7.3	EXCAVATION METHODS FOR THE MDC´S .....	81
5.1.5	Summary and conclusions .....	57	7.3.1	Introduction .....	81
5.2	CURRENT STRESS FIELDS IN THE PYRENEES .....	57	7.3.2	Construction of a support system above the cavern dome .	82
5.2.1	Introduction .....	57	7.3.3	Cavern excavation sequence.....	84
5.2.2	The Alpine paleostresses.....	58	7.3.4	Support system for the MEMPHYS caverns .....	86
5.2.3	Establishing the stress tensor by analysing the seismic focal mechanisms in the region.....	58	7.4	NUMERICAL MODELLING OF THE MDC.....	86
5.2.4	Interpretation of the results.....	61	7.4.1	Initial modelling.....	86
5.2.5	The data concerning in situ stress .....	63	7.4.2	Geometric description of the final model.....	89
5.2.6	Results of stress orientation using the CRATOR program and the Right Diedra .....	63	7.4.3	Geological description and calculation properties.....	91
5.2.7	Conclusions .....	68	7.4.4	Support elements.....	91
5.2.8	Bibliography .....	69	7.4.5	Excavation sequence .....	94
6.	GEOMECHANICAL CHARACTERIZATION .....	72	7.4.6	Calculation results.....	98
6.1	PREVIOUS INFORMATION .....	72	7.5	MEMPHYS SAFETY AND TECHNICAL ASPECTS.....	111
6.1.1	Rock quality.....	72	7.5.1	Ventilation (construction works and final ventilation) .....	111
6.1.2	Temperature of the rock mass.....	73	7.5.2	Radon free ventilation system .....	112
6.2	BOREHOLES .....	74	7.5.3	Cooling and Heating.....	113
6.2.1	New boreholes in the tunnel .....	74	7.5.4	Handling of dangerous substances.....	113
6.2.2	Preexisting boreholes.....	77	7.5.5	Fire protection system and evacuation .....	113
6.2.3	Laboratory Testing .....	77	7.5.6	Filling and emptying procedure facilities.....	117
7.	MEMPHYS EXPERIMENT .....	79	7.5.7	Liquid handling facilities.....	117
7.1	MDC´S AND TANK DESCRIPTION.....	79	7.5.8	Access.....	118
7.1.1	Dimensions.....	79	7.5.9	Fire event .....	118
7.1.2	Technological specifications .....	79	7.5.10	Energy supply .....	118
7.1.3	General layout.....	80	7.5.11	Bulk transport and stocking.....	118
			7.5.12	External installations.....	119
			7.6	MEMPHYS TANK .....	119

7.6.1	Tank structure .....	119	8.5.8	Access .....	134
7.6.2	Assembling procedure .....	119	8.5.9	Fire event .....	134
7.6.3	Mechanical and thermal interaction with rock .....	119	8.5.10	Energy supply .....	134
7.6.4	Drainage system .....	119	8.5.11	Bulk transport and stocking .....	134
7.6.5	Handling of leakage .....	120	8.5.12	External installations .....	135
<b>8.</b>	<b>LENA EXPERIMENT .....</b>	<b>121</b>	<b>8.6</b>	<b>LENA TANK .....</b>	<b>135</b>
8.1	MDC'S AND TANK DESCRIPTION .....	121	8.6.1	Tank structure .....	135
8.1.1	Dimensions .....	121	8.6.2	Assembling procedure .....	135
8.1.2	Technological specifications .....	121	8.6.3	Mechanical and thermal interaction with rock .....	135
8.1.3	General layout .....	121	8.6.4	Drainage system .....	135
8.1.4	Auxiliary caverns .....	122	8.6.5	Handling of leakage .....	136
8.2	GEOMECHANICAL DESCRIPTION OF THE SITE .....	122	<b>9.</b>	<b>GLACIER EXPERIMENT .....</b>	<b>136</b>
8.3	EXCAVATION METHODS FOR THE MDC .....	122	9.1	MDC'S AND TANK DESCRIPTION .....	136
8.3.1	Introduction .....	122	9.1.1	Dimensions .....	136
8.3.2	Previous stages of excavation and placement of cables ...	123	9.1.2	Technological specifications .....	136
8.3.3	Cavern excavation sequence .....	124	9.1.3	General layout .....	137
8.3.4	Support system for the LENA cavern .....	125	9.1.4	Auxiliary caverns .....	137
8.4	NUMERICAL MODELLING OF THE MDC .....	126	9.2	GEOMECHANICAL DESCRIPTION OF THE SITE .....	137
8.4.1	Elastic modelling .....	126	9.3	EXCAVATION METHODS FOR THE MDC .....	138
8.5	LENA SAFETY AND TECHNICAL ASPECTS .....	127	9.3.1	Introduction .....	138
8.5.1	Ventilation (construction works and final ventilation) .....	127	9.3.2	Cavern excavation sequence .....	139
8.5.2	Radon free ventilation system .....	128	9.3.3	Support system for the GLACIER caverns .....	141
8.5.3	Cooling and Heating .....	129	9.4	NUMERICAL MODELLING OF THE MDC .....	142
8.5.4	Handling of dangerous substances .....	129	9.4.1	Elastic modelling .....	142
8.5.5	Fire protection system and evacuation .....	130	9.5	GLACIER SAFETY AND TECHNICAL ASPECTS .....	143
8.5.6	Filling and emptying procedure facilities .....	133	9.5.1	Ventilation (construction works and final ventilation) .....	143
8.5.7	Liquid handling facilities .....	133	9.5.2	Radon free ventilation system .....	144



9.5.3	Cooling and Heating.....	145	10.4	MATERIALS ANALYSIS REGARDING THE DISPOSAL OF THE WASTE MATERIAL.....	159
9.5.4	Handling of dangerous substances.....	146	10.5	THE ENVIRONMENTAL IMPACT ASSESSMENT PROCESS IN SPAIN.....	162
9.5.5	Fire protection system and evacuation.....	146	10.6	ENVIRONMENTAL MONITORING PLAN.....	164
9.5.6	Filling and emptying procedure facilities.....	149	10.7	CONCLUSIONS.....	165
9.5.7	Liquid handling facilities .....	149	11.	COST ESTIMATES .....	166
9.5.8	Access.....	150	11.1	MEMPHYS.....	167
9.5.9	Fire event .....	150	11.2	LENA .....	175
9.5.10	Energy supply .....	150	11.3	GLACIER.....	183
9.5.11	Bulk transport and stocking .....	150	12.	TECHNICAL TIMESCALE FOR REALIZATION .....	191
9.5.12	External installations .....	150	12.1	INTRODUCTION.....	191
9.6	GLACIER TANK.....	151	12.2	MEMPHYS.....	191
9.6.1	Tank structure.....	151	12.3	LENA .....	191
9.6.2	Assembling procedure .....	151	12.4	GLACIER.....	191
9.6.3	Mechanical and thermal interaction with rock .....	151	APPENDIX Nº 1:	DRAWINGS .....	195
9.6.4	Drainage system.....	151			
9.6.5	Handling of leakage.....	152			
10.	ENVIRONMENTAL ASPECTS.....	152			
10.1	INTRODUCTION .....	152			
10.2	COMPENDIA OF ENVIRONMENT LEGISLATION APPLICABLE TO THE AREA OF THE LSC.....	153			
10.2.1	European Regulations .....	153			
10.2.2	National Regulations.....	153			
10.2.3	Regional regulations.....	156			
10.3	ANALYSIS OF PROTECTED AREAS RELATED TO THE LOCATION .....	157			
10.3.1	Areas protected by European Law.....	157			
10.3.2	Areas protected by Regional Law .....	158			
10.3.3	Areas of Recommended Protection.....	158			

## 1. FOREWORD

The Feasibility Study for Large Underground Openings and Auxiliary Infrastructure that is resumed in this document is the result of 8 months of engineering work. It has been carried out by a multidisciplinary team. The Contract for this Feasibility Study was awarded by the Canfranc Underground Laboratory Consortium (LSC) to IBERINSA, one of the leader engineering companies of Spain, in April, 2009. The team leader for the technical works development is Mr. Manuel Romana, Doctor in Civil Engineering and Professor of Rock Mechanics in the Civil Engineering School of the Universidad Politécnica de Valencia, a recognized specialist engineer in underground works design and construction, who leads his own organization STMR, which has been associated to IBERINSA all along the study. IBERINSA team has been leaded by Mr. Clemente Sáenz, Civil Engineer, manager of the Geology and Geotechnics department of the company, and Assistant Lecturer of Engineering Geology of the Civil Engineering School of the Universidad Politécnica de Madrid .

The LSC team has been led by Mr. Luis Labarga, professor of Physics at the Universidad Autónoma de Madrid, and Mr. José Jiménez, from the LSC. The General Manager of the LSC, Mr. Alessandro Bettini, has supervised the works during their development. Periodical meetings between the LSC team and the IBERINSA-STMR team have been held monthly.

Works have been divided in different stages:

- First, data about the area of Canfranc was collected. Due to the vicinity of the Somport tunnel, it was important to achieve geotechnical information regarding to the tunnel construction. As special advisor for this phase, IBERINSA and STMR have counted on Mr. Rafael López-Guarga, General Manager for the Aragón National Road Network, who directed the tunnel works some years ago.

- In a second stage, lots of information regarding different caverns around the world was analysed. This information shows that the LAGUNA Feasibility Project is exceptional in terms of the dimensions of the caverns to be designed, comprising great depth and huge spans. Collected data included cavern support, cavern excavation methods and so on.
- Once the geological information was collected, some more studies were carried out: geological and seismological patterns were identified, and some selected rock parameters were obtained, in order to develop calculations. Seismological patterns of the Pyrenees area have been assessed by Mr. Ramón Capote, Professor of Tectonics in the Geological faculty of the Universidad Complutense de Madrid.
- Calculations have been conducted by ITASCA, one of the world's leader companies in soil and rock modelling. Once basic parameters and geometry of the caverns were agreed, some initial elastic calculations were carried out, in order to analyze some previous aspects about underground openings performance.
- In a second phase of calculations, vault and cavern walls support has been modelled and analyzed in more detailed models, with different hypothesis, and including constructive procedures.
- While numerical modelling went in progress, definitive layouts for the different experiment schemes were discussed. In this phase, it was necessary to count on with installations design, specially those ones regarding to ventilation of the caverns and working areas, fire protection, water and liquid supplies and emergency facilities. The final design of the layouts of this phase is the result of team work and discussion, both from the LSC team and from the technical partners, IBERINSA and STMR.
- Drawings of the layouts, of excavations and supports and of different installations have been generated for each experiment, allowing to submit a first

draft of civil works quantities. In this final phase, the technical partners have had the assessment of an experienced Spanish civil works contractor, Obras Subterráneas, S.A. in order to establish different unit prices for the main works to be done.

- Finally, environmental issues for the area of the experiment have been taken in mind. Although most work to develop is underground one, some particular aspects of the work should be taken in mind in further designs, and Environmental Assessment Plans and Monitoring Plans will have to be considered. At this stage, the main environmental issue regards to how to manage excavation muck in dump areas.

Apart from this works, the LAGUNA Spanish Feasibility Study is included in a multinational organisation, which comprises national groups from England, France, Italy, Poland, Romania and Finland. Those countries present different possible sites for the LAGUNA experiment development, and their particular site characteristics allow for different solutions and layouts of the experiments.

Regular meetings have been held along the course of the works in different countries: Wroclaw (Poland, May 2009), Pyhasälmä (Finland, September 2009), and Boulby (England, December 2009). With the result of these meetings, in which the technical works in progress have been presented, the European Group is trying to analyze the different proposals for the LAGUNA experiment installation in the abovementioned countries. The meetings have been helpful to exchange technical advances and experiences.

The final result of this extensive process is this document, drafted in December, 22, 2009. Its general index resumes the work at the above mentioned different stages.

## 2. INTRODUCTION TO THE SITE

The Canfranc Underground Laboratory (LSC) is a new facility for Underground Science. It is conceived as a Consortium of the Spanish Ministry of Science and Innovation, the Aragon Regional Government and the University of Zaragoza.

In 1985, the Nuclear and Astroparticle Physics research group from the University of Zaragoza, led by Prof. Angel Morales, set off the Canfranc Underground Laboratory in the Central Pyrenees (Spain). This Laboratory consisted of a main hall of about 120 m<sup>2</sup> and two halls of about 18 m<sup>2</sup>. The scientific program of the Laboratory has had more than 50 researchers belonging to 12 institutions from 8 different countries taking part on the investigation that basically focused on:

- a) Search for double beta decay with germanium (IGEX).
- b) Search for Dark Matter with scintillators (NAI-32 and ANAIS), semiconductors (IGEX-DM) and bolometers (ROSEBUD).
- c) R&D program for the development of ultralow background detectors (AMBAR).

The construction of a new road tunnel in Canfranc and the support from both national and regional governments, made it possible to perform a substantial enlargement of the experimental space available in 2005. In particular the new facilities will allow to have a new experimental hall at a depth of about 2500 m.w.e. measuring 40 × 15 × 10.5 m, oriented towards CERN so that a neutrino beam from such Laboratory may reach a detector in the LSC, as well as a new ultralow background laboratory measuring 15 × 10 × 7.5 m. Furthermore, a Clean Room will be built (underground) for the development of new detectors prototypes. The new Laboratory can be accessed through the newly-built road tunnel and it features its own independent entrance gallery in such tunnel.

Located under the Pyrenees mountain “El Tobazo”, the over burden at the site provides 2.500 meters water equivalent of shielding from cosmic rays and offers a



low background environment for the next generation of experiments exploring the frontiers of particle and astroparticle physics.

The “Consortio para el Equipamiento y Explotación del Laboratorio Subterráneo de Canfranc” (LSC) has taken the Leadership for the Spanish studies. IBERINSA, a leading Spanish company in civil engineering, is the contractor for the Feasibility Study. Mr. Manuel Romana, a recognized Spanish geotechnical professor and engineer, leads the design team, which includes geologists, engineers, environmental assessment, and other specialities.

## 2.1 GENERAL FEATURES

Canfranc is a small village located in Northern Spain, near the French border. The village belongs to the province of Huesca, in the Comunidad Autónoma de Aragón (Regional Government of Aragón). The local administrative division to which Canfranc belongs is called La Jacetania, whose main city is Jaca, a village located 25 km South.

The Somport international mountain pass connects Spain and France in this region, and has provided communication since ancient times. Somport is the Spanish transcription for the latin *Summo Porto*, that is, the summit of the Pyrenees Roman road crossing this part of the Pyrenees Range. In the early Middle Age, the pilgrims on the Way of Saint James to Santiago de Compostela crossed this mountain pass, which was one of the main communication networks of the Central Pyrenees for hundreds of years, and Canfranc began to grow as a small city nearby the road to Santiago.

Figure 2.1.1 shows the general location of the Canfranc area in Northern Spain, and figure 2.1.2 shows the area at more detailed scale.

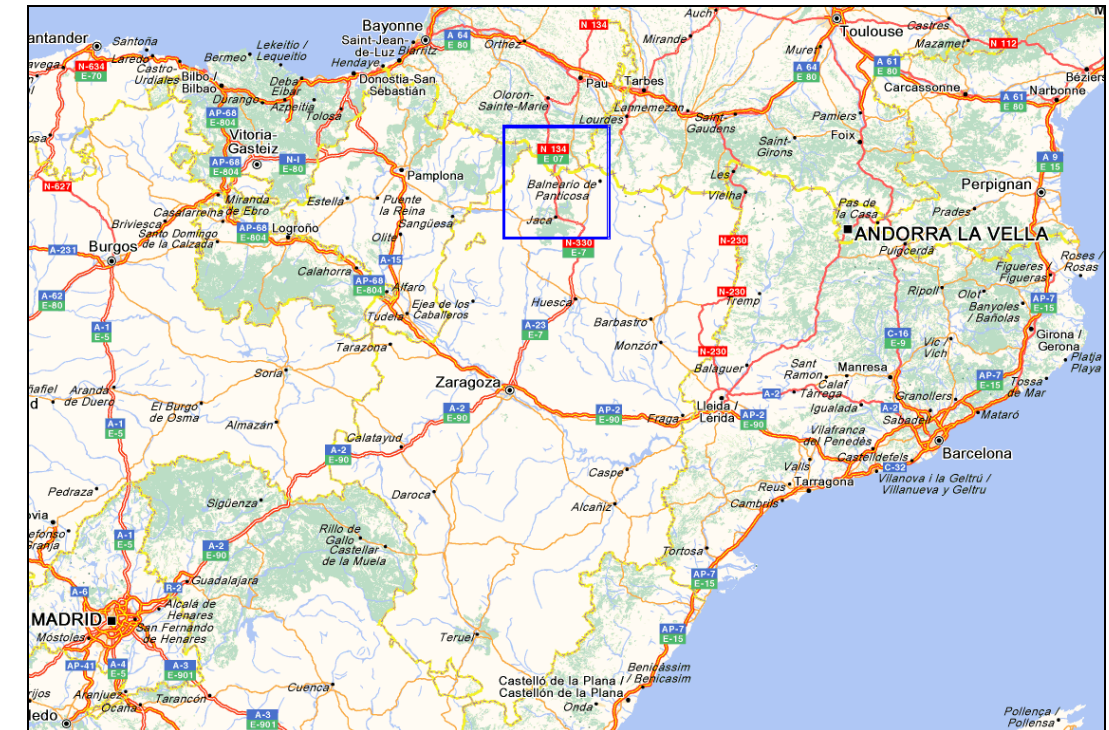


Figure 2.1-1. Location of Canfranc in Northern Spain.

In the early 20's of the 20<sup>th</sup> century, an international railway tunnel was built, and the Canfranc Station area began to develop around the place of Arañones, north from Canfranc. The railway operated for a few years, but the tunnel is currently abandoned. So are different buildings that were built for the occasion, such as the beautiful railway station. Road networks did not improve till the final years of the century, in which a new road tunnel was planned, designed and built.

This road tunnel (the Somport Tunnel) links the Jaca area –that is, Northern Huesca-, with the French Pyrenees Department, and the cities of Oloron and Pau. It is 8,6 km long, 5,7 in the Spanish side of the border and 2,9 in the French side. Works in the tunnel progressed between years 1994 and 2003, in which the tunnel began to operate. Due to safety and emergency reasons, the tunnel needed of an emergency gallery, and the abandoned railway tunnel was slightly conditioned and connected with the road tunnel for this purpose. Connection galleries between the two infrastructures were built each 400 meters.

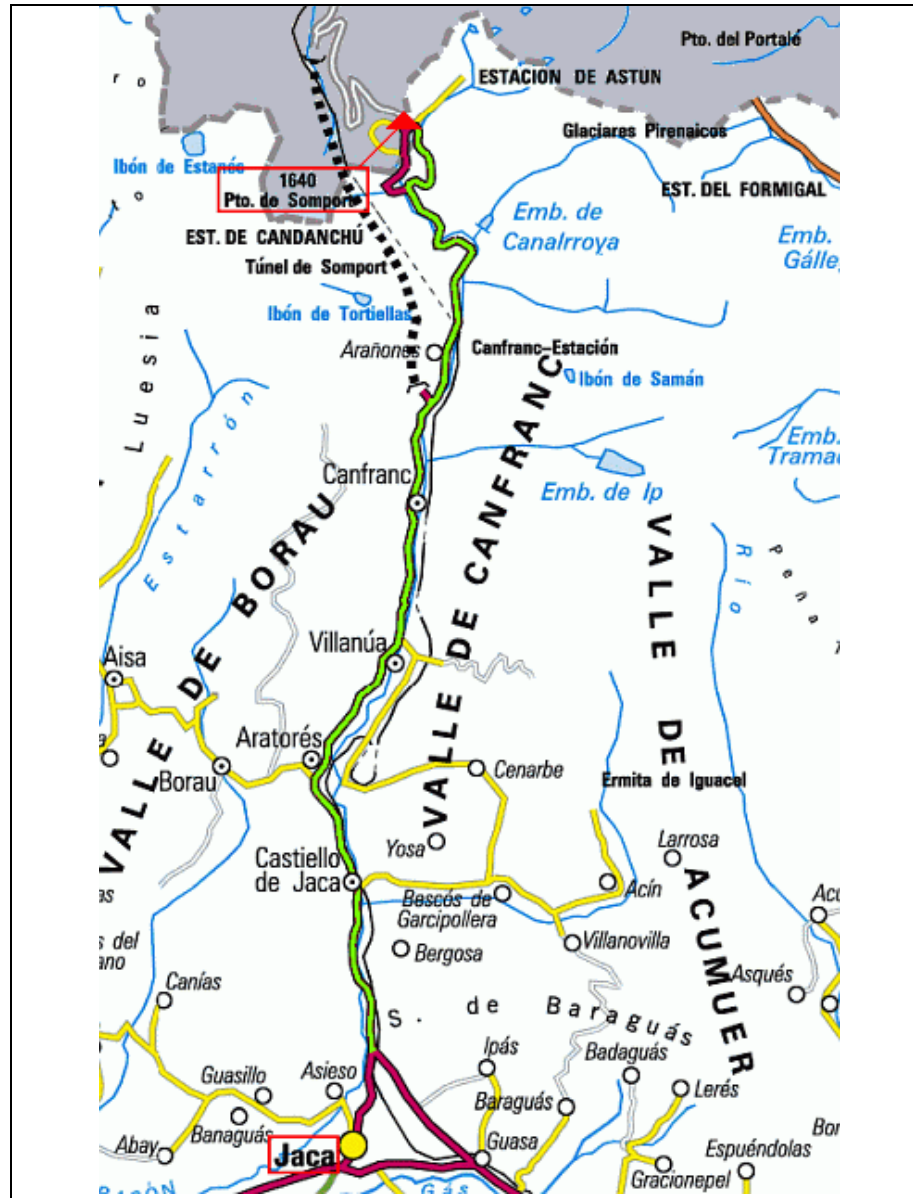


Figure 2.1-2. Location of Canfranc and the Somport pass. Jaca is located on the lower side of the figure.

Tunnel portals of both tunnels are located in different places. The old railway tunnel portal is located nearby the town of Canfranc Station. The road tunnel portal is placed south from the railway one, with a modern building in which a modern control office rules the ventilation, TV, safety and emergency facilities of the tunnel.



Figure 2.1-3. General view of the abandoned Canfranc Station. Taken from [www.franciscoperez.com](http://www.franciscoperez.com)

Both the road and railway tunnel underpass the Central Pyrenees. The highest mountain in the Canfranc area is Mount El Tobazo (1.850 m a.sl.). There is a ski resort in this mountain, named Candanchú.

## 2.2 SITE CHARACTERISATION

### 2.2.1 Climate

Data about climate have been collected from the National Meteorological Institute of Spain. A station for rainfall and temperature monitoring is located 10 km South from Canfranc (at the village of Castiello de Jaca), and the most remarkable data are the following:

#### 2.2.1.1 Temperatures

Average, maximum and minimum temperatures are shown, month by month, in the next table:



Month	Average (° C)	Maximum (°C)	Minimum (°C)
January	2,7	20,0	-19,0
February	3,8	22,0	-18,0
March	6,1	25,0	-14,0
April	8,0	27,0	-8,0
May	11,9	32,0	-6,0
June	16,2	36,0	-2,0
July	19,3	39,0	1,0
August	19,4	40,0	-1,0
September	15,6	36,5	-3,0
October	10,9	31,0	-6,0
November	6,0	23,5	-12,5
December	3,4	21,0	-15,5

Table 2.2-1. Temperatures collected from the “Castiello de Jaca” Meteorological Station.

### 2.2.1.2 Rainfall

Average rainfall is collected in next table. The total amount is around 850 mm per year. Monthly rate of rainy days is also shown:

Month	Rainy days per month	Average (mm)
January	5	71,7
February	4	56,1
March	6	80,6
April	7	78,5
May	10	85,1
June	7	65,7
July	4	37,5
August	5	50,8

September	6	81,6
October	7	69,9
November	6	78,5
December	6	93,1

Table 2.2-2. Rainy days and amount of rainfall at the “Castiello de Jaca” Station.

A typical season distribution would be: 27% of rainfall in winter, spring and fall, and 19% in summer.

There are different climate classifications. Attending to the Papadakis one, the area of Canfranc belongs to the “*Mediterranean temperate cool*” area.

### 2.2.2 Hydrography

The valley of Canfranc is the River Aragón valley. The river is one of the main tributaries to river Ebro from its left side, and it is constantly supplied by snow areas or by inflow of mountain springs. Some small hydroelectrical power stations are located at both sides of the river, taking advantage of local glacier lakes (named *ibones*), combined with small dams along the river.

Next figure shows the volume that River Aragón provides each year at Canfranc, controlled by the Ebro Basin Hydrographical Authority in different flow gauges. It also shows daily minimums of water volumes that have been registered. According to these data, the amount of river volume flow ranges from 17 to 138 Hm<sup>3</sup> per year, being the average 58,84 Hm<sup>3</sup>. Average daily maximum volume exceeds 30,7 m<sup>3</sup>/sec, and instantaneous maximum volumes reach an average of 55 m<sup>3</sup>/sec, reaching as much as 111 m<sup>3</sup>/sec.



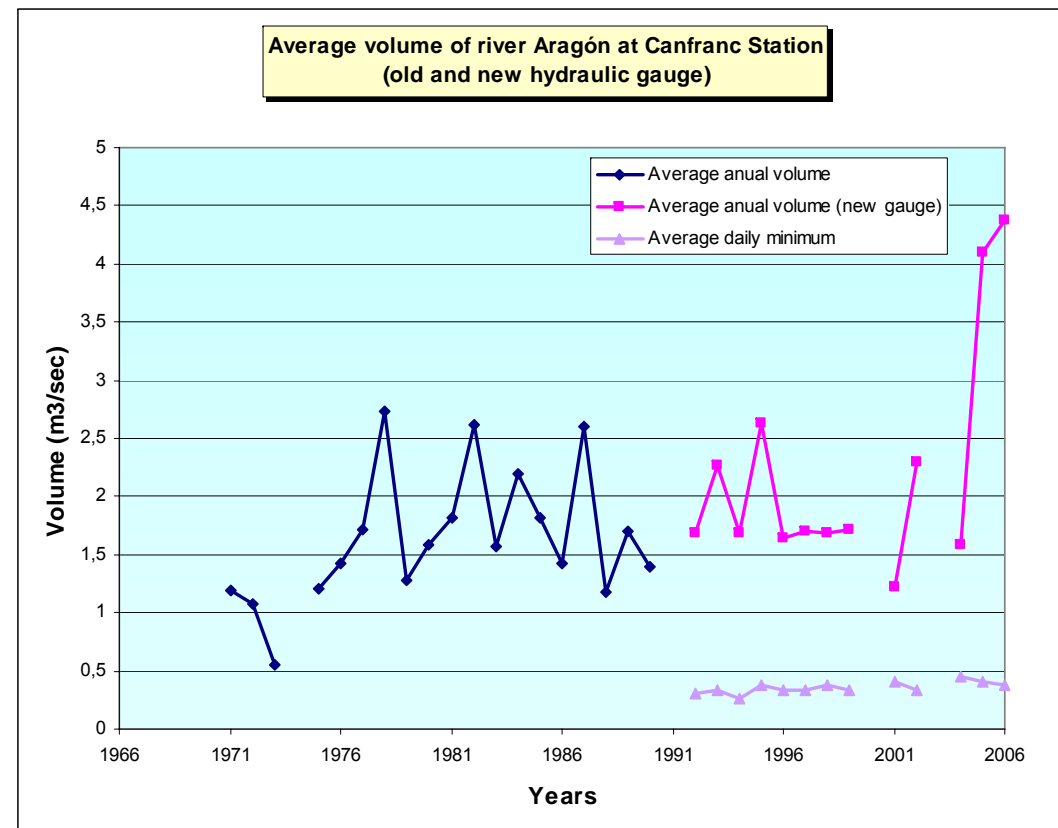


Figure 2.2-1. Volumes of River Aragón, attending to data from Ebro River Authority

### 2.2.3 Population

The main village of the Canfranc area is Jaca: the population census shows 13193 inhabitants (data from 1<sup>st</sup> January 2008). Canfranc has two different villages: Canfranc and Canfranc Estación, that gather 523 residents. Castiello de Jaca and Villanua are also nearby villages, with around 200 residents each one.

Public facilities and services are located mostly around Jaca:

- Public hospital, belonging to the Social Security Services and public health center.
- Police station, with 31 police members.

- Two public and two private schools for elementary education, and two public and one private school for secondary education.
- Public day-nursery.

Two fire brigades are located in Jaca and Canfranc Estación, both depending of the Emergency Services of the Regional Government of Aragón. The Guardia Civil (Spanish Military Police) is detached both in Canfranc Estación and in Jaca. The Spanish Army Mountain Rescue Group has also its operation base in Jaca.

Apart from this services, the Canfranc area offers lots of tourism possibilities comprising cultural activities (Jaca is one of the main historical cities beside the Way of Saint James), and snow sports in the Candanchú and Formigal ski resorts. Candanchú ski runs are located vertically over the Somport Tunnel, partially in the North Face of the Tobazo Mountain. Jaca is applying for the Winter Olympic Games in 2014, and can offer lodging and housing enough for these activities.

## 2.3 EXISTING INFRASTRUCTURES

### 2.3.1 Roads and railways network

Canfranc is located beside the road N-330, which is the local network that connects Spain and France, from Jaca to Oloron Saint Marie, in Southern France, nearby Pau. The Spanish section of this road was renovated when the International Somport Tunnel was built, and allows travelling from Jaca to Canfranc in 20 minutes.

Road N-330 connects also to the main highways under construction A-21 and A-23, which connect the different Pyrenean valleys between Pamplona, Huesca and Zaragoza, parallel to the Pyrenees, providing communication with the Central Ebro Basin, Barcelona and Madrid. See previous figures 2.1.1 and 2.1.2.

There is also a local train, connecting Huesca, Jaca and Canfranc. It travels twice a day from Huesca and Jaca to Canfranc. Travel time from Jaca to Canfranc is 30 minutes. This railway allows also freight trains, and there is a huge railway yard beside the old Canfranc station which can be used for construction purposes.

The main railway network connects Madrid, Zaragoza and Barcelona with a high speed railway train. Zaragoza is located 170 km far away from Canfranc. There are also trains from Zaragoza to Huesca.

### 2.3.2 Underground facilities

At its actual configuration the area in which the LSC laboratory is located is surrounded by two main underground facilities:

- The new international road tunnel (Somport tunnel), which runs under the Pyrenees Range from Spain to France and through the El Tobazo mountain. This tunnel was built between 1994 and 2002, and provides access to the LSC Laboratory, as above mentioned. The owner is the Spanish Ministry of Public Works (Dirección General de Carreteras. Demarcación de Carreteras del Estado en Aragón).

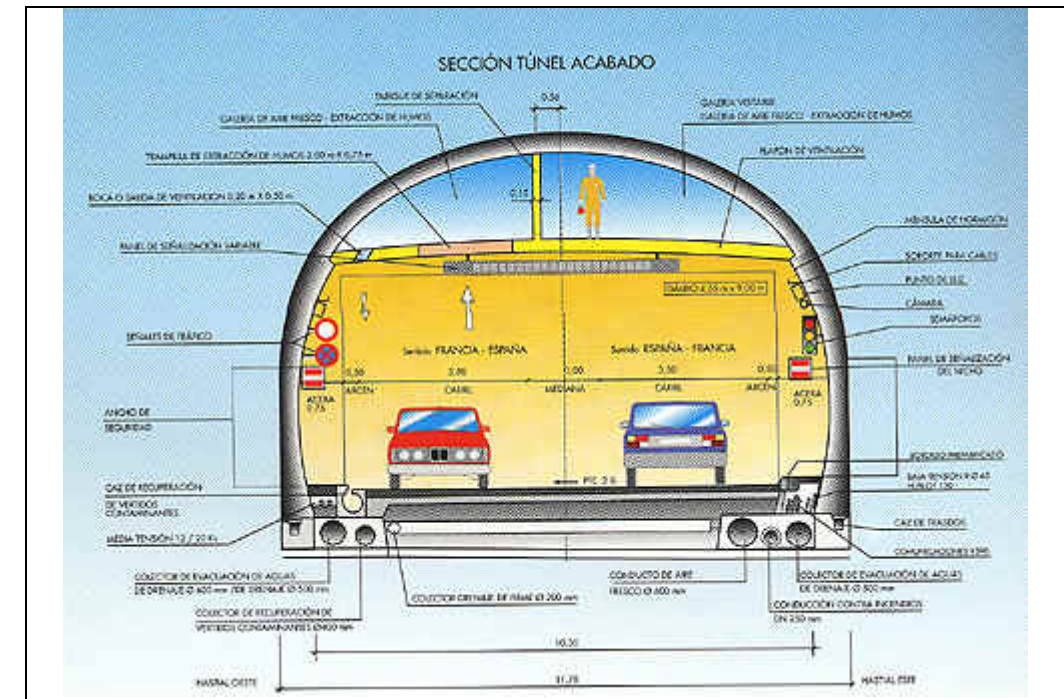


Figure 2.3-1. Section of the new Somport road tunnel, with different roof ducts.



Figure 2.3-2. View of the new Somport road tunnel at the access to LSC

- The old railway tunnel. This tunnel is currently abandoned and it runs almost parallel to the road tunnel. It was built between 1915 and 1925 and it serves as an emergency exit to the road tunnel with emergency galleries distributed throughout its length. The railway tunnel's cross section is reduced allowing only traffic of small vehicle. The LSC Laboratory could also be reached through this tunnel, although security management of the Somport tunnel requires clearance in the gallery and, thus, no traffic is allowed through it.



Figure 2.3-3. At left, cross section of the railway tunnel. At the right, emergency gallery connecting the railway tunnel with the road one.

Though in service, future underground constructions should have independent access from the Canfranc area, both during construction and for maintenance and in order to ensure future experiment developments. This condition has been kept in mind in the conceptual phase of the design, although the existence of these two main underground infrastructures gives easier access, and escape ways to the designed underground detector installations, both for construction and for operation purposes.

## 2.4 DETECTOR OPTIONS CONSIDERED FOR THE SITE

Three detector options have been considered for the Canfranc site. The names MEMPHYS, LENA and GLACIER are those for the Water Cherenkov, Liquid Scintillator and Argon technologies.

The general layout is similar for both MEMPHYS and LENA options, due to their location along the existing tunnel, although the Water Cherenkov experiment has been pre-designed with three large MDC's and the LENA experiment only needs one. Rock cover requirements have been taken in mind in conceptual design, and allow for almost 900 m of rock overburden in both cases, the existing maximum one along the Somport Tunnel.

In the case of the GLACIER (Argon) type, rock cover requirements are not so demanding, so the location has been selected in the aim to find the best rock quality along the tunnel, whose properties have been confirmed both with geomechanical data compiled from the excavation of the Somport tunnel face and from some selected boreholes.

### 2.4.1 Water Cherenkov technology (MEMPHYS)

The Water Cherenkov technology needs three caverns. The dimensions are the following ones

Diameter	Height (cavern)	Height (tank)
68 m (each)	86,5 m	≈70 m

Due to operational reasons, rock cover should be enough to fulfil experiment requirements, and location should not be far away from the actual LSC laboratory. The LSC actual installation is located below El Tobazo Mountain, almost 2.000 meters high, as previously mentioned.



The conceptual design deals with the alignment of the three tanks along a N30°W axis, almost parallel to the railway tunnel. The base of the caverns will reach level +1.000 (above sea level) and the summit of the vault reaches +1.085 a.s.l., so vertical rock cover is 890 m for the Southern cavern, and 855 m for the Northern one. This rock cover means 2.300 equivalent m.w.e. shielding, according to expected rock density.

For construction purposes and for future operation, an access gallery must be built, reaching the base of the vault of the caverns. The gallery portal should be located nearby to the one of the abandoned railway tunnel. Other locations for this access portal would lead to very steep galleries, and have been discarded for operational reasons. First stage design consists of a 5,12% slope gallery, more than 2.370 m long, reaching the base of the vaults at an upper chamber at level +1.073 a.s.l. This tunnel would be a cardinal importance infrastructure for construction purposes and for future definitive access.

A connection gallery from this chamber would communicate the three MDC's. At the end of this gallery, a deep vertical shaft could be excavated from the railway tunnel, if communication between the actual LSC and the LAGUNA experiment caverns is needed.

An elevator could provide rapid access from LSC to the MDC's. This shaft could be located at the Northern side of the MDC's location. Evacuation facilities would also take advantage of this implement.

Other auxiliary tunnels running from the access gallery to the base of each MDC complete the initial construction scheme. The longer tunnel saving the elevation difference between vault and base is 1.000 m long, and the slope is 7%. Apart from these, different auxiliary caverns (AC's) have been incorporated to the overall layout, where different utilities can be located:

- Cavern AC1: clean storage, power transformation, main control and offices.

- Cavern AC2: water and air purification system of the experiment (one for each MEMPHYS tank).

Finally, a ventilation auxiliary facility consisting in a gallery and a vertical shaft has been also designed. The scheme of this infrastructure is similar to the one that operates for the road tunnel. The shaft entrance is designed to be located in the Rioseta area, and environmental considerations should be taken in mind for this area in future detailed designs. The shaft would be 220 meters deep, and the ventilation gallery 1182 meters long.

Drawings at the end of this document show a comprehensive scheme for this LAGUNA technology infrastructure, both in plan and in perspective. A detailed scheme is shown in figure 2.4.1.

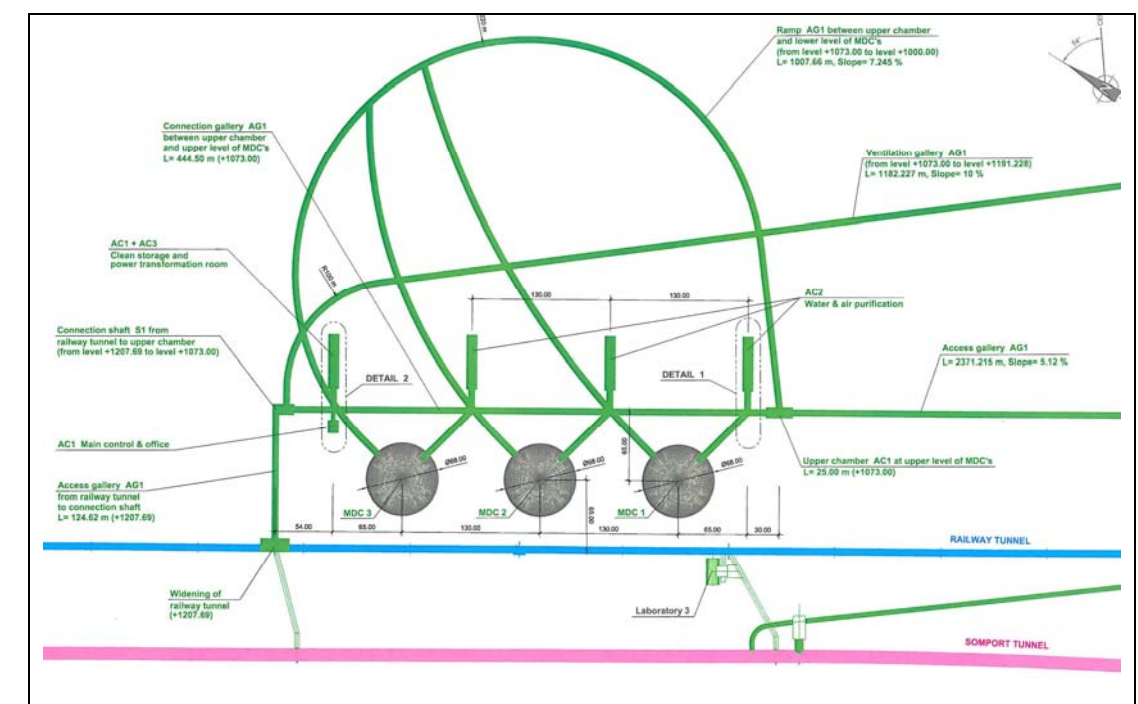


Figure 2.4-1. Detail of the MEMPHYS MDC's and auxiliary galleries.

Attending to geological considerations, caverns will be located in the Atxerito Formation, and, thus, primary rock support should deal with this fact. Geotechnical

modelling has taken in mind these aspects at this stage, according to predicted rock quality.

#### 2.4.2 Liquid Scintillator technology (LENA)

This experiment needs of a single underground cavern. Dimensions are the following ones:

Diameter (cavern)	Target diameter (tank)	Height (cavern)	Height (tank)
34 m	26 m	120 m	≈105 m

The requirements of rock cover are higher in this case. The optimal requirement is to reach 3.500 equivalent m.w.e. The LSC location does not allow this rock cover, unless the cavern is located very deep, in which case difficulties to access from the actual underground facilities would increase. The optimal first design for the Canfranc site leads to locate the MDC in the same site than the northernmost of the three MEMPHYS caverns, so the scheme for access construction galleries and communication with the LSC is be very similar.

The level of the base of this cavern would be 965 a.s.l. The slope of the gallery reaching the upper level of the vault would be 4,90%, and 2.536 m long, attending to the conceptual design. The gallery ends at an upper chamber, as in the MEMPHYS case, from which another horizontal gallery reaches the base of the vault. Portal location is the same than the one considered for the MEMPHYS technology scheme, and the tunnel would run parallel to the railway one.

The underground communication net between LSC and MDC would have a similar scheme than the one of the MEMPHYS case. Also an auxiliary construction tunnel from the access gallery to the base of the cylindrical cavern is needed. Auxiliary caverns (AC's) are located around the entrance to the vault, and provide room for the next items:

- Cavern AC1: clean room, liquid and gas handling. Electronics, low background laboratory, main control and offices.
- Cavern AC2: purification system of the experiment.

Drawings show also a comprehensive scheme for this LAGUNA technology infrastructure, and a detail of the layout is annexed in the next figure.

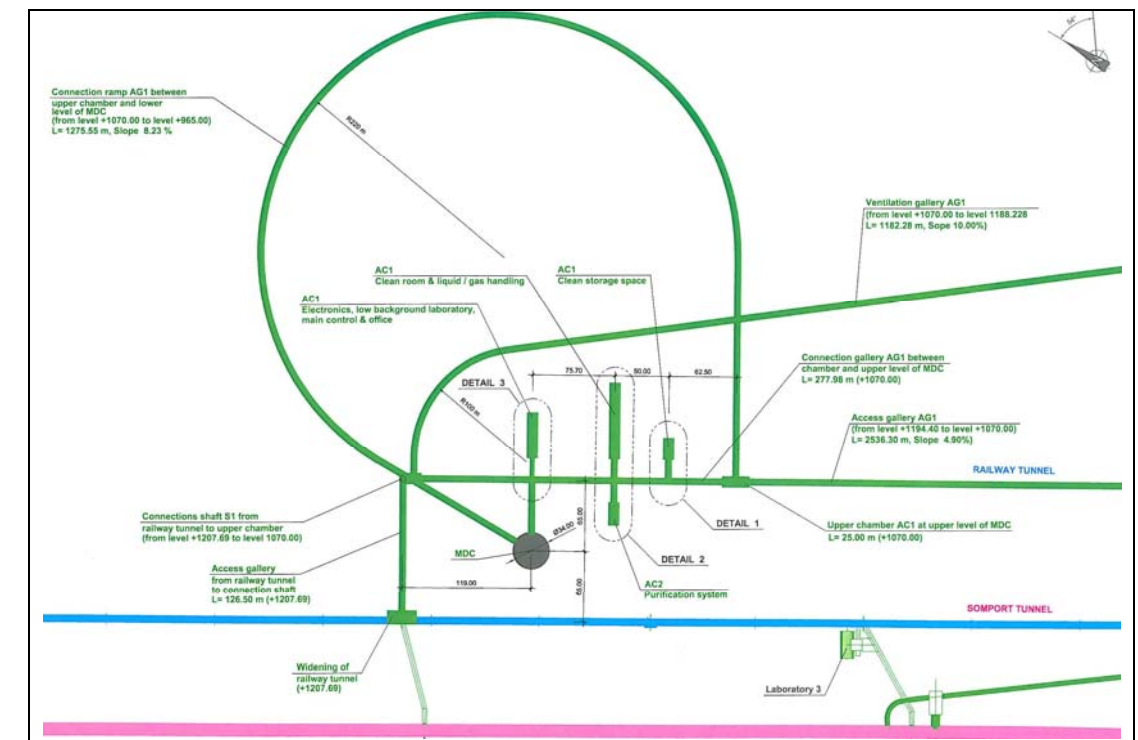


Figure 2.4-2. Detail of the LENA MDC and auxiliary galleries.

Attending to geological considerations, the MDC for LENA will be located in the Atxerito Formation. Primary rock support should deal with this fact. Vault dimensions are smaller, but cavern walls are higher.

#### 2.4.3 Liquid Argon Technology (GLACIER)

A single cavern would also be needed. In this case, dimensions are the following:

Diameter	Height (cavern)
75 m	40 m

The diameter outgoes any existing dimensions for any kind of underground installation. This experiment requires 600 m.w.e., so this rock coverage can be easily fulfilled in many sections, and the best rock quality can be chosen to locate the cavern. The top level of the cavern has been selected to be below the level of the railway tunnel.

In the Canfranc site, limestone rocks that form El Tobazo mountain are the best quality ones, and the excavation of the Somport road tunnel confirmed this, as it has been mentioned. A location where the entire vault is excavated in best-quality rock has been chosen, attending to the data collected. In agreement with these, the MDC should be located 600 m North from the actual LSC installation.

Since it is farther away, the access ramp can be built from a new portal, 1.500 m North from the railway existing one. From this portal, a 2050 meters long access gallery would be excavated. The first 1500 meters of this gallery would have a 6,2% slope and the remaining 550 metres would have a gentler slope of 0.9% and it would reach an upper chamber at elevation +1201 a.s.l. From this chamber an auxiliary gallery (L=37,5 metres) would be excavated to reach the working area at the base of the vault. Another access gallery connecting the LSC to the upper chamber could be easily excavated communicating both structures.

The cavern would be completely installed in the coralline Tobazo limestones.

Another auxiliary tunnel would run from the access gallery to the base of the MDC, completing the scheme. Auxiliary caverns (AC's) provide both room for electronic, main control and office facilities, and for storage space and power transformation.

Comprehensive drawings for this LAGUNA technology infrastructure have been generated. A detailed scheme is shown in the next figure.

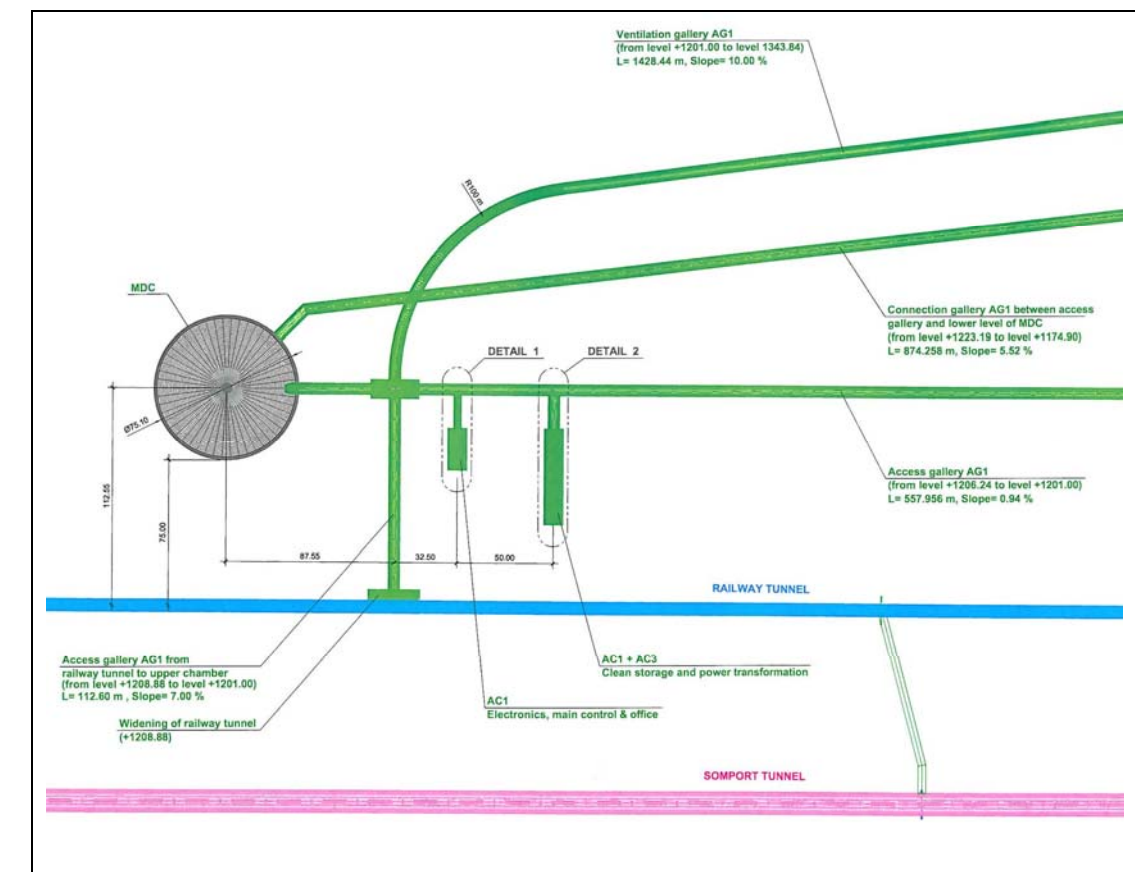


Figure 2.4-3. Detail of the GLACIER MDC and auxiliary galleries.



## 2.5 ADVANTAGES OF THE SITE AND THE CONSIDERED LAYOUT

Many arguments for sitting LAGUNA at Canfranc are presented in detail throughout this Feasibility Study and this chapter provides an overview and summary of the reasons.

- The Somport Tunnel is a permanent bi-national facility that is not expected to close in the next 50 to 100 years. No bi-national tunnel in Europe has been closed in such time period. The Somport Tunnel would provide permanent control on the site; such as safety, communication, ambulances, etc...
- The Canfranc site would be dedicated exclusively to LAGUNA and would not have any interference by other activities, such as mining.
- The access to the underground facilities from the exterior for both, construction and operation purposes, is through an independent tunnel with dimensions and slope similar to those of any road tunnel and therefore capable of carrying car, bus or truck traffic.
- The future LAGUNA underground facilities at Canfranc can be operated independently from the Somport Road Tunnel in the case of eventual unfavorable conditions, such as fire, heavy traffic, accidents, etc...
- The current design has separate entrances for people located at two distant ends, one being through the access tunnel and the other the connection with the Somport tunnel. This increases the safety of the site in the case of an incident at any location within the facility.
- Current plans have a ventilation system with two different openings: the access tunnel and the ventilation shaft to the outside. Safety is therefore increased even in the case of fire at any location within the facility. On the

other hand the ventilation shaft provides the intake of radon-free air. These aspects are well-explained on further paragraphs of this document.

- Current plans have an independent connection to the outside, through the access tunnel, capable of providing the needed water and power to the facilities from a nearby dam, and from other industrial facilities.
- The area of the experiment will be located in the vicinity of a developed area, with all kind of housing facilities, and a good communication network.

### 3. OVERVIEW ON LARGE UNDERGROUND CAVERNS AROUND THE WORLD

#### 3.1 PRECEDENTS OF LARGE UNDERGROUND CAVERNS

The caverns needed for the LAGUNA experiments are of considerable dimensions requiring large unsupported spans (up to 80 m) at depths ranging from a few hundred metres to well over 1200 m. In fact the needed spans are larger than any actual cavern in operation. Furthermore the depths are also bigger than usual although in this case no deeper than some of the existing underground caverns. It is the combination of depth and size of caverns needed for LAGUNA what makes them extraordinary in dimensions

For this reasons it is very important to search for precedents of the construction of existing permanent large underground caverns worldwide in order to establish some data bank which could give some insight in the scope of the LAGUNA caverns construction problems.

To this effect a thorough search of caverns (of any use) has been done, referred to caverns with spans bigger than usual or very deep.

Furthermore, the caves researched that are considered suitable as precedents for LAGUNA are divided here, by use, into:

- Caverns built for physics experiments,
- Permanent mining installations,
- Hydrocarbon storage caverns,
- Power plant caverns,

- Others (like underground sport arenas and some published military facilities).

##### 3.1.1 Caverns for physics experiments

As indicated by Laughton (2007), there are over a dozen caverns worldwide built to house physics detectors with spans larger than 20m, among them are:

- Super Positron Super Synchrotron and the Large Electron Positron (LEP), European Particle Physics Laboratory (CERN), France-Switzerland: Six **21m** span caverns, between 50 to 175m deep in a weak interbedded series of sandstones, siltstones, and marls
- Large Hadron Collider (LHC), France-Switzerland: Two 35m span caverns
- Gran Sasso Laboratory, Italy: Two **20m** span caverns, 1500m deep in a dolomitic rock mass
- Kamioka Mine, Japan: One **20m** span cavern (KamLAND) and one **40m** span cavern (Super-KAMIOKANDE), approximately 1000m deep in hard metamorphic rock unit
- Sudbury Neutrino Observatory (SNO), Creighton Mine, Canada: One **20m** span cavern, nearly 2000m deep in norite

Due to the relevance that Super-KAMIOKANDE has for LAGUNA, a more detailed description of the Japanese observatory will be provided. Figure 6.1-1 shows a schematic view of the underground openings and observation facilities built for the Super-KAMIOKANDE project. The cavern is 40 m in diameter and 57.6 m deep and has been excavated at a depth of approximately 1 Km.

The site is situated close to the synclinal axis in the central mass of complicated folding structures of the Hida gneiss, being composed of amphibolite, hornblende

gneiss and so-called the “Inishi migmatite” partly with little limestone and skarn minerals. They are fresh/unweathered and competent enough with very little mineralization. The rock properties as measured in the construction site are shown on table 3.1-1. (Nakagawa, 1997).

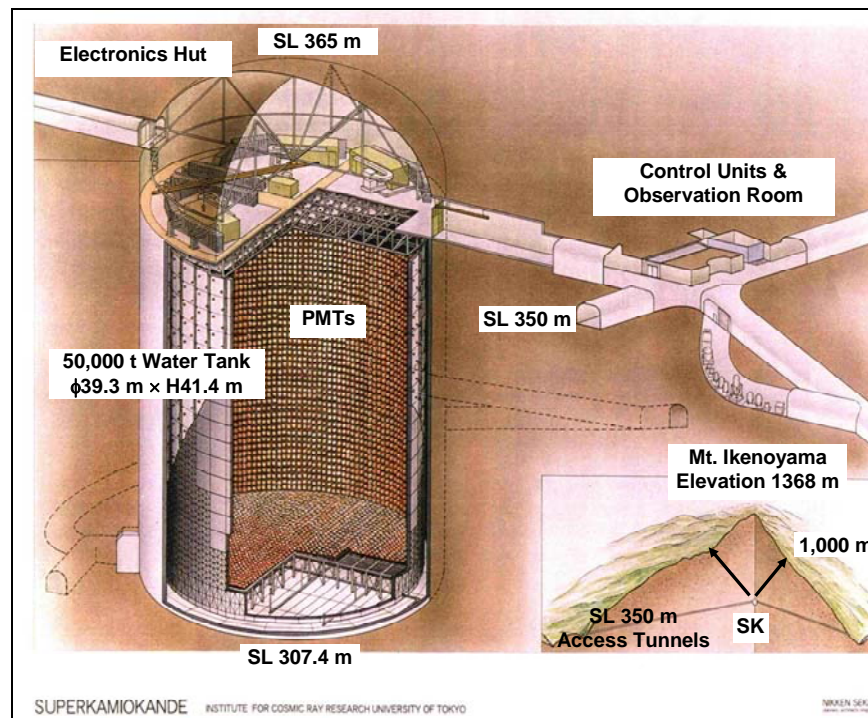


Figure 3.1-1. A schematic view of the Super-KAMIOKANDE (from the Institute for Cosmic Ray Research, University of Tokyo)

Items	Values
Rock types	Amphibolite and gneiss
Density	0.026 MN/m <sup>3</sup>
Compressive strength	149 MPa
Tensile strength	9.7 MPa
Young's modulus	49.9 GPa
Elastic wave velocity	4930 m/s
Initial state of stresses	$\sigma_1$ 28.8 MPa (068/309)
	$\sigma_2$ 18.9 MPa (008/060)
	$\sigma_3$ 6.1 MPa (020/153)
RQD	84%
RMR	84 - 94

Table 3.1-1. Engineering properties of the rock and measured in-situ stresses at the construction site

It is also worthwhile mentioning the development of the Deep Underground Science and Engineering Laboratory (DUSEL) in the U.S. The former Homestake gold mine near Lead, South Dakota, was the site selected in 2007 for the future underground laboratory. DUSEL will be a multidisciplinary deep underground science facility where investigations in physics, biology, earth science, and engineering will be carried out. It will have campuses at different depths ranging from a few metres deep to 2400m under ground.

In its conceptual design DUSEL houses Water Cherenkov (MEMPHYS) detectors of 50m diameter and 50m height located at 1480 metres deep. Figure 3.1-2 shows the preliminary design of the tanks obtained from the conceptual design posted in the Lawrence Berkeley National Laboratory – Nuclear Science Division web page (<http://www.lbl.gov/nsd/homestake/conceptualdesign.html>).

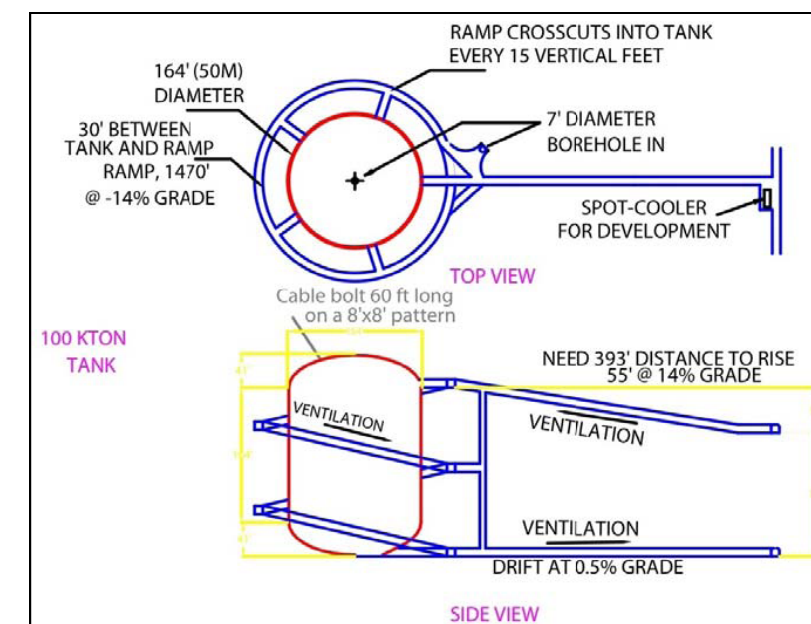


Figure 3.1-2. Preliminary design for a single cavity with nominal dimensions of 50m diameter and 50m height to house a 100kt mass water Cherenkov detector. The upper ramp for access to the cavity will be at 1480m deep.  
(<http://www.lbl.gov/nsd/homestake/conceptualdesign.html>)

In mid May 2009 the mining team working at the Homestake site successfully completed dewatering to an approximate depth of 1,5 Km below the surface. The



exact location of the caverns is not yet defined as the site investigation work continues. Construction is scheduled to start in 2013.

Likewise, another next-generation observatory is in a planning phase in Japan, the Hyper-KAMIOKANDE. Even though in a conceptual stage, the Hyper-KAMIOKANDE is expected to be almost 20 times larger than the Super-KAMIOKANDE (Nakagawa, 2005). The design requirements of the Hyper-KAMIOKANDE include, among others, a huge 1,000,000 m<sup>3</sup> cavern located 700 to 850 metres deep (at least 500m). Multiple caverns are considered even though the single cavern is preferred. Figure 3.1-3 shows the baseline configuration of the Hyper-KAMIOKANDE.

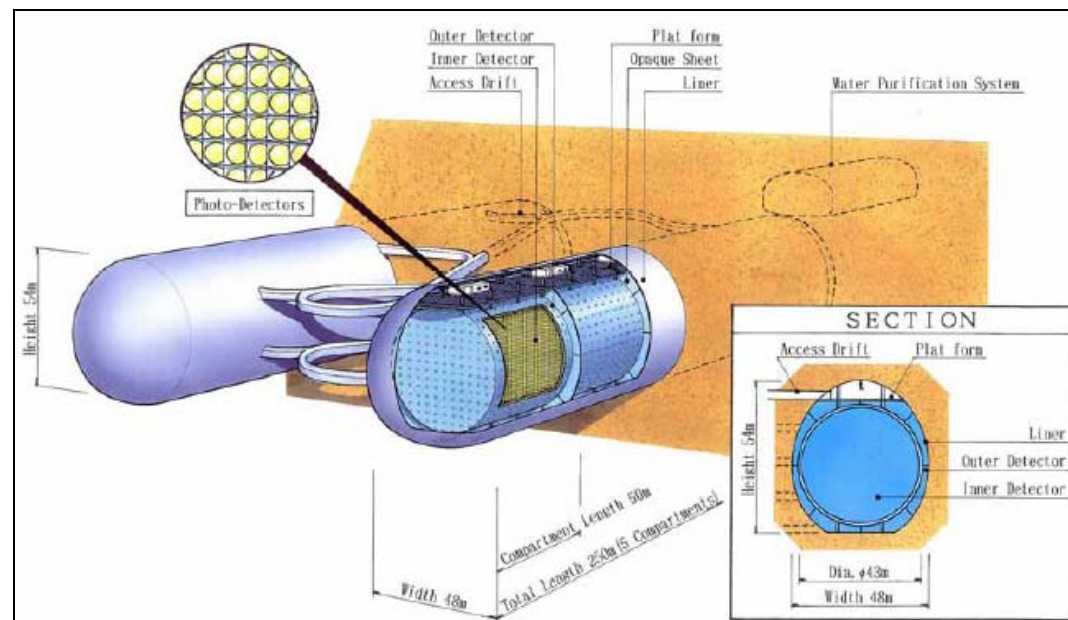


Figure 3.1-3. Baseline configuration of the Hyper-KAMIOKANDE (Nakagawa, 2005)

### 3.1.2 Permanent mining caverns

Even though construction techniques used in deep mining are of little use in the construction of the caverns for LAGUNA, some permanent mine caverns are of interest; some because of their unsupported spans and others for the depth

reached during mining. Some examples of mines of interest for this project are presented next:

- Tytyri Limestone Mine, Lohja, Finland: **60m** wide, 160m high and 109m long.
- Vihanti Mine, Finland: **40m** wide, 60m high, 150m long and 200m deep in dolomite.
- Joma Copper Mine, Norway: **70m** wide, 20m high.
- Anjou Slate Mine, France: **30m** wide, 70m high and 350m deep.

South African mines are very deep (because the high prices of mined gold and/or diamonds) so permanent deep installations are economically feasible due to the high cost of transportation to the surface. Two of the deeper ones are:

- Western Deep Mine, permanent crushing installation, South Africa: 17 m span approximately and almost **3 km** deep
- President Steyn: gold mine hoist chamber, South Africa: 16m span and over **2 Km** deep.

### 3.1.3 Underground fuel storage facilities

Regarding underground fuel storage facilities, a common practice is to store hydrocarbon in rock salt layers resulting in caverns of considerable unsupported spans at depths well above 1000 m. The following three hydrocarbon storage caverns in salt located in France are presented as examples of the dimensions and depth of such openings:

- Terzanne, Etrez Storage Facility: **80m** wide, 150m high and **1402m** deep.

- Manosque Storage Facility: **80m** wide, 350m high and 600m deep.
- Hauterives Storage Facility: **120m** wide, 250m high and **1300m** deep.

Although these caverns are wide and deep they do not represent good precedents for the caverns in this project because of the construction methods involved (the salt layer is diluted and the saline solution extracted to create the cavern) are not compatible with mining or civil engineering excavation methods.

Alternatively, a novel concept for storing natural gas was developed in Sweden, the Lined Rock Cavern (LRC) concept and consists of storing pressurized natural gas in steel-lined caverns excavated in rock. The LRC system provides more flexibility than the conventional underground gas storage cavern which requires the existence of salt domes or thick salt layers.

The LRC concept involves the excavation of cylindrical caverns 20 to 50m in diameter, 50 to 115m high with domed roof and rounded inverts.

These caverns are located at depth from 100 to 200m underground and are lined with 1-m thick reinforced concrete and 12 to 15mm thick carbon steel liners that act as an impermeable barrier. The gas is stored at maximum pressures from about 15 to 25 MPa. (<http://www.netl.doe.gov>)

A full-scale LRC demonstration facility has been constructed (with European Union funding), at Skallen, a site near the coastal city of Halmstad in southwest Sweden.

The facility has undergone extensive pressure testing and has been in regular operation since 2003 (<http://www.usgastech.com/products/LinedRock/linedrock.htm>). Figure 3.1-4 shows the characteristics and a sketch of a tank

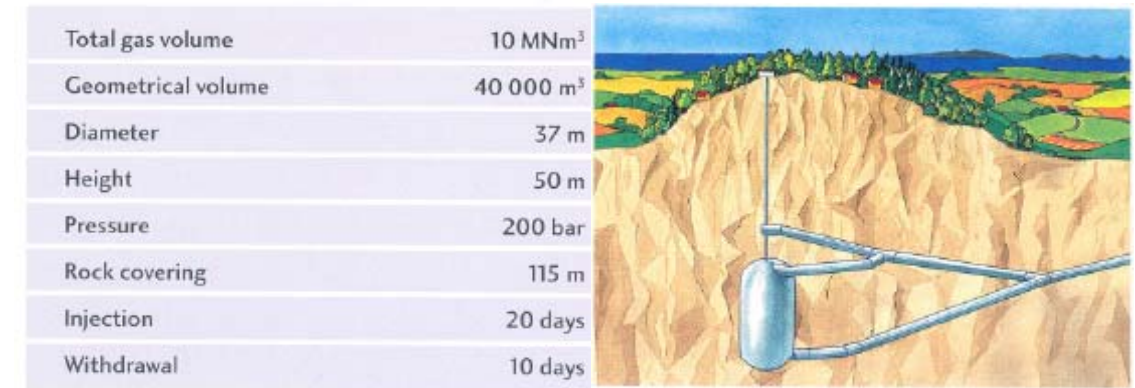


Figure 3.1-4. Tank characteristics of the first storage facility built using the LRC concept in Sweden (<http://www.usgastech.com/products/LinedRock/linedrock.htm>)

### 3.1.4 Power plant caverns

There are many large underground caverns built to house turbines, electrical generators and transformers in hydroelectric power plants worldwide. Even though these caverns vary greatly on size and depth, they constitute good precedents for the constructions of the LAGUNA caverns, especially those with larger spans. Table 3.1-2 shows some power plant caverns with spans larger than 30m.

Site	Cavern Dimensions and Depth	Rock Type (reference)
La Sautet power station, France (1933)	B = 31 m H = 20 m L = 35 m D = 100 m	Limestone (Leith, 2001)
Liujiaxia powerhouse, China (early 1960's)	B = 31 m H = 64 m L = 86 m	(Leith, 2001)
Hongrin power station, Switzerland (1970)	B = 30 m H = 27 m L = 137 m D = 50-150 m	Limestone and limestone-schist with several sets of vertical fractures and clay. (Hoek, 1980)
Waldeck II power station, Germany (1973)	B = 33,5 m H = 50 m L = 105 m D = 350 m	Interbedded shale and greywacke, faulted and jointed. Faults form wedges in cavern roof. (Hoek, 1980)
Rio Grande No. 1 hydroelectric project, surge	B = 38 m H = 62 m	Exfoliated gneiss (very good quality)

tank, Cordoba, Argentina (1980)	L = 106 m	(Moretto, 1993)
Imaichi Power Station, Japan (1982)	B = <b>33,5</b> m H = 51 m L = 160 m D = 400 m	Sandstone, breccia (Hibino, 1995) (Hoek, 1989)
Cirata power station, Indonesia (1988)	B = <b>35</b> m H = 49.4 m L = 253 m D = 109 m	Breccia, Andesite (Hoek, 1989)
Kazunogawa Power Plant, Japan (1999)	B = <b>34</b> m H = 54 m L = 210 m D = 500 m	Sandstone/mudstone alternation, highly jointed (10/m average and 30/m max.) (Kudoh, 1999) (Koyama, 1999)
Masjed-E-Soleiman Powerhouse Cavern, Iran (2002)	B = <b>30</b> m H = 50 m L = 112 m D = 250-320 m	Siltstone, claystone, sandstone and conglomerate (Shahabi, 2003) (Ahmadi, 2007)

Table 3.1-2. Some hydroelectric underground caverns with spans larger than 30m.

### 3.1.5 Caverns for other uses

Underground caverns have also been built to house other types of facilities such as warehouses, museums, military installations and sports centres, the most famous being Gjøvik Hall in Norway, an underground sport facility with a 61m unsupported span, 24m high and set 25-50m deep in hard metamorphic rock under favourable stress-field conditions.

The stresses measured in-situ indicate that the horizontal stress is 4 times larger than the vertical one and therefore the most critical unsupported length would be its height (24m) and not the span. (Aarvold, 1994)

Other examples of underground sports facilities include the following three located in Finland:

- Hervanta underground ice rink, 1982: **32m** wide, 9m high and 133m long.

- Kauniainen indoor sports centre, 1987: **28,7m** wide, 12m high and 44,5m long.
- Turku underground ice rink: **31m** wide and 80m long.

Also as a reference it is worth mentioning the Takayama Festival Art Museum in Japan, which is of hemispherical shape having an unsupported span of 40,5m, a height of 20m. At only 30m deep the museum is set in Colluvium and pyroclastic welded tuff.

### 3.1.6 Summary

The caverns presented in this section are summarized in a scatter plot of span vs. depth (Figure 3.1-5). The most relevant caverns are included. For the sake of simplicity the hydroelectric caverns with span < 30 metres have been omitted.

A similar plot (with less data) has been published about the DUSEL project.

In this plot it can be clearly appreciated that openings of such magnitude as those needed for LAGUNA are unprecedented except for the liquid scintillator.

The plot shows two facts worth of mention:

- In fact the maximum up-to date achieved span is 40 metres (Gjovik hall 65 meters span is no relevant due to the fact that critical opening for Gjovik is the height and not the span, as previously explained. A Gjovik “equivalent” has been plotted
- In caverns below 1 kilometer deep (there are very few) the span diminishes very quickly to less than 20 meters.



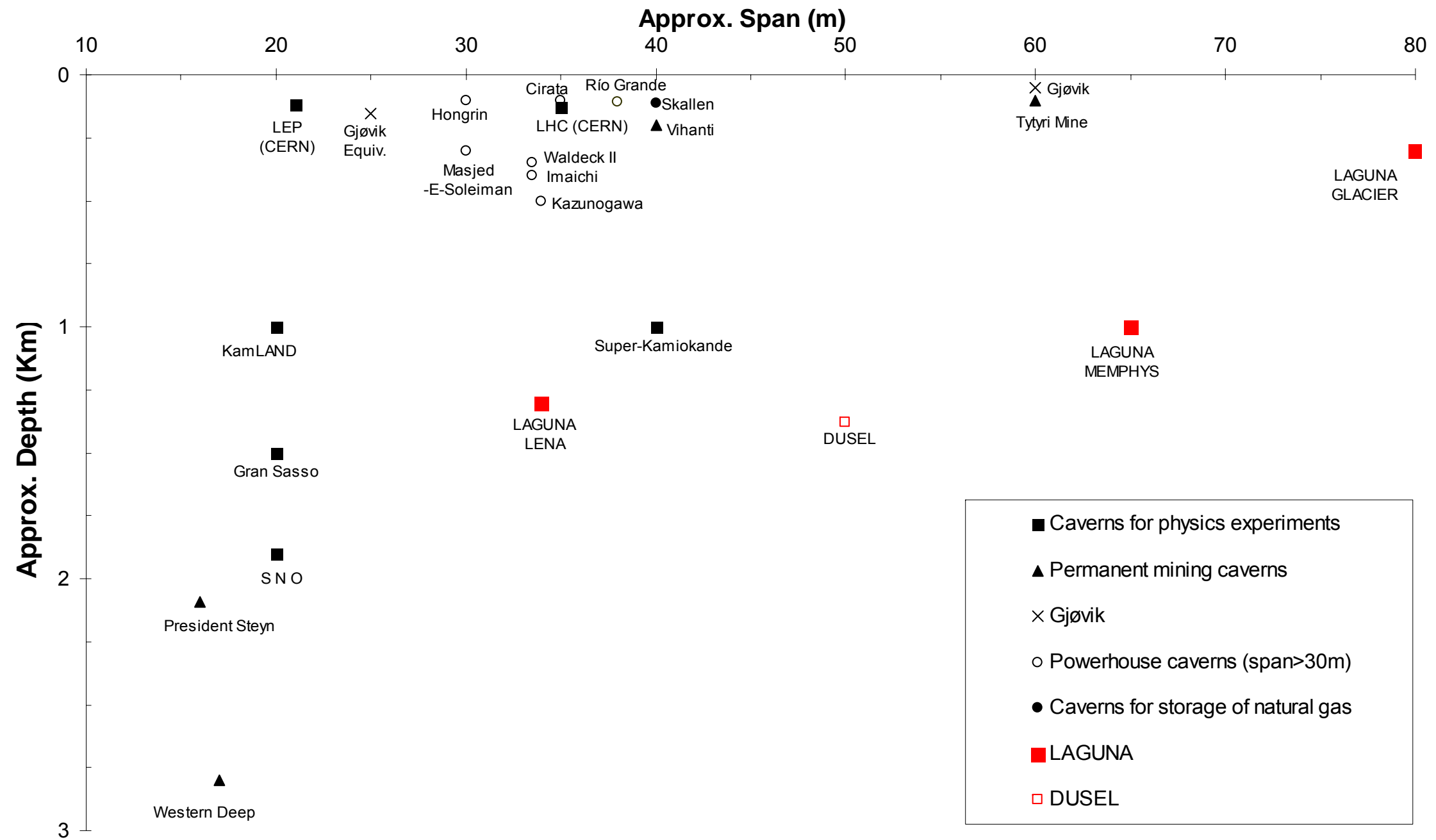


Figure 3.1-5. Scattered plot span vs. depth of permanent large caverns classified by use.

## 3.2 EXCAVATION METHODS AND SUPPORT SYSTEMS OF SOME LARGE PERMANENT UNDERGROUND CAVERNS

In this section, the excavation procedures and support systems used in the construction of some large caverns will be presented as precedents for the proposed excavation sequence and support for the Main Detector Caverns (MDC) in this feasibility study.

### 3.2.1 Super - KAMIOKANDE

The information presented in this sub-section is obtained from Nakagawa, 1997 and Yamatomi, 1999.

#### General excavation procedures

ANFO and emulsion explosives with NONEL detonators were used for the excavation of the Super-KAMIOKANDE cavern. For the beginning of the excavation track-less mining systems and NATM concepts were applied.

About 120,000 m<sup>3</sup> of blasted material was hauled through the access tunnels and ramps to an existing dome (150 m away at elevation 350) where water purification and degassing facilities were later placed. The material was finally extracted through a main tunnel to the waste disposal.

Figure 3.2-1 shows the excavation sequence used for the Super-KAMIOKANDE cavern. The excavation was divided into 4 blocks, where Block 1 was the first one to be excavated followed by blocks 2, 3 and 4. Block 1 was in turn excavated in subsections 1 to 8 as shown in figure 6.

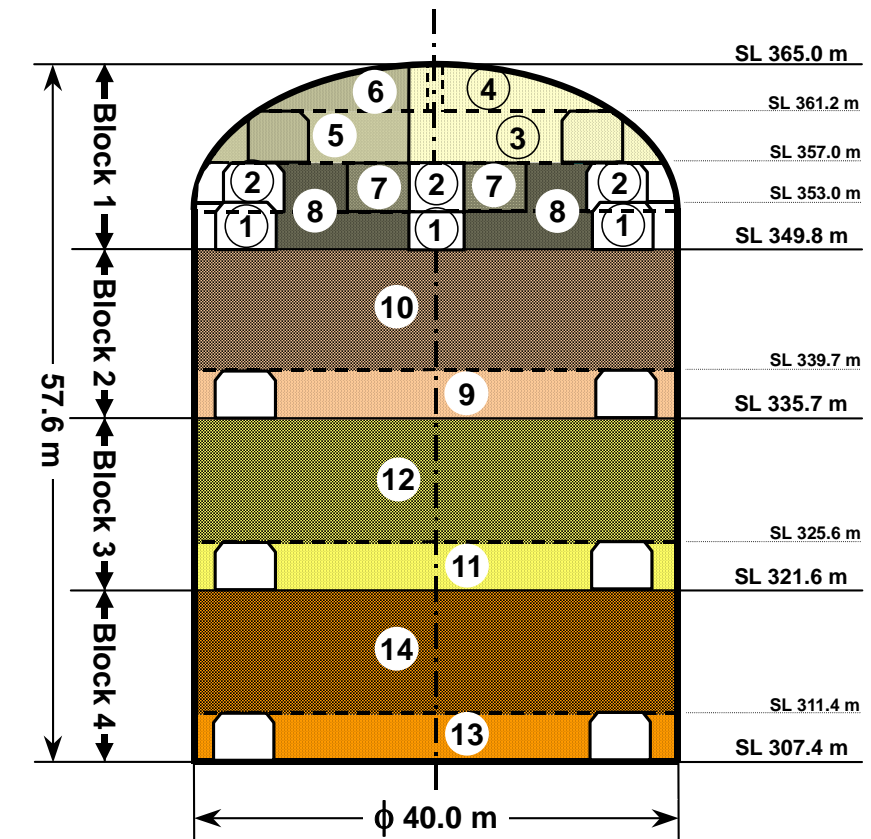


Figure 3.2-1. Excavation sequence for the Super-KAMIOKANDE cavern

#### Excavation and support of the vault

Support:

- The overhand cut & fill stopping method was used.
- Doubled layered 16 cm thick wet-shotcrete mixed with 80 kg/m<sup>3</sup> steel-fiber was sprayed on the peripheral surface of the dome.
- Cement grouted cablebolts:  $\phi 15.2$  mm x L8 m, 7 strand PC steel, 2 wires/hole, every 4 m<sup>2</sup>
- Cement grouted rockbolts:  $\phi 22$  mm x L 2 m, steel rebar, every 1 m<sup>2</sup>
- During excavation, temporary shotcrete and rockbolts were placed

#### Excavation procedure:

- Circular tunnel at elevation 349.8 and 2 m inside of the periphery of the dome, followed by smooth blasting to finish it (stage 1)
- The roof of the circular tunnel was stoped at two stages upward to stand on the piles at elevation 357 (stage 2)
- Internal rock pillar was horizontally stoped (stage 3) to expose intermediate roof at elevation 361.2
- Pre-cablebolts were installed at elevation 361.2 before blasting upward (stage 4, see figure 3.2-2a)
- Blasting of stage 4 was done with parallel drillholes of different lengths to achieve the curved rooftop (figure 3.2-2b)
- Shotcreting and rockbolting of the curved rooftop (figure 3.2-2c)
- The other half (stages 5 and 6) were carried out in the same manner (figure 3.2-2d)
- The internal core of Block 1 (stages 7 and 8) was excavated by bench blasting along with removing the piled rock used before as the working floor.
- Pulling test was carried out confirming up to 30 ton capacity.

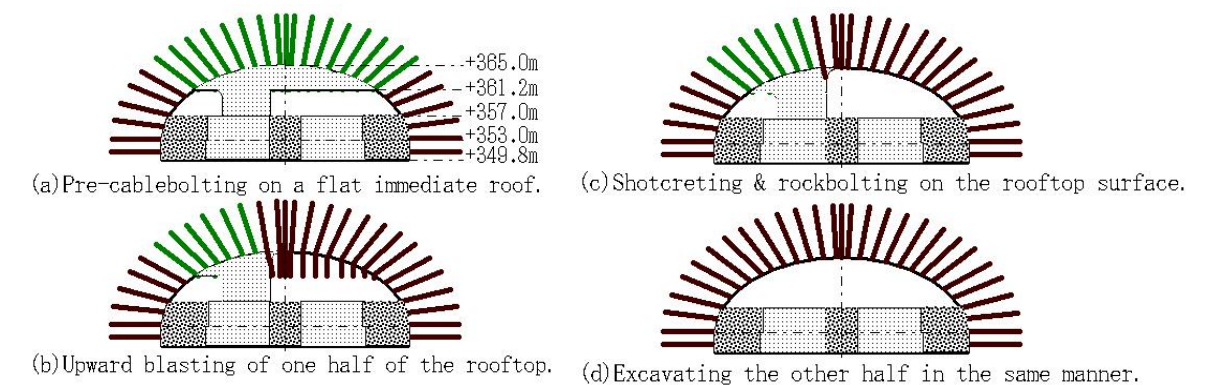


Figure 3.2-2. Excavation procedure for the rooftop of the cavern with pre-cablebolt installation.

#### Excavation and support of the side walls

##### Support:

- Doubled layered 16 cm thick wet-shotcrete mixed with 80 kg/m<sup>3</sup> steel-fiber was sprayed on the peripheral surface of the dome.
- Cement grouted cablebolts:  $\phi 15.2$  mm x L8 m, 7 strand PC steel, 2 wires/hole, every 6 m<sup>2</sup>
- Cement grouted rockbolts:  $\phi 22$  mm x L 2.35 m, steel rebar, every 1 m<sup>2</sup>, installed to stick 19 cm out of the shotcreted wall (to be connected to tie-rods welded on the detector tank, the resulting space was filled with lining concrete)
- During excavation, temporary shotcrete and rockbolts were placed

##### Excavation procedure:

- Prior to excavation of Blocks 2, 3 and 4, a spiral ramp was tunneled from elevation 349.8 to 307.4 and branched at elevation 335.7 and 321.6

- To excavate Block 2 a circular tunnel was excavated first (at elevation 335.7) 2 m inside the cavern. Smooth blasting to finish and placement of design support
- Sublevel horizontally opened leaving 2 or 3 pillars
- Stage blasting with 10.1 m long vertical blasting holes (from elevation 339.7 to 349.8). Lowering of the slope of the blasted rock pile contributed to support the peripheral wall.
- Blocks 3 and 4 were excavated in the same manner as Block 2.

Grouting of typical faults was carried out before construction and also systematically below elevation 335.7 inside the cavern by drilling 9m to 12m long, 4 to 6 check holes after 2 or 3 blasts. The outer zone of the cavern below elevation 335.7 was also curtain-grouted downward from each sublevel before each longhole blasting.

### 3.2.2 Gjøvik Olympic Mountain Hall, Norway

The information presented in this sub-section is obtained from Aarvold, 1994 and Barton, 1991.

The Gjøvik Olympic Mountain Hall in Norway was constructed between 1991 and 1993 to be used as an ice rink for the winter Olympics at Lillehammer in 1994. It is 61 meters wide, 91 meters long and 24 meters high and between 25 and 40 meters deep.

The excavation started with the construction of two access tunnels (with cross sections of 20m<sup>2</sup> and 45 m<sup>2</sup>) driven as shown on figure 3.2-3. From the tunnel located at the top, a 10m wide Center Top Heading was driven throughout the entire length of the stadium. After the heading excavation was completed two 14m wide lateral tunnels were blasted bringing the span at this stage to 38m.

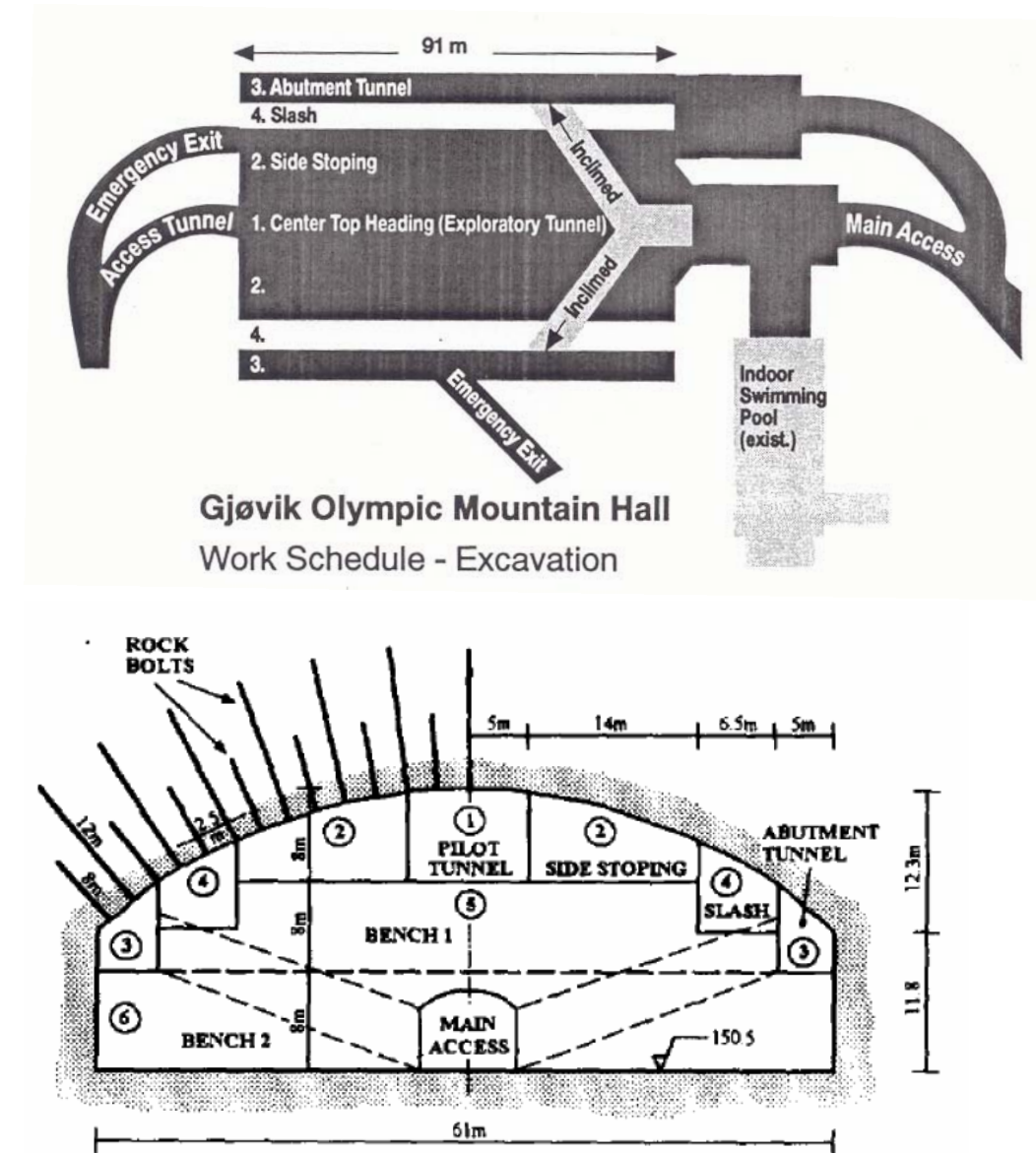


Figure 3.2-3. Excavation stages for The Gjøvik Olympic Mountain Hall in Norway

While works on the top of the cavern were carried out, including the permanent support, the main access tunnel was driven to the base level of the cavern. From this access tunnel, two secondary inclined tunnels were excavated to reach the abutments. The rest of the roof excavation consisted on blasting the remaining rock mass between the abutments and the side stopping. After supporting the span



the rest of the cavern was excavated by bench blasting techniques with a maximum bench height of 12m.

The support system consisted of 10-cm-thick steel fiber reinforced shotcrete layer both (twin strand, 12m long, and spacing of 5m x 5m) and steel bolts ( $\varnothing$  25mm) were placed at the vault. On the side walls, in addition to the shotcrete, untensioned, grouted bolts were used (see figure 3.2-4).

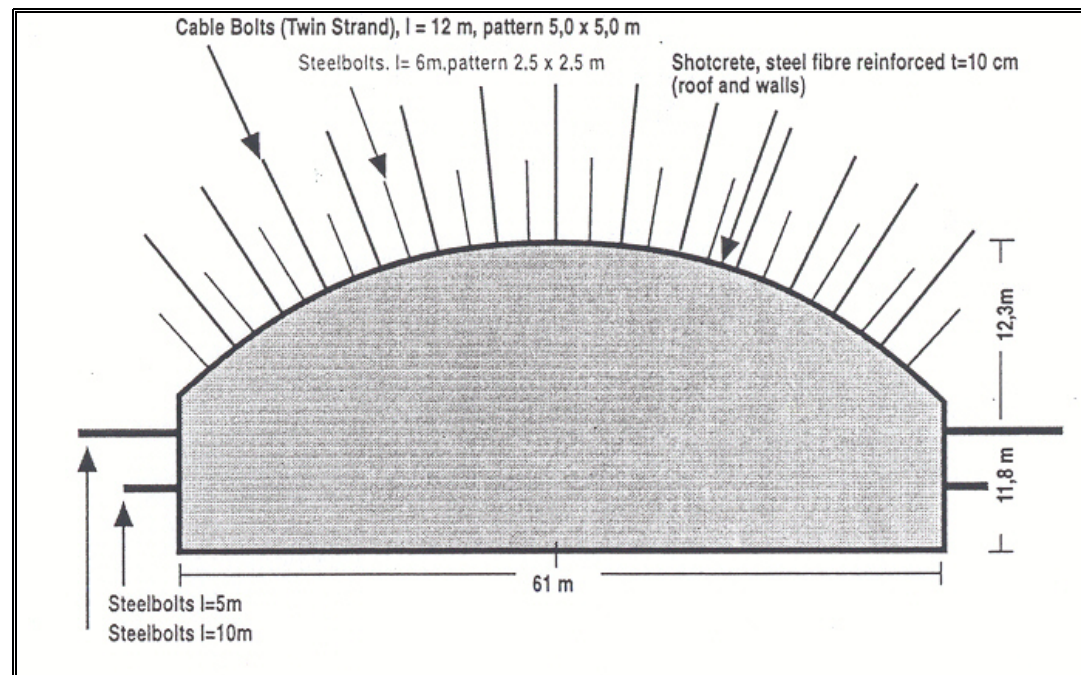


Figure 3.2-4. Support system of Gjøvik Olympic Mountain Hall in Norway

### 3.2.3 Power Plants

A typical power plant cavern excavation is carried out in stages and starts by drilling a pilot tunnel along the entire length of the opening. After this top gallery is supported, the rest of the vault is excavated usually by side stoping and then properly supported to complete the first stage. The rest of the excavation is carried out by benching until the bottom of the cavern is reached, appropriate support is pro-

vided for the walls before moving to the next level. Figure 3.2-5 shows a typical example of a power plant excavation stages.

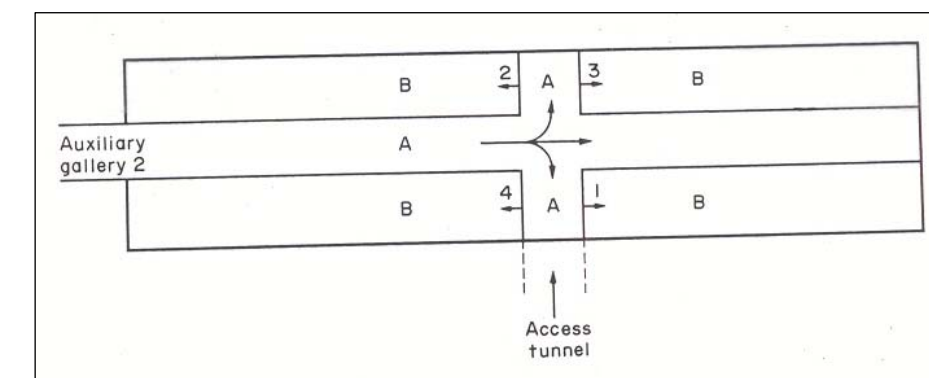
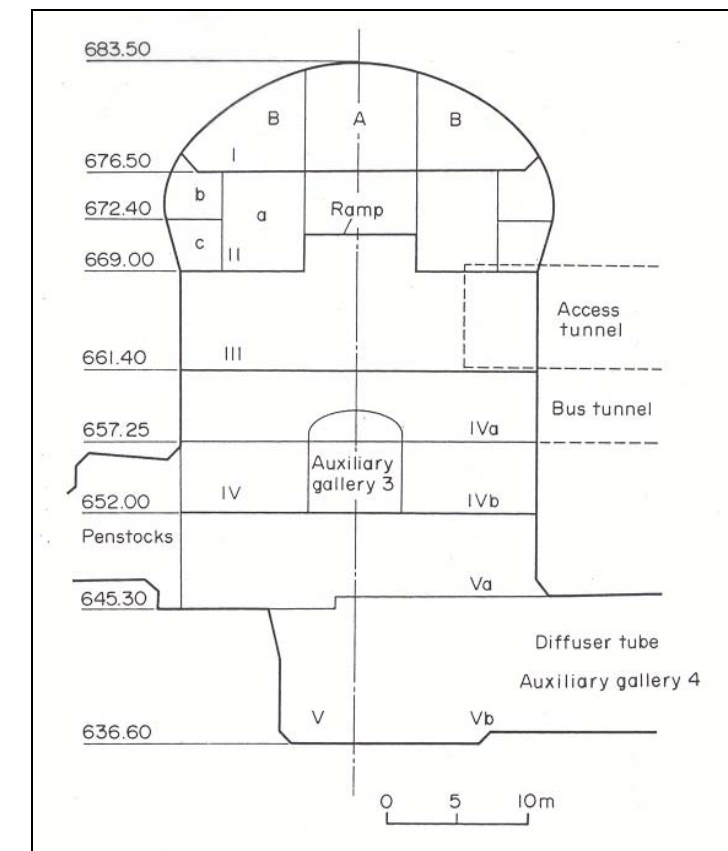


Figure 3.2-5. Excavation stages of the powerhouse cavern of Rio Grande No.1 in Córdoba, Argentina.

### 3.3 SUPPORT SYSTEMS ADOPTED IN SOME LARGE PERMANENT UNDERGROUND CAVERNS

The data gathered regarding the support used in some large permanent underground caverns is summarized in table 3.3-1. This table includes dimensions and depth of the cavities as well as crown and wall support systems and comments when available.

Site	Cavern Dimensions and Depth (1)	Support used	Comments
Tumut I power plant, New South Wales, Australia (1959)	B = 23,5 m H = 33,5 m L = 91,4 m D = 335 m	<b>Crown:</b> 2,5 cm Ø, 1,2m x 1,2m spacing, 4,6 m long, 23 k yield, ungrouted <b>Walls:</b> 2,5 cm Ø, 1,5m x 1,5m spacing, 3,7 m long	$\sigma_v = 10,3$ MPa $\sigma_h = 0 - 12,4$ MPa
NORAD Cheyenne Mountain Complex, Colorado Springs, Colorado, U.S.A. (military defense facility) (1964)	B = 31 m H = 25,6 m	Pattern rock bolting <b>Roof:</b> reinforced by recessed rock anchors, deformed 32mm Ø bar with perforated sleeve by 7,3m long, S=1,7m x 1,7m. Fully grouted hollow core deformed 25,4mm Ø bar bolts, 2,4m long, S = 1,2m x 1,2m <b>Walls - upper half:</b> fully grouted recessed rock anchors, deformed 32mm Ø bar with perforated sleeve by 3,6m long, S=2,4m x 2,4m. Fully grouted hollow core deformed 32mm Ø bar bolts, 2,4m long, S = 1,2m x 1,2m.	
Rainier Mesa, Nevada, cavities I and II (1965)  $\sigma_v = 6,9$ MPa $\sigma_h = 3,45$ MPa  (hemisphere on end, crown is dome-shaped) (Cording, 1971)	B = 24,4 m H = 42,6 m L = 36,6 m D = 396 m	Tensioned bolts, back 2,5m anchored in grout, rest ungrouted. <b>Crown:</b> 2,86 cm Ø, 1m x 1m spacing, 9,8 m long <b>Walls:</b> 2,86 cm Ø, 1,8m x 1,8m spacing, 7,3 m long <b>After stabilization, Cavity II Wall:</b> 2,86 cm Ø, 1m x 1m spacing, 14,6 m long	Gunite added to prevent drying and cracking in crown, after excavation was completed.  Cavity I wall stable under design bolting, Cavity II has joints and bedding planes intersecting wall which formed an unstable wedge.

(1) B = Width, H = Height, L = Length, and D = Depth.

Table 3.3-1. Support systems used in some large underground caverns.

Site	Cavern Dimensions and Depth	Support used	Comments
Boundary Dam power plant, Washington (1967)  (Cording, 1971)	B = 23,2 m H = 53,3 m L = 145 m D = 152,4 m	<b>Crown:</b> 2,5 cm Ø, 1,8m x 1,8m spacing, 4,6 m long (*) <b>Haunches:</b> alternate 4,6m and 6m bolts, 1,5m x 1,5m spacing <b>Walls:</b> bolted only where required <b>Draft tube pillars:</b> 8 636k tendons per pillar (**)	(*) Additional bolts 9m long, installed where joints appeared to form wedges. Wire mesh used. Some gunite. Attention given to reinforcement of rock around reentrants.  (**) Placed to support jointed and slickensided rock in pillars.
Churchill Falls power plant (machine hall), Canada (1970) (Hoek, 1980)	B = 25 m H = 47 m L = 296 m D = 294 m	<b>Roof:</b> 4,6 to 7,6m long 28mm Ø expansion shell rock bolts on 1,5m centres with chain like mesh. <b>Wall:</b> similar but no mesh	$\sigma_h = 1,7 \sigma_v$
Hongrin power station, Switzerland (1970) (Hoek, 1980)	B = 30 m H = 27 m L = 137 m D = 50-150 m	Excavated by series of small galleries. Supported by 650 pre-stressed anchors 11 to 13m long and shotcrete installed soon after excavation.	
El Toro power plant, Chile (1973)  (Cording, 1971)	B = 24,4 m H = 38,4 m L = 102 m	<b>Crown:</b> 400k, 6m x 6m spacing, 15m to 16,8m long. Plus: 40k, 2,4m x 2,4m spacing, 4m long bolts <b>Walls:</b> 400k, 6m x 6m spacing, 15m long	
Waldeck II power station, Germany (1973) (Hoek, 1980)	B = 33,5 m H = 50 m L = 105 m D = 350 m	18-24cm thick shotcrete reinforced with wire mesh and 996 pre-stressed rock anchors up to 23m long and 3800 4 or 6m long rock bolts.	
Western Deep gold mine hoist chamber, South Africa (1974) (Hoek, 1980)	B = 16,6 m H = 12 m L = 32 m D = 2750 m	Steel ropes 32mm diameter, cemented grouted, 7m long at 1,5m centres with wire mesh and 7cm shotcrete	
President Steyn gold mine hoist chamber, South Africa (1975) (Hoek, 1980)	B = 16 m H = 13 m L = 27 m D = 2090 m	10m long pre-stressed tendons at 4m centres plus 3m long bolts at 2m centres with wire mesh reinforced shotcrete 5-7cm thick.	

Table 3.3-1. Support systems used in some large underground caverns. (Cont.)



Site	Cavern Dimensions and Depth (1)	Support used	Comments
Shintakase power station, Japan (1978) (Hoek, 1980)	B = 27 m H = 55 m L = 165 m D = 250 m	<b>Roof:</b> 5m long 25mm Ø and 2m long and 22mm Ø rock bolts. <b>Walls:</b> bolts and 15 and 20m long anchors tensioned to 1200kN. 16 to 24cm thick mesh reinforced shotcrete on roof and upper walls. Lower walls concreted.	$\sigma_v = 5,9 \text{ MPa}$ $\sigma_h = 2,0 \text{ MPa}$
La Grande power station, Canada (1979) (Hoek, 1980)	B = 27 m H = 47 m L = 483 m D = 100 m	<b>Roof:</b> 6,1m grouted rock bolts tensioned to 200 kN <b>Wall:</b> bolting, spacing =1,5 to 2,1 m squared grid, with shotcrete applied locally.	
Imaichi power station, Japan (1982) (Hibino, 1995) (Hoek, 1989)	B = 33,5 m H = 51 m L = 160 m D = 400 m	<b>Roof and walls:</b> 15m long cable bolts	$\sigma_v = 9,1 \text{ MPa}$ $\sigma_h = 7,6 \text{ MPa}$
Hervanta underground ice rink, Finland (1982) (Leith, 2001)	B = 32 m H = 9 m L = 133 m	Grouted rock dowels at 1,5 c/c	
Surge tank, Rio Grande No. 1 hydroelectric project, Cordoba, Argentina (1986) (Moretto, 1993)	B = 38 m H = 62 m D = 106 m	<b>Vault:</b> anchored bolts and unreinforced gunite. <b>Wall:</b> Unlined	Hemispherical vault. Cavern is connected to surface by a 3m diameter vertical shaft, 106m long excavated from the surface by blasting.
Powerhouse cavern, Rio Grande No. 1 hydroelectric project, Cordoba, Argentina (1986) (Moretto, 1993)	B = 25 m H = 50 m L = 105 m D = 160 m	<b>Vault:</b> No systematic bolting needed, 25mm Ø fully cemented grouted anchor bolts, 3-10 m long, prestressed at 14 kN on unstable blocks only.	Larger displacements measured (doubled in most cases) than previously estimated. This is believed to be because the disturbed rock condition and weakened faults were not taken into account during calculations.
Cirata power station, Indonesia (1988) (Hoek, 1989)	B = 35 m H = 49.4 m L = 253 m D = 109 m	<b>Roof and walls:</b> 18m long cable bolts	

Table 3.3-1. Support systems used in some large underground caverns. (Cont.)

Site	Cavern Dimensions and Depth	Support used	Comments
Gjøvik Olympic Hall, Norway (1993)  (Aarvold, 1994) (Barton, 1991)	B = 61 m, H = 25 m, L = 91 m D = 25-40 m,  Beq= 25 m Heq = 61 m Deq= 155 m	<b>Roof:</b> Cablebolts: Twin strand, L=12m, pattern 5mx5m Steelbolts: L=6m, pattern 2,5mx2,5m Shotcrete: Steel fibre reinforced, t=10cm.  <b>Walls:</b> Steelbolts: L=5m and 10m Shotcrete: Steel fiber reinforced, t=10cm.	Given the stress conditions present on the site ( $\sigma_v = 1 \text{ MPa}$ , $\sigma_h = 4 \text{ MPa}$ ) the most critical dimension is H (instead of B); therefore this structure should be viewed as to having the equivalent dimensions and depth shown.
Sanchung powerhouse, Korea (1993-1999) (Han-Uk, 2003)	B = 25 m H = 49.5 m L = 116 m D = 250 m	Rockbolt: length: 10m and 15m, spacing: 2m Shotcrete: 10 cm thick	$\sigma_v = 5.5 - 7.1 \text{ MPa}$ $\sigma_h = 8.9 - 6.9 \text{ MPa}$
Super-KAMIOKANDE, Japan (1994)  $\sigma_1 = 28,8 \text{ MPa}$ $\sigma_2 = 18,9 \text{ MPa}$ $\sigma_3 = 6,1 \text{ MPa}$	B = 40 m H = 41.4 m D = 1000 m	Dome: Wet shotcrete: 16 cm thick mixed with 80 kgm3 steel fibre Cemented grouted cablebolts: Ø 15,2mm, L=8m, 7 strand PC steel, 2 wires/hole, spaced 4m2. Cemented grouted rockbolts: Ø22mm, L=2m, steel rebar, spaced 1m2.  Cylindrical part: Wet shotcrete: 16 cm thick mixed with 80 kgm3 steel fibre Cemented grouted cablebolts: Ø 15,2mm, L=8m, 7 strand PC steel, 2 wires/hole, spaced 6m2 Cemented grouted rockbolts: (*) Ø 22mm, L=2,35 m, steel rebar, spaced 1m2.	(*) Rockbolts were installed to stick 19 cm out of the shotcreted wall to be connected to tie-rods welded on detector tank. The resulting space was filled with lining concrete.  (**) Additional support in the SE and NW parts of the dome: Block 1: 33 15m cablebolts, every 16 m2, 65 5m cablebolts, every 20 m2 Block 2: 15 15m cablebolts, every 12 m2, 50 5m cablebolts, every 12 m2
Tehri powerhouse, India (1996-2003)  (Rechitski, 2007)	B = 22 m H = 47 m L = 197 m D = 300-350 m	Crown: Rockbolts 2,5 cm Ø, 2m x 2m spacing, 6m to 10m long, prestressed 9-12t, shotcrete  Walls (*): Rockbolts 3,2 cm Ø, 1,5m x 2m spacing, 6m to 15m long, prestressed 9-12t, shotcrete	(*) Additional 62 prestressed cable anchors were placed in upstream wall: 7 steel tendons, 15,2mm Ø, 18m long, 80t

Table 3.3-1. Support systems used in some large underground caverns. (Cont.)

Site	Cavern Dimensions and Depth	Support used	Comments
Takayama festival art museum, Japan (1998) (Hemispherical) (Chikahisa, 1999)	B = 40,5 m H = 20 m D = 30 m	Rock anchors: 7 steel wire strands, L=8.5 to 11.5m, inner lining, and shotcrete	$\sigma_v = \text{MPa}$ $\sigma_h = \text{MPa}$
Joma copper mine, Norway (closed in 1998) (Leith, 2001)	B = 70 m H = 20 m	Unreinforced flat roof	
Kazunogawa power plant, Japan (1999) (Kudoh, 1999) (Koyama, 1999)	B = 34 m H = 54 m L = 210 m D = 500 m	<b>Crown:</b> anchor length: 15 – 20m, anchor pre-stress: 0.21 – 0.31MPa, Shotcrete: 32 – 40cm <b>Walls:</b> anchor length: 15 – 20m, anchor pre-stress: 0.18 – 0.31MPa, Shotcrete: 24cm	$\sigma_v = 12,3 \text{ MPa}$ $\sigma_h = 9 \text{ MPa}$
Chungsong powerhouse, Korea (2000-2007?) (Han-Uk, 2003)	B = 27.5 m H = 55.7 m L = 114.6 m D = 180 m	Rockbolt: length: 12m and 15m, spacing: 2m Shotcrete: 10 cm thick	$\sigma_v = 4.9 - 5.1 \text{ MPa}$ $\sigma_h = 6.2 - 6.5 \text{ MPa}$
Masjed-E-Soleiman powerhouse cavern, Iran (2002) (Shahabi, 2003) (Ahmadi, 2007)	B = 30 m H = 50 m L = 112 m D = 250-320 m	Roof: 20cm double reinforced shotcrete layer, Rockbolts: 6m long, every 4m2, 100KN. Wedge anchors: 10m long, every 4m2, 200KN (pre-stressed to 100KN).  Additional support (*): 4 rows of wedge anchors, grid 2x2, 200KN. 4 row of 264 KN monobars in grid 2x2 pre-stressed to 500KN in mudstone. 2 additional rows of 264KN monobars in grid 2x2 in 2 meters of wall.	Monitoring consisted of 42 extensometers and 65 load cells and 18 convergence sections  (*): After back analysis with monitoring results additional support was placed on the walls.
Siah Bisheh powerhouse cavern, Iran (200?) (Sharifzadeh, 2007)	B = 25 m H = 46,5 m L = 132 m D = 250 m	Shotcrete wire mesh: 20cm in side walls and 25 cm in roof. Temporary support: 3, 5, and 8 m long grouted rockbolts, 140 KN Permanent support: 15, 20, and 22m double protected tendons, pre-tensioned up to 850 KN  Drainage holes with 4m long pipes, Ø 48 to 56mm, spaced 4x4m in roof and walls.	Six grouted rod extensometers in the roof and sidewalls, convergency points, piezometers and cable anchor load cells.

Table 3.3-1. Support systems used in some large underground caverns. (Cont.)

### 3.4 REFERENCES

Aarvold, V (1994). "Gjøvik Olympic Mountain Hall, Norway", Proceedings of Tunneling'94, 7th International Symposium, London.

Ahmadi, M. Goshtasbi, K. Ashjari, R. (2007). "Numerical Analyses of Masjed-E-Soleiman Powerhouse Cavern, Iran". Proceeding of the 11th Congress of the International Society for Rock Mechanics, Lisbon, Portugal.

Barton N. et al. (1991). "Norwegian Olympic ice hockey cavern of 60 m span". Vol.2. Proceeding of the 7th International Congress on Rock Mechanics. Aachen, Germany.

Chikahisa, H. et al. (1999). "Estimation of measurement results concerning deformation behavior of large-scale rock cavern used as underground museum in excavation". Vol. 1. Proceedings of the 9th International Congress on Rock Mechanics, Paris, France.

Cording, E. et al (1971). "Rock Engineering for Underground Caverns". Underground Rock Chambers, ASCE National Meeting on Water Resources Engineering, Phoenix, Arizona, January 13-14.

Han-Uk, L. Chee-Hwan, K. (2003). "Comparative study on the stability analysis methods for underground pumped powerhouse caverns in Korea". Vol. 2. Proceedings of the 10th Congress of International Society of Rock Mechanics, South Africa.

Hibino, S. Motojima, M. (1995). "Characteristic behavior of rock mass during excavation of large scale caverns". Vol. 2. Proceeding of the 8th International Congress on Rock Mechanics. Tokyo, Japan.

Hoek, E. Brown, E. T. (1980). "Underground Excavations in Rock". London: Institution of Mining and Metallurgy, 527 pages.

Koyama, T. et al (1999). "Observational construction management for large underground cavern excavation". Vol. 1. Proceedings of the 9th Congress of International Society of Rock Mechanics, Paris, France.

Kudoh, K. et al. (1999). "Support design of a large underground cavern considering strain-softening rock". Vol. 1. Proceedings of the 9th International Congress on Rock Mechanics, Paris, France.

Leith, W. (2001). "Geologic and engineering constraints on the feasibility of clandestine nuclear testing by decoupling in large underground cavities". Department of the Interior, U.S. Geological Survey, Virginia, USA (<http://geology.er.usgs.gov/eespteam/pdf/USGSOFR0128.pdf>)

Moretto, O. Sarra, R. Del Rio, J (1993). "A case history in Argentina – Rock mechanics for the underground works in the pumping storage development of Rio Grande No.1". Ch. 8, Vol. 5 of Comprehensive Rock Engineering. Pergamon Press.

Nakagawa, T. et al (1997). "Qualified underground technologies for excavation of the Super-KAMIOKANDE cavern". Proceedings of the 1st Asian rock mechanics symposium, Seoul, Korea: 125-130

Shahabi, M. Kashfi, M. (2003). "Method statement for excavation of powerhouse cavern considering mudstone layers in Masjed Soleiman dam". Vol. 2. Proceedings of the 10th Congress of International Society of Rock Mechanics, South Africa.

Sharifzadeh, M. et al. (2007). "Long term stability assessment of Siah Bisheh pumped storage powerhouse cavern under saturated condition". Proceeding of the 11th Congress of the International Society for Rock Mechanics, Lisbon, Portugal.

Rechitski, V.I. et al (2007). "Results of Monitoring for Underground Excavations behavior during Construction of Tehri Dam Project, India". Proceeding of the 11th Congress of the International Society for Rock Mechanics, Lisbon, Portugal.

US Army Corp of Engineers; Engineer Manual 1110-1-2907 Rock Reinforcement, 1980.

Yamatomi, J. et al. (1999). "Waste-less mining – The Super-KAMIOKANDE and subsurface space utilization at Kamioka Mine, Japan". Vol. 3. Proceedings of the 9th International Congress on Rock Mechanics, Paris, France.

## 4. GEOLOGICAL FEATURES OF THE CANFRANC SITE

### 4.1 INTRODUCTION

The aim of this paragraph is to make an approach to the geology with a view to preparing the Feasibility Study for the LAGUNA Experiment in the Underground Laboratory at Canfranc.

The following bibliography was referred to when preparing this part of the document:

- National Geology Map (MAGNA) Page nº 144 - Ansó. E. 1:50.000. ITGE, 1994.
- National Geology Map (MAGNA) Page nº 145 - Sallent. E. 1:50.000. ITGE, 1989.
- The Geological, Hydrogeological and Geotechnical Study of the Somport Tunnel (Huesca). Carried out in 1990 by the Joint Venture (U.T.E) GHESA-INARSA-COTAS INTERNACIONAL (INGICO), for the General Directorate of Roads, dependent upon the Spanish Ministry of Public Works and Urban Planning.

Other publications referred to were as follows:

- Geology of Spain / Vera, J. A. Madrid: Spanish Geology Society; Spanish Institute of Geology and Mining, 2004.
- Tectonic Map of the Iberian Peninsula and the Balearic Isles, to a scale of 1:1.000.000 published by the Spanish Institute of Geology and Mining, 1980.

From a geographical viewpoint, the area where it is planned to construct the caverns (MDC's) lies in the Central Pyrenees, close to the frontier between the Prov-

ince of Huesca and France, to be specific, under Monte El Tobazo, which is located in the vicinity of the Candanchú Skiing Resort. The mountainous terrain that characterises the zone is crossed by valleys that run south, the largest one in the area being the valley of the River Aragón.

### 4.2 GEOLOGICAL FRAMEWORK

From a geological perspective, the zone studied for the location of the LAGUNA Experiment, lies on the southern limb of the Pyrenean Axial Zone, very close to where it comes into contact with the South Pyrenean Zone. The point of contact between the two zones is marked by the Larra thrust fault, lying to the south of the zone. A diagram is shown below of the Pyrenees Mountain Range (Cordillera).

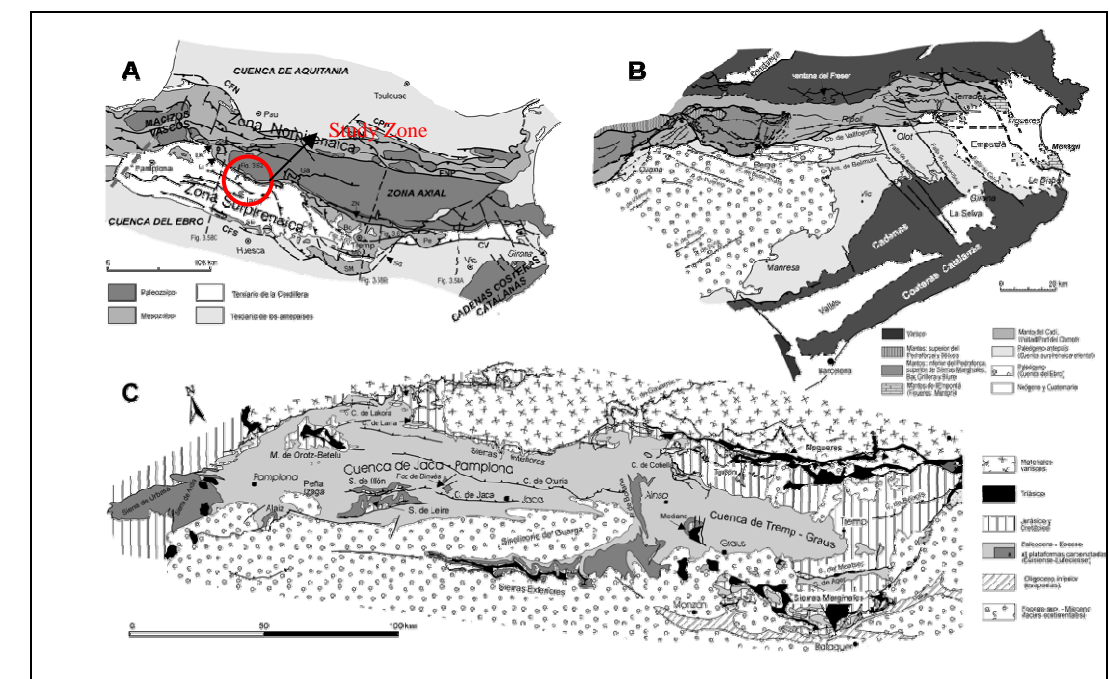


Figure 4.2-1. General geological location

The current morphology of the Pyrenees Mountain Range is a result of the major process of deformation associated with the Alpine Orogeny, which took place dur-



ing the Tertiary, and whose main phase, the Pyrenean Phase took place in the Eocene-Oligocene transition, around 35 million years ago.

The materials involved in this deformation, and thus earlier or synchronous ones, can be split into two distinct and major groups. On the one hand, a base composed of Palaeozoic materials, which contains representation from all the levels from the Cambrian to the Carboniferous, and whose deformation and main structure are inherited from older Orogenic phases, Variscan Orogeny. On the other hand, a discordant sedimentary cover overlies these materials, which contains representation from the Permian to the Eocene-Oligocene.

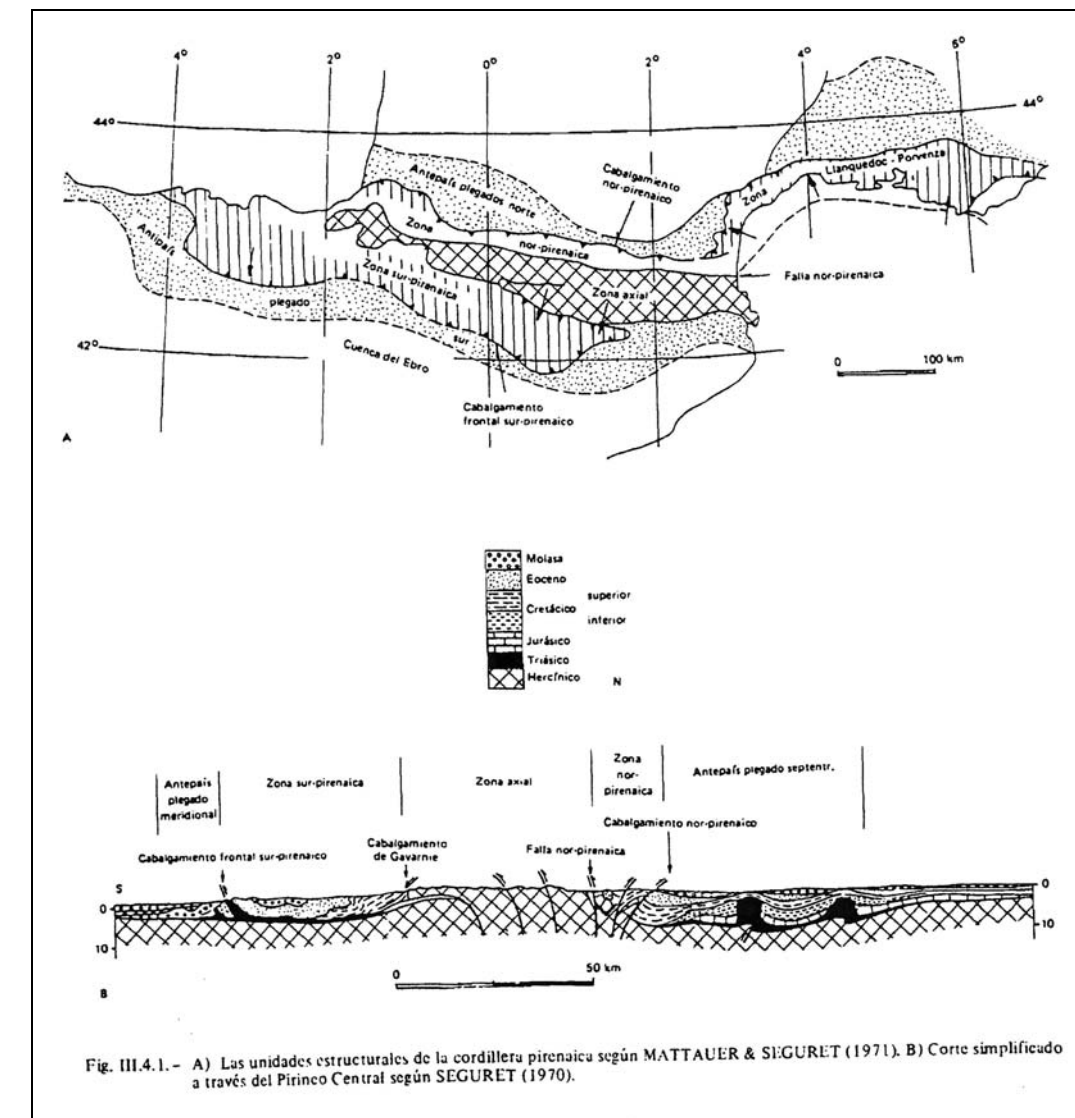
There are a series of differences between the Pyrenees and other mountain ranges that were formed during the Alpine Orogeny. These differences the rectilinear arrangement, the only slight development of the metamorphic processes related to Alpine deformation phases, and the low magmatic activity associated with the Alpine Orogenic phases.

The most recent structural arrangements account for the formation of the Pyrenean Mountain Range (Cordillera) as a result of their most internal zones (Axial Zones) being subjected to a raising process, with the uplifting of the ancient Palaeozoic base. This uplifting process gave rise to a “*positive flower*” arrangement, characteristic of ranges, brought about by the collision between continental plates. The cover materials would have built up not only on the French side (north) but also on the Spanish side (south), albeit as a result of two different tectonic and structural processes:

- The Spanish zone is an area where the Tertiary and Mesozoic cover would have become displaced along a decollement and slipped surface as a consequence of the raising of the Axial Zone, generating major displacements towards the south caused by different imbricated splays and their associated structures. Certain fragments of the Axial Zone would have been involved in this gravitational movement, because they would have been displaced over the

Mesozoic and Tertiary cover; one such example of these thrust faults is the Manto de Gavarnie Cover); the Study Zone lies within this cover.

The next figure shows a structural diagram of the Pyrenees, in which the major divisions on the chain can be seen:



less displacement than in the Axial Zone. Only occasionally is their evidence of gravitational slides similar to the ones on the southern slopes. In contrast to the southern zone, basal outcrops are frequent, although the structure is complicated by the presence of the North Pyrenean fault, which brings the Axial Zone into contact with the North Pyrenean Zone (French slopes), and different authors are of the opinion that it is a first range fault responsible for the relative movements of the Iberian Peninsula with respect to France.

The next figure shows a structural diagram of the Pyrenean Axial Zone:

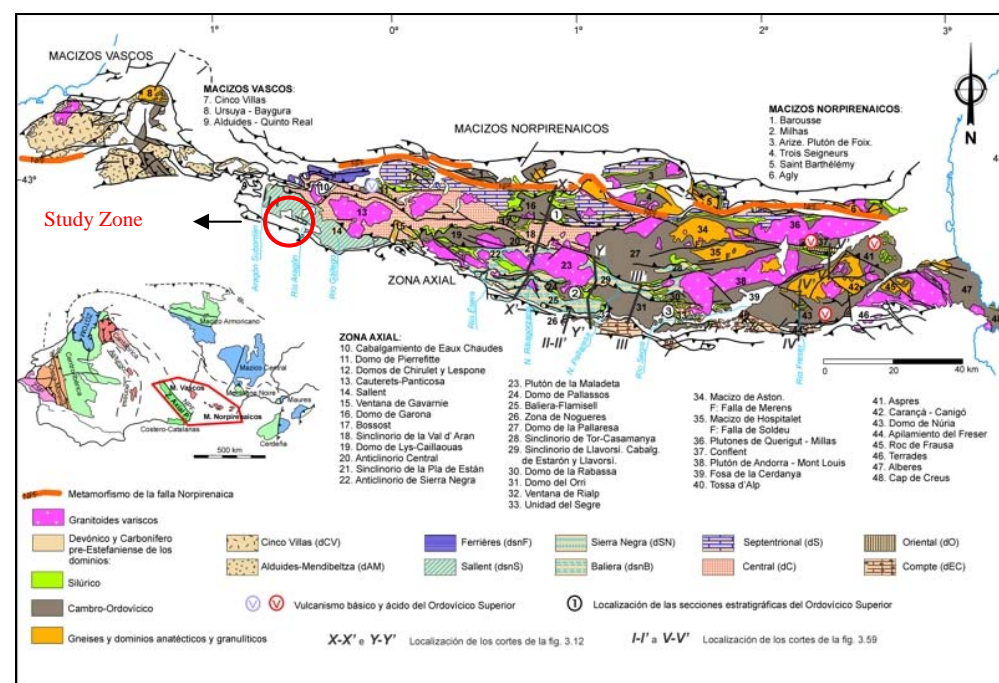


Figure 4.2-3. Structural diagram of the Pyrenees

However, for the purposes of this study, it is clear that the materials on which the excavation of possible MDC's is to take place are entirely Palaeozoic materials, originally deformed during the Variscan Orogeny and subsequently transformed by the Alpine Orogeny, which is the cause of the current landforms.

The appendix to this document contains geological plans of the study zone at different scales.

## 4.3 STRATIGRAPHY

### 4.3.1 Introduction

The Palaeozoic pattern intrinsic to the Axial Zone, where it is planned to locate the LAGUNA experiment in the Canfranc zone, contains materials deposited during the Devonian. During that period, the materials are calcareous and dolomitic in many sectors, although detritic facies are also evident in the Study Zone, not only at the base but also at the top. The carboniferous materials, deposited in a concordant way over the Devonian, start with variable thicknesses of limestones and continue with a thick series of flysch and greywackes that run as far as the main phases of the Variscan deformation. The discordant and post-orogenic materials first started to build up during the "Estefaniense" or Upper Pennsylvanian, with highly discontinuous lacustrine facies, and carried on into the Permian and Permian-triassic with very variable facies ranging from argillites and slates to thick masses of conglomerates with sandstones.

The excavations for the MDC's affect the formations that lie deep under *Monte El Tobazo*. This mountain is currently crossed by two tunnels, one of which is a rail tunnel and the other a road tunnel, which connect Spain and France. The information that was compiled at the project stage and during construction, especially of the road tunnel, has served to obtain extensive knowledge about the materials that are crossed, including the Devonian materials in *Monte El Tobazo*, where the MDC's are planned to be excavated.

### 4.3.2 Lithologies

This section contains an analysis of the lithologies affected by the excavations that are needed to construct the future MDC's. In spite of the fact that several lithologies have been mapped on the surface, a description is given only of the ones that could be affected by the excavations. The information yielded by the Somport Tunnel together with what is known about the geology in the zone, has made it

possible to establish that the lithologies that are affected belong to the Devonian, to be specific, they belong to the Atxerito Series (D-1) and Coralline limestones (D-2). A description of these two formations is given below.

#### **4.3.2.1 Mudstones, slates and limestone of the Lower Devonian. Atxerito Series (D-1)**

This is a formation in which there are very few outcrops and they are far from the study zone. That is why the description of them that has been given is based upon bibliographical data and the research work and surveys of the face that were carried out on the Somport Tunnel

MAGNA Page nº 144 says the following about these materials: *these rocks would appear to be made up of alternating layers of claystones and centimetric or millimetric layers of sandstones. Decimetric layers of limestones are occasionally to be found.*

From a lithological perspective, it is made up of alternating layers ranging from centimetric to metric of mudstones and claystones that are black and occasionally green, schists with millimetric or centimetric levels of grey sandstones whose grain size ranges from very fine to medium. Sandy and calcareous levels appear locally, with 30 to 40% quartz content, light grey to dark grey, somewhat re-crystallised, containing a large amount of macrofauna.

It is difficult to estimate the thickness of this formation, but it is assumed that it ranges from 150 to 200 meters.

According to the bibliography referred to, it is a formation dating back to the Lower to Middle Devonian.

#### **4.3.2.2 Coralline limestone of the Middle Devonian (D-2)**

It is a formation that appears at the top of the aforementioned, outcrops abounding on the surface, in view of the fact that it forms extensive walls of Monte Tobazo.

From a lithological perspective it is composed of recifal limestones, which emerge in layers (of metric dimensions) that contain large amounts of coral. These limestones are normally packstone or wackestone. These thick layers of limestones alternate with limestones of the mudstone type, in between which fine interbedded shales are frequently found. In the Study Zone they take the form of limestones with a light grey patina, occasionally dark grey, microcrystalline, sometimes highly recrystallised and partially (dolomitized). They contain metric interlayers of metric siliceous and calc-schists and millimetric coating, possibly of algar origin. Thick packets of intraformational breccias are fairly common.

All the levels that are included in this formation usually have abundant calcite seams and occasional networks of stilolite joint patterns.

These facies contain variable and very abundant fauna, especially polypes. There are also coralline bioherms of up to 100 meters wide and 20 meters thick.

The "Geological, Hydrogeological and Geotechnical Study of the Somport Tunnel" describes these materials, on the basis of microscope observations of the fine coating, as: *"... rocks whose textural composition is essentially micrite with a content of pseudo-sparite that varies on the basis of the extent to which it is recrystallised, with percentages of less than 10% dolomite, micas and quartz somewhat sandy, opaque, and as accessory minerals, pyrites, zircon and apatite".*

The thickness of this formation ranges from 200 to 400 meters; it is generally well stratified at the base and massive towards the top, it being very difficult to measure the direction and the dip of the bedding planes, because this occurs at the slope that comes into contact with the Rioseta del Monte Tobazo cirque.



This formation has been dated as being Middle Devonian.

#### 4.4 TECTONICS

The “Pre-Estafaniense” materials, that is to say the Devonian and Carboniferous ones in the Study Zone and its vicinity were affected by two generations of well-characterised Hercynian folding. Subsequently, during the Alpine orogeny, these materials underwent a series of deformations that, without penetrating to a great extent, did modify the final layout of the crests of the Hercynian folding. In this sense, and as has already been pointed out, the study area lies in the allocthonous block of Gavarnie, which has come to affect the Pre-Hercynian materials in the Axial Zone, bringing about the tilting of all the earlier structures.

An analysis is given below of the structures generated during each one of the orogenies that have affected the materials where it is planned to excavate the MDC's:

##### 4.4.1 Variscan Orogeny

During this orogeny, different authors make a distinction between two phases of deformation that generate different structures, which can be distinguished *in situ*.

##### First phase:

It is a formation that generates tight isocline folds, with South vergence, whose axes and axial planes run from East to West. In spite of the fact that no major structures have been detected in the Study Zone that are associated with this phase of deformation, such structures have been detected nearby. So, the rock mass structure between the southern entrance to the Somport Tunnel and the fault running from East to West that runs to the south of the Coll de Ladrones Fort, is composed of a series of anticlines and synclines, whose wave-length is around 500 meters, and whose origins are attributed to this deformation phase.

##### Second phase:

Folds were generated at this phase that range from very tight to simple flexures, whose angle between limbs is greater than 90°. These folds run from North to South, showing evidence of immersion towards the North, where as their axial planes run from East to West, which is given by the position of the schistosity that is associated with these structures..

The vergence of these folds, on a regional scale is conditioned by the presence of the folds from the first deformation phase, and they generally run westwards.

The most typical microstructure at this deformation phase is the (axial plane schistosity), which constitutes the regional scale foliation, which in slaty and lutite materials can be regarded as a slaty cleavage, whereas in sandstone and calcareous materials, it can be regarded as a “rough slaty cleavage”, but it may not necessarily appear.

The main macrostructure of this generation of folding corresponds to the Monte Tobazo anticline; this fold runs N 150° and 25° immersion to the North. A short limb can be observed, upright or somewhat inverted, and a normal limb lying almost horizontal or dipping gently towards the North East. Regional foliation is associated with this structure, which makes it possible to establish the direction of crest of the fold.

This macrostructure, defined earlier in the geology mapping, was confirmed, with some reservations, during the excavation of the Somport Tunnel, which confirmed the presence of the Atxerito Formation occupying the nucleus of decametric folds that are associated with the main structure.

The superimposing of the second phase over the first one, also affects the immersion of the crests of the first phase folds.



With respect to the fracturing caused during the Variscan Orogeny, two main families of faults have been detected.

**Family 1: East to West (N 70°):**

This is a family of faults that compartmentalise different structural domains in the vicinity of the study zone. The fault that lies closest to the study zone lies to the North of it, under the Candanchú Skiing Resort. It is a fault with considerable slip, because it brings Middle Devonian materials in the South Block (Monte Tobazo) into contact with Culm materials in the North Block. It is a fault that strikes N 90° and dips 40° North.

**Family 2: North to South (N 140° E):**

The faults detected in the Monte Tobazo zone belong to this second family, Monte Tobazo being the zone under which the location of the MDC's is planned. The largest of these faults is the one detected at Pista Grande, which divides the anticline that is formed by that mountain, sinking its normal limb. This fault, which is easily recognisable on the surface, appears to dip 80 to 85° towards the East.

**4.4.2 Alpine Orogeny**

During this orogeny, the deformations that the Palaeozoic materials that form the Axial Zone underwent gave rise to readjustments, generally in the fragile regime, of the original Variscan structure. A description is given below of the most significant Alpine structures that affect these materials:

- Structural inversion faults. These are fractures that bring Permian materials into contact with other Pre-Hercynian Palaeozoics, which are generally arranged sub-horizontally.
- These were originally sin-sedimentary faults, in such a way that the Permian was deposited on-lapping the faults. These structures subsequently

acted as thrust faults during the Alpine deformation, bringing about their characteristic inversion. The thrust fault mapped to the North of Monte Tobazo at Candanchú belongs to this type of fault; it brings Permian materials into contact with the Pre-Estafaniense units.

- Rotation of Variscan structures. This tilting could be due to the superimposing of Alpine thrust faults that took place in this part of the Axial Zone, which gave rise to an antiformal pile-up. This rotation would account for the current anomalous arrangement of the crests of the crests of the Variscan folds.
- Finally, there are a series of faults running from North to South, which affect all the materials as a whole.

**4.5 METAMORPHISM OF THE MATERIALS IN THE AXIAL ZONE**

The most intense metamorphism associated with the materials in the Axial Zone occurred in the Variscan area of the Pyrenees. This metamorphism affects areas to different extents. Thus, there are not only areas with high-grade metamorphic rocks, with frequent magmatic processes, but also others formed by low-grade metamorphic rocks, or even non-metamorphic rocks. The limit between the two tectonic "levels" does not have the same stratigraphic position, leading off from the easternmost zones (Mediterranean) towards the Valle de Arán sector, before descending to the westernmost zones of the axial zone, which is where the study section lies.

The outcrops of granitoids are extensive in some zones and are of two distinct types of granites: granites with muscovite, which are invariably closely related to the metamorphic infrastructure and which lie not very far above it, and granodiorites with biotite, which in many cases penetrate into the metamorphic superstructure, up to the highest levels, even the Carboniferous. In both cases it is assumed that they were produced via migmatisation, leading off from the Lower Cambrian rocks, in the case of the former, or from the older levels of the Palaeozoic series, in

the latter case. The granodiorites would have been more mobile, and they would have taken longer to consolidate, although as it is only logical to assume, the migmatization in both cases would have been synchronic and would have taken place at the same time as the periods of Variscan deformation.

Within these metamorphism zones, the materials studied belong to the highest levels within the Pre-Hycernian stratigraphy, their degree of metamorphism being either low or without metamorphism; they are affected by what could be referred to as deep diagenesis, although this does not prevent it from being frequently the case that the original structures are faded by recrystallisation or from them having been subjected to intense processes of deformation.

#### 4.6 GEOMORPHOLOGY

The geomorphology in the study area is severely marked by the rugged structure and the complex geological history of the region. The current orography is a result of the interactions between the geomorphologic processes that have taken place from the beginning of the uplifting to the present time.

It is clear that the lithological and structural factors are largely responsible for the current forms, in a young mountain range like the Pyrenees. However, the surface topography is not always consistent with this lithological and structural control, and in many cases certain landforms are rather evolutionary or a consequence of a phenomenon that has since disappeared without trace, and they linger on as residual landforms, until such time as other more living morphological processes resulting from current causes can absorb and remove them.

This is a frequent occurrence in geomorphologic processes, which accounts for the differences in landforms, which starting from a series of initial determinants (lithology and structure), gradually become eroded, evolving and becoming modified as they cross different structural “levels”. During this evolutionary process, the morphology of the ground will invariably endeavour to adapt itself to the extent that it

can, to internal factors (materials and initial structure) and external factors (climate, altitude, gradient, etc.).

On a regional level, it could be stated that the current geomorphology is basically inherited and evolutionary in the sense that, while on a local level importance is attached to the lithological and structural factors, the logical and continuous interferences between the two processes invariably play their part.

With respect to the study zone under which it is planned to excavate the future MDC's, this can be regarded as a zone in which landforms are basically affected by lithological and structural factors, which determine the vertical calcareous cliffs that characterise Monte Tobazo.

#### 4.7 HYDROGEOLOGY

The carbonated Devonian materials, which include the Coralline Limestones, constitute a Devonian aquifer on a regional level. The hydrogeological performance of this aquifer is complex. The information that can be deduced from the existing reports, suggests that the aquifer is extensively divided up by a normal fracture system, (running from NNE to SSW).

The piezometric elevations for the slight inflows located in these materials prove to be disjointed, and major degrees of confinement are observed on occasions, which leads to genuine spring wells occurring.

In the study zone, this aquifer is drained by springs in Candanchú, at around elevation 1610. These springs yield flow rates ranging from 6 to 10 l/sec, according to collected data.

The permeability of this rock mass is determined by several factors, which are described below:

### **Lithology:**

There are lithologies within the materials that make up the rock mass underlying Monte Tobazo, which can be regarded as virtually impervious (detritic formations with a high percentage of lutites and/or slates from the Atxerito Formation), and lithologies that can be regarded as permeable and thus potentially constituting part of an aquifer (coralline limestones).

### **Karstic Processes:**

The permeability of the calcareous formations (coralline limestones), is basically due to karstic processes. The development of these processes is considerable on the surface, which structural limestone pavements and sinkhole areas. These materials have been crossed by the Somport Tunnel, and it has been observed that at depth there is no major evidence of karstic processes, which accounts for the fact that there was no significant water inlet during tunnel excavation. However, the nature of karstic processes inside a rock mass (irregularity and randomness) means that certain precautions have to be taken where this phenomenon is concerned.

### **Fracturing:**

The zones where there is a great amount of fracturing such as mylonites associated with fault and other highly tectonized zones have an effect like the two aforementioned factors, and could cause confined aquifers to be connected together or the presence of major channels of water underground, where their lithological composition would not make these types of problems likely, because the ground is practically impervious. Furthermore, in those cases where the fracturing is sufficiently developed (with a major band of mylonite) and it crops out on the surface, the fractures can be subjected to natural recharging and act as genuine free aquifers.

A combination of these three factors could serve to give an acceptable image of the hydrogeological characteristics of the rock mass under Monte Tobazo. Therefore, it is possible to summarise it as being a rock mass that is considerably permeable at the surface because of the karstic processes and the decompression of the rock mass itself, which causes the fractures to open wider, so during spells of heavy rain and when ice and snow thaw, the piezometric level could be fairly close to the surface. However as a result of its orography, the drainage processes can be assumed to take place quickly.

## 5. SEISMOLOGICAL PATTERNS OF THE CANFRANC AREA

### 5.1 SEISMOTECTONIC STUDY

#### 5.1.1 Introduction

##### 5.1.1.1 Background

The following information was used to carry out this seismotectonic study:

- Earthquake Proof Spanish Construction Standard (NCSR-02, *Norma de Construcción Sismorresistente*).
- List of earthquakes within a radius of 200 km from a centre point located at the dam (provided by the National Geographical Institute, IGN).
- Isoseismic contour maps for the 20th Century and for the above list (provided by IGN).
- Lists of earthquakes in the Hautes Pyrenees Department from the Sisfrance Seismic Database.
- Secanell, R., Irrizarry, J., Susagna, T., Martín, C., Goula, X., Combes, P. and Fleta, J. *Unified Evaluation of the Seismic Hazard in the Vicinity of the frontier between France and Spain*. 2nd National Seismic Engineering Conference 439-447. Malaga (2003).
- Secanell, R., Bertil, B., Martin, C., Goula, X., Susagna, T., Tapia, M., Dominique, P., Carbon, D. & Fleta, J. *Probabilistic Seismic Hazard Assessment of the Pyrenean Region*. J. Seismol (2008) 12:323-341.

- Ambraseys, N. *The Prediction of Earthquake Peak Ground Acceleration in Europe*. Earthquake Engineering and Structural Dynamics, Vol. 24, 467-490 (1995).

##### 5.1.1.2 General geological information

As summary of previous paragraphs, from a geological perspective, the zone that has been proposed for the location of the LAGUNA Experiment, lies on the southern slope of the Pyrenean Axial Zone, very close to where it comes into contact with the South Pyrenean Zone. The limit between the two zones is the Larra overthrust fault, lying to the south of the zone.

The materials involved in this formation, and thus earlier or synchronic to it, can be classified into two major groups: a base that is composed of Palaeozoic materials, which contains evidence of all the divisions from the Cambrian until the Carboniferous, and whose deformation and main structure are inherited from the most ancient orogenic phases (Hercynian Orogeny); a sedimentary cover overlies these materials in an uncomfortable way, ranging from the Permian to the Eocene-Oligocene.

The “Pre-Estefaniense” materials as a whole (Devonian and Carboniferous) lying in the zone and its immediate vicinity, were affected by two well-defined generations of Hercynian folding. Subsequently, during the Alpine Orogeny, these materials underwent a series of deformations, which without proving to be very penetrative, did nevertheless manage to modify the eventual arrangement of the axes of the Hercynian folding. In this sense, as has already been pointed out earlier, the study area has been located in the allochthonous unit or block of Gavarnie, which affects the pre-hercynian materials in the axial zone, bringing about a tilting of all the earlier structures. A more detailed description of the tectonics in the zone is contained in previous geological descriptions.



### 5.1.2 Pyrenean Seismotectonic Zoning

Seismogenetic zones are defined on the basis of the distribution of seismic epicentres and their association with areas whose tectonic characteristics are assumed to be homogeneous. This defining process is carried out by delimiting zones based on observations of the distribution of the seismic epicentres, especially those whose epicentral intensities are greater than VII, and their association with tectonic characteristics that are assumed to be homogeneous.

A series of seismotectonic zoning activities have been carried out by different authors that roughly coincide, because they are invariably determined by the main tectonic features. The differences lie in the way that the data have been interpreted in each one of the cases. By way of example, the figures shown below contain the results of each one of these works (García Fernández et al, 1989; Martín, 1983).

For example, in the work carried out by Martín (1983), possible seismogenetic sources are identified from the overall consideration of the main geotectonic units on the Iberian Peninsula, the spatial distribution of the seismicity and maps of the maximum intensities perceived and the general direction of the intensity isolines.

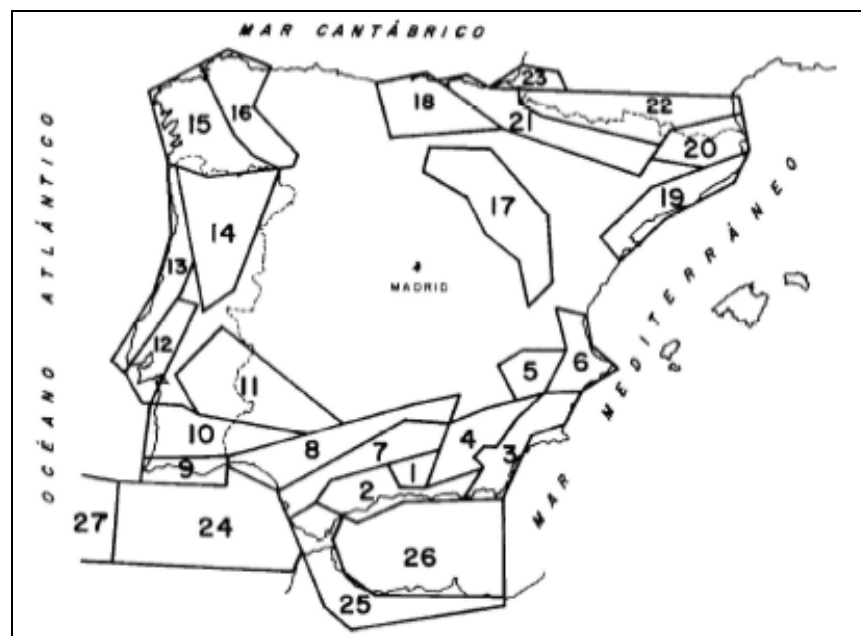


Figure 5.1-1. Seismogenetic zones on the Iberian Peninsula, according to Martín (1983).

The location and size of the seismogenetic zones that are defined in this group are closely linked to two aspects: the first of these is the need to obtain a cross-section sample that is sufficiently representative of earthquakes to enable us to estimate the seismic parameters of the source, and the second, is to find out the effects that the size and geometry might have on the seismic hazard results in specific areas. The diagrams of the seismogenetic zones used by the different authors thus vary from one author to another.

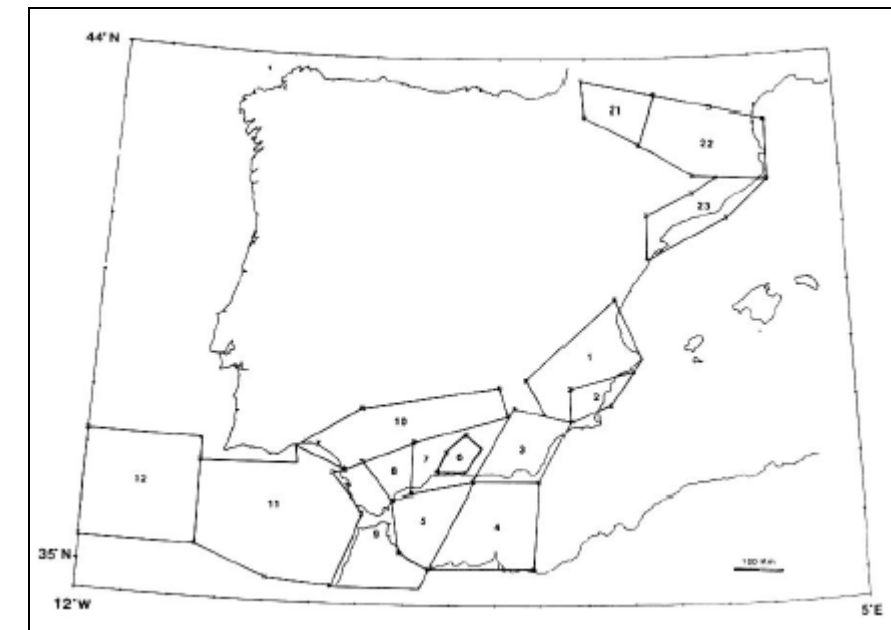


Figure 5.1-2. Seismogenetic zone used by García Fernandez (1989) and modified with respect to the one used by the working group on the NCSR-02 (IGN; 1991).

An update of the Pyrenean seismogenetic zones has recently been published; this was done with a view to standardising the data and the geometry that are used by French and Spanish research workers. The zoning concerned is published by Secanell et al (2003) and can be seen in the following figure.

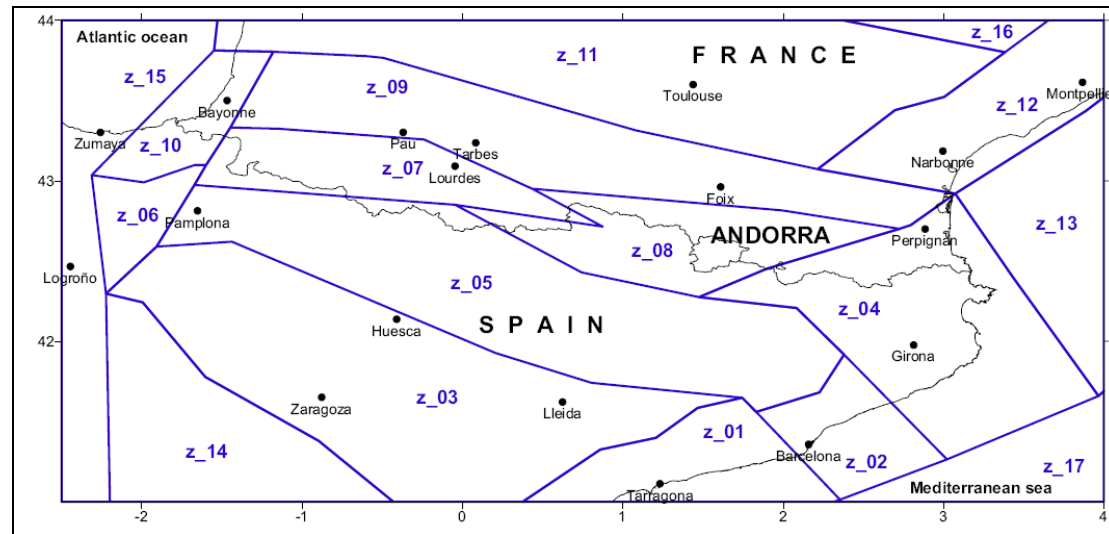


Figure 5.1-3. Seismotectonic zoning for the Pyrenean Region (Secanell et al, 2003).

Furthermore, this region has been redefined within the SESAME Project (Seismotectonics and Seismic Hazard Assessment of the Mediterranean Basin. IUGS-UNESCO IGCP-382), for similar reasons: to obtain a map of seismogenetic zones that is unified for the whole of Europe. The result of this work can be seen in the following figures 5.1-4 and 5.1-5, which contain the seismogenetic zoning that has been carried out, together with the enlargement for the Iberian Peninsula. (Jimenez et al, 2001).

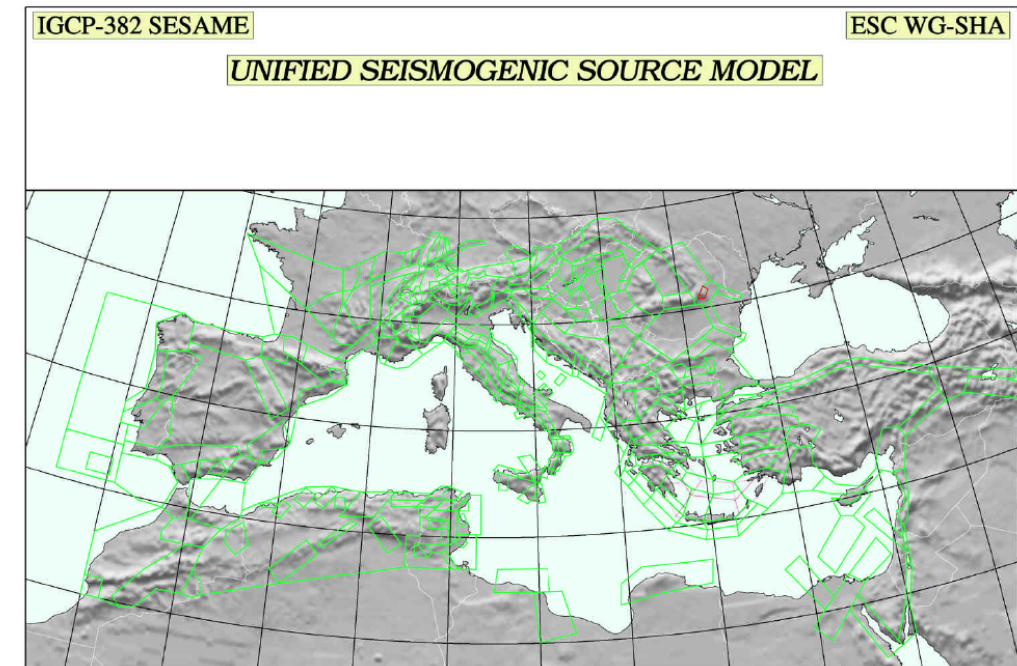


Figure 5.1-4. Seismogenetic zoning for Europe (SESAME Project).

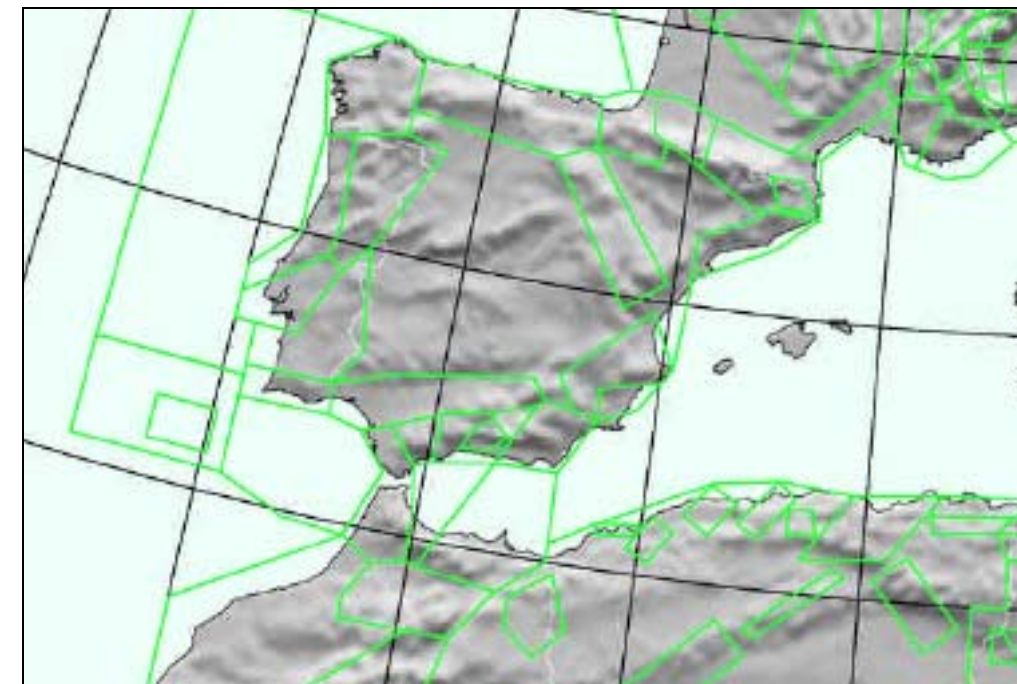


Figure 5.1-5. Seismogenetic zoning for the Iberian Peninsula (SESAME Project).

### 5.1.3 Determinist Study

#### 5.1.3.1 Seismicity

The seismicity of this zone has been studied using the earthquake catalogue provided by the IGN, which includes all the record for a zone that covers an area of 200 km from the site. Furthermore, a catalogue has been analysed of earthquake intensity isolines that affected the study zone. The data concerned has been used to prepare the following table of intensities perceived.

Epicentre	Coordinates	Date	Distance	Max. Intensity	Intensity perceived
Lisbon (PT)	10° W / 37° N	1-Nov-1755	~750 km	X	III
Arnedo (Logroño)	2° 05' W / 42° 15' N	18-Mar-1817	~150 km	VIII	III
Cauterets (FR)	0° 02' E/42° 42' N	13-Jul-1904	~ 30 km	VIII	VIII
Monte Perdido (Huesca)	0° 0' /42° 42' N	22-Jul-1904	~ 45 km	VI	IV
Martes (Huesca)	0° 57' W/42° 33' N	10-Jul-1923	~ 35 km	VIII	IV
Viella (Lerida)	0° 50' E/42° 41' N	19-Nov-1923	~ 90 km	VIII	VI
Laruns (FR)	0° 31' W/43° 02' N	22-Feb-1924	~ 30 km	VIII	VI
Viella (Lerida)	0° 47'E/42° 41' N	27-Feb-1924	~ 120 km	VI	IV
Turruncun (Logroño)	2° 06'W/42° 08' N	18-Feb-1929	~ 130 km	VII	II
Bagnères de Bigorre (FR)	0° 12' E/43° 07' N	31-Jan-1950	~ 55 km	VII	IV
Quillán (FR)	0° 5,9'E/42° 51,7'N	25-Nov-1958	~ 50 km	VI	IV
Lourdes (FR)	0° 3,8 W/43° 07' N	29-Aug-1964	~ 40 km	V	II
Arette (FR)	0°40,6'W/43° 7,7'N	13-Aug-1967	~ 35 km	VIII	V-VI
Tarbes (FR)	0°21,5'W/43°11'N	29-Feb-1980	~ 50 km	V	V

**Table 5.1-1.** Summary of the earthquakes that affected the site for which an isoseismic contour map is available.

It can be observed from the data contained in this catalogue, which covers a period of 585 years (1396 to 1981), that the maximum intensity perceived in the zone was VIII, although there have been a further 5 earthquakes with an intensity of VIII in the Pyrenees and one more in Logroño.

Other maps are also available showing epicentres. They have been prepared by different organisations and universities and can be seen below.

National Geographic Institute (IGN). This Centre possesses the following seismicity maps for the Iberian Peninsula:

- Epicentre Map: there are data for the Pyrenean zone concerning earthquakes whose intensities reach VIII and intensities greater than 5. Figure 5.1-6.
- Seismic Hazard Map in terms of intensity: in the study zone, the intensity can range from VI to VII. Figure 5.1-7.
- Seismic Hazard Map in terms of acceleration for a return period of 500 years: the study zone lies within an acceleration zone that ranges from 0.08g to 0.12. Figure 5.1-8.

These maps are shown in the following pages.



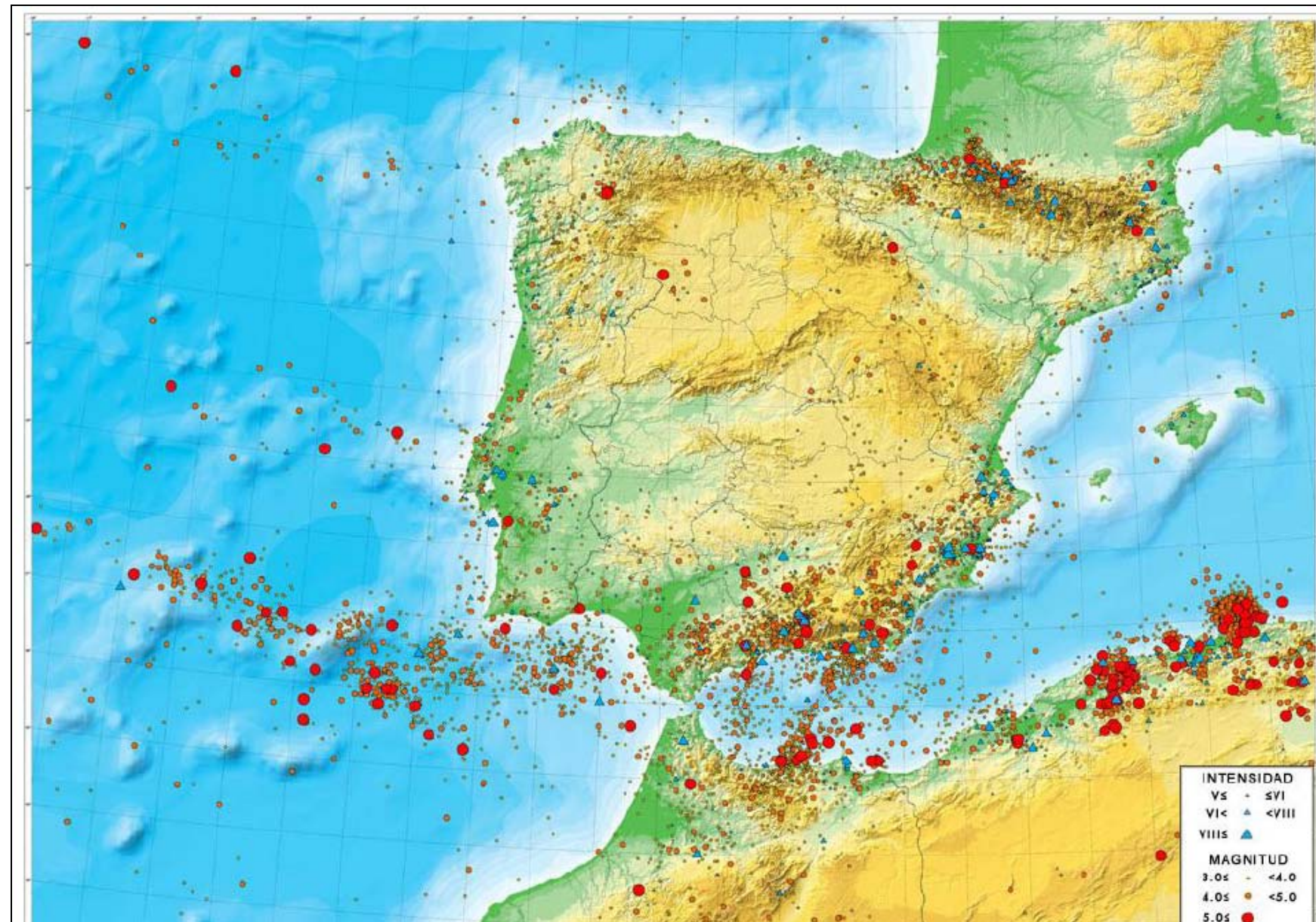


Figure 5.1-6. Epicentre Map. IGN.





Figure 5.1-7. Seismic Hazard Map. Intensity on 500 year period. IGN.

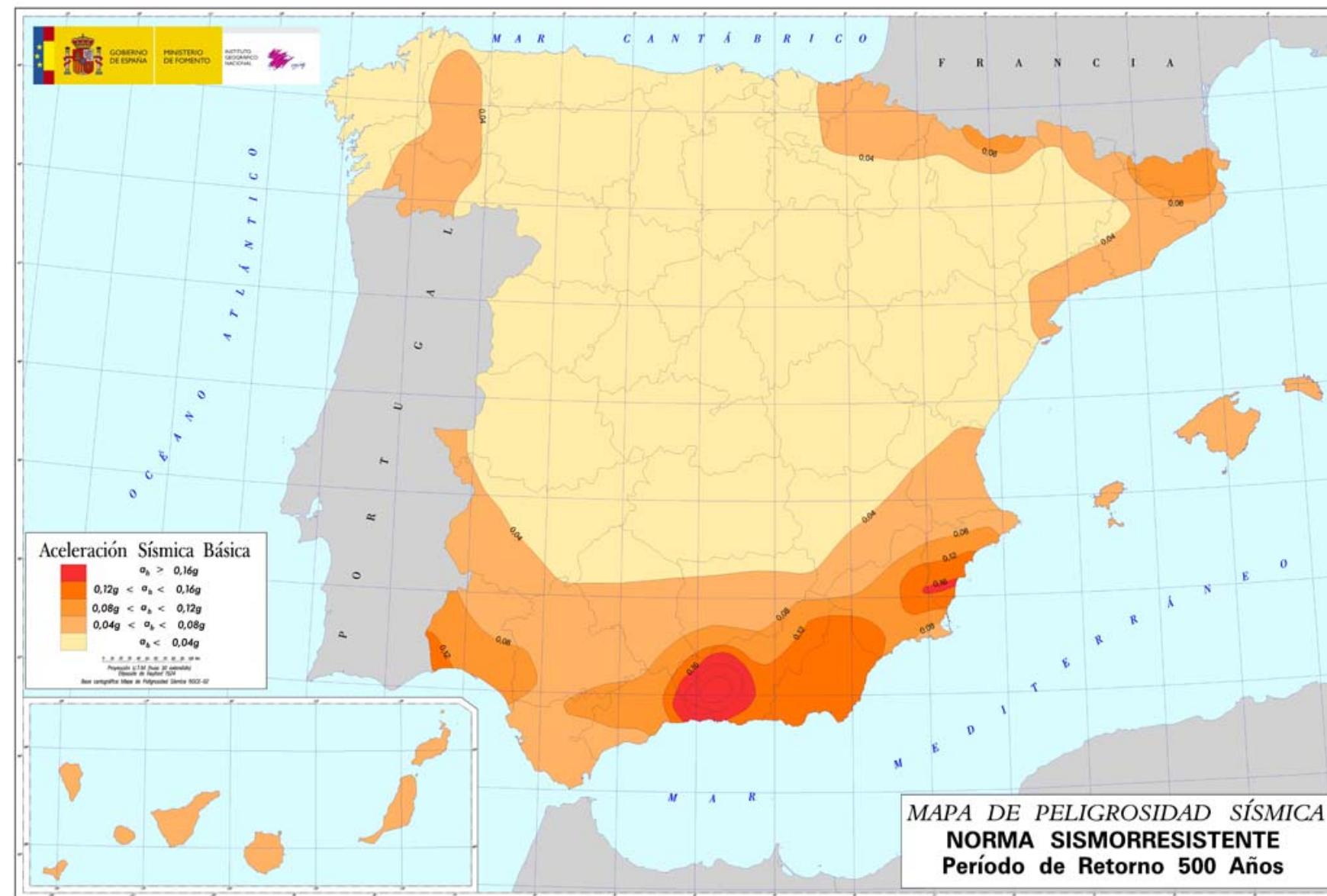


Figure 5.1-8. Seismic Hazard Map. Basic Seismic Acceleration for 500 year period. IGN



Sisfrance.- Information prepared by the BRGM (Bureau de Recherches Géologiques et Minières) and by the IRSN (Institut de Radioprotection et de Sûreté Nucleaire), as well as other official French organisations.

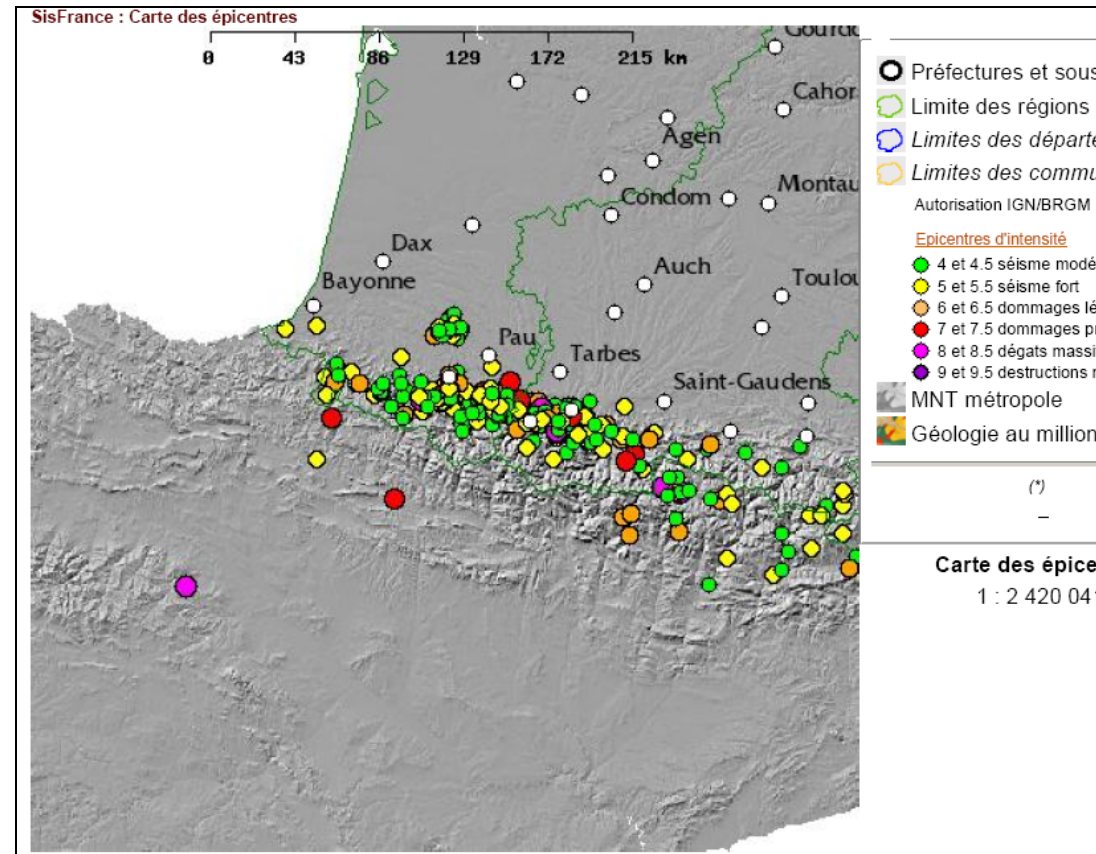


Figure 5.1-9. Epicentre Map. Pyrenees. Sisfrance

Observatoire Midi-Pyrénées. This Centre provides the following maps of intensity perceived and magnitude in the Pyrenees. Intensity data of up to VIII are picked up and magnitude data of over 5.

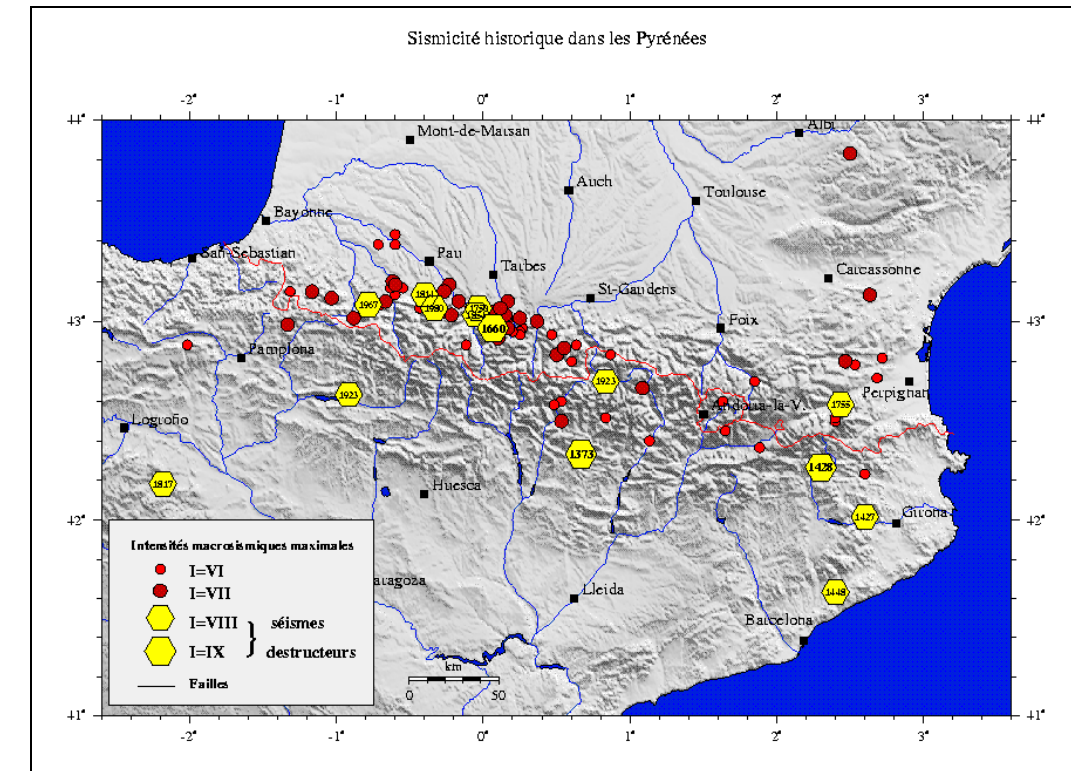


Figure 5.1-10. Seismic Intensity Map. Observatoire Midi-Pyrénées.

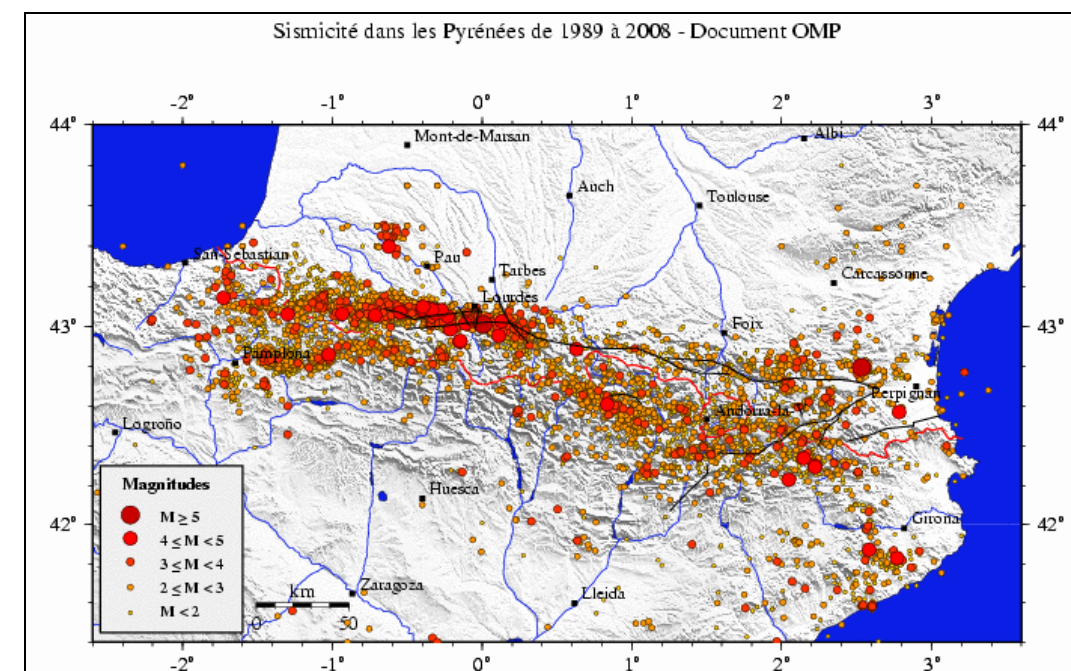


Figure 5.1-11. Magnitude Map. Observatoire Midi-Pyrénées

The data from the maps provided by the aforementioned bodies and from the updating of the catalogue of isoseismic contours indicate that the maximum intensity and magnitude values that can be expected in the zone would be as follows:

- Intensity: VII – VIII
- Magnitude 5 – 5.5

### 5.1.3.2 Intensity / acceleration at the site

The IGN provided us with the attenuation laws that they generally use. These are the intensity attenuation laws calculated by A. J. Martín (1983) for different seismogenic zones in Spain on the basis of isoseismic contours observed. A distinction between two possibilities is made in several zones (G: “Large”, P: “Small”), depending on whether the epicentral intensity is above or below VIII.

- General G:  $I = I_e + 12'55 - 3'53 * \ln(R+25)$
- General P:  $I = I_e + 5'23 - 2'21 * \ln(R+5)$
- Azores-Gibraltar Fault:  $I = I_e + 21'41 - 4'02 * \ln R$
- South Spain G:  $I = I_e + 11'23 - 3'10 * \ln(R+25)$
- South Spain P:  $I = I_e + 11'68 - 3'24 * \ln(R+25)$
- South-Eastern Spain G:  $I = I_e + 15'51 - 4'40 * \ln(R+25)$
- South-Eastern Spain P:  $I = I_e + 5'92 - 2'61 * \ln(R+5)$

In this case, the general attenuation laws for the whole of the Iberian Peninsula will be used to obtain the intensity perceived at the site being studied on the basis of

the maximum intensity of each earthquake. These laws have been plotted in the figure 5.1-12 shown below.

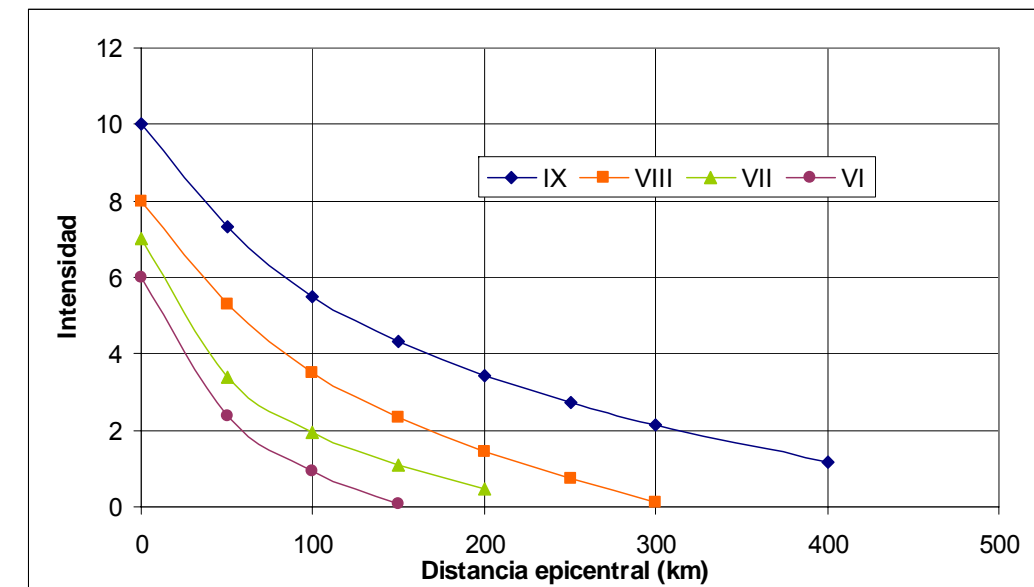


Figure 5.1-12. The general Attenuation Laws for the Iberian Peninsula, as provided by the IGN.

A comparison has been made between the intensity perceived at the site and the intensity calculated using the expressions for the earthquakes for which isoseismic maps are available. The results can be seen in the figure 5.1-13.



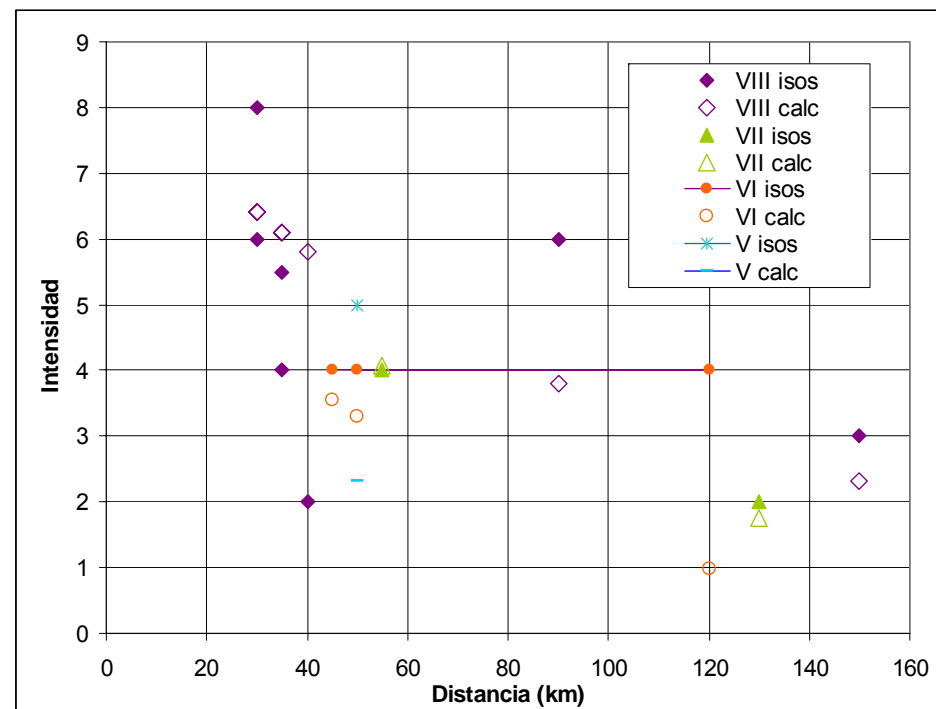


Figure 5.1-13. Comparison between the intensity values perceived at the site and the intensity values calculated using the IGN's general attenuation law.

The comparison between the intensity perceived at the site and the intensity calculated by means of the general attenuation law provided by the IGN for the earthquakes that are included in the previous table show the following behaviour patterns:

- Intensity = VIII. The values calculated are greater than the values noticed in the case of distances of less than 50 km, whereas the opposite is the case for distances greater than 50 km.
- I = VII.- the values calculated are approximately the same as the values noticed.
- I = VI.- the values calculated are less than the values perceived for distances of more than 50 km; for shorter distances they are similar.

- I = V.- the values calculated are less than the values perceived

These differences could be put down either to inaccuracies in defining the iso-seismic contours, or to local effects at the site that cause the isoseismic contours not to be concentric lines around the epicentre as forecast by the laws of attenuation.

Whatever the case may be, the maximum intensity perceived corresponding to the isoseismic plans provided by the IGN lead to a maximum intensity value at the site between VII and VIII. If we take the results obtained by the attenuation law used, the maximum value of intensity is 6.8, although this is the value only for those earthquakes for which a map of isoseismic contours is available, so there is no reason why it should be the same as the maximum expected value.

As far as the acceleration value is concerned, the accelerations at the site have been obtained from the magnitude data and intensity data take from the IGN Catalogue. In the first case, earthquakes were considered whose magnitudes were equivalent to or greater than 4, whereas in the second case, the earthquakes with intensities greater than VI were considered. In this case, the intensities noticed have been transformed into magnitudes by means of the formula devised by López Casado et al (2000) (see the figure of the relationships between intensity and magnitude on further paragraphs).

The expression proposed by Ambraseys (1995) was used to obtain the acceleration value for the site. Several expressions are proposed in this work, from which one has been selected that is independent of the depth of the focus, because this information is not available. It is as follows:

$$\log(a_h) = -1,43 + 0,245 \cdot M_s - 0,0010 \cdot r - 0,786 \cdot (r) + 0,24 \cdot P$$

Where:

$$r = (d^2 + 6^2)^{0,5}$$

P = 0 for values corresponding to the percentile of 50% and 1 for values for the 84 percentiles.

It was thus possible to obtain the following maximum values for the acceleration perceived:

Data	Date	Distance	Horizontal acceleration $a_H$
M=4,2	04/10/1999	15,40 km	0,076 g
I=VII	07/08/1914	1,07 km	0,257 g

An acceleration has thus been obtained that is similar to the one proposed by the earthquake proof standard NCSR-02 on the basis of the magnitude data. However, a much higher value has been obtained from the intensity data for historic earthquakes, in view of the fact that the epicentre and the tunnel of Somport lie very close to each other. As we shall see below, this value is similar to the results yielded by probabilistic studies that have been published recently.

#### 5.1.4 Probabilistic approach

The aim of this study is to obtain the magnitudes of the earthquakes that are likely to occur, for 100-, 500- and 1,000-year periods.

The procedure for the probabilistic study revolves around 4 basic hypotheses:

- The seismic activity within a seismotectonic zone is uniformly distributed in space.
- The occupation rate of earthquakes of any intensity within any seismotectonic zone, is the same as what has been observed in the past.

- The distribution of intensities in any seismotectonic zone can be likened to a truncated exponential or to a Gumbel distribution.
- If no premonitories or replicas are considered, the time distribution for earthquakes for a given intensity can be regarded as Poisson type. Therefore, the likelihood of occurrence of n earthquakes P(n) in a period of time t, will be given by the following:

$$P(n) = \exp(-Nt) * (Nt)^n / n!$$

n = number of earthquakes with a given intensity or magnitude, which occur in a specific period of time.

In this study, the probabilistic analysis contains the following sections:

- Seismicity.- the data belonging to all the earthquakes recorded has been compiled, when their epicentre lies within a circle whose radius is 200 km, taking the LAGUNA site as the centre of the circle. More general seismic information has also been compiled, such as maps of epicentres.
- The earthquake occurrence rate has been established on the basis of the earthquake frequency distributions. These distributions follow a potential law known as the Gutenberg-Richter equation.
- Finally, the aforementioned distribution is used to establish the value of the intensity or magnitude of the earthquake that is most likely to occur for return periods of 100, 500 and 1,000 years.

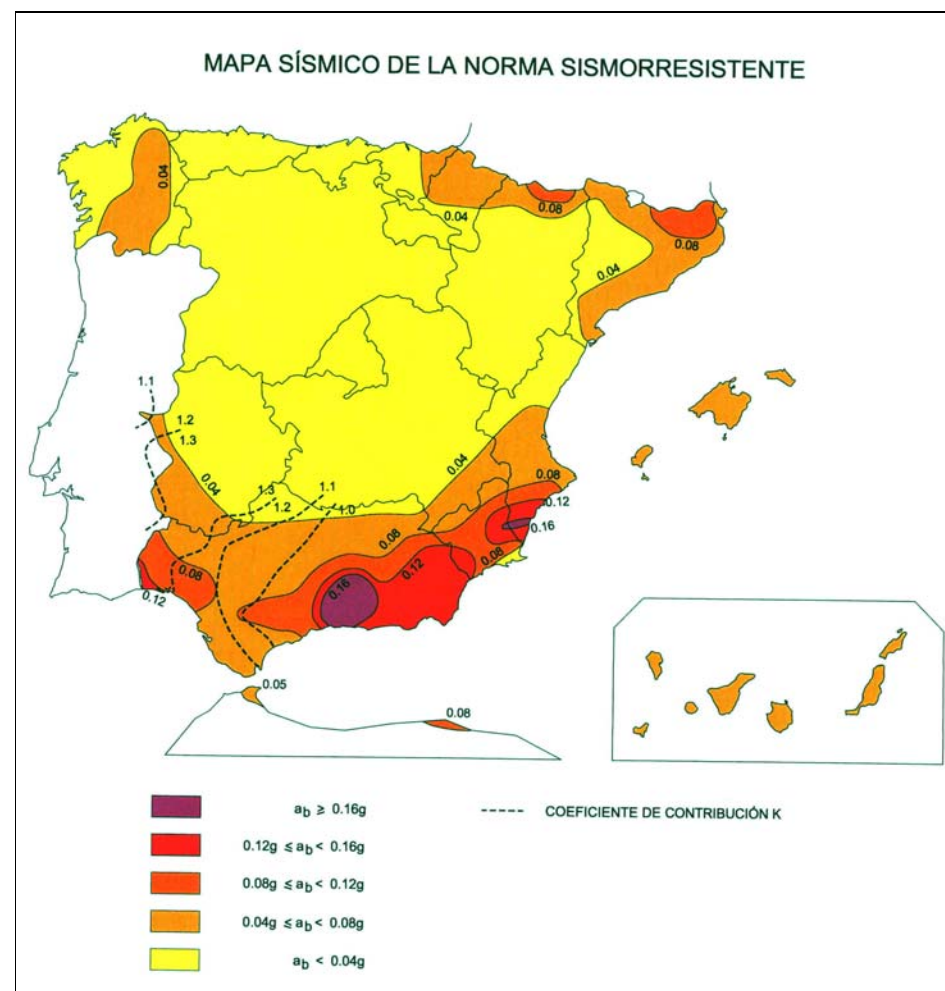
##### 5.1.4.1 General list of earthquakes

A general list of earthquakes that has been furnished by IGN, including the records of historical and instrumental seismic movements recorded within a radius of 200 km around the LAGUNA site has been analysed.

#### 5.1.4.2 Seismicity at the site

The Somport Tunnel lies in the southern zone of the Pyrenees. The documentation presented above indicates that the seismic activity in this zone has been considerable not only historically but also during the instrumental period.

The map that is shown below, included in the earthquake proof standard, plots these trends. According to this Standard (NCSE-02), the zone where the tunnel is located could be affected by seismic accelerations greater than 0.08 g.



Furthermore, in the light of the data compiled in this work, it is known that in this zone the historical records indicate that there have been earthquakes with very high intensities (up to IX), and that there are instrumental records of earthquakes of considerable magnitudes within the range of time under consideration (up to 5), although the zone with the greatest seismic activity lies to the north of the border between France and Spain.

#### 5.1.4.3 Earthquake Occurrence Rate

The earthquake occurrence rates are established on the basis of the frequency distributions for the number of earthquakes that exceed a particular intensity.

Their analytical expression takes the following form:

$$\ln N = a + b * I_0$$

N.- number of earthquakes per year whose epicentral intensity is equivalent to or greater than  $I_0$ .

a, b.- constants that represent the seismic characteristics in each province.

$I_0$ .- epicentral intensity (MSK).

The relationship between the frequency and intensity is obtained using the list of earthquakes furnished by the IGN. This catalogue includes both historical and instrumental data for the earthquakes. The data varies in quality, and also with respect to the completeness of the records.

As we have already pointed out, the seismic database used in this work comes directly from the catalogue furnished by the *Servicio de Sismología e Ingeniería Sísmica* of the IGN.

The fields that make up the database are as follows: agency that provides the Information, essentially the *Servicio de Sismología e Ingeniería Sísmica* of the IGN, geographical coordinates for the epicentre, year, month, day, time, magnitude, maximum intensity perceived or epicentral, name of the nearest settlement to the epicentre and the post code for the province.

The scale of Intensity used in the IGN Catalogue is the MSK scale. However, from 1997 and on the EMS (European Macroseismic Scale) has been used. The EMS scale can be regarded as an update of the MSK incorporating modern construction methods, so it is considered feasible to compare the two scales.

The scale of magnitude used in the catalogue is the body waves mb calculated on the maximum wave amplitude Lg. It must be stressed that the method used for calculating the magnitude varies considerably depending on how old the records are.

The seismic database used comprises 4,940 seismic events. The catalogue covers the period ranging from the year 1373 until 30th May 2006.

With a view to enabling the user to study the occurrence and characteristics of the seismicity in the definition of seismogenetic sources, it is first necessary to subdivide the catalogue into time periods that are homogeneous in terms of the completeness of the records, the variability of the value of the magnitude and the precision where the location is concerned. These periods have to be defined taking into account the progress and development of the National Seismic Network in time, and its effects on the data contained in the seismic catalogue.

Although the first seismograph was installed in Spain in 1897, it was not until the 1920s that the first National Seismic Network came into operation. This fact is recorded in our database on the one hand, with an increase in the frequency of events located in the sea, and on the other hand, with the first record with magnitude calculated (1919, Jacarilla, Alicante, mb = 5.2). Approximately as from 1920,

events began to be recorded with an intensity of II, and the magnitude is calculated for events with an intensity of VII or greater, with only a few exceptions.

Towards the end of the 1950s, the National Seismic Network underwent a major instrumental update, although the number of recording stations remained virtually the same as in the preceding period. It can be clearly observed in our catalogue how there was an increase in the records for seismic movements whose magnitudes were less than 3.5, especially in the provinces of Almeria, Murcia and Alicante. It can also be seen that the first measurements of the location error took place in those years.

Later, midway through the 1980s, the National Seismic Network once again underwent a process of improvement accompanied by a major increase in the number of recording stations. At the present time in our work zone, all the seismographs installed were manufactured after 1984. Finally, it must be pointed out that since 1990, the new Digital Seismic Network has been implemented; it involves the creation of new stations and improvements to the existing ones.

On the basis of the aforementioned considerations, the seismic catalogue has been subdivided into the following time periods: Historical (up to 1920), Precarious Instrumental (up to 1960), Old Instrumental (up to 1985) and Modern Instrumental (since 1985). The limits between each period must be regarded as approximate, because the passing from one period to another is not homogeneous throughout the work zone.

The average annual rate of earthquake occurrence must be estimated by carefully considering the completeness of the records contained in the catalogue for the magnitude and/or intensity values. Table 5.1-2 shows the intervals of completeness that have been deduced on the basis of an analysis of the data in each time period in the catalogue.



		Completeness (first year)	Total period that records were kept (years)
Intensities	VIII – IX	1000 – 1500	920 - 420
Magnitudes	= 4.0	1920	83
	4.0 – 3.0	1960	43
	< 3.0	1985	18

Table 5.1-2

#### 5.1.4.4 Probabilistic Study

This study was conducted using the database provided by the IGN for all the earthquakes recorded in both the historical and instrumental periods within a radius of 200 km around the study zone.

The total number of records amounts to 4,940 and includes records of historical earthquakes catalogued with estimations of seismic intensity as instrumental records that yield magnitude values for the earthquake.

The catalogue available at the website [www.sisfrance.net](http://www.sisfrance.net) prepared by the BRGM (Bureau de Recherches Géologiques et Minières) and by the IRSN (Institut de Radioprotection et de Sûreté Nucleaire) and other official French bodies was also analysed. The data that have been selected for the Hautes Pyrenees Region are those for the zone lying close to the tunnel of Somport location. These records are macroseismic intensity data. A total of 179 records have been used, ranging from the year 1518 to 2007.

It has been possible to use this information to establish the earthquake occurrence rate adjusting the potential Gutenberg-Richter law that characterises the time distribution of the earthquakes on the basis of their magnitude or intensity.

These adjustments have been made not only from the intensity but also the magnitude records for the earthquakes, with a view to comparing the results later. The first adjustment is made with the intensity data. As has already been pointed out,

the intensity record can only be considered complete for high intensity values, in view of the fact that for more than 600 years, the historical records include earthquakes whose intensity is greater than VII. Up to the start of the instrumental records data are not available for seismic events whose intensities are lower.

The instrumental catalogue lacks data for high-magnitude earthquakes, so it is only regarded as complete for magnitudes below 5 and all the major earthquakes for which there are historical records would be missing. The catalogue has been completed with the data from those earthquakes for which there is an intensity record. Two relationships between intensity and magnitude have been used for this purpose. The first is the one proposed by López Casado et al (2000):

$$m_b = 3,00 + 0,032 \cdot I_o^2 + 0,40 \cdot P$$

Where P has been taken as being equivalent to 0. It has been found that, when relating the seismic catalogue data used for intensity and magnitude for one single event, taking a value of P equivalent to zero, a better approximation to the results is obtained (see figure 5.1-15, purple line).

This figure also shows the relationship between intensity and magnitude that is obtained directly from the data in the seismic catalogue provided by the IGN (black line), whereas the purple line refers to López Casado's expression with a value of P equivalent to zero.

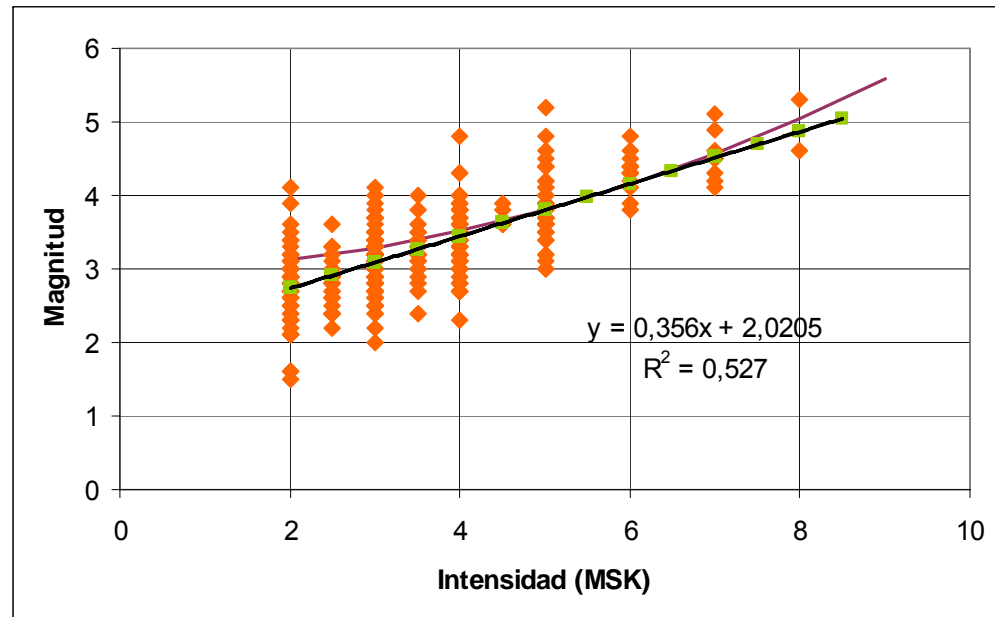


Figure 5.1-15. Relationship between intensity and magnitude obtained from the catalogue used in this study (black line) and the López Casado et al (2000) relationship (purple line).

Gutenberg-Richter's straight lines have been obtained in this study not only for the intensity and magnitude data that are provided in the catalogue directly, but also for the values that are obtained from these using the relationship found in this study (see previous figure) as the formula used by López Casado et al (2000). The results are shown below.

#### Results yielded from the Intensity data contained in the Seismic Catalogue.

Gutenberg-Richter's straight line has been obtained from the Intensity data contained in the seismic catalogue provided by the IGN. These data first appeared in the year 1373 and the most recent data is from 11th January 2006. The results are shown in the figure 5.1-16.

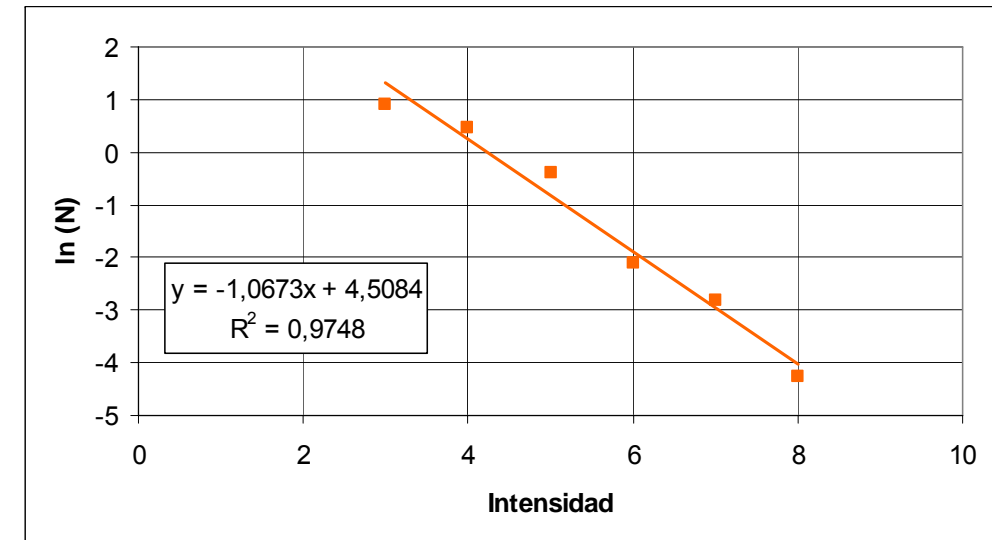


Figure 5.1-16. Gutenberg-Richter Law obtained from the intensity data taken from the IGN seismic catalogue.

The results obtained from the seismicity data for the Hautes Pyrenees Region contained in the French catalogue are also included.

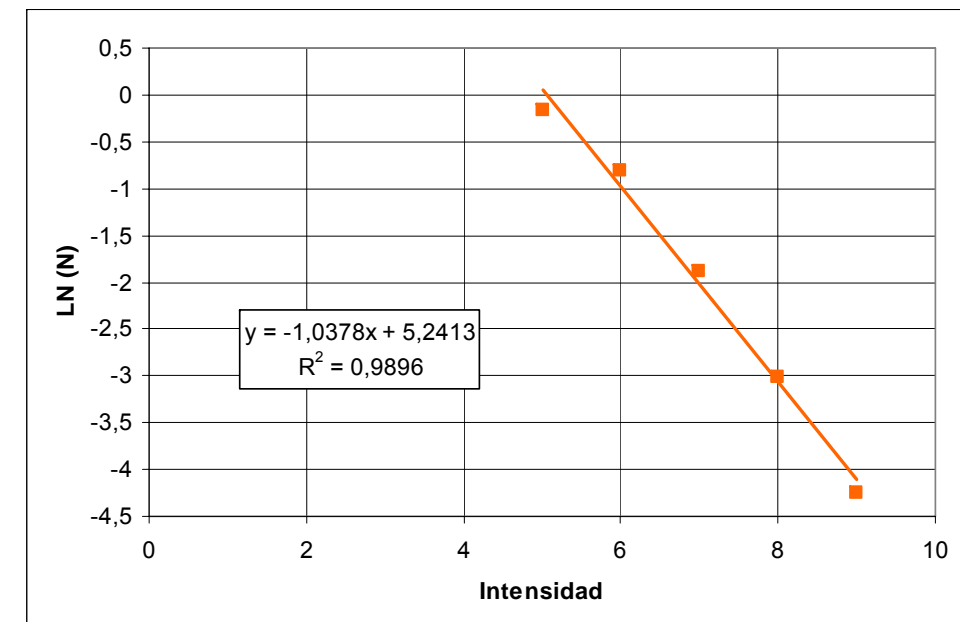


Figure 5.1-17. Gutenberg-Richter Law obtained from the intensity data taken from the French seismic catalogue for the Hautes Pyrenees Region.

These two catalogues yield similar values for parameters “a” and “b” of the Gutenberg-Richter Law:

Catalogue	A	B
IGN	4.5084	-1.0673
Sisfrance	5.21413	-1.0378

Results for the Intensity data obtained from the magnitude values in the Seismic Catalogue.

In this case, the intensity values were obtained from the instrumental data concerning magnitude, from the IGN seismic catalogue using the relationship between intensity and magnitude obtained in this work. The results are shown below. The regression line that is obtained yields values of “a” and “b” that are higher than in the previous case.

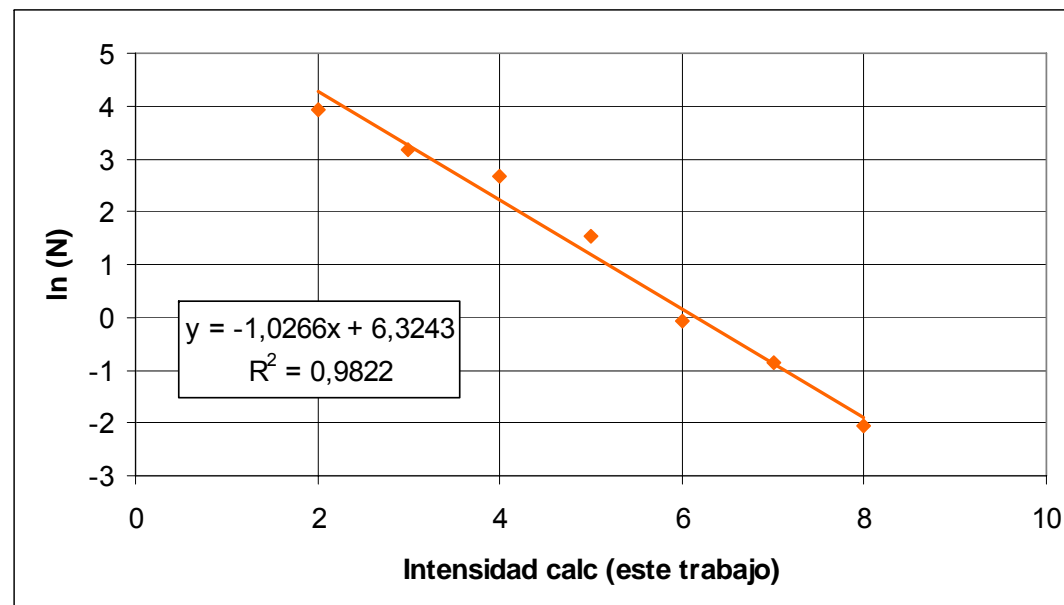


Figure 5.1-18. Gutenberg Richter relationship established from the intensity data obtained from the magnitude values in the seismic catalogue.

Results obtained from the magnitude data contained in the IGN Seismic Catalogue.

The figure 5.1-19 shows the results obtained from the magnitude data obtained directly from the catalogue. Not only the relationship obtained for the magnitude data from the seismic catalogue ( $m_b$ ) but also the data obtained when transforming this data into moment-magnitude ( $M_w$ ) are included. This transformation was made using the relationship proposed by Rueda and Mezcuca (2002) from the peninsular earthquake data recorded by the National Seismic Network:

$$M_w = 0,311 + 0,637 \cdot m_b + 0,061 \cdot m_b^2 \quad (1.7 < m_b < 5.7)$$

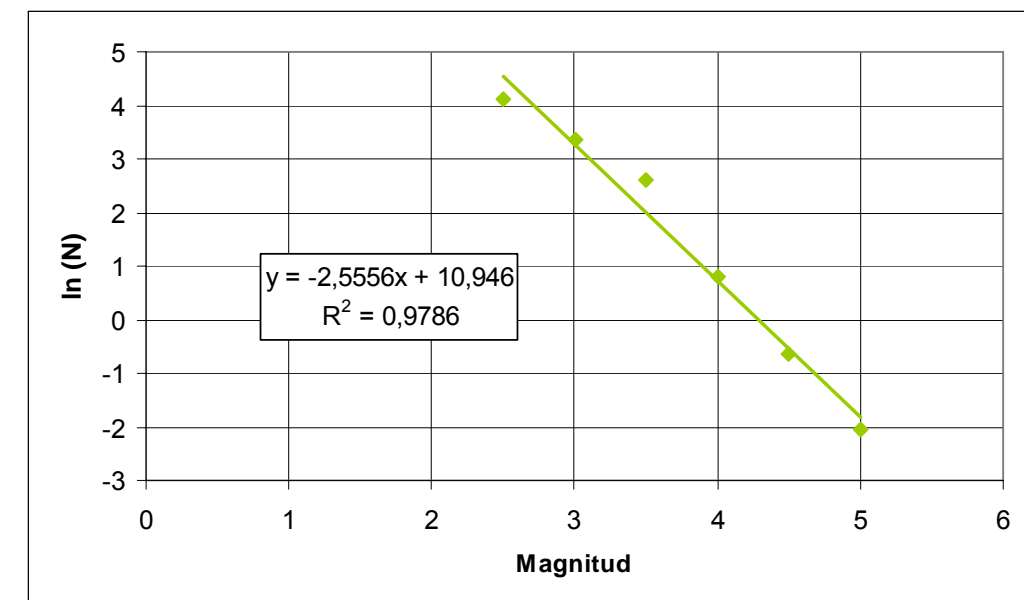


Figure 5.1-19. Gutenberg-Richter Law obtained from the magnitude data taken from the seismic catalogue

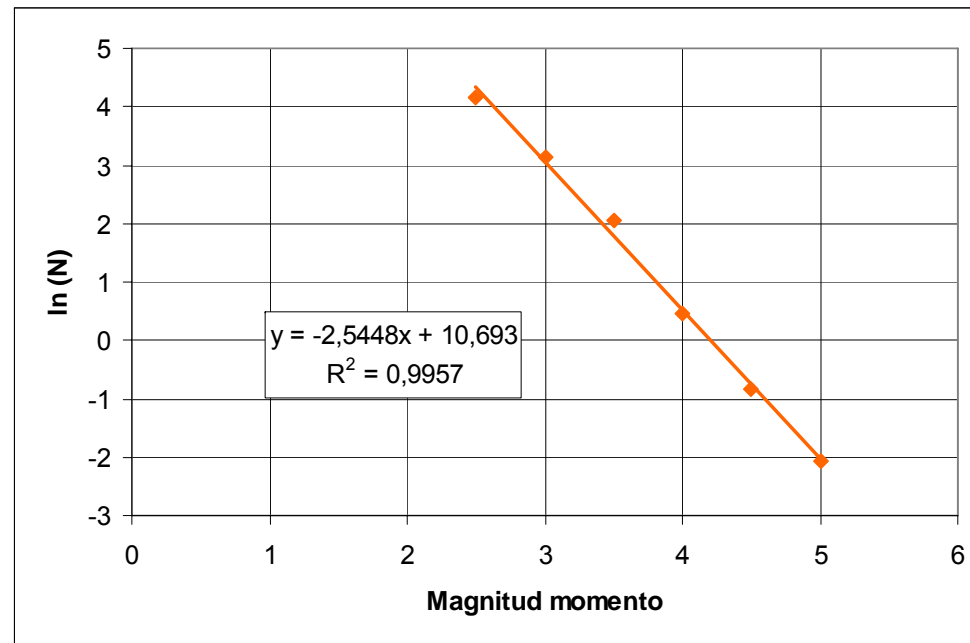


Figure 5.1-20. Gutenberg-Richter Law obtained from the moment magnitude data taken from the seismic catalogue using the relation proposed by Rueda and Mezcua (2002).

#### Results from the magnitude data obtained from the intensity data in the seismic catalogue.

In this case, the intensity data have been transformed into magnitude data, using the relationship found in previous figures, as well as the López-Casado formula.

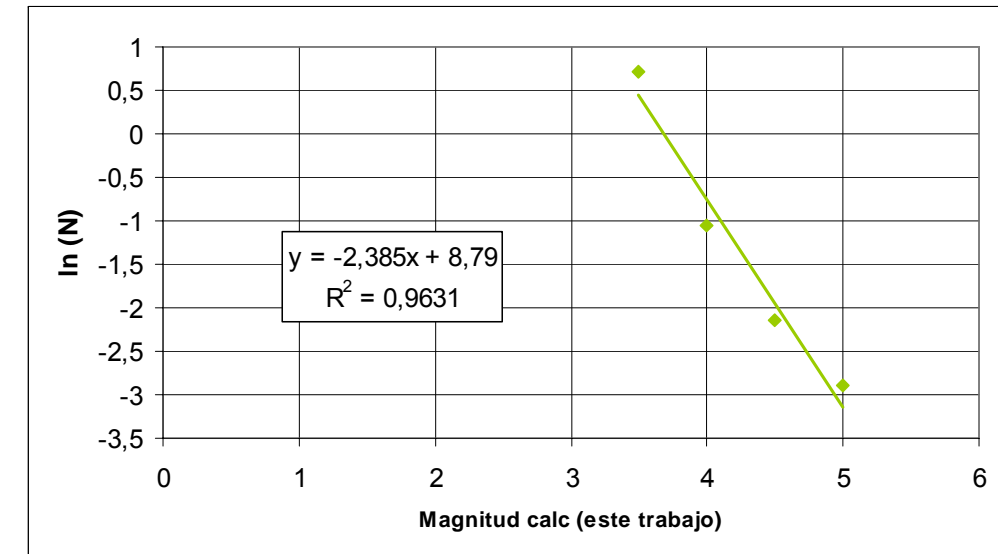


Figure 5.1-21. Gutenberg Richter relationship established on the basis of the magnitude data obtained from the intensity values in the seismic catalogue. Relationship obtained in this work.

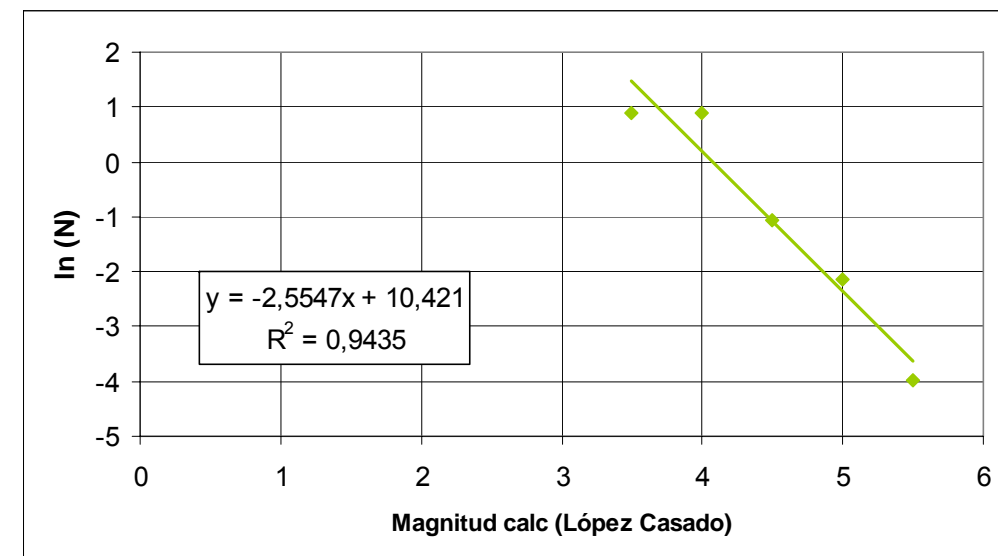


Figure 5.1-22. Gutenberg Richter relationship established on the basis of the magnitude data obtained from the intensity values in the seismic catalogue. López Casado Relationship.

In each one of the figures shown, N is the number of earthquakes whose intensity is equivalent to or greater than a given earthquake. The values of the parameters



in the Gutenberg-Richter equation would thus be the following for each one of the cases studied:

Table 5.1-3. Gutenberg-Richter Law parameters for different databases.

		a	B
Intensity	IGN Catalogue	4.5084	-1.0673
	Catalogue SisFrance	5.2413	-1.0378
	Magnitude (relationship this work)	6.3243	-1.0266
Magnitude	IGN Catalogue	10.946	-2.5556
	Intensity (relationship this work)	8.790	-2.385
	Intensity (López Casado et al, 2000)	10.421	-2.5547
Moment Magnitude	IGN Catalogue	10.693	-2.5448

These results have been compared with others that have been published for this same zone. To be specific, the results have been used from the following articles

- Secanell, R., Irizarry, J., Susagna, T., Martín, C., Goula, X, Combes, P. and Fleta, J. "Unified Evaluation of the Seismic Hazard in the Vicinity of the frontier between France and Spain". 2nd National Seismic Engineering Conference,. 439-447. Málaga (2003).
- Secanell, R., Bertil, B., Martin, C., Goula, X., Susagna, T., Tapia, M., Dominique, P., Carbon, D. & Fleta, J. "Probabilistic Seismic Hazard Assessment of the Pyrenean Region". J. Seismol (2008) 12:323-341.

These authors have carried out a probabilistic study in the Pyrenees zone for the purpose of which they have used data from the following seismic catalogues, which have been brought together in one single catalogue called ISARD:

#### Macroseismic Data:

- Catalogue issued by the Servei Geològic de Catalunya –SGC- (1999).
- Catalogue issued by the Instituto Geográfico Nacional –IGN- (1983)
- Catalogue issued by Sisfrance –BRGM and others - (2004)
- Catalogue issued by Levret et al (1996).

#### Instrumental data:

- Laboratoire de Détection Géophysique (LGD) which began in 1962.
- Instituto Geográfico Nacional (IGN) since 1961.
- Other regional catalogues whose data series are not as extensive (SGC, OMP, etc.)

For the cases where there is an evaluation not only of the intensity but also the magnitude, a relationship has been obtained between both results; it is included in the figure 5.1-23. This relationship is similar to the one found in this work, but it shows a lower value for the independent term and a steeper slope.

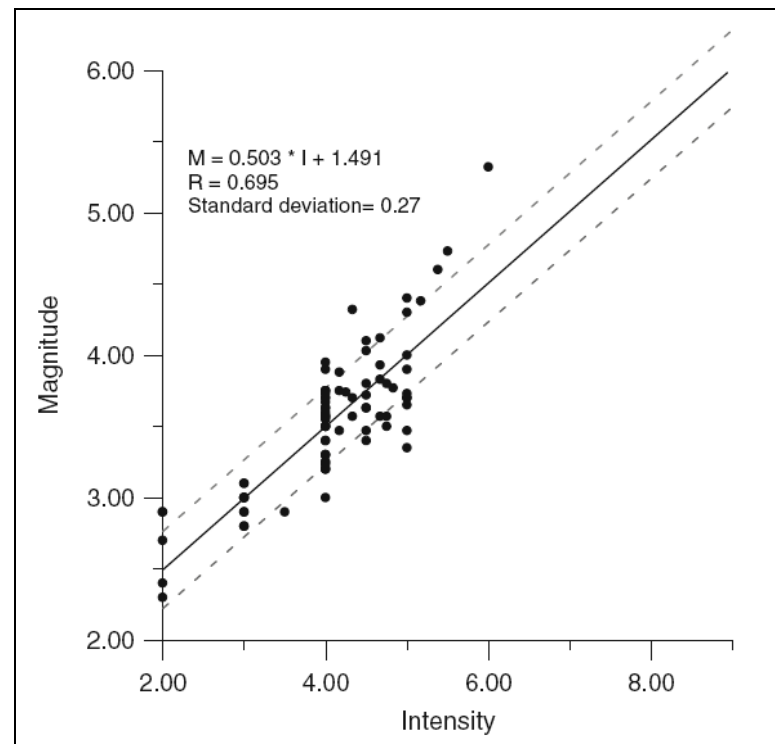


Figure 5.1-23. Relationship between intensity and magnitude proposed by Secanell et al (2008).

This relationship has been used to complete the catalogue, finding magnitude values for those earthquakes for which only historical records are available. The following time distribution for the seismicity has been found.

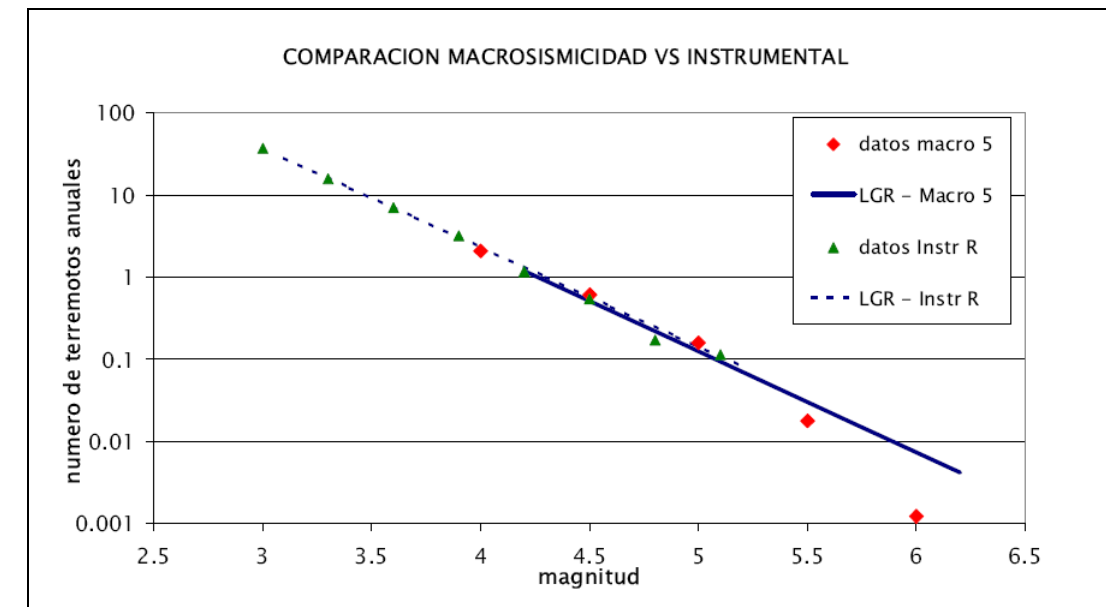


Figure 5.1-24. Gutenberg-Richter adjustments to the historical and instrumental seismicity (Secanell et al, 2003)

The results of our analysis and the analyses of these authors have been analysed jointly. The following tables show the results for the different regressions found concerning the number of earthquakes per year for a given intensity / magnitude and a return period in years for every intensity / magnitude.

Tables 5.1-4 and 5.1-5.

		Number of earthquakes per year								
Intensity		a	b	II	III	IV	V	VI	VII	VIII
	IGN Catalogue	4,5084	-1,0673	10,74	3,69	1,27	0,44	0,15	0,05	0,02
	SisFrance Catalogue	5,2413	-1,0378	23,71	8,40	2,97	1,05	0,37	0,13	0,05
Magnitude	Magnitude (relationship for LAGUNA)	6,3243	-1,0266	71,60	25,65	9,19	3,29	1,18	0,42	0,15
				3	3,5	4	4,5	5	5,5	6
	IGN Catalogue	10,946	-2,5556	26,55	7,40	2,06	0,57	0,16	0,04	0,0124
Magnitude	Intensity (relationship for LAGUNA)	8,79	-2,385	5,13	1,56	0,47	0,14	0,04	0,01	0,0040
	Intensity (López Casado et al, 2000)	10,421	-2,5547	15,75	4,39	1,22	0,34	0,10	0,03	0,0074
	Secanell et al.	12,854	-2,9949	47,91	10,72	2,40	0,54	0,12	0,03	0,0060

		Recurrence period (years)								
Intensity		a	b	II	III	IV	V	VI	VII	VIII
	IGN Catalogue	4,5084	-1,0673	0,09	0,27	0,79	2,29	6,66	19,35	56,26
	SisFrance Catalogue	5,2413	-1,0378	0,04	0,12	0,34	0,95	2,68	7,56	21,35
Magnitude	Magnitude (relationship for LAGUNA)	6,3243	-1,0266	0,01	0,04	0,11	0,30	0,85	2,37	6,61
				3	3,5	4	4,5	5	5,5	6
	IGN Catalogue	10,946	-2,5556	0,04	0,14	0,49	1,74	6,25	22,42	80,45
Magnitude	Intensity (relationship for LAGUNA)	8,79	-2,385	0,19	0,64	2,12	6,98	22,99	75,75	249,64
	Intensity (López Casado et al, 2000)	10,421	-2,5547	0,06	0,23	0,82	2,93	10,51	37,71	135,26
	Secanell et al.	12,854	-2,9949	0,02	0,09	0,42	1,86	8,34	37,26	166,57

The above results have been shown in the following figures 5.1-25 and 5.1-26. Where the intensity data are concerned, it can be observed that the results are widely dispersed, in view of the fact that the number of earthquakes per year that is obtained from the catalogue provided by the IGN is about half the number that is obtained with the Sisfrance catalogue, and much less than the number that is obtained when transforming the data from the catalogue to intensity. This could be due to the fact that the historical catalogue is not sufficiently complete and that, as a result, the seismicity in the zone is being underestimated.

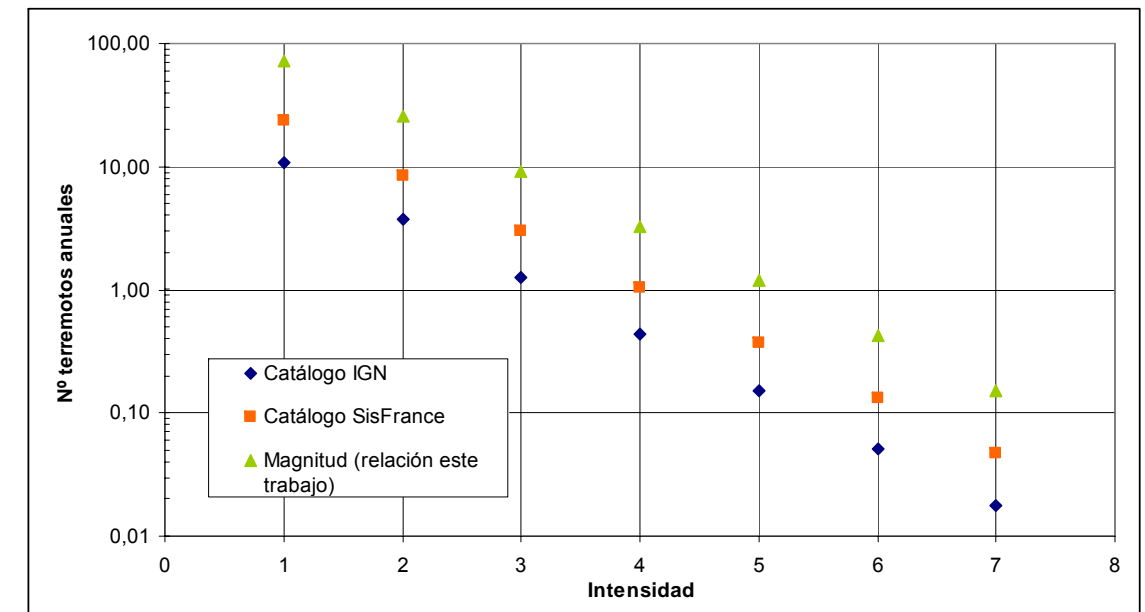


Figure 5.1-25. Gutenberg-Richter's relationship for the different series of Intensity data considered.

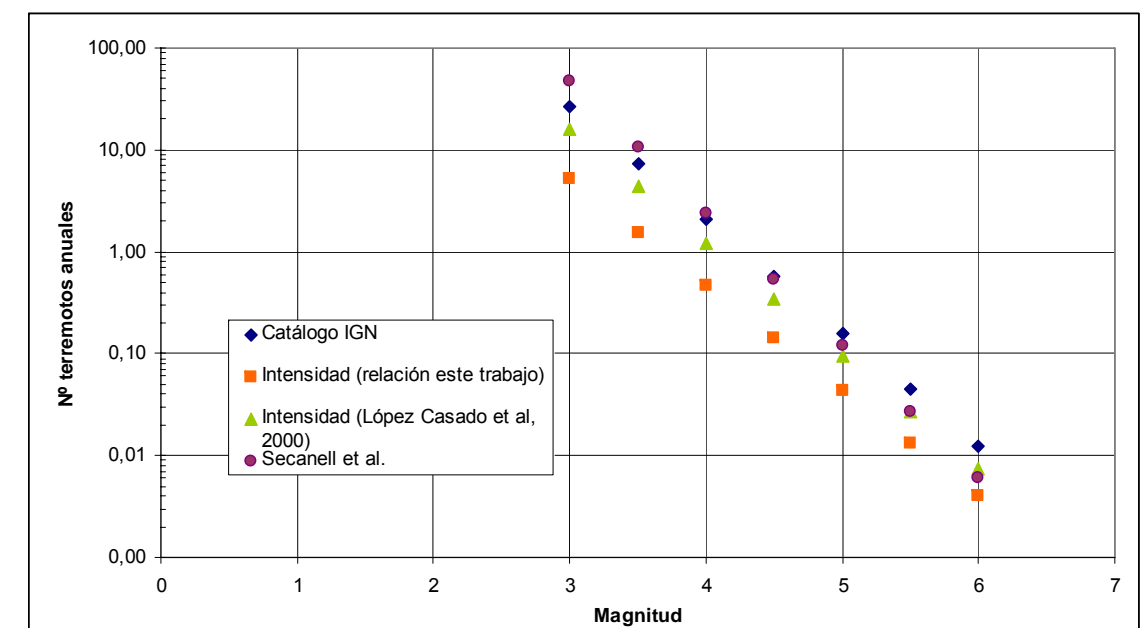


Figure 5.1-26. Gutenberg-Richter's Relationship for the different series of magnitude data considered.

As far as the magnitude data are concerned, the results are similar to the ones obtained from the IGN Catalogue and from Secanell et al, although the latter do



predict lower annual frequencies for major earthquakes ( $M > 4.5$ ) and greater annual frequencies for minor earthquakes ( $M < 4.5$ ). The data that are obtained when transforming the intensity values from the IGN seismic catalogue into magnitude values, are much lower than the former, which would appear to confirm the above idea that this catalogue is incomplete.

Therefore, if we consider the results obtained with magnitude data from this study (IGN) as being the results obtained by Secanell et al (2003, 2008), the magnitudes that are obtained for the reference periods are as follows:

Period	This Study (IGN)	Secanell et al (2003, 2008)
2000 years	7.3	6.8
500 years	6.7	6.4
100 years	6.0	5.8

Finally, in view of the similarity between these results, it is proposed to use the acceleration values obtained by Secanell et al (2008). These results were obtained using the following attenuation laws:

- The laws established by Ambraseys (1995) and Ambraseys et al (1996) for the European domain and adapted to the Pyrenean seismic context. In the case of Ambraseys (1995), the attenuation law depends upon the distance from the focal point, whereas in the case of Ambraseys et al (1996), the law is not dependent.
- The second was established by Tapia et al (2004) as part of the ISARD Project and updated by Tapia et al (2007).

The results that these authors obtain can be seen in the following figures.

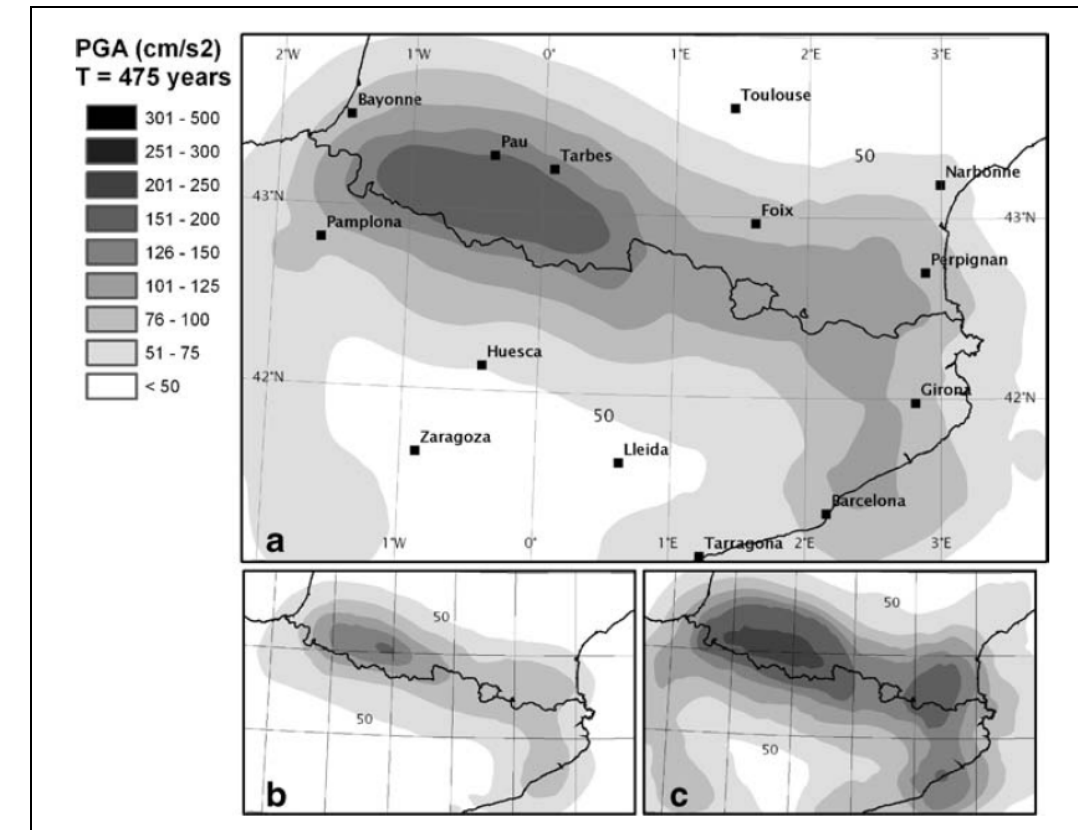


Figure 5.1-27. Acceleration (PGA "Peak ground acceleration") obtained by Secanell et al for a return period of 475 years.

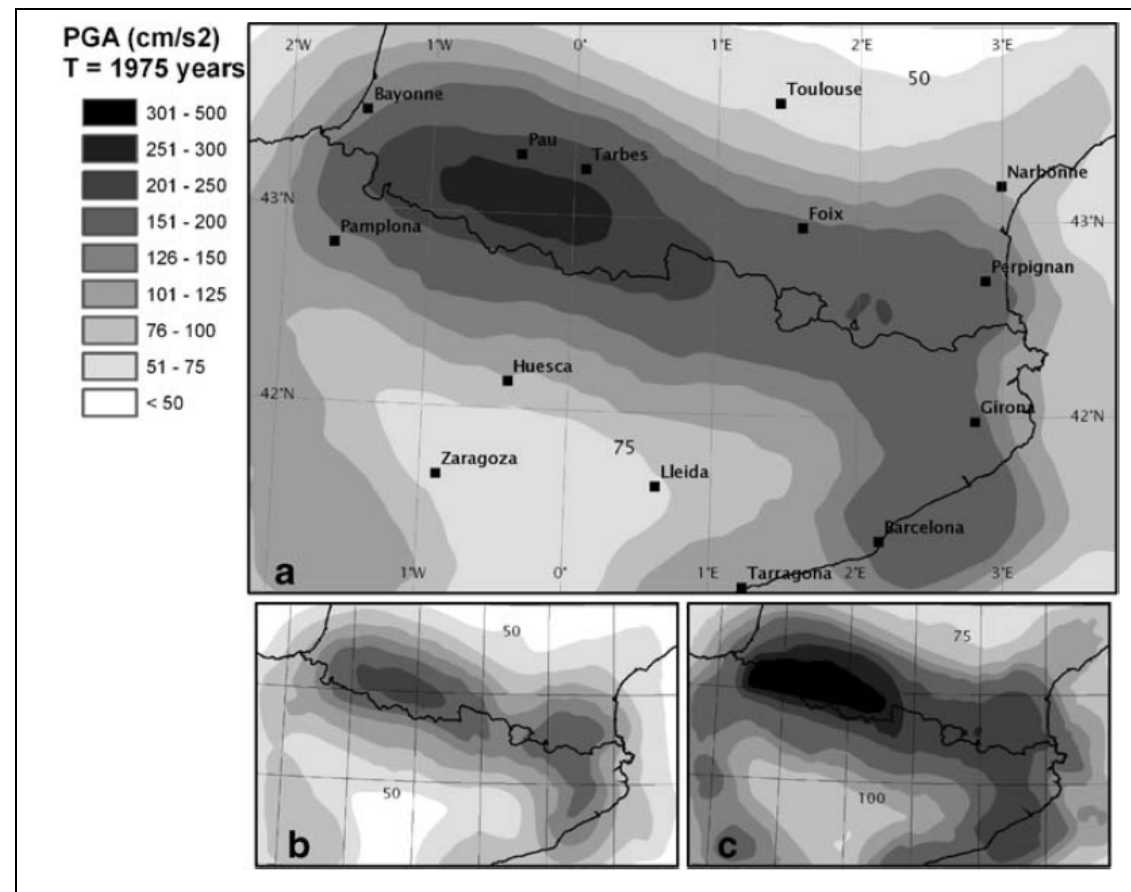


Figure 5.1-28. Acceleration (PGA “Peak ground acceleration”) obtained by Secanell et al for a return period of 1975 years.

It can be deduced from the above results that the maximum acceleration to be expected in the zone for the two return periods analysed is as follows:

- Return period = 475 years; acceleration = 1.26 – 1.5 m/s<sup>2</sup>
- Return period = 1975 years; acceleration = 1.5– 2 m/s<sup>2</sup>

These values are greater than the ones indicated in the Spanish Earthquake Proof Standard NCSR-02, in which the basic seismic acceleration to be considered in this zone is 0.08 g (0.8 m/s<sup>2</sup>).

Similar results have been found in those obtained by the SESAME Project. This project has studied the seismic hazard in a unified way for the whole of Europe. Some of its results can be seen in the next figure. On this map, accelerations are expected in the Pyrenean zone close to the zone that concerns us, ranging from 0.12 to 0.25 g, with a 10% probability of these values being exceeded in 50 years.

In view of these results, the basic acceleration proposal to be used as given by the Earthquake Proof Standard (NCSE-02) is not a very conservative estimate and it is recommended that higher acceleration values be calculated:

- 0.12g – 0.16 g, for return periods of 500 years.
- 0.16g – 0.20 g, for return periods of 2000 years.

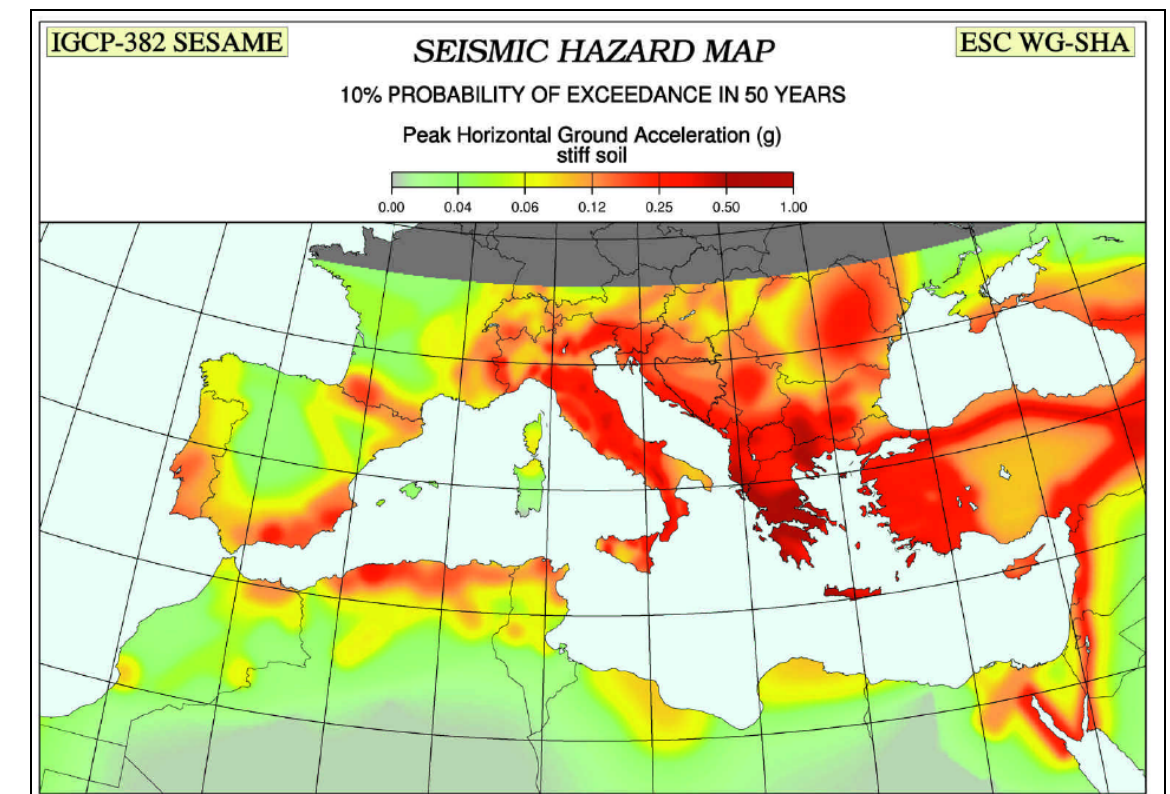


Figure 5.1-29. Seismic hazard map of Europe for the SESAME Project (Jimenez et al, 2001).

### 5.1.5 Summary and conclusions

The seismicity in the zone has been reviewed and updated on the basis of the seismicity data provided by the IGN, as well as the data obtained from the Sisfrance base. These data have been used to conduct both a deterministic and a probabilistic analysis of the seismicity.

An initial analysis suggests that the seismicity in the zone could be characterised by earthquakes with the following properties:

$I_{max} = VII \text{ to } VIII$

$M_{max} = 5 \text{ to } 5.5$

$a_{max} = 0.257 \text{ g}$

The following values are yielded from the probabilistic analysis:

Period	This Study (IGN)	Secanell et al (2003, 2008)
2000 years	7.3	6.8
500 years	6.7	6.4
100 years	6.0	5.8

Where the acceleration values are concerned, the Spanish Earthquake Proof Standard (NCSE-02) associates values close to 0.08 g with the tunnel site and an acceleration value of 0.07 g with the village of Canfranc. The maximum acceleration values included in that standard reach 0.16 g, so we would be a long way from the worst cases, but that does not mean to say that these values are of no significance.

However, an analysis has been carried out of recent studies conducted in the zone in which greater acceleration values have been yielded. Taking these results into

account and bearing in mind the similarity between the data concerning the expected magnitude for different periods, it is recommended that the following design accelerations be used:

- 0.12 g – 0.16 g, for return periods of 500 years.
- 0.16g – 0.20 g, for return periods of 2000 years.

## 5.2 CURRENT STRESS FIELDS IN THE PYRENEES

This paragraph has been prepared by Mr. Ramón Capote, Professor of Tectonics of the Geological Faculty of the Universidad Complutense de Madrid.

### 5.2.1 Introduction

The aim of this section is to assess the potential tectonic regional stress fields that might have a bearing on the stress states in the Somport Tunnel zone.

A certain number of papers that have been published endeavour to establish the natural stress fields that affect the Pyrenean Range as a whole. Some of these works consider the orientation and the tectonic regime during the Alpine compression era, that gave rise to the formation of the *Cordillera*: we consider these stress fields to be paleostresses, different from the current ones. However, an awareness of these serves to give greater insight into the transmission of intraplate stresses in this sector, thereby helping to provide an interpretation of the current stress field. A comprehensive synthesis of the Alpine paleostresses can be found in a recent work (Liesa and Simón, eds.) (2009). The method used involves analysing the geological data, specifically establishing the paleostress tensor by means of fault population analysis.

As far as the current stresses are concerned, the problem revolves around the relative lack of reliable and available geological data on the current tectonic activ-



ity, which means that it is necessary to resort to other types of data. Two main courses of action have generally been followed when establishing the current stress field: establishing the stress tensor by analysing the earthquake focal mechanisms and establishing the orientation of the main stress axes on the horizontal plane on the basis of the ovalisation and “breakouts” from oil boreholes. Information about the stress fields has been obtained from several works that have been published, but the complexity of the results has prompted us to make our own interpretation of the data published.

### 5.2.2 The Alpine paleostresses

According to Liesa and Simón (2009), the Alpine paleostress fields have developed throughout time and are a result of the overlaying of several intraplate stress fields transmitted from a distance by tectonic stresses that were generated at the Iberian plate boundary. These overlying fields are as follows:

Intraplate stress field (ESE to WNW). Caused by a combination of Mid-Atlantic ridge stress and compression on the eastern boundary of Iberia, from the Eocene.

Stress field (NE to SW). Caused by a compression on the northern boundary of Iberia and the Mid-Atlantic ridge), without there being any compression transmitted at that time from the SE of the Iberian subplate. This stress field is the one that deforms and uplifts the Pyrenean Range and the Iberian Cordillera, between the Eocene and the Oligocene. In the Pyrenees, its exact direction is NNE to SSW, whereas in the Iberian Cordillera it is NE to SW.

Stress field NW-SE to NNW-SSE. Caused by a compression of the Mid-Atlantic ridge and a compression from the SE boundary of Iberia. It dates back to the Oligocene to Lower Miocene and is the stress field that is responsible for the deformation and elevation of the Central System.

Intraplate stress field (NNE to SSW) affecting the Pyrenees, the Ebro Basin and the eastern centre-sector of the Iberian Cordillera. It dates back to the Oligocene to

Lower Miocene and it is caused by a compression at the northern boundary of Iberia, without the Mid-Atlantic ridge force being important.

Figure 5.2-1 shows the general orientation of the stresses affecting the Sub-Pyrenean zone and the Iberian Cordillera within the Pyrenean stress field, NE to SW (Eocene to Oligocene).

### 5.2.3 Establishing the stress tensor by analysing the seismic focal mechanisms in the region

The data coming from different studies carried out in the range as a whole and in specific areas. Data from the earthquake focal mechanisms included on the Geotectonic Map of France (Grellelet, 1993) and from the Sigma Project (Herraiz et al, 2000) have been used in the general work. The data from 9 scattered earthquakes (Earthquakes 41, 47, 49, 55, 57, 61, 62, 67 and 69, Figure 5.2-2) have been extracted from the former, three located at the eastern end, a couple of them from the central zone, close to the tunnel, and the other four from the western sector of the Cordillera. The latter 6 earthquakes have been brought together for analysis purposes into one single central-western group. The ones from the SIGMA Project (Figure 5.2-3) amount to 23, which we have also grouped into two sets, one western set, with 4 events (earthquakes 129, 130, 131 and 132), and the other central-western, with the other 19 earthquakes (between 110 and 128). Although some earthquakes are common to both groups, the focal mechanism solution in them differs considerably, so we have analysed them as two independent groups.

The overview that is obtained from the two aforementioned earthquake groups is too general and undefined, even for the scale of the Cordillera. Fortunately, some earthquake studies have been conducted in an area lying close to Somport. It is the area between Pau, Lourdes and Bagneres, to the north of the tunnel zone (Rigo et al, 2005). This study aims to correlate the earthquake focal mechanisms not only with the stress field but also with the North Pyrenean Fault activity. The work has been carried out from a population of 30 earthquakes that took place



between 1999 y 2003. Our analysis focuses particularly on the latter data (Figure 5.2-4).

Several calculation methods and computer programs have been used, developed to solve the reverse problem, stress tensor inversion. To be specific, the following programs have been used: TENSOR by Delvaux (Delvaux and Sperner, 2003), the program MyFault, by Pangea Scientific (Michael, 1984 and 1987), and CRATOR (by Vicente). Both nodal planes from the focal mechanism solution have been considered when analysing the focal mechanisms, in view of the fact that *a priori* we had not established the plane for the real fault. Figure 5.2-5 and Figure 5.2-6 show examples of data analysis.

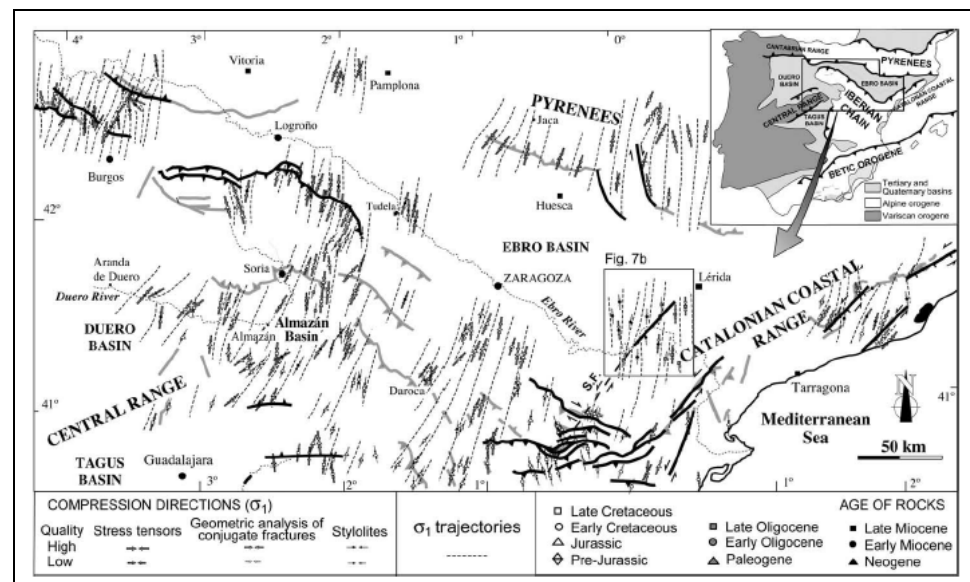


Figure 5.2-1. Paleostress paths in the Pyrenees and the Iberian Range during the Eocene compression. Taken from Liesa and Simón (2009)

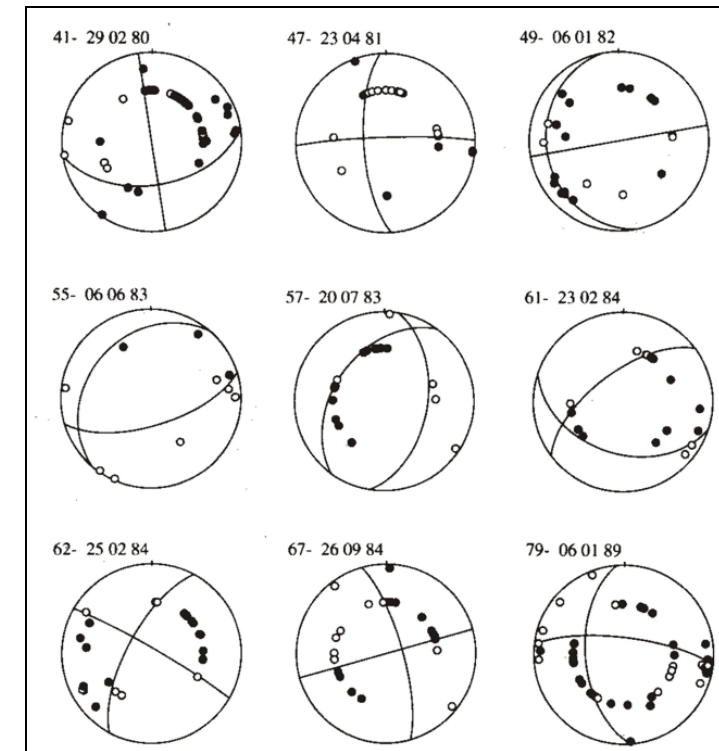


Figure 5.2-2.- Focal spheres of the 9 earthquakes analysed taken from the geotectonic map of France (Grelet et al 1993)

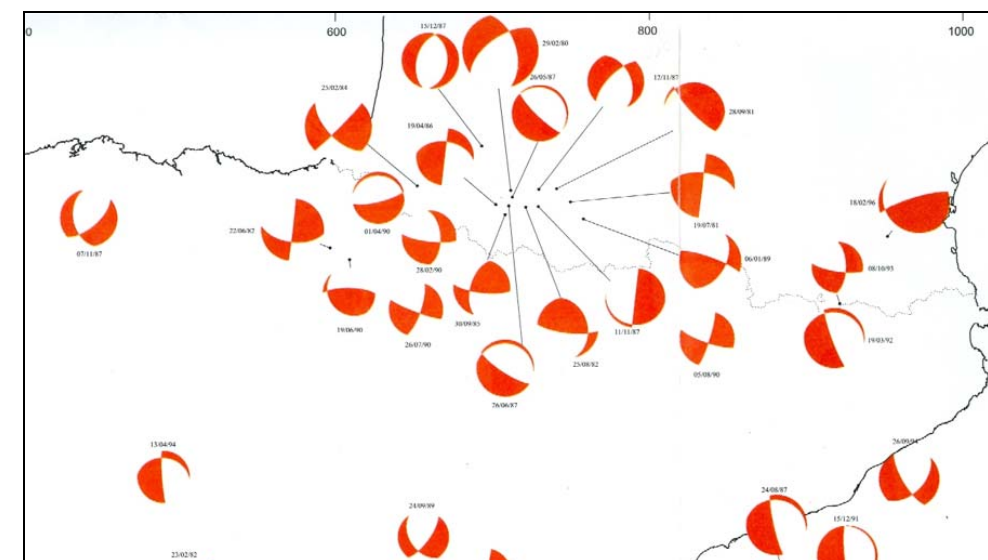


Figure 5.2-3.- SIGMA Project Catalogue (Herraiz, 1998)

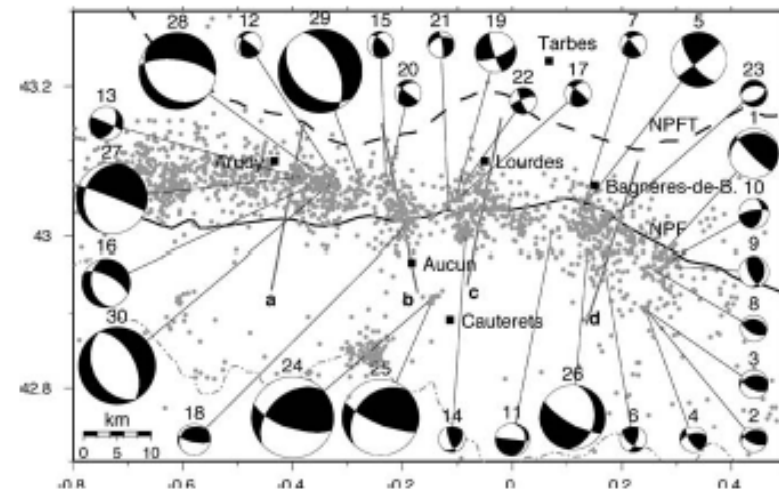


Figure 5.2-4.- Focal spheres of the earthquakes analysed taken from the work by Rigo et al (2005)

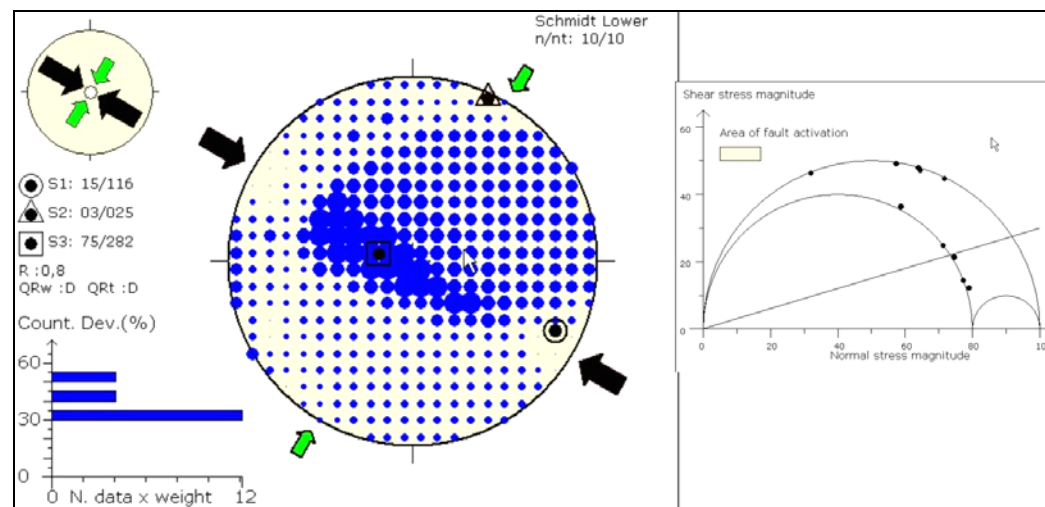


Figure 5.2-5.- Example of graphic outputs when analysing earthquake focal mechanisms using the TENSOR Program by Delvaux applied to the earthquakes in the Aucun Zone (Central Pyrenees). On the left is the Right Dihedra diagram. On the right is Mohr's circle. It is a tectonic regime of the reverse type, with SHmax running NW to SE.

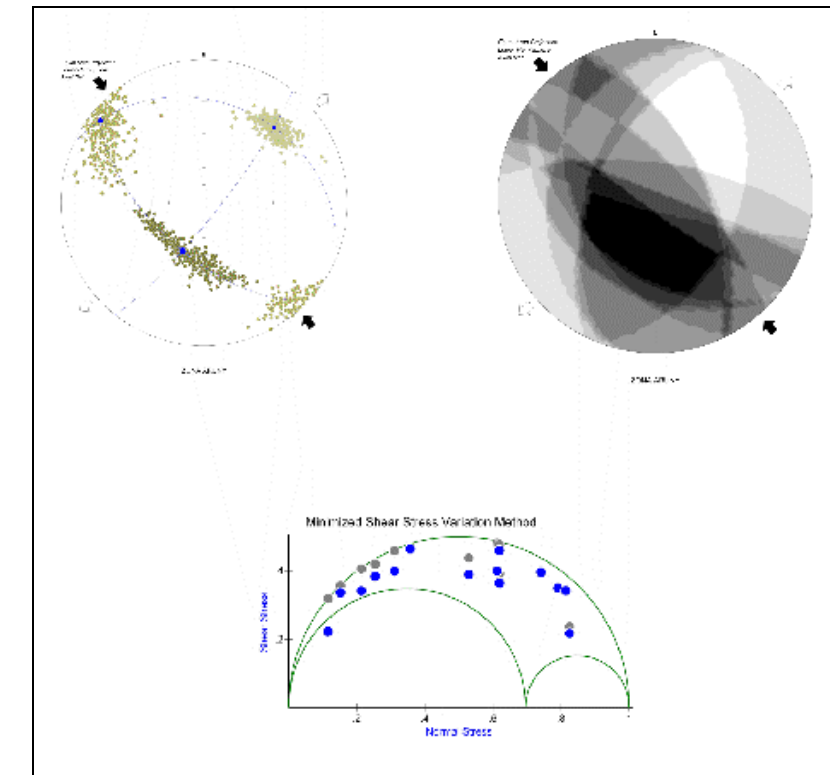


Figure 5.2-6.- Right Dihedra Diagram, axes for the stress tensor (indicating errors) and Mohr's circle for the Arunty earthquakes. MyFault Program.

The focal mechanisms yield a heterogeneous table of the deformation and of the regional stress fields, with a certain amount of incompatibility between tensors associated with the set of faults, as if two different tensors were acting in the region. This leads, for example, to the right dihedra diagrams not being very indicative. That is why it has been necessary to examine the results and try to incorporate them into a consistent table. The following figures show the diagrams that are yielded by the analysis.

The analysis of the earthquakes on the Neotectonic Map of France (Figure 5.2-7) using the Delvaux method gives as a strike-slip regime result for the Western-Central sector of the Pyrenees, with a compressive axis running from NNW to SSE (25/153) and an ENE to WSW (05/245) horizontal extension direction. A similar result is obtained with the MyFault program, that is to say, a shortening direction closer to N to S yet still NNW to SSE and an ENE to WSW extension (Figure 5.2-8). In the eastern sector, the result yielded by the TENSOR program by Delvaux is

also a strike-slip regime with an NNW (N153) compression and an extension running towards N245. With the MyFault program, the direction  $\sigma_1$  once again approaches North (N170).

However, the analysis of the earthquakes data considered in the SIGMA Project yields a field with the shortening direction as in N13, but the fact that the number and the events used in this case are different must be taken into account (Figure 5.2-7). The tectonic regime is also of the strike-slip type for the western sector, but the direction of  $\sigma_1$  is N27, close to N to S, but lying in the NE quadrant. In the eastern zone, the regime is not as clearly defined, with a tensor index of 0.5 and the direction of the main stress axis is N8.

These results are scattered and correspond to data obtained from earthquakes located beyond the environment lying close to the Somport Tunnel. That is why we have resorted to closer and more detailed data that are contained in the work down by Rigo et al (2005). The results by zones are as follows:

- Arudy Zone. The TENSOR program has an extensional regime whose extension direction as in 228 (Figure 5.2-8). The direction of the maximum axis is like that according to N138. The tensor has the index  $R = 0.5$ . The focal mechanisms are predominantly of the normal fault type, in accordance with the tectonic regime concerned. The MyFault program gives a tectonic regime with a NE to SW extension and a NW to SE compression, which is compatible with the aforementioned result. This sector lies to the West of the tunnel zone and there is every indication that there is a  $\sigma_1$  axis in the NW to SE and a predominant extension tectonic regime.
- Aucion Zone. The regime is clearly compressive in this zone (Figure 5.2-8) according to the results of the TENSOR program, with a direction  $\sigma_1$  according to N116 and  $\sigma_2$ , according to N25 ( $R = 0.8$ ). The MyFault program obtains similar results, but once again with the main axis  $\sigma_1$  nearer to N to S. If one observes the individual focal mechanisms in this zone, it can be seen that although some of them are normal faults and strike-slip faults, most of them are reverse faults.

- Lourdes Zone. In this zone, the tensor clearly changes in such a way that the axis  $\sigma_1$  remains facing NE to SW (14/235), whereas the minimum axis  $\sigma_3$  is facing as in 29/333 (Figure 5.2-8).  $R = 0.25$  for the tensor calculated. It can be seen in Figure 5.2-8 that the predominant focal mechanisms are of the reverse type, although there are also strike-slip and normal mechanisms.
- Bagneres Zone. In this sector, the results yielded by the TENSOR program indicate that there is a compressive regime with the maximum horizontal stress running in direction N80, and another somewhat slighter compressive direction N170 (Figure 5.2-8), as well as an index  $R = 0.67$ . A compressive regime is also obtained with the MyFault program but with a maximum compression permuting to the orientation N150 and the lower horizontal compression into N58 ( $R = 0.32$ ). This compressive regime in two horizontal leads to the existence of focal mechanisms that are predominantly of the reverse type, only two being in normal regime.

#### 5.2.4 Interpretation of the results

By and large, the results of the population analysis of the focal mechanisms for this sector are consistent with the results of the analysis of the earthquakes from the Neotectonic Map of France. A maximum horizontal shortening direction of  $\sigma_1$  can be deduced running NW to SE (between N138 and N116), with an extensional regime in the westernmost part (Arudy) and one that is clearly compressive in the Aucion area. In the Lourdes Zone, there is clearly a major general change, and it goes on to be a compressive regime, but with the axis of maximum horizontal force facing a different way, in the NE quadrant, between N55 and N80.

The seismicity of this sector between Arudy and Bagneres was traditionally associated with the activity of the North Pyrenean fault, a feature running approximately E to W, which constitutes the limit between the Iberian plate and the Euroasian plate during the Alpine orogeny). The work done by Rigo et al (2005) considers the distribution of focal points at depth and comes to the conclusion that the earthquakes occurred on a plane that dips to the North down to a depth of as much as



18 km and this does not in the same zone as the North Pyrenean fault. Furthermore, this same work stresses the fact that the deformation (and associated seismicity) in this sector of the Pyrenees is very heterogeneous, with no clear and single tectonic regime, to the extent that there is a maximum main stress  $\sigma_1$  in at least two directions that are perpendicular to each other, one running NW to SE and the other running NE to SW. They also point out that the extension axes are more frequently orientated in a NE to SW direction. The complexity of the seismicity would be accounted for by the combined effect of the changes in the pressure of the cortical fluid and triggering phenomena.

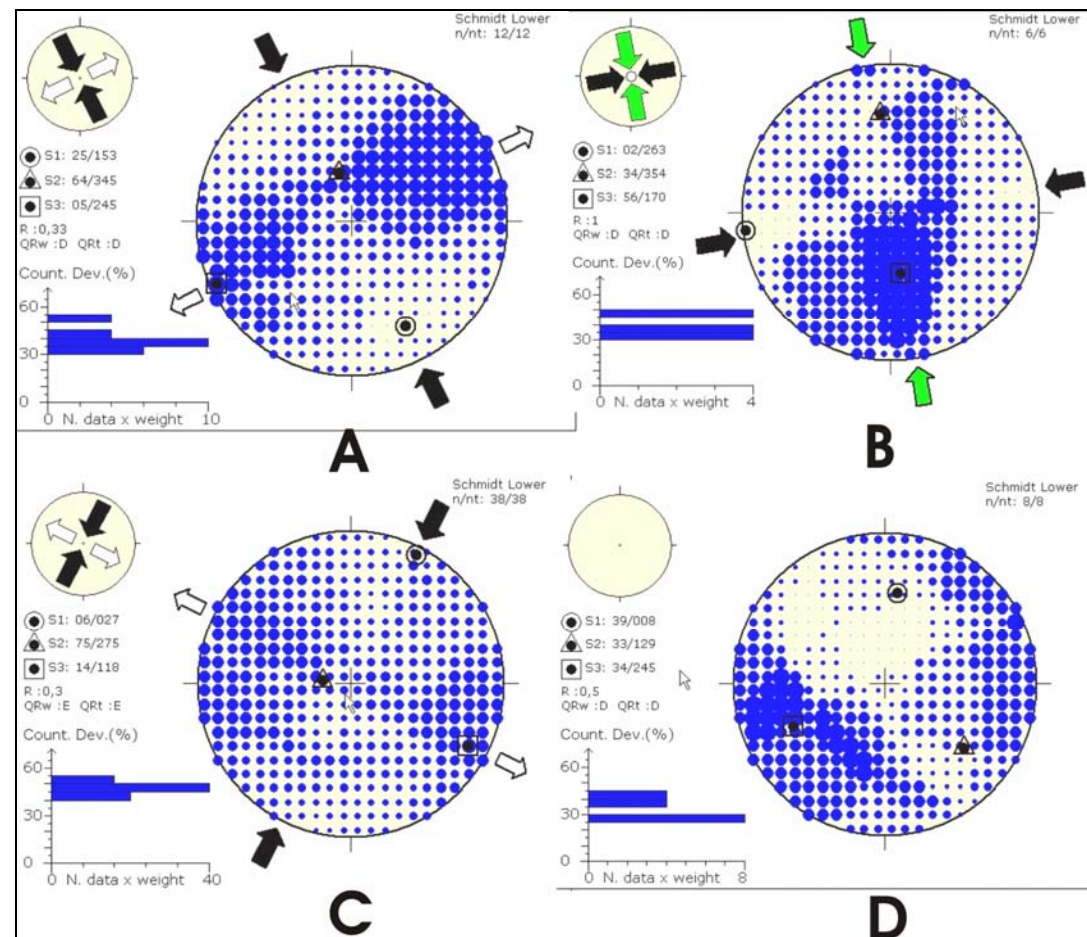


Figure 5.2-7.- Stress tensors obtained using the TENSOR Program using earthquake data taken from the Geotechnic Map of France (A and B) and from the SIGMA Project (C and D). A and C belong to the Central and Western Pyrenees. B and D are from the eastern third of the Pyrenees.

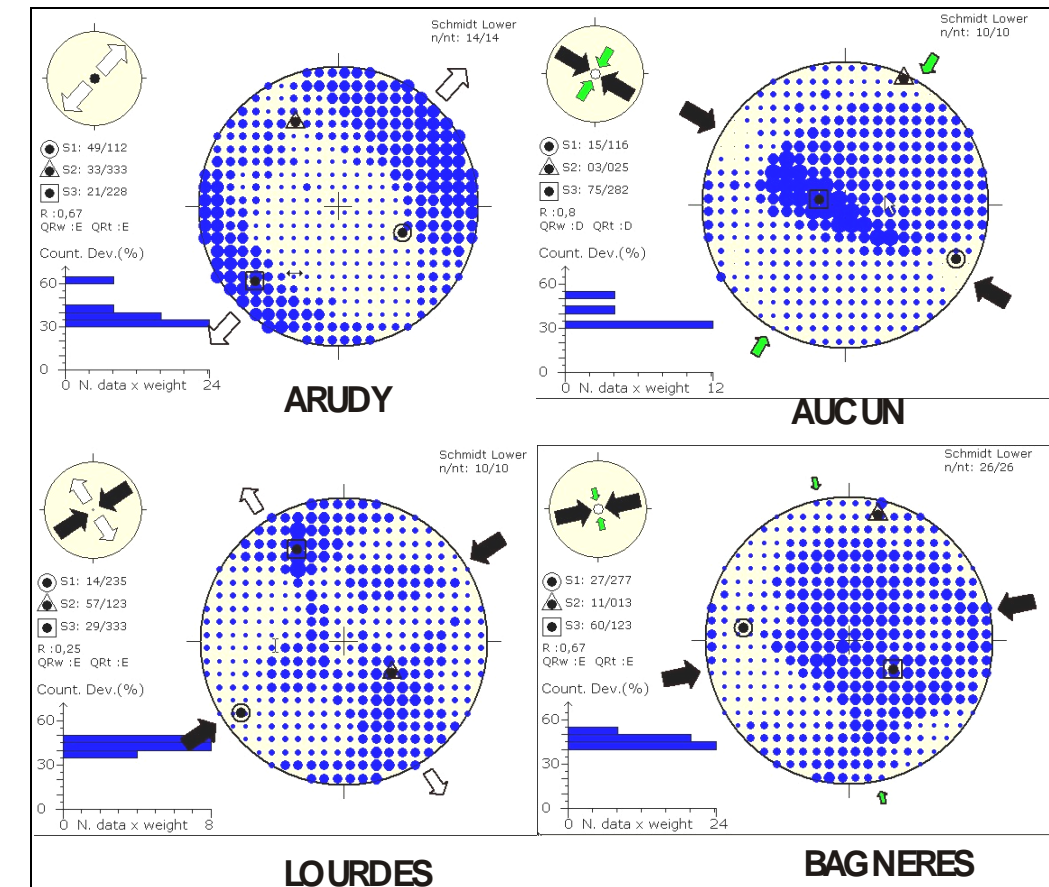


Figure 5.2-8- Right Dihedra Diagrams and stress tensors for the zones analysed using the data provided by Rigo et al (2005).

We are of the opinion that the NW to SE direction of the axis  $\sigma_1$  in the western part of Arudy and Aucun must be consistent with the stress direction of the westernmost zone of Europe, a stress field transmitted at a distance by the Mid-Atlantic Rift. A change of direction in the maximum stress to the NE quadrant took place between Arudy and Lourdes as well as from the Bagneres the tectonic regime, compressive, involved a field with  $\sigma_1$  (ENE to WSW). This change is also consistent with a change in orientation of the concentration of epicentres, which goes from E-W to NE-SW. This field is more in relation with the stresses transmitted from the alpine collision borders. The complexity of this zone is a consequence of



the interference of the two fields and the aforementioned triggering phenomenon and the changes affecting the fluid pressure.

The work done by some authors also reveals this complexity. In the central and eastern part of the Pyrenees, Lindo et al (1996) obtain two maximum main stress directions  $\sigma_1$ , on the basis of an analysis of a set of earthquakes that took place between 1977 and 1996, one running NW to SE (Central Zone and South Pyrenean), and another one, which affects the northernmost part of the Eastern Pyrenees, running NE to SW. Herranz et al (2000) also detect a change of orientation in the maximum stresses from the eastern sector to the westernmost sector. However, they explain it as one single field with progressive variation in the stress paths.

#### 5.2.5 The data concerning in situ stress

Very few works have been done in Spain to describe the current stresses using instrument techniques, and in situ stress data are particularly few in the Pyrenees as a whole. The most comprehensive work was done by Jurado and Müller (1997). It is based upon the analysis of breakouts from oil boreholes, with a view to obtaining the orientation of the horizontal stress axes. It has been shown that the horizontal stress is greater than the vertical stress, which can be put down to a field of compressive tectonic stresses. The maximum horizontal stress axis SH, is obtained from the orientation of the long ovalisation axis of the boreholes. In this study only 7 boreholes are within the Pyrenees and of these, 3 (*Cantonegro*, *Cadialso* and *Traspaderne*) lie within what is referred to as the Western Pyrenees, which is, in fact, the Basque-Cantabric Cordillera. 4 boreholes are analysed within the actual Pyrenees (*Surpirenaica-1*, *Cajigar-1*, *Comilos-1* and *Serrat-1*).

The depths at which the ovalisation processes are to be found range from 50 to 3,220 meters and interpreting the results is also a very complex process. The results from the *Surpirenaica* and *Cajigar* boreholes, lying in the central zone of the range, give a NW to SE orientation for the axis of maximum horizontal stress SH: N115  $\pm$  36 for the *Surpirenaica-1* borehole and N127  $\pm$  6 for the *Cajigar-1* borehole.

The results are different for the other two boreholes. *Comilos-1* gives an SH of 81  $\pm$  23, whereas the *Serrat-1* borehole gives 61  $\pm$  42. In these two, in spite of a variability in the SH, two peaks can be observed, one NE to SW and the other NW to SE. These results are fairly consistent with the results of the focal mechanisms analysis: One is an orientation of  $\sigma_1$  NW to SE in the western and central sector, corresponding to the field caused by the Mid-Atlantic ridge and the other NE to SW, more represented in the eastern sector of the range, although there are also NW to SE compression directions.

In the Aquitaine Basin, the foreland basin in the central and western sector of the Pyrenees, the ovalisation processes of a large number of oil boreholes have also been studied (Bell et al, 1992), providing stress orientation data in a zone lying close to the Pyrenean range that are relevant to this study. The results indicate that the stress fields are complex, with two predominant maximum horizontal stress directions (SH), NE to SW and NW to SE. The zones in which each one is predominant are interbedded with each other, and they cannot be clearly separated. The interpretation stems for the idea that two stress fields are involved in this zone, whose origins lie in different external forces, the aforementioned stress of the Mid-Atlantic ridge and the compressive stress field of Central Europe. The fact that they alternate with another one is interpreted as being indicative of the fact that the two main horizontal stresses have a very similar value, in such a way that the horizontal stress ellipse is almost circular in nature. The slight local variations could thus be made to permute in the position of the two axes.

#### 5.2.6 Results of stress orientation using the CRATOR program and the Right Diedra

##### 5.2.6.1 Right Diedra Method

This is one of the most extensively used methods. It was devised by Pegoraro (1972) and can be applied directly not only to faults but also to earthquake focal mechanisms. It is a geometrical method that is based upon limiting for each fault,

the space zones that are compatible where both compression and extension are concerned, superimposing these fields in stereographic projection.

In view of the fact that the axis  $\sigma_1$  is located in the compressive diedro and that the axis  $\sigma_3$  is located in the extensive one, when a set of faults has been activated under the same stress regime, the two main axes of maximum and minimum stresses must be included in the same diedro for all the focal mechanisms. In cases where there are numerous focal mechanisms, a compatibility percentage is used. The program Cratos 1.0 was used for this study.

After it was developed, several authors carried out works aimed at improving the right diedra method. This led to a series of conditions being imposed when applying the method:

- The maximum compression and extension axes must be perpendicular
- The two axes must be in opposing pairs of diedra

The advantages of this method are that they provide a rapid and clear display of the positions of the maximum compression and extension zones.

### 5.2.6.2 Stress Tensors

The following populations of focal mechanisms have been analysed individually:

- The nine planes coming from the French Catalogue
- 23 planes coming from the SIGMA Project; in the latter case, the two potential fault planes were analysed separately.
- 55 planes coming from a joint analysis of the above populations.

The following procedure was followed with each one of the populations analysed. These analyses were carried out using the program (CRATOS)

A series of figures are shown below that have been extracted using this program for each one of the cases.

a) Data extracted from the French Catalogue.

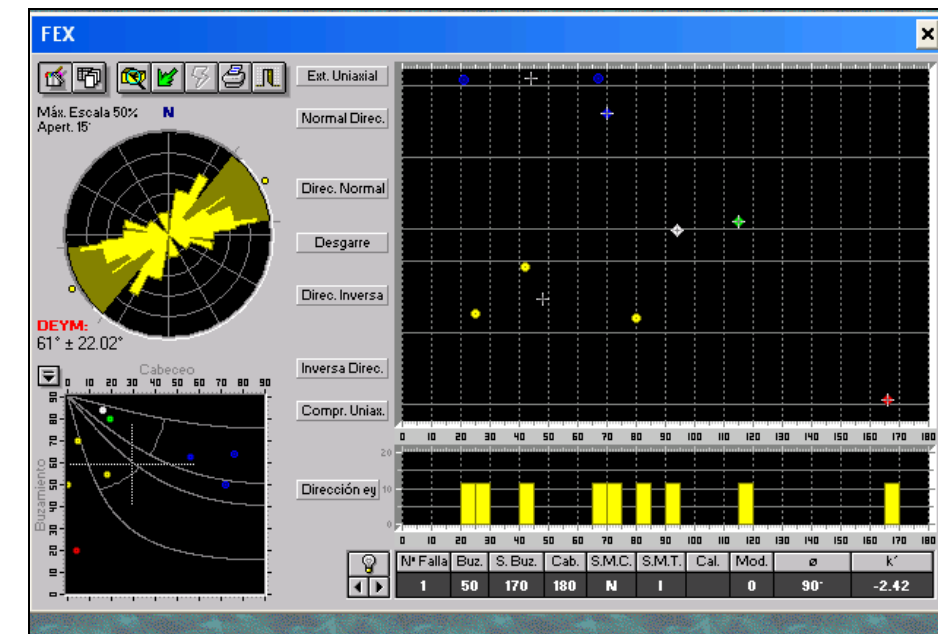


Figure 5.2-9.- The figure shows a representation of the planes selected on a plunge / dip graph. The stress regime that was generated and the main shortening direction ENE to WSW is also shown for each one of the faults.

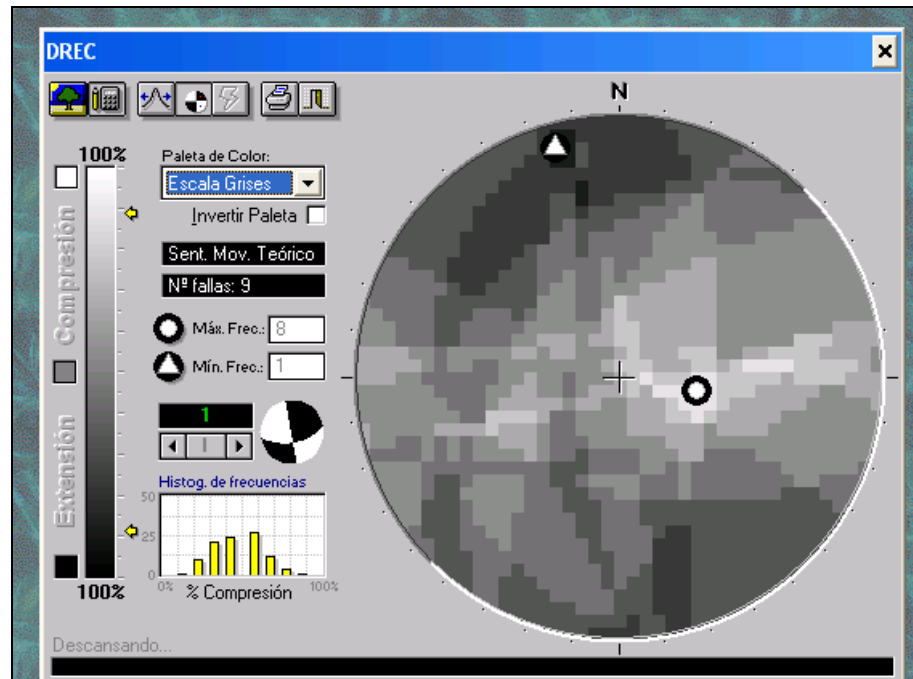


Figure 5.2-10.- This figure shows the right diehedral method, where the compression and extension quadrants can be observed.

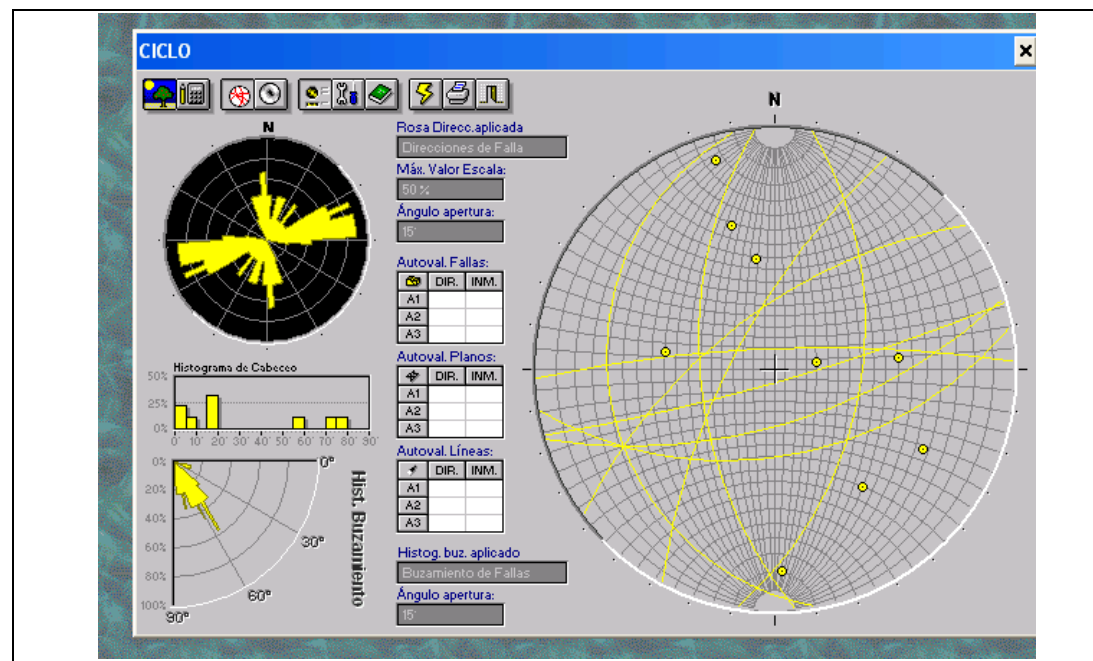


Figure 5.2-11.- This figure shows a block diagram of dips, from which it can be deduced that most of the planes analysed have raised dips. It can likewise be deduced that there are two populations of planes, a first one with an ENE to WSW orientation, which is close to the maximum shortening direction, and a second population that is almost N to S. The

dip block diagram also shows an average dip close to 60°, which could indicate that in the first of the cases, the faults would be strike-slip faults, whereas in the second population they would be normal faults.

b) Data from the SIGMA Program (Population 1).

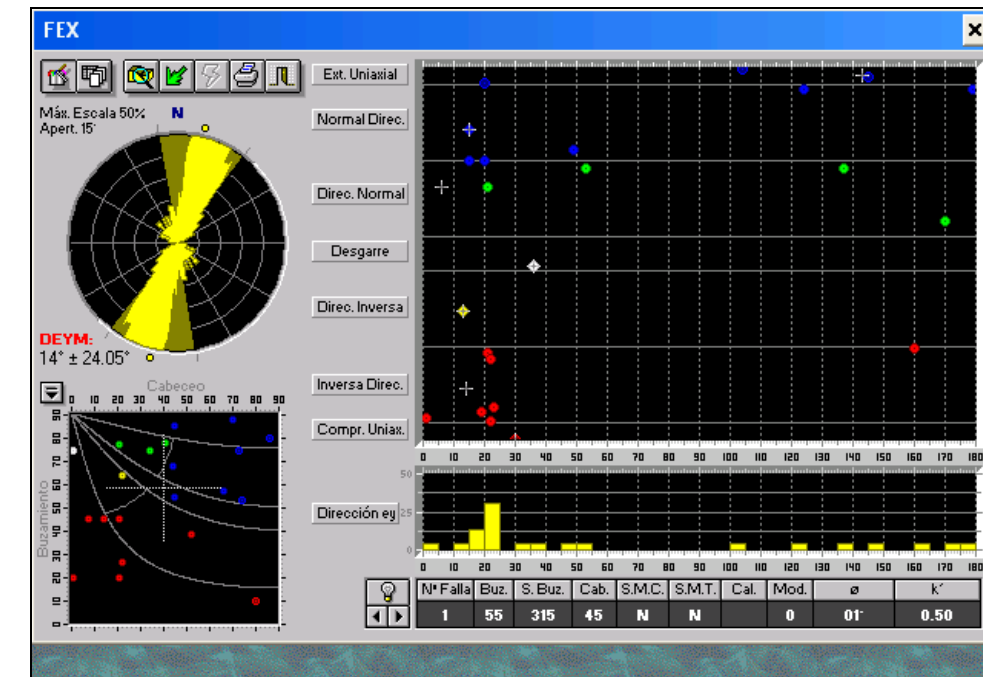


Figure 5.2-12.- This figure shows a representation of the planes selected on a plunge / dip graph. It also shows, for each one of the faults, the stress regime that has generated it and the main shortening direction close to N to S.



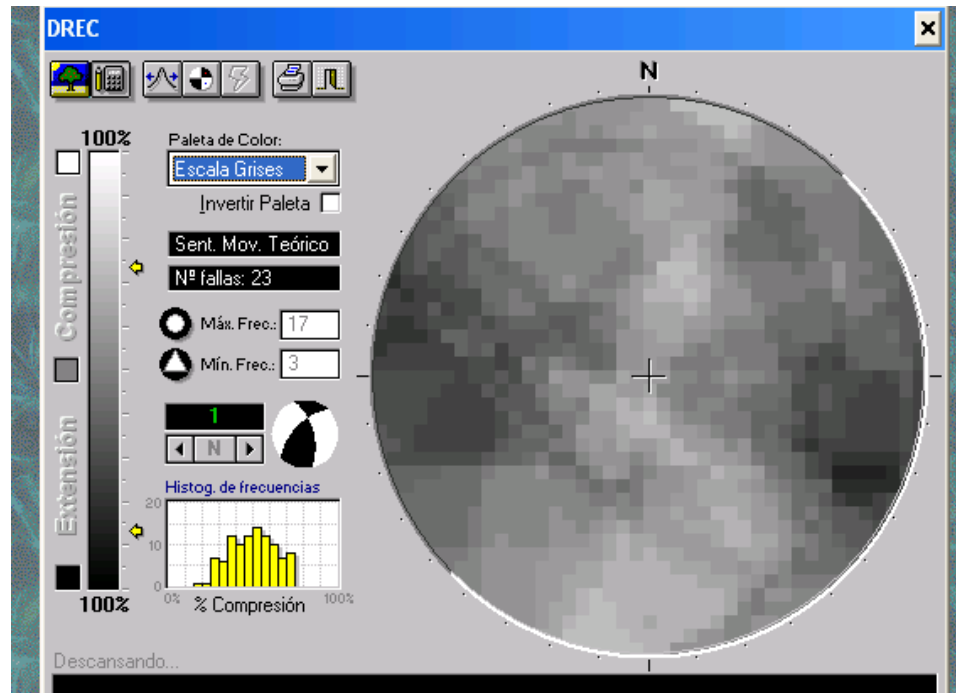


Figure 5.2-13.- This figure shows the right diedra method, in which the compression and extension quadrants can be observed.

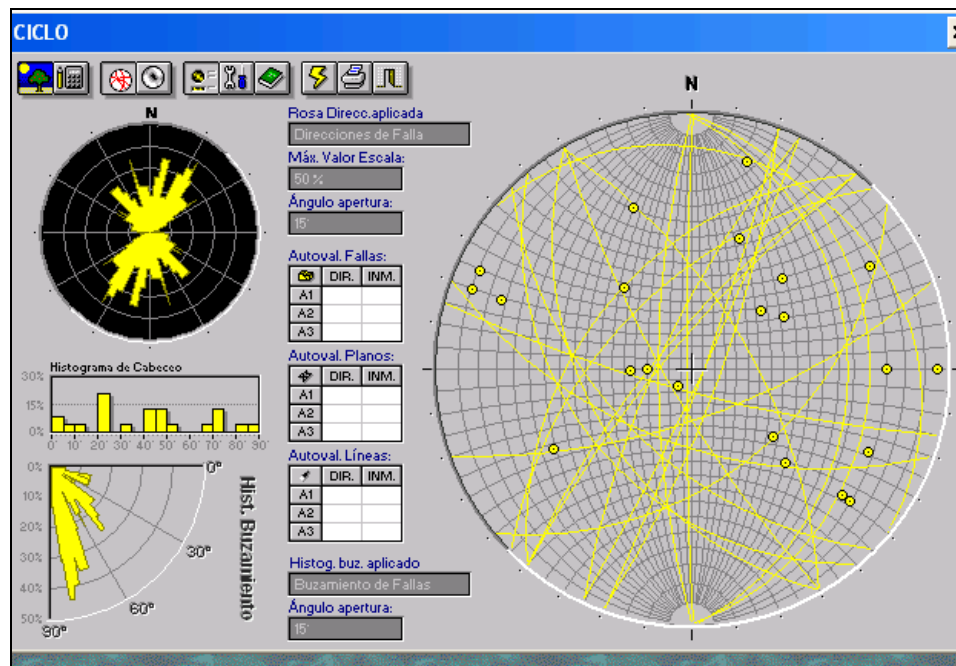


Figure 5.2-14.- This figure shows a block diagram of dips, from which it can be deduced that most of the planes analysed have raised dips. It can likewise be deduced that there are two populations of planes, a first one with a NNE to SSW orientation, with certain variations, which is close to the maximum shortening direction. The dip block diagram also

shows scattering in the dip that would indicate normal, strike-slip and reverse faults, the former two clearly predominating.

c) Data from the SIGMA Program (Population 2).

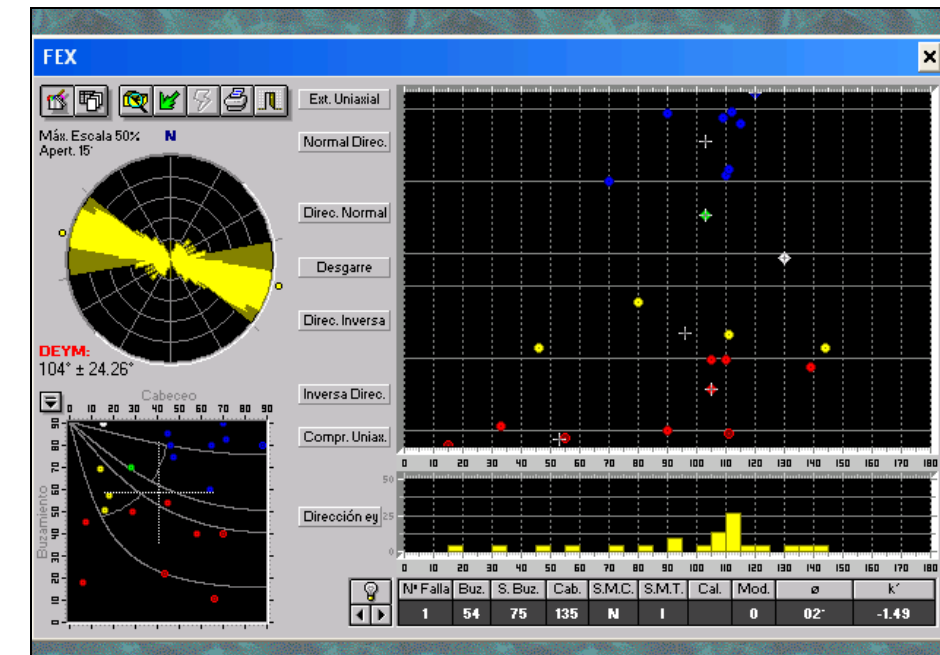


Figure 5.2-15- The preceding figure shows a representation of the planes selected on a plunge / dip graph. It also shows, for each one of the faults, the stress regime that has generated it and the main shortening direction close to E to W, which is to be expected given that it is the auxiliary plane.

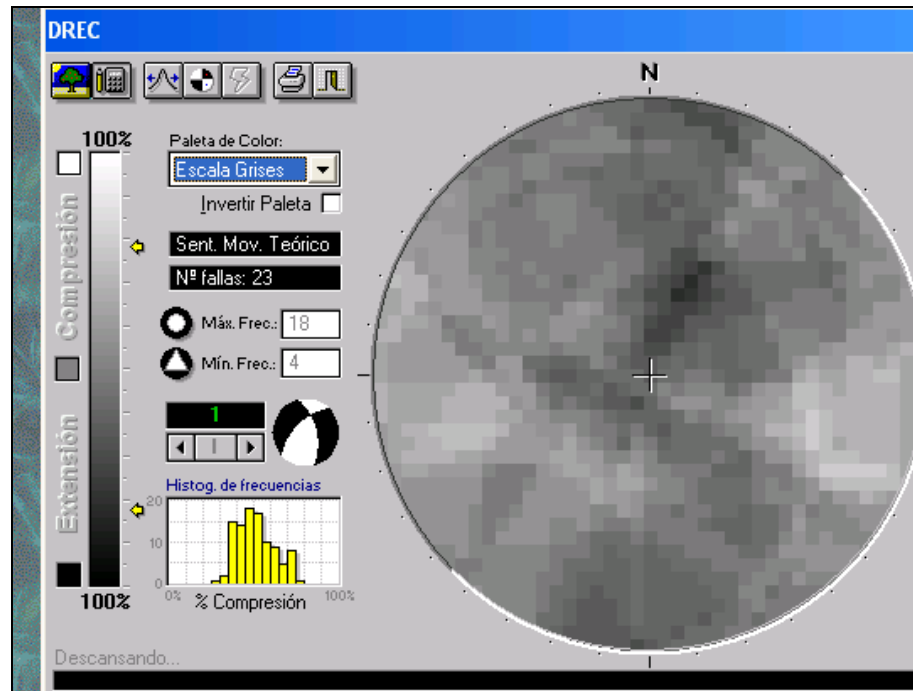


Figure 5.2-16. This figure shows the right diedra method, in which the compression and extension quadrants can be observed.

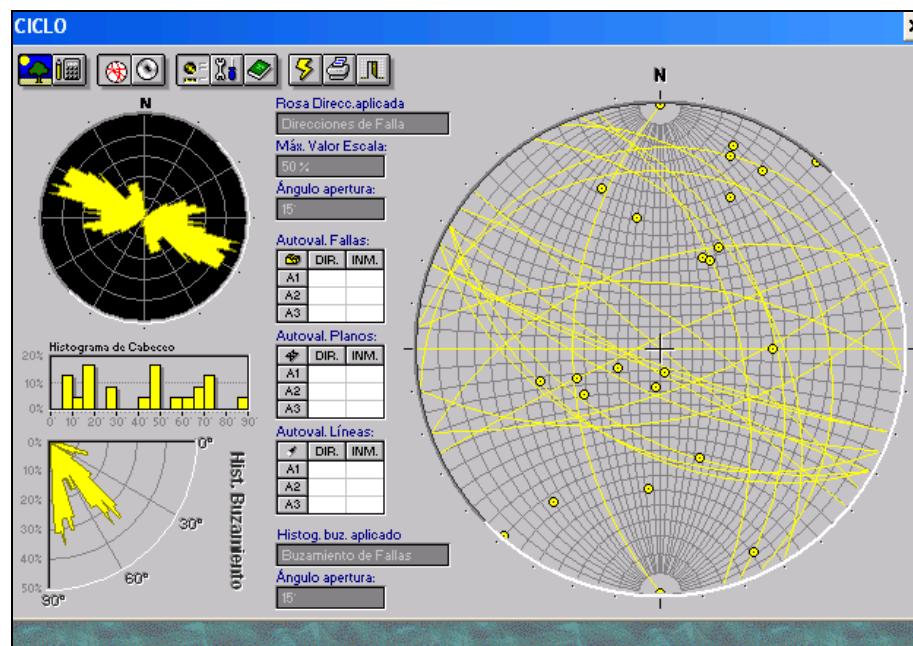
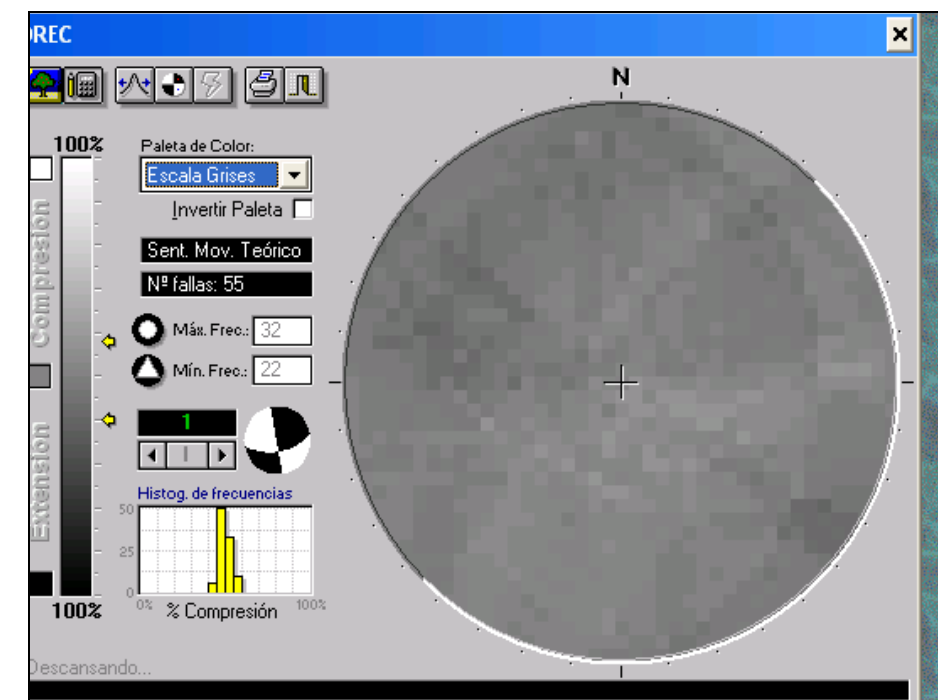
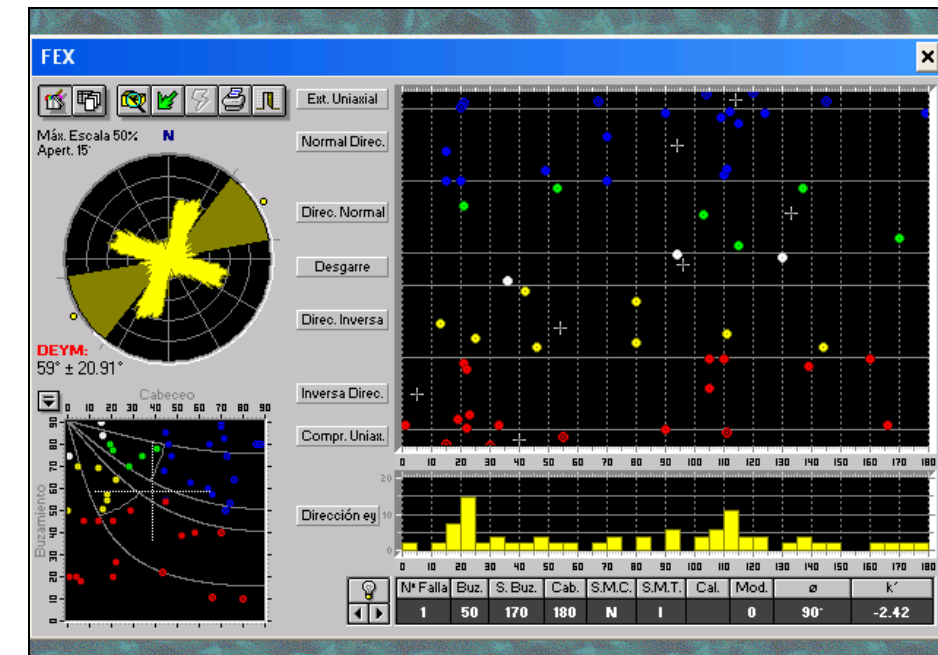


Figure 5.2-17.- This figure shows a block diagram of dips, from which it can be deduced that most of the planes analysed have raised dips. There is also a diagram of roses for the direction of the planes analysed, in which it can be observed that there is a main direction WNW to ESE, with certain variations, which is close to the maximum shortening direction.

The dip block diagram also shows scattering in the dip that would indicate normal, strike-slip and reverse faults, the former two clearly predominating.

d) Joint analysis of the data



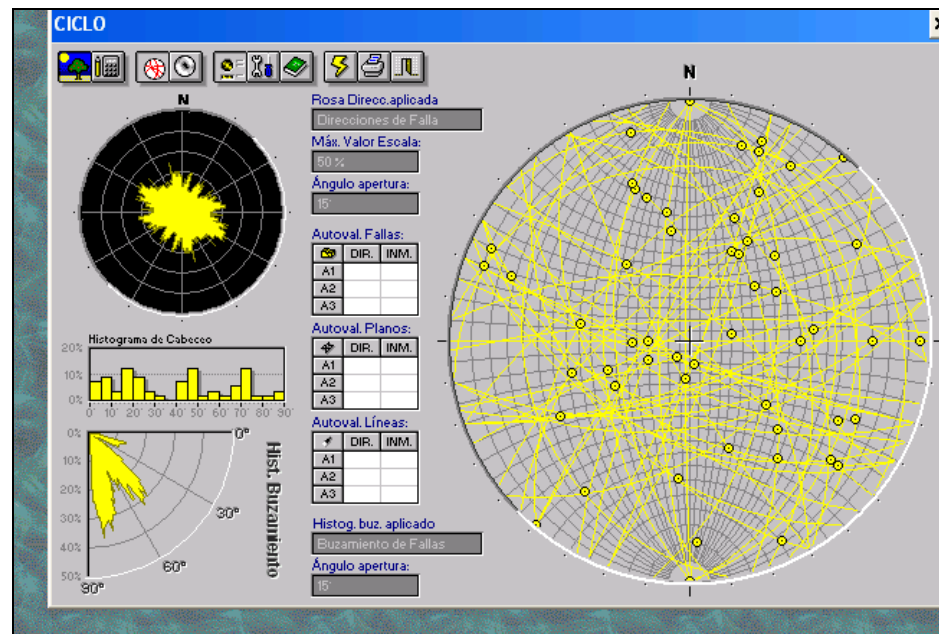


Figure 5.2-18.- In this case a great of scattering was observed as a result of representing different stress fields depending on which plane was selected, in the case of the data coming from the SIGMA Program. Therefore, it is not possible to reach any major conclusions.

### 5.2.7 Conclusions

The earthquake focal mechanisms have been analysed in the Pyrenees with a view to obtaining data about the current tectonic stress fields that are responsible for the tectonic and seismic activity at the present time. The analysis methods have been based upon obtaining the stress tensor that adapts best to the faults that cause the seismicity. Where some methods are concerned, an attempt has been made to find out which of the nodal planes in the local sphere is the fault, but two planes have been taken in others. The analysis has been approached with several tensor calculation programs, CRATOS, MyFault, TENSOR and the Right Diedra by Angelier. The results have been completed with the results obtained from several works that have been published. All these results have proved to be fairly consistent with each other.

Reference has been made to works that establish the stress data by taking *in situ* measurements in the Pyrenees and in the Aquitaine Basin. These measurements were “breakouts” from oil boreholes. The results were found to be consistent with the cortical level data that were obtained from the analysis of the focal mechanisms.

It has been found that the Pyrenean stress fields are complex, appearing to alternate in a complicated way in different zones. Along general lines, a distinction can be made between two main stress lines, one general NE to SW direction and another running from NW to SE, with variations in the details of the orientation. The NW to SE direction, arising from the stress field of the Mid-Atlantic ridge, is predominant in the central and western part of the Cordillera, and the faults can either be strike-slip faults, reverse faults or distensive type ones. In the eastern sector, apart from this direction, the field with SH running NE to SW also appears to a greater extent.

Where the Somport Tunnel zone is concerned, the closest data are for the seismicity developed between the Arudy and Bagnères zones. Both maximum stress directions are found once again in this zone, with the same problems as in the rest of the Cordillera. The zones lying closest to the Somport Tunnel are the Arudy and Auzan zones. The most likely maximum horizontal stress axis (SH) for both is orientated between N112 and N116 (TENSOR Program by Delvaux), although the tectonic regime is rather extensional in Arudy, and it is clearly compressive in Auzan, or N136 to N172 (MyFault Program).

If these results are taken into account, it can be considered that the most likely orientation of the tectonic SH axis is direction  $N136 \pm 25$ . The local effects (topography, lithological change) can bring about modifications to this direction.

These conclusions will have to be confirmed with further rock mass investigations such as in-situ stress tests in boreholes.



## 5.2.8 Bibliography

Angelier, J., and P. Mechler, Sur une méthode graphique de recherche des contraintes principales également utilisable en tectonique et sismologie: La méthode des droites, Bull. Soc. Geol. Fr., 19(6), 1309-1318, 1977.

Arlegui, L. E., Diaclasas, fallas y campo de esfuerzos en el sector central de la Cuenca del Ebro: Relación con el campo de esfuerzos neógenos, tesis doctoral, Univ. de Zaragoza, Zaragoza, Spain, 1996.

Bell, J.S., Caillet, G. and Le Marrec, A. 1992. The present-day stress regime of the southwestern part of the Aquitaine Basin, France, as indicated by oil well data. J. Struct. Geol., 14: 1019-1032

Bordonau, J., Vilaplana, J.M., 1986. Géomorphologie et tectonique récente dans le Val d' Aran (Zone axiale des Pyrénées Centrales, Espagne). Rev. Géol. Dyn. Géogr. Phys. 27 (5), 303-310.

Cabañas, L., R. Lindo, and M. Herraiz, MF96: Un programa interactivo para la determinación gráfica de mecanismos focales, Geogacela, 20(6), 1377-1379, 1996.

Capote, R., G. De Vicente, and J. M. González Casado, An application of the slip model of brittle deformations to focal mechanism analysis in three different plate tectonics situations, Tectonophysics, 191. 399-409, 1991.

Capote, R., Muñoz, J.A., Simón, J.L., Liesa, C.L., Arlegui, L.E., 2002. Alpine tectonics 1: the Alpine system north of the Betic Cordillera. In: Gibbons, W., Moreno, T. (Eds.), The Geology of Spain. The Geological Society, London, pp. 367-400.

Carey, E., Recherche des directions principales de contraintes associées au jeu d'une population de failles, Rev. Géol. Dyn. Géogr. Phys., 21, 57-66, 1979.

Carey, E., and M. B. Brunier, Analyse théorique et numérique d'un modèle mécanique élémentaire appliqué à l'étude d'une population de failles, C.R. Acad. Sci. Ser. D. 279, 891-894, 1974.

Choukroune, P. (1992) Tectonic evolution of the Pyrenees. Annu. Rev. Earth Planet. Lett. 20: 143-158

Choukroune, P., ECORS team, 1989. The ECORS Pyrenean deep seismic profile reflection data and the overall structure of an orogenic belt. Tectonics 8, 23-39.

Cortés, A. L., and A. Maestro, Recent intraplate stress field in the eastern Duero Basin (N Spain), Terra Nova, 10, 287-294, 1998.

Cortés, A. L., and J. L. Simón, Campos de esfuerzo recientes en la fosa de Alfabra- Teruel-Mira, in Aportaciones al Conocimiento del Terciario Ibérico, edited by J.P. Calvo and J. Morales. pp.65-68, Univ. Complutense de Madrid and Museo Nacional de Ciencias Naturales, Madrid, 1997.

Delouis, B., Haessler, H., Cisternas, A. & Rivera, L. (1993) Stress tensor determination in France and neighbouring regions. Tectonophysics, 221: 413-437

De Vicente, G., J. L. Giner, A. Muñoz-Martín, J. M., González-Casado, and R. Lindo, Determination of present-day stress tensor and neotectonic interval in the Spanish Central System and Madrid Basin, central Spain, Tectonophysics. 266, 405-424, 1996.

ECORS Pyrenees Team, 1988. The ECORS deep reflection seismic survey.

Nature 311, 508-511.

Gallart, J., Banda, E., & Daignères, M. (1981) Crustal structure of the Paleozoic Axial Zone of the Pyrenees and transition to the North Pyrenean Zone. Ann. Geophys., 37: 457-480

Giner, J. L., Análisis Neotectónico y Sismotectánico en el Sector Centro-Oriental de la Cuenca del Tajo, tesis doctoral, Univ. Complutense de Madrid, Madrid, 1996.

González de Vallejo, L.I., Serrano, A.A., Capote, R., De Vicente, G. 1988. The state of stress in Spain and its assessment by empirical methods. In: Romana (Ed.), Rock Mechanics and Power Plants. Balkema, Rotterdam: 165-172

Goula, X., L. Talaya, A. Tennens, I. Colomina, I., Fleta, B. Grelle and T. Granier, Evaluació de la potencialitat sísmica del Pirineu Oriental, Terra, 28(11),41-58,1996.

Goula, x., C. Olivera, I. Fleta, B. Grelle R. Lindo, L.A. Rivera, A. Cisternas, and D. Carbon, Present and recent stress regime in the eastern part of the Pyrenees, Tectonophysics, 308, 487-502, 1999.

Grelleet, Ph., Combes, P., Granier, Th., and Philip, H. Sismotectonique de la France Metropolitaine, Mem. Soc. Geol. Fr., vol.I, 76 pp., Mem. de la Soc. Geol.de Fr., Paris, 1993a.

Gregersen, N. Pavoni, O. Stephansson, and C. Ljunggren, Regional patterns of tectonic stress in Europe, J. Geophys. Res., 97, 11,783-11,803, 1992.

Herraiz, M. et al., Proyecto Sigma: Análisis del Estado de Esfuerzos Tectónicos, Reciente y Actual en la Península Ibérica, 240 pp., 2 maps, Cons. de Seguridad Nucl., Madrid, 1998.

Herraiz, M., De Vicente, G., Lindo-Ñauparí, R., Giner, J., Simón, J.L., González Casado, J.M., Vadillo, O., Rodríguez Pascua, M.A., Cicuéndez, J.I., Casas, A., Cabmias, L., Rincón, P., Cortés, A.L., Lucini, M., 2000. The recent (upper Miocene to Quaternary) and present tectonic stress distribution in the Iberian Peninsula. Tectonics 19 (4), 762-786.

IGN, 2006. Servicio de información sísmica del Instituto Geográfico Nacional de España (<http://www.ign.es/ign/es/IGN/SisIndice.jsp>)

Jurado, and Müller (1997) Contemporary tectonic stress in northeastern Iberia: New results from borehole breakout analysis. Tectonophysics, 282 (1): 99-115

Moya, J., Vilaplana, J.M., 1992. Tectónica reciente en el Macizo de la Maladeta, sector del Alto Esera (Pirineo Central). In: Cearreta, A.; Ugarte, F.M. (Eds.), The Late Quaternary in the Western Pyrenean Region. Servicio Editorial Universidad del País Vasco, Bilbao, Spain, pp. 385-403.

Müller, B., V. Wehrle, R Zeyen, and K. Fuchs, Short-scale variations of tectonic regimes in the western European stress province north of the Alps and Pyrenees, Tectonophysics, 275. 199-219,1997.

Müller, B., M. L. Zoback, K. Fuchs, L. Mastin, S. Gregersen, N. Pavoni, O. Stephansson, and C. Ljunggren, 1992. Regional patterns of tectonic stress in Europe, J. Geophys. Res., 97, 11,783-11,803,.

Muñoz, I.A., 1992. Evolution of a continental collision belt: ECORS-Pyrenees crustal balanced cross-section. In: McClay, K.R. (Ed.), Thrust Tectonics. Chapman and Hall, London, pp. 235-246.

Nicolas, M., Santoire, J.P. & Delpech, P.Y. (1990) Intraplate seismicity: New seismicity data in western Europe. Tectonophysics, 179: 363-369

Njike-Kassala, J.D., Souria, A., Gagnepain-Beyneix, J., Martel, L. & Vadell, M. (1992) Frequency-magnitude relationship and Poisson's ratio in the Pyrenees, in relation to earthquake distribution. Tectonophysics, 215: 363-369

Nivière, B., Duhos-Sallée, N., Lacan, P., Hervouet, Y., 2006. A structural model for the seismicity of the Arduy (1980) epicentral area (western Pyrenees, France). Geophys. Res. Abstr. 8.

Olivera, C., T. Susagna, A. Roca, and X. Goula, Seismicity of Ibe Valencia Trough and surrounding areas, *Tectonophysics*, 203, 99-109, 1992.

Ortuño. M., Perca, H., Masana, E., Santanach, P., 2004. La falla del norte de la Maladeta, ¿fuente sísmica del terremoto de Vielha (19 de Noviembre de 1923)? *Geotemas-VI Congreso Geológico de España, Zaragoza, 12-15 julio 2004*, vol. 6(3), pp. 171-174.

Ortuño, M., Queralt, P., Martí, A., Ledo, J., Masana, E., Perea, H. & Santanach, P. (2008) The North Madaleta Fault (Spanish Central Pyrenees) as the Vielha earthquake seismic source: Recent activity revealed by geomorphological and geophysical research. *Tectonophysics*, 453: 246-262

Philip, H., I. C. Bousquet, 1. Escuer, J. Fleta, X. , Goul •• and B. Grellel, Presence de failles inverses d'age quaternaire dans rEst des Pyrénées: [implications sismotectoniques, *C. R. Acad. SeL Ser. 11*, 3[4,1239-1245,1991.

Rebaï, S., H. Philip, and A. Taboada, 1992. Modern tectonic stress field in the Mediterranean region: Evidence for variation in stress directions at different scales, *Geophys. J. Int.*, 110, 106-140,.

Rigo, A., Pauchet, H., Souriau, A., Grésillaud, A., Nicolas, M., Olivera, C. and Figueras, S., 1997, The February 1996 earthquake sequence in the eastern Pyrenees: First results, *J. Seismology* 1, 3-14.

Rigo, A., Souria, A., Dubos, N., Sylvander, M. & Ponsolles, Ch. (2005) Analysis of the seismicity in the central part of the Pyrenees (France), and tectonic implications. *Journal of Seismology*. 9: 211-222

Rivera, L. and Cisternas, A., 1990, Stress tensor and fault plane solutions for a population of earthquakes, *Bull. Seismo Soc. Am. SO*, 600-614.

Santanach, P.F., Sanz de Galdeano, C., Bousquet, J.C. 1980. Neotectónica de las regiones mediterráneas de España (Cataluña y Cordilleras Béticas). *Bol. Geol. Min. XCI-XCII*: 417-440

Sibuet, J.C., Srivastava, S.P., Spakman, W., 2004. Pyrenean orogeny and plate kinematics. *J. Geophys. Res.* 109, B08104. doi: 10.1029/2003JH002514.

Simón, J. L., Late Cenozoic stress field and fracturing in the Iberian Chain and Ebro Basin (Spain), *J. Struct. Geol.*, 11(3),285-294,1989.

Sis France, 2002. Sismicité de la France, Catalogue des sismes du BRGM (<http://www.sisfi.llnce.net> ).

Souriau, A. and Pauchet, H., 1998, A new synthesis of Pyrenean seismicity and its tectonic implications, *Tectonophysics* 290, 221-244.

Souriau, A., Sylvander, M., Rigo, A., Fels, J.-F., Douchain, J.-M. and Ponsolles, C., 2001, Sismotectonique des Pyrénées: Principales contraintes sismologiques, *Bull. Soc. géol. France* 172, 25-39.

Srivastava, S.P., Roest, W.R., Kovacs, L.C., Oakley, G., Lévesque, S., Verhoef, J., Macnab, R. 1990. Motion of Iberia since the Late Jurassic: Results from detailed aeromagnetic measurements in the Newfoundland Basin. *Tectonophysics*, 184: 229-260

Susagna, T., Roca, A., Goula, X., Batlló, J., 1994. Analysis of macroseismic and instrumental data for the study of the 19 November 1923 earthquake in the Aran Valley (Central Pyrenees). *Nat. Hazards* 10, 7-17.

Wells, D.L., Coppersmith, K.J., 1994. New empirical relationships among magnitude, rupture length, rupture area and surface displacement. *Bull. Seismol. Soc. Am.* 84, 974-1002.



Westaway, R., 1991. Present-day kinematics of the plate boundary zone between Africa and Europe, from the Azores to the Aegian. Earth Planet. Sci. Lett. 96, 393-406.

Zoback, M. L., First- and second-order patterns of stress in the lithosphere: The World Stress Map project. J. Geophys. Res., 97, 11,703-11,728, 1992.

## 6. GEOMECHANICAL CHARACTERIZATION

### 6.1 PREVIOUS INFORMATION

#### 6.1.1 Rock quality

Although the Somport Tunnel was excavated during the late 90's, limited information could be collected from the road authorities. The most significant one is the collection of geological characterisation made during the excavation of the tunnel face, both in the Atxerito Formation and in the Coralline Limestones.

The analysis of the tunnel head excavation leads to the following figure, which shows that rock concerning Coralline Limestones is good to very good, attending to Bienawski (1989). No adjustment has been made in the case of the graph for strike and dip orientations.

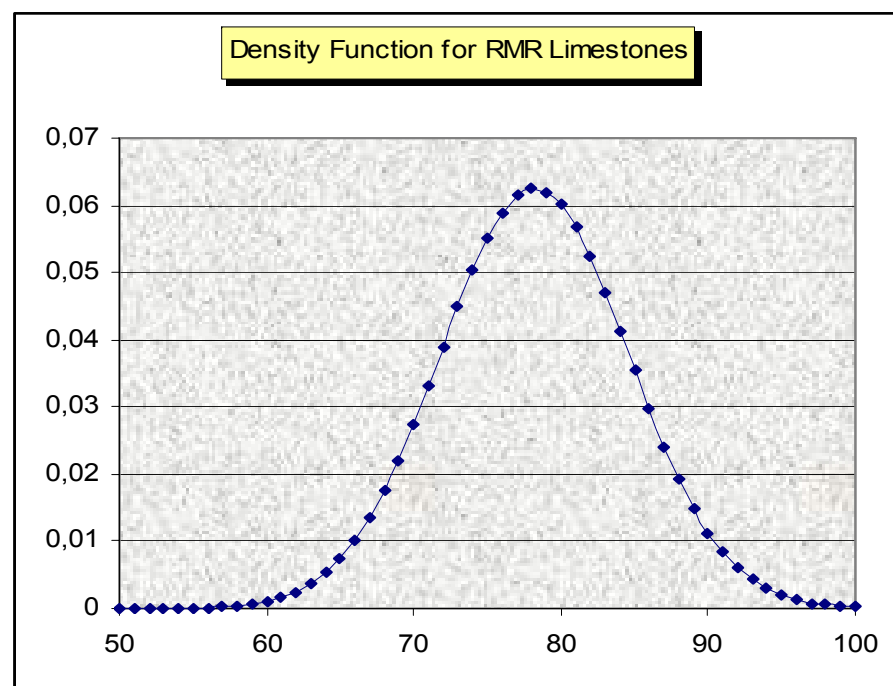
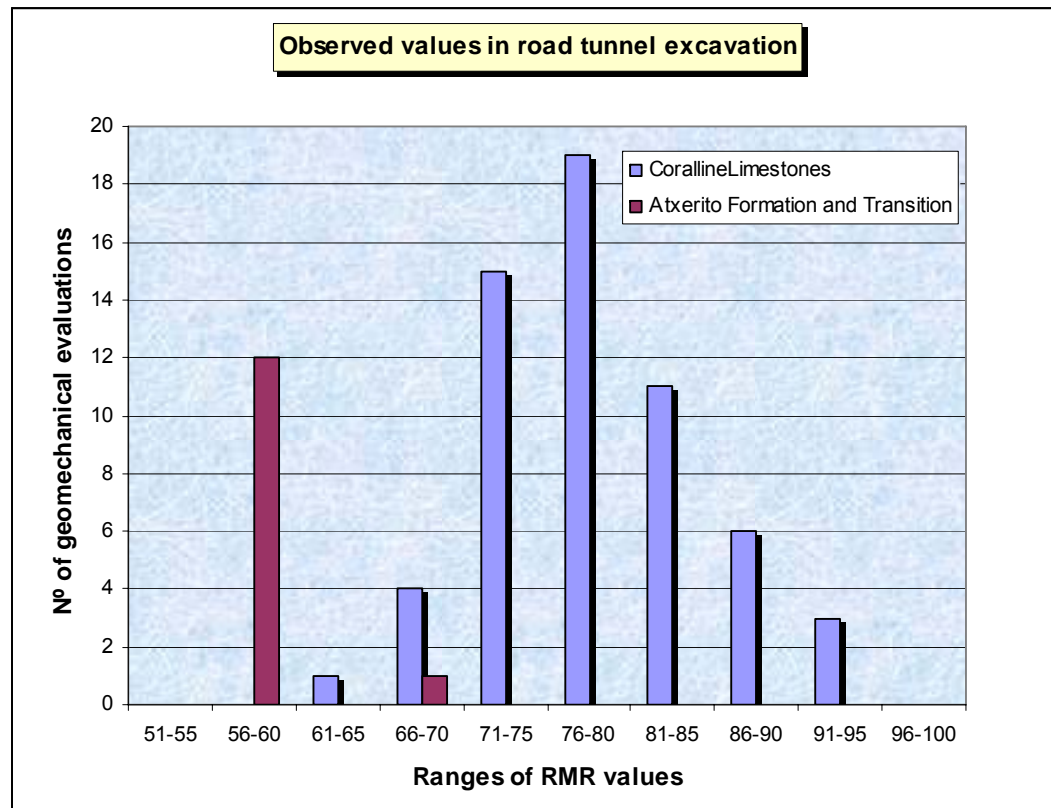
The characteristic values for RMR classification are:

- 25% 1st quartile value: RMR=62,4.
- 50% mean value: RMR=78,2.
- 75% 3rd quartile value: RMR=94

The expression  $\ln Q' = (RMR - 44) / 9$  leads to a mean value of  $Q' = 44,7$ .

Atxerito Formation lies always in the upper range of the "Fair rock" classification. Recovered data do not allow statistical analysis, and a RMR value = 56 can be chosen as minimum.

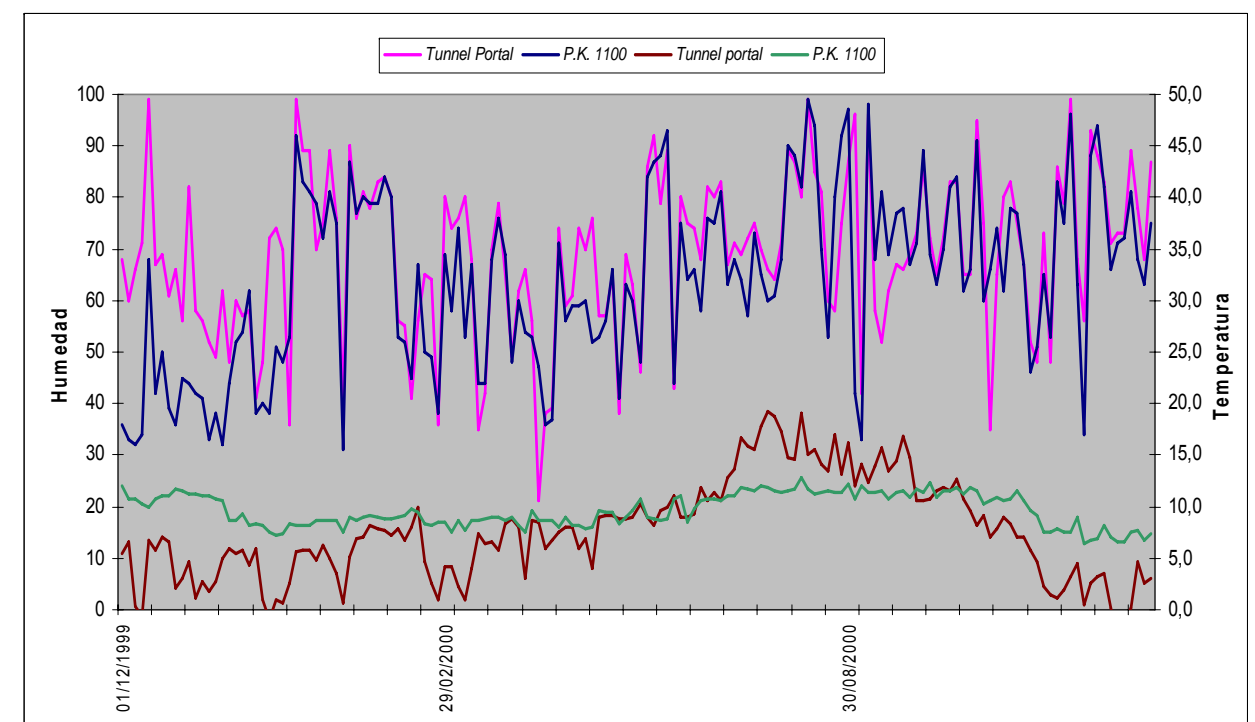
No special problems concerning rock spalling or creep were recorded while excavating both limestones and Atxerito Formation. Rock cover of the tunnel lies in the range of 750 meters in the area where these formations were found.



### 6.1.2 Temperature of the rock mass

The only available data about this particular aspect has been collected from observation of temperatures during the Somport road tunnel construction. The following figure 6.1-1 shows the difference between outside conditions and the ones measured 1 kilometre away from the tunnel portal, inside the tunnel.

Data was collected during more than one year, from 01<sup>st</sup> December 1999 to 23<sup>rd</sup> January 2001:



It can be noticed that a very constant temperature is measured into the tunnel (9 to 10 °C as average value, see the green line), although humidity ranges in a similar way than tunnel portal. The average humidity is 64% (blue line). In the case of temperature, the datum is good for underground experiment construction.

Further rock exploration could collect some precise data about this parameter.

## 6.2 BOREHOLES

### 6.2.1 New boreholes in the tunnel

Two boreholes were drilled in the railway tunnel during the Feasibility Study. Since this tunnel is the emergency one for the road tunnel, limited locations could be considered when preparing the borehole machine.

The elected locations were finally two widened zones of the railway tunnel, in which the boring machine would not hold up potential evacuation through the tunnel. This was a key consideration when deciding where to locate drillings. A fire practice was conducted during the drill, so the boring machine, was evacuated during the practice.

The aim of these two borehole drills were the following ones:

- The definition the geological context of the MDC's area into the regional stratigraphy, which is well-known in the base of the experience of the Somport Road Tunnel.
- The characterization of the petrology of the rock at the site.
- The characterization of the geomechanical properties of the rock cores (recovery, RQD, spacing of discontinuities, weathering of rock cores and rock joints, joint condition)
- The laboratory testing of selected rock samples, to determine their bulk density, porosity, confined and unconfined strength, brittleness, and other rock properties.
- The aim to classify rock mass by means of usual geomechanical classifications.

The main characteristics of the two boreholes were the following ones:

Borehole	Location in the railway tunnel	Length (m)	Drill diameter /Core diameter (mm)	Observations
S-1	Widening at gallery 9	40,00	101/85	Coralline limestones from top to end
S-2	Widening between galleries 11 and 12, next to the LSC	70,00	101/85	Black coralline limestones with laminated calcareous shales

As expected, borehole S-1 found light grey coralline limestones.

Borehole S-2 was located in a zone in which the geological profile of the tunnel showed the Atxerito formation. The closest emergency gallery, named nº 11, was excavated in this material, and dark grey and black slates had been previously observed, since the primary support had some local spalling, and rock outcrops were visible. The entrance to the new laboratory of Canfranc, that is being excavated at this time, is located at gallery nº 12. The Atxerito formation is also visible at this site, both at walls of the gallery and at the vault of the LSC main new hall, which partially collapsed due to inadequate rock support.

Although when planning the borehole it was clear that the Atxerito Formation was to be found at the site, finally the column of S-2 showed black limestones, partially laminated, and secondary recrystallization processes.

The following pictures show some typical drilled materials:



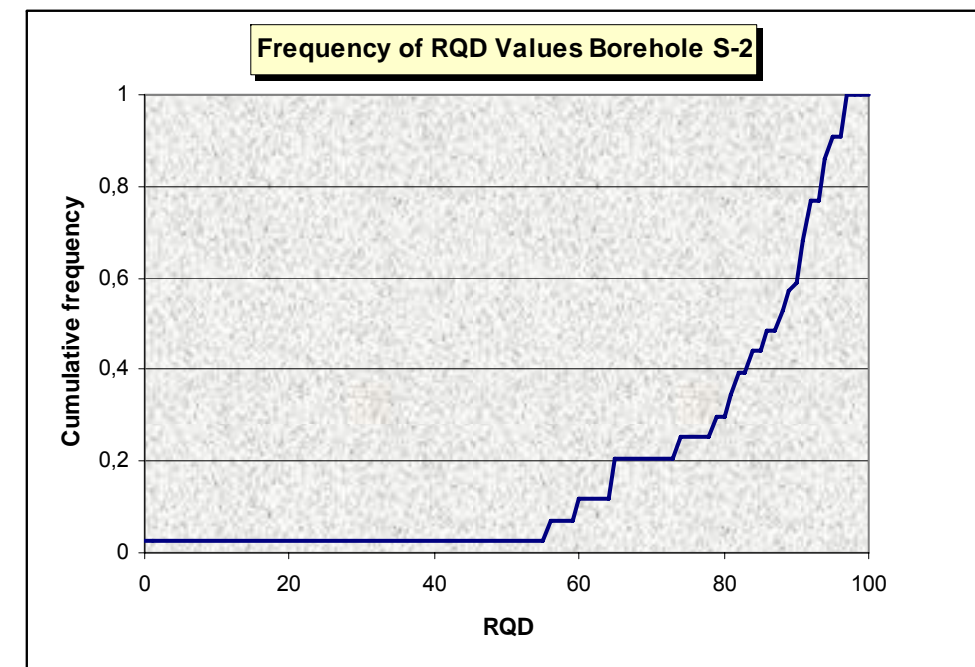
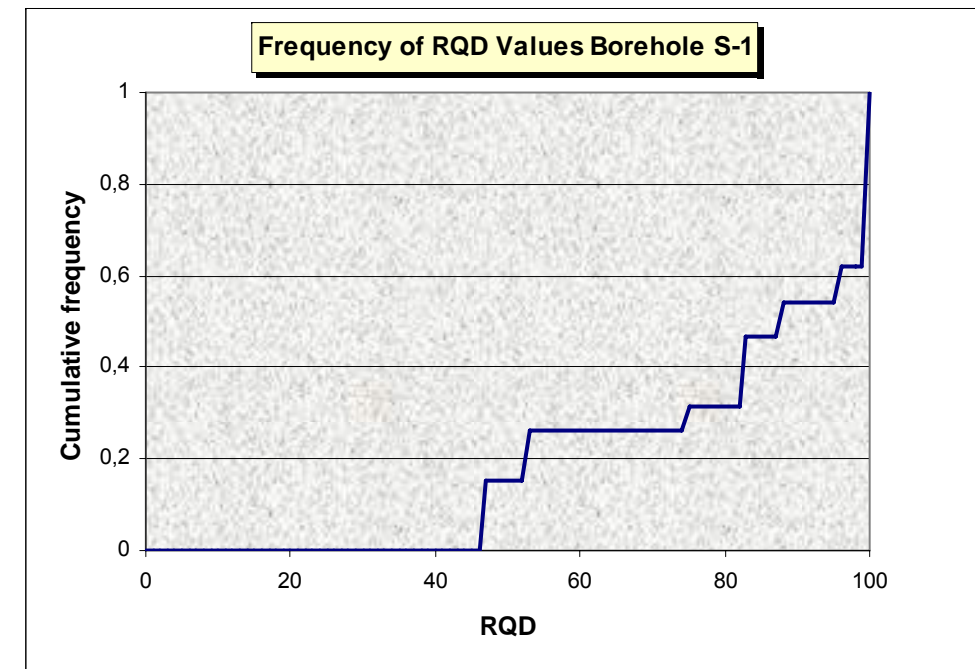


Two boxes of S-1. At left, from 11,00 to 13,25 meters deep. At right, from 37,00 to 39,20.



Two boxes of S-2. At left, from 25,90 to 28,20 meters deep. At right, from 44,20 to 46,420.

Next figures show RQD analysis for boreholes. No laboratory tests have been conducted to the date.



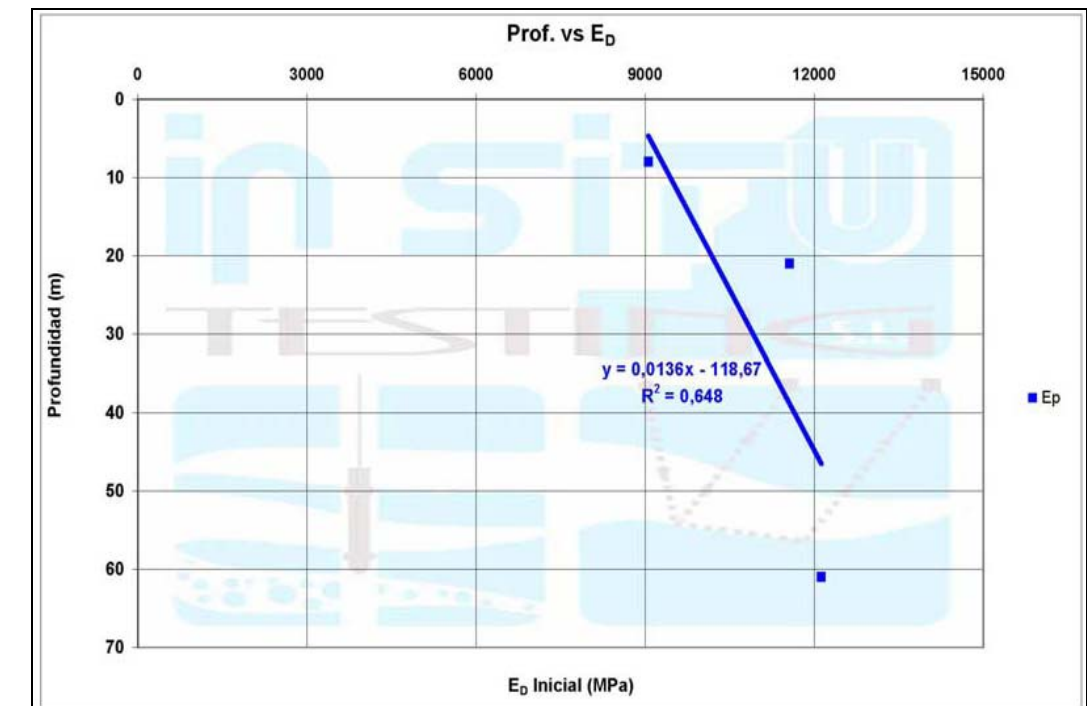
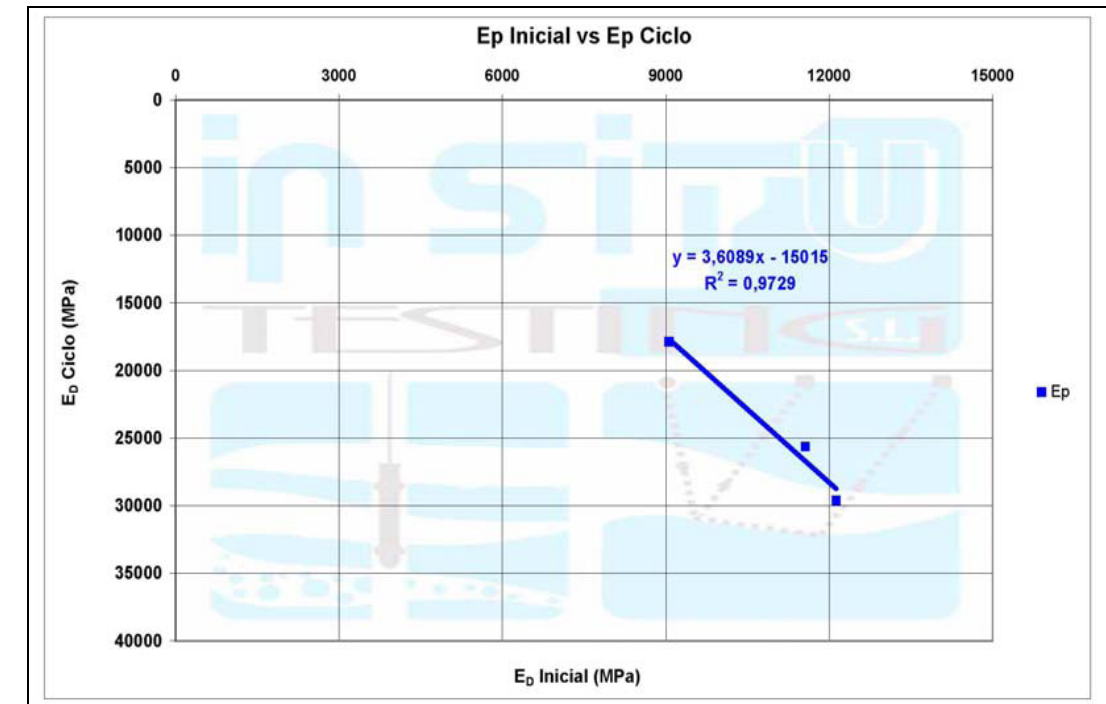
Three dilatometer tests were performed in borehole S-2. Different kind of limestones were chosen, both fractured and sound ones. Dilatometric moduli can be obtained in different axes. Both compression and re-compression tests were con-

ducted, shown that the relationship between both parameters lies in the range of 2,0 to 2,5.

The following table summarizes test results, for a Poisson ratio  $\nu=0,25$ :

Depth	E modulus (MPa) Compression	E modulus (MPa) Re-compression	Relationship	Observations
8,00	9.058	17.872	1,97	Fractured lime- stones RQD=56
21,00	11.560	25.636	2,22	Fined grain lime- stones, dark grey. Some slicken- sides. Calcite veins. RQD=65
61,00	12.126	29.617	2,44	Recrystallized limestones RQD=79

Next figures show the relationship between initial and recompression moduli, an also initial moduli vs depth of the borehole.



### 6.2.2 Preexisting boreholes

Limited information was also obtained from a horizontal borehole that was drilled previously to the excavation of the new underground facilities and main hall for the LSC extension. The borehole was 54 meters deep. It drilled the Atxerito formation shales and some tectonized joints. Due to folding and local faulting, coralline limestones were observed in some sections, which means that the borehole penetrated the contact area.

According to these data, that include some laboratory testing and rock core descriptions, different rock quality intervals were defined as follows:

From	To	Basic RMR	E rock mass (MPa)	Description
0,00	15,90	45	3.080	Milimetric layering of shales and fine grained sandstones. Faulted zone.
15,90	42,10	57	6.145	Shales and claystones with milimetric sandstone layering
42,10	43,40	48	3.660	Broken and possible fault zone
43,40	49,80	55	5.475	Shales and claystones with milimetric sandstone layering
49,80	52,40	49	4.350	Broken and possible fault zone
52,40	54,10	62	8.195	Shales and claystones with milimetric sandstone layering

### 6.2.3 Laboratory Testing

Some selected samples were tested in order to check rock properties. Only limestone specimens were recovered from boreholes, as previously noted in borehole descriptions.

Main laboratory characteristics of rock samples are the following ones:

- Average bulk density 27,1 kN/m<sup>3</sup>
- Unconfined compressive strength UCS=34,5 MPa
- Intact rock modulus of deformation  $E_i=37,7$  GPa
- Poisson's coefficient  $\nu=0,28$
- Tensile strength 5,10 MPa
- Point Load Test 2,69 MPa
- Slake Durability Index (2<sup>nd</sup> cycle) 98,7%
- Wave propagation  $V_p = 5.707$  m/s
- Porosity 0,86%



FEASIBILITY STUDY FOR THE LAGUNA PROJECT AT THE LSC (CANFRANC)  
LABORATORY TEST RESULTS OF BORINGS S-1 AND S-2

BORING	LITHOLOGY	SAMPLE	DEPTH		WET DENSITY (T/M <sup>3</sup> )	DRY DENSITY (T/M <sup>3</sup> )	WATER CONTENT (%)	UNIAXIAL COMPR. STRENGTH			TENSILE STRENGTH (Mpa)	TRIAXIAL STRENGTH			SHEAR STRENGTH THRU JOINTS		POINT LOAD TEST IS0 (Mpa)	SLAKE (%)	ABSORPTION (%)	POROSITY (%)	SONIC VELOCITY (m/s)	NOTES
			FROM	TO				$\sigma_c$ (Mpa)	E (Mpa)	$\nu$		$\sigma_1$ (Mpa)	$\sigma_3$ (Mpa)	E (Mpa)	C (Mpa)	$\phi$ (°)						
S-1	CORALLINE LIMESTONE	TP	2,75	3,25	2,72	2,70	0,6										2,37	98,88	0,30	0,50	6086	
S-1	CORALLINE LIMESTONE	TP	8,55	9,00							1,94											
S-1	CORALLINE LIMESTONE	TP	16,70	17,05	2,70	2,70	0,1										3,72	98,77	0,30	0,70	5781	
S-1	CORALLINE LIMESTONE	TP	22,70	23,15				15,09	41531	0,35												
S-1	CORALLINE LIMESTONE	TP	27,25	27,55	2,71	2,71	0,1										2,18	98,52	0,20	0,40	5701	
S-1	CORALLINE LIMESTONE	TP	36,65	37,00				14,27	62103	0,32												
S-2	FINE GRAINED LIMESTONES	TP	5,65	5,98	2,71	2,71	0,1	48,30											0,20		4883	
S-2	FINE GRAINED LIMESTONES	TP	8,67	9,00	2,67	2,66	0,4	32,20	43303	0,31	3,42											
	Idem	TP	id	id	2,59	2,58	0,3				2,83											
S-2	FINE GRAINED LIMESTONES	TP	12,60	13,00																		
S-2	FINE GRAINED LIMESTONES	TP	18,30	18,61	2,68	2,68	0,1				5,52											
	Idem	TP	id	id	2,63	2,63	0,2				6,92											
S-2	FINE GRAINED LIMESTONES	TP	21,40	21,67	2,70	2,70	0,1	14,13											0,20		5843	Failure through longitudinal calcite vein
S-2	FINE GRAINED LIMESTONES	TP	28,20	28,45	2,71	2,69	0,6	29,70	35676	0,21												
S-2	FINE GRAINED LIMESTONES	TP	31,05	31,34	2,70	2,70	0,1												0,10		4513	
S-2	FINE GRAINED LIMESTONES	TP	34,00	34,33																		
S-2	FINE GRAINED LIMESTONES	TP	36,92	37,23													2,57					
	Idem	TP	id	id													2,59					
S-2	FINE GRAINED LIMESTONES	TP	42,52	42,87	2,71	2,69	0,6	54,10	38921	0,21												
S-2	FINE GRAINED LIMESTONES	TP	46,65	47,00	2,70	2,70	0,1				9,74											
	Idem	TP	id	id	2,65	2,65	0,2				8,81											
S-2	RECRYSTALLISED LIMESTONE	TP	52,48	52,81	2,83	2,82	0,3	77,30										99,03	0,40	1,20	6305	
S-2	RECRYSTALLISED LIMESTONE	TP	53,82	54,12				12,74	4803	0,29	0,92											
S-2	RECRYSTALLISED LIMESTONE	TP	56,88	57,18	2,83	2,82	0,3	30,50										98,83			6125	
S-2	RECRYSTALLISED LIMESTONE	TP	65,49	68,45	2,82	2,81	0,3	50,80										98,36	0,50	1,50	6125	

N° values	17	17	17	11	6	6	8										5	6	8	5	9	
Average value	2,71	2,70	0,3	34,47	37723	0,28	5,01										2,69	98,73	0,28	0,86	5707	
Standard deviation	0,06	0,06	0,2	20,95	18598	0,06	3,26										0,60	0,25	0,13	0,47	610	
Maximum value	2,83	2,82	0,6	77,30	62103	0,35	9,74										3,72	99,03	0,50	1,50	6305	
Minimum value	2,59	2,58	0,1	12,74	4803	0,21	0,92										2,18	98,36	0,10	0,40	4513	

## 7. MEMPHYS EXPERIMENT

### 7.1 MDC'S AND TANK DESCRIPTION

#### 7.1.1 Dimensions

The dimensions of each MDC that will be necessary to build are:

Diameter	Height (cavern)	Height (tank)
68 m (each)	86,5 m	≈70 m

Each cavern will allocate a water tank. The caverns are cylindrical shaped, and have been designed with a vault, with 15 meters spire from the horizontal upper level of the cylinder. The lower level of the cavern is at 1000 a.s.l. and the walls are 70 meters high. The summit of the dome elevation is 1085 a.s.l

#### 7.1.2 Technological specifications

##### 7.1.2.1 Tanks

According to Technodyne conceptual design, the tank needs of two different parts:

- The outer shell of the detector is a stainless-steel tank. According to the Super Kamiokande experiences, it is necessary backfill this tank against the rock, to support water pressure once the tank is filled, and to ensure high purity water demand.
- There is also a inner structure in the tank, to which photomultipliers (PMT's) will be held. This structure allows to isolate a certain volume of water between

the inner and the outer structure. This volume acts against muon veto, and should be 2 meters thick.

A complementary isolation must be installed, provided by a light-proof membrane, adhered to the PMT's structure. This scheme provides an outer detector (OD) and an inner one (ID).

According to these dimensions, the ID tank would be 58.3 m diameter. A primary support thickness of 35 cm and 40 cm backfill concrete have been considered. The support structure for PMT's has been taken from the Super Kamiokande dimensions (55 cm), and 10 additional centimeters allow for different liners. This dimensions lead to a 173.516 m<sup>3</sup> inner water volume (H=65 m). The volume of the OD is 25.076 m<sup>3</sup>.

##### 7.1.2.2 Water

Water procurement can be done by using natural resources of water, that can be taken from River Aragón, which provides natural fresh water to the Canfranc area. When describing site characterization some statistical values concerning River Aragón average flow volumes have been explained.

Water purification system would be very similar to the one described for the Super Kamiokande<sup>1</sup>. It consists of:

- Particle filters (1μm) and reverse osmosis
- Two heat exchangers to reduce PMT dark noise and suppress growth of bacteria.
- Cartridge polisher to eliminate heavy ions.

<sup>1</sup> Fukuda et al. *Nuclear Instruments and Methods in Physics Research A* 501 (2003) 418–462

- UV sterilizer which kills surviving bacteria.
- A Reverse Osmosis (RO) system, and a tank to dissolve Rn-reduced air. The RO step removes additional particulates. The introduction of Rn-reduced air into the water increases radon removal efficiency in the next step: the vacuum degasifier (VD), which removes dissolved gases in water.
- Ultra filter and membrane degasifier, to achieve radon reduction.

### 7.1.3 General layout

The conceptual design deals with the alignment of the three tanks along a N30°W axis, almost parallel to the railway tunnel. The base of the caverns will reach level +1.000 (above sea level) and the summit of the vault reaches +1.085 a.s.l., so vertical rock cover is 890 m for the Southern cavern, and 855 m for the Northern one. This rock cover means 2.300 equivalent m.w.e. shielding, according to expected rock density.

For construction purposes and for future operation, an access gallery must be built, reaching the base of the vault of the caverns. The gallery portal should be located nearby to the one of the abandoned railway tunnel. Other locations for this access portal would lead to very steep galleries, and have been discarded for operational reasons.

First stage design consists of a 5,12% slope gallery, more than 2.370 m long, reaching the base of the vaults at an upper chamber at level +1.073 a.s.l. This tunnel would be a cardinal importance infrastructure for construction purposes and for future definitive access.

A connection gallery from this chamber would communicate the three MDC's. At the end of this gallery, a deep vertical shaft could be excavated from the railway tunnel, if communication between the actual LSC and the LAGUNA experiment caverns is needed. An elevator will provide rapid access from LSC to the MDC's.

This shaft can be located at the Northern side of the MDC's location. Evacuation facilities in case of emergency would take advantage of this implement.

Other auxiliary tunnels running from the access gallery to the base of each MDC complete the initial construction scheme. The longer tunnel saving the elevation difference between vault and base is 1007 m long, and the slope is 7,2%.

Finally, a ventilation auxiliary facility consisting in a gallery and a vertical shaft ( $\Phi=5,70$  m) has been also designed. The scheme of this infrastructure is similar to the one that operates for the road tunnel. The shaft entrance is located in the Rioseta area, and environmental considerations should be taken in mind for this area in future detailed designs. The ventilation shaft is 220 m deep, and the ventilation gallery communicating the experiment area and the Rioseta place is 1182 m long.

Drawings at the end of this document show a comprehensive scheme for this LAGUNA technology infrastructure.

Attending to geological considerations, caverns will be located in the Atxerito Formation, and, thus, primary rock support should deal with this fact. Geotechnical modelling has taken in mind this aspects at this stage, according to predicted rock quality.

### 7.1.4 Auxiliary caverns

Apart from the above mentioned MDC's and access tunnels, different auxiliary caverns (AC's) have been incorporated to the overall layout, where different utilities can be located:

- Cavern AC1: clean storage, main control and offices.
- Cavern AC2: water and air purification system of the experiment (one for each MEMPHYS tank).



- Cavern AC3: power transformation equipment. It can be comprised in the clean storage AC1.

## 7.2 GEOMECHANICAL DESCRIPTION OF THE SITE

A general review on geomechanical characterization has been stated in paragraph 6. Two different rock formations are to be considered for the different experiments. Regarding to the MEMPHYS one, the basic characterization of the Atxerito Formation is resumed in the above mentioned paragraph.

Final parameters used for calculation purposes are resumed in Table 7.4-1. that is shown below.

## 7.3 EXCAVATION METHODS FOR THE MDC'S

### 7.3.1 Introduction

As explained in section 7.1.3 General Layout, the access to the experiment caverns is reached by a 7 m high, 2371 m long tunnel running from the portal, located adjacent to the railway tunnel, to the base of the dome at elevation 1073 (future working area). The bottom of each cavern would be accessed by an additional 7 m high gallery. The 7-meter high access tunnels (both upper and lower) have the necessary dimensions to house the machinery and the ventilation required during construction.

The upper access tunnel would have a slope of 5.1% which is considered acceptable. Even though steeper tunnels can be found in Norway (up to 10% in sub-sea tunnels, Henning et al, 2007), in Spain such steep slopes in tunneling are virtually unheard of. The steepest descendent tunnel to reach an underground work in Spain, at the moment, is the intermediate access to the Pajares tunnel which is part of the high speed railway system (AVE), where 5.5 Km were bored with TBM (tunnel boring machines) at 6.13% slope. Although uphill excavations with TBM can be steeper, downhill excavations with slopes larger than 6.5% are not recommended. The upper access tunnel could be excavated with TBM, roadheaders or by the drill-and-blast method.

The lower ramps are curved, have a slope of 7,2% and are about 1000 m long. The use of TBM for the excavation for these ramps is not recommended because of their curvature and slope, alternative excavation methods such as roadheaders or drill-and-blast would be more convenient. These lower ramps will be used during construction and to access the tanks for maintenance and eventual reparations.

The excavation of the main caverns and additional underground facilities could be carried out by the drill-and-blast method which has been the main construction method of underground spaces for decades and still is the only feasible method

due to the involved big dimensions. The shafts will be excavated mechanically with raise boring.

The next paragraphs will cover the excavation sequence and support needed for the construction of the experiment caverns:

### 7.3.2 Construction of a support system above the cavern dome

When pre-designing the support system for the cavern roof widely used approaches were considered. The United States Corp of Engineers recommendation, from the manual “Engineering and Design – Tunnels and Shafts” (EM 1110-2-2901), states that for spans between 18 and 30 m the rockbolt length should be a quarter of the span (there is no mention of structures with larger spans than 30 m). This means that for a MEMPHYS cavern with a 68 m span the minimum rockbolt length recommended is 17 m.

Dr. Evert Hoek’s recommendations (from the on-line book *Practical Rock Engineering*) state that the cable length needed to support a cavern should be at least 40% its span, this means 27-meter long cables in the case of a MEMPHYS cavern. Regarding the minimum length for rockbolts, Hoek recommends 12-meter long bolts (according to the equation:  $L=2+0.15*\text{span}$ ).

Cables and bolts of such lengths are outside of what is normally available and easily installed. This suggests that the use of cables and rockbolts as the only support for the cavern roof might not be adequate.

Another issue considered was the potential wedge instability of the cavern roof. Even with excellent quality rock there have been instances of wedge instability reported, as it was the case of the powerhouse from the Río Grande Project in Argentina. The 25-meter span powerhouse cavern is located in massive tonalitic gneiss of excellent quality with an average uniaxial compressive strength of 140 MPa. Three intersecting joint sets were found at the location of the cavern which created potential roof instability. Figure 7.3-1 (a) shows the largest possible

wedges formed and figure 7.3-1 (b) shows a scaled down wedge determined in-situ based on average joint trace length. This scaled down wedge was properly secured and no problems were encountered during the construction of the powerhouse.

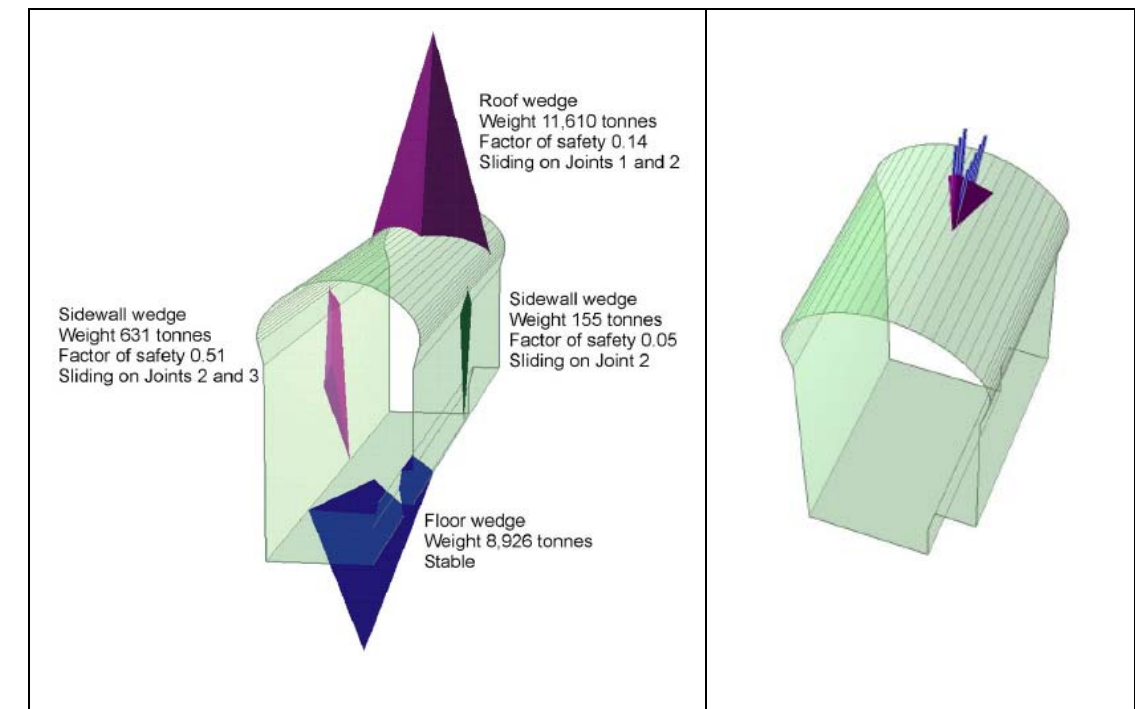


Figure 7.3-1. (a) Possible wedges formed in the Río Grande powerhouse cavern  
(b) Scaled down wedge formed in the Río Grande cavern roof.

Another example worth pointing out, because of the monetary damage involved, is the case of the Chuquicamata copper mine failure in Chile. In July 2006 there was a collapse of a wall in the transfer station tunnel (21 m wide by 26 m high by 33 m long) that halted two-thirds of production at the mine, which represents about 2% of the world copper output. The information available regarding the failure is scarce for being in the midst of litigation, however it seems that an audit of the situation was carried out and concluded that the main cause of the collapse of the cave was the inadequacy of the support system as designed.

At the end, when selecting the support system there are two major concerns to address:

- The local stability and the relief of tensions close to the walls and vault, and
- The possible failure of a large wedge on the cavern roof

These problems can general be solved with the use conventional support, such as cables, bolts and shotcrete. However, for the MEMPHYS experiments the conventional approach is not adequate due to the unprecedented dimensions of the caverns and it is apparent that an additional support system would be necessary to ensure the cavern stability.

This additional support system would be located above the cavern roof and would consist on two horizontal galleries and eight diametrical ribs that meet at the top in an upper chamber, as shown in figure 7.3-2. This vault system needs to be in place before starting with the cavern excavation.

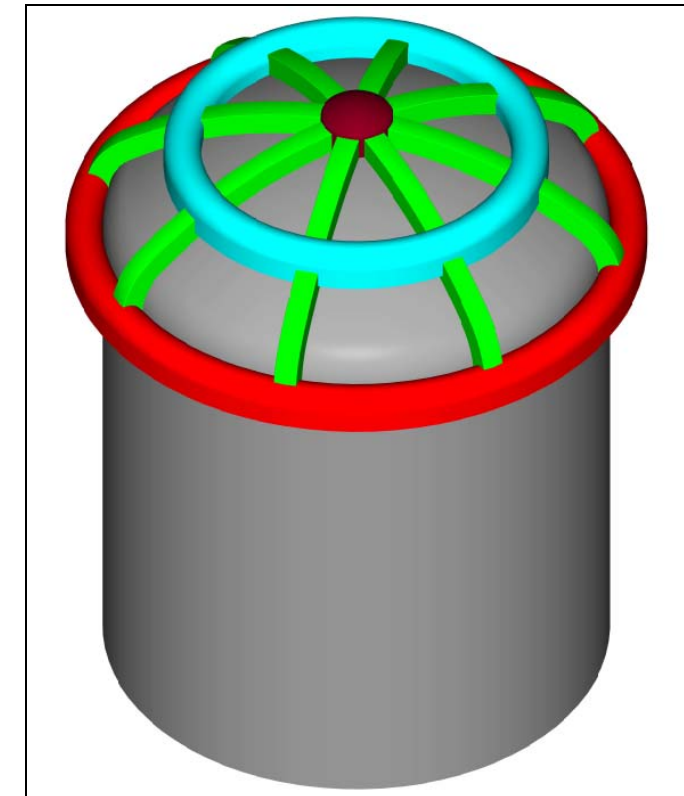


Figure 7.3-2. Perspective view of the vault system.

The excavation sequence of the ribs and galleries shown in figure 7.3-2 is expected to be as follows:

- Excavation and support of upper access tunnel at elevation 1073 (H = 7 m)
- Excavation and support of the lower perimeter gallery (5.0 m x 5.5 m) at elevation 1067.
- Excavation of lower part of structural ribs (2.5 m x 3.0 m) up to elevation 1080.9
- Excavation and support of intermediate gallery (5.0 m x 5.5 m) at elevation 1080.9

- Excavation of the top part of structural ribs (from intermediate gallery to upper cavern)
- Excavation and support of upper cavern (elevation 1086.3)

The galleries and ribs of the vault support structure will be concrete-filled at a later stage; however, based on the results obtained by the numerical modeling, the concrete filling must be done in stages to avoid overstressing the concrete. By allowing the rock mass to deform before filling the galleries and ribs with concrete, the stress on the galleries and ribs would be reduced. The concrete-filling sequence will be explained in the next paragraph.

### 7.3.3 Cavern excavation sequence

Following the excavation of the galleries and ribs above the crown, the cavern is excavated following the sequence shown in figure 7.3-3.

Explained more in detail, the excavation stages for the MEMPHYS caverns are as follows (the stage numbers correspond to the numbering shown on the excavation sequence drawing):

**Stage 1:** Excavation and support of the first ring of the dome, at elevation 1073 by the drill-and-blast method

**Stage 2:** Excavation and support of the second ring of the dome, by the drill-and-blast method

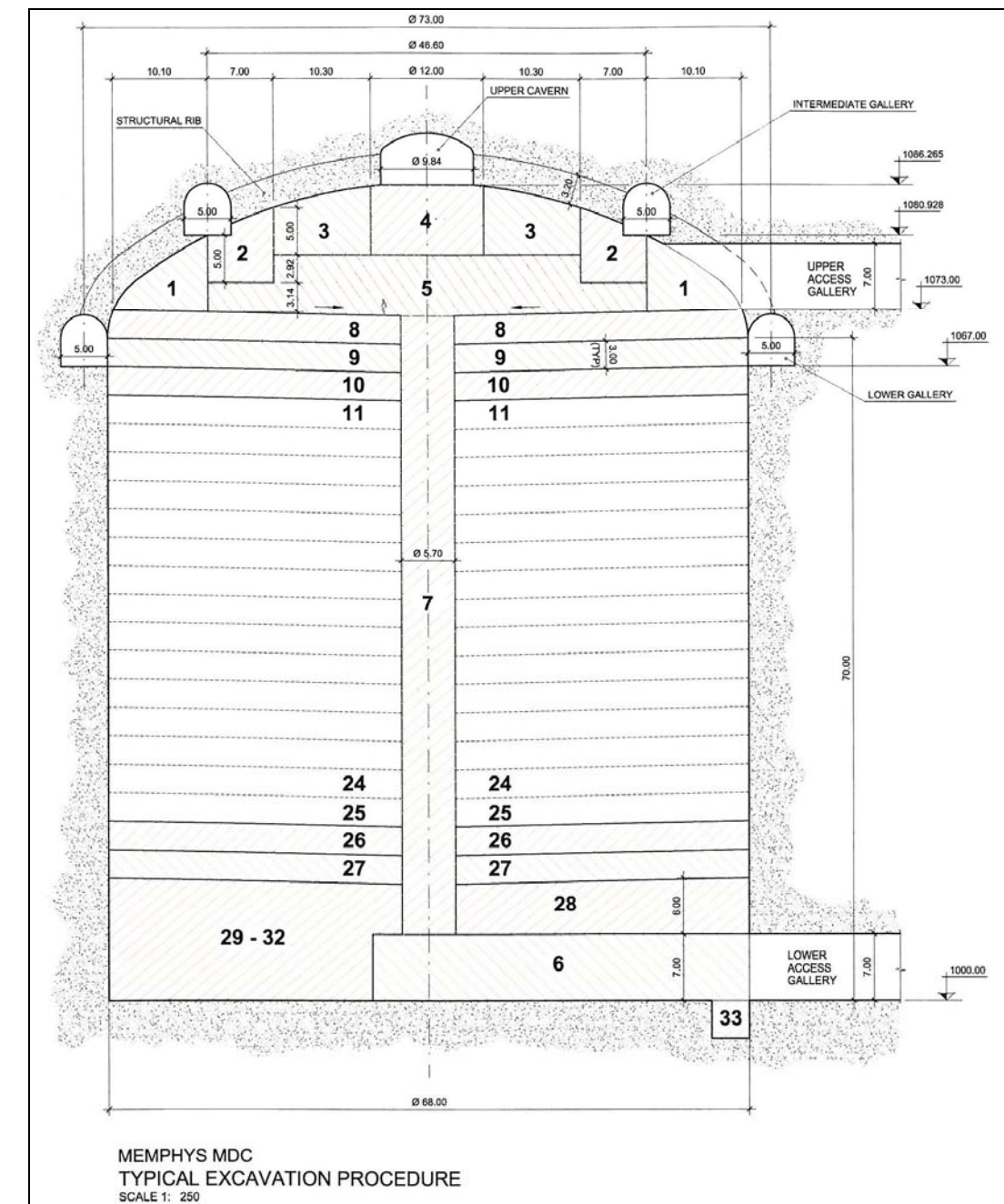


Figure 7.3-3. Excavation sequence for the MEMPHYS caverns.

After the completion of stages 1 and 2, the following elements of the pre-support system are concrete-filled:



Upper cavern

- Drilling of pilot hole

Upper part of ribs (from upper cavern to intermediate gallery)

- Installation of the drill string

Intermediate horizontal gallery

- Installation of the reamer head

Following the partial concrete-filling of the galleries and ribs, the excavation of dome continues:

Stage 3: Excavation and support of the third ring by the drill-and-blast method

- Excavation of the shaft from the bottom up
- Mucking out through lower access tunnel

Stage 4: Excavation and support of the top part of the dome by the drill-and-blast method

Stages 8 to 27: Excavation of the cavern to elevation 1013:

- Excavation in 3 m benches slightly sloped toward the shaft (~ 5%)
- Mucking out through lower access tunnel
- Support of the walls immediately after mucking out

After stages 3 and 4 are completed, the lower part of ribs (from the intermediate gallery to the lower gallery) and the lower horizontal gallery of the vault system are concrete filled.

The excavation of the dome is completed following the concrete filling of the vault system in the next stage:

Stage 28: Excavation of the rock on top of the lower access tunnel with the drill-and-blast method

Stage 5: Removal of the remaining rock on the dome by the drill-and-blast method

Stages 29 to 32: Excavation of the rock on top of the lower access tunnel below elevation 1013:

- Excavation of three 3-meter benches and one 4-meter bench
- Mucking out through lower access tunnel
- Support of the walls immediately after mucking out

The construction of the lower access tunnel should be completed before starting with the excavation of the cylindrical part of the cavern:

Stage 6: Excavation and support of lower access tunnel at elevation 1000 (H = 7 m) to the centre of the cavern

Stage 33: Excavation of the drainage pit

The excavation of the cylindrical section of the cavern will be carried out by raise boring in the next sequence:

Stage 7: Excavation of a shaft ( $\phi$  5.7m) with raise boring:

### 7.3.4 Support system for the MEMPHYS caverns

The support system for the dome and the walls of the MEMPHYS caverns are presented in this section.

#### Dome:

Besides being supported by the vault structure previously described (and shown in figure 7.3-2), the dome will have cables, rockbolts and shotcrete with the following specifications:

- Cables: 18 m long, 7 strand, cement grouted (grouted bulb length of 6 m), in a 2 m x 2 m pattern
- Rockbolts: 6 m long rebar steel bar,  $\phi 38$  mm, cement or resin grouted, in a 2 m x 2 m pattern
- Shotcrete: 35-cm thick steel fibre reinforced shotcrete

#### Walls:

The cavern walls will be supported by cables, rockbolts and shotcrete with the following specifications:

- Cables: 18 m long, 7 strand, cement grouted (grouted bulb length of 6 m), in a  $L_V = 3$  m,  $L_H = 1.33$  m pattern
- Rockbolts: 6m long rebar steel bar,  $\phi 38$  mm, cement or resin grouted, in a  $L_V = 3$  m,  $L_H = 1.33$  m pattern
- Shotcrete: 35-cm thick steel fibre reinforced shotcrete

## 7.4 NUMERICAL MODELLING OF THE MDC

This paragraph describes the numerical modelling analyses developed to validate the excavation sequence and support elements projected for the MEMPHYS type cavern, to be constructed in the Canfranc Underground Laboratory in Huesca.

A three-dimensional model using the finite difference code FLAC3D has been developed, which reproduces, with a reasonable precision, both the problem geometry and the construction phases planned.

### 7.4.1 Initial modelling

In a first stage, an elastic analysis of the problem was made. This stage allows for an initial approach to the excavation, with analysis not only of plastic areas to be developed around the excavation and safety factors, but of movements at the roof, the walls and at the floor of the MDC's. Rock was considered to be elastic, and a plasticity criterion was also considered. The original Hoek-Brown criterion was conceived with the aim to describe both intact rock cores and rock masses. The evolution of this criterion has led to the following expression:

$$\sigma_1^{cr} = \sigma_3 + \sigma_{ci} (m \sigma_3 / \sigma_{ci} + s)^a$$

Where  $\sigma_1^{cr}$  and  $\sigma_3$  are minor and major principal stresses at failure,  $\sigma_{ci}$  is the uniaxial compressive strength of rock cores and m & s are two parameters, different for each rock mass. The plastic zones of the rock mass can be evaluated comparing the principal stresses in relation with the critical  $\sigma_1^{cr}$  of the Hoek Brown criterion.

A safety factor can be defined as:

$$FS = (\sigma_1^{cr} - \sigma_3) / (\sigma_1 - \sigma_3)$$

When this safety factor is more than 1, no failure is to be expected, and the rock mass behaves as intact,

This kind of model underestimates plasticity areas, but allows for primary detection of the extension of plasticity in the model to be carried out with more precision in further stages.

For the MEMPHYS experiment, three MDC's have been modelled. The geometrical mesh used for ground modelling is shown in the following figures:

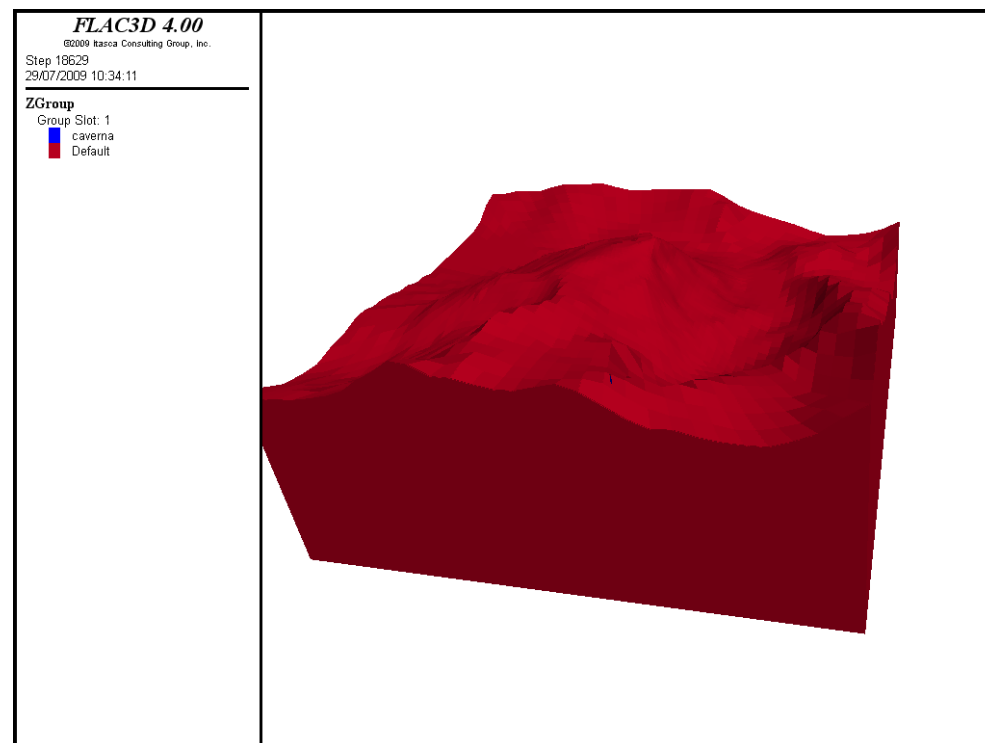


Figure 7.4-1. Ground modelling for the MDC's.

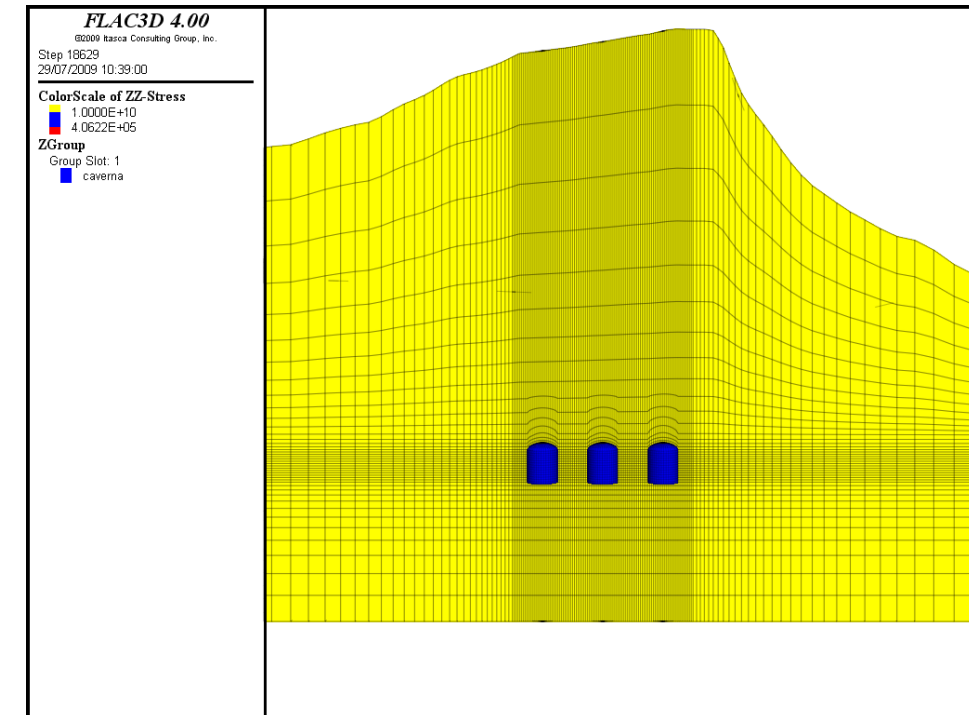


Figure 7.4-2. Typical section for the MEMPHYS MDC's.

Rock properties are described below:

Material	$E$ (GPa)	$\nu$	$\sigma_{ci}$ (MPa)	$m_i$	$D$	$GSI$	$m_b$	$s$	$a$
Shales	4.9	0.3	60	12	0	50	1.677	0.0039	0.506

Table 7.4-1. Calculation properties

Figure 7.4-3 shows plastic elements around the excavation of the caverns, and local safety factor of these elements, once the first of the caverns has been excavated, with no support.

Figures 7.4-4 and 7.4-5 show both the perspective and the frontal view of the three caverns, once they have been excavated.

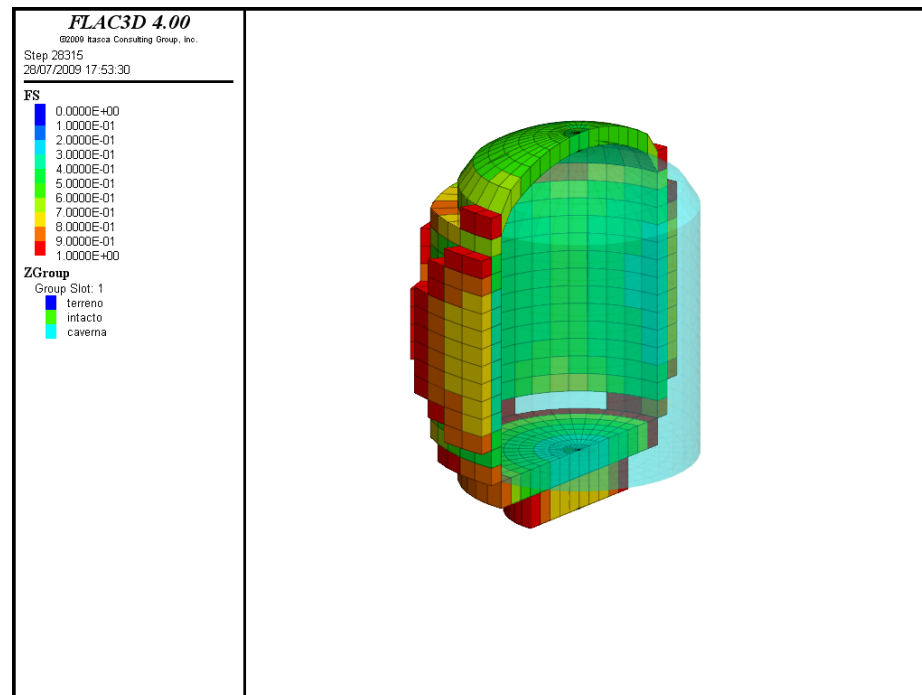


Figure 7.4-3. Plastic elements around one MEMPHYS MDC.

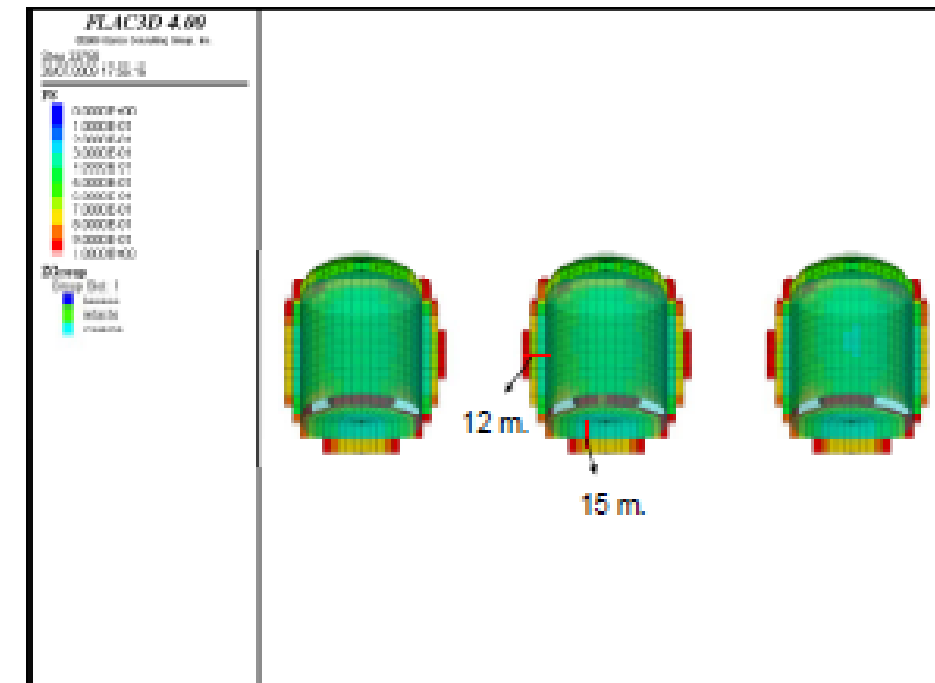


Figure 7.4-5. Plastic elements around the three MEMPHYS MDC's.

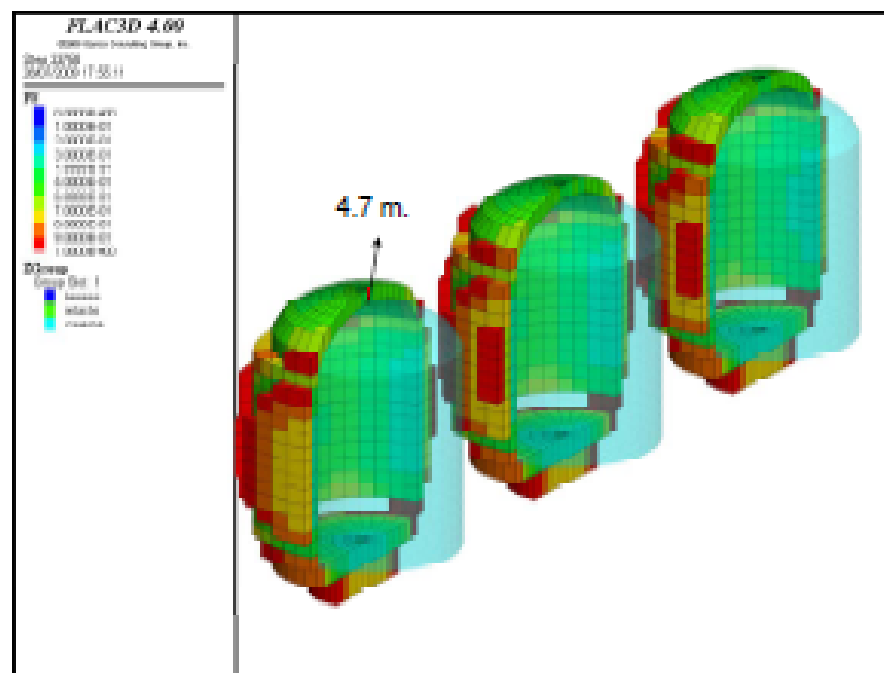


Figure 7.4-4. Plastic elements around the three MEMPHYS MDC's.

The important fact is that no interaction is expected between the caverns at the separation that has been designed for the general layout, so individual detailed analysis can be carried out for next calculations. Plastic zones are almost the same for each of the three MDC's.

The results show that plastification reaches 4.7 m at the summit of the vault, 12 m at the cavern walls and 15 m in the floor area. Since a single excavation phase has been considered, these values should be conservative, because no progressive stress relief is considered.

Plastic zones are almost the same for each MDC modelled and it is apparent from the results that no interaction between the caverns is expected to take place with the separation specified in the layout. Since the effect that multiple caverns have on each other is negligible, only one cavern is modelled in subsequent more detailed analyses.



A description of the detailed calculation model used, the different hypothesis considered in the analysis and the results obtained are described below.

#### 7.4.2 Geometric description of the final model

The calculation model developed reproduces as realistic as possible both the geometry of the MDC and the support elements. The model includes the real topography of the area in which the cavern will be constructed.

A general view of the model is shown in Figure 7.4-6, with dimensions of 3000 m in the X direction and 3000 m in the Y direction (horizontal axes), in order that the boundaries were far enough from the MDC area, and avoid affections to the results from topography effects (if topography was flat, 1000 m would have been enough). In the vertical direction, as the real surface topography has been considered, the model has a variable height, with 2675 m in the area with greatest height. In this figure, the dimensions of the cavern compared to those of the calculation model can be appreciated.

The maximum cover on the cavern is roughly 890 m, although it varies due to the surface topography. Figures 7.4-7 and 7.4-8 show two transversal sections in the model, with the location of the cavern compared to the ground surface.

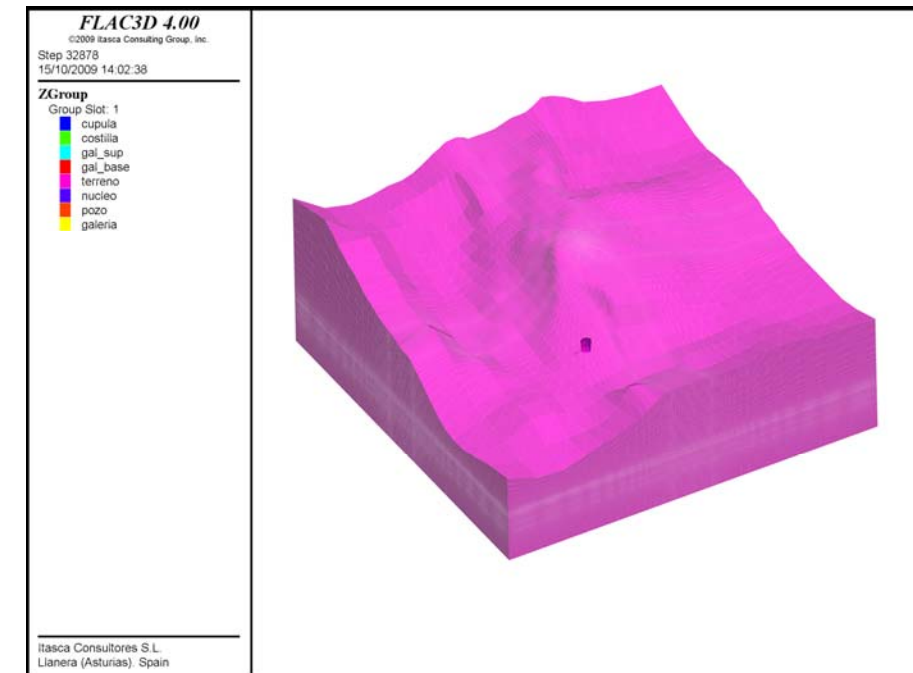


Figure 7.4-6. Calculation model general view.

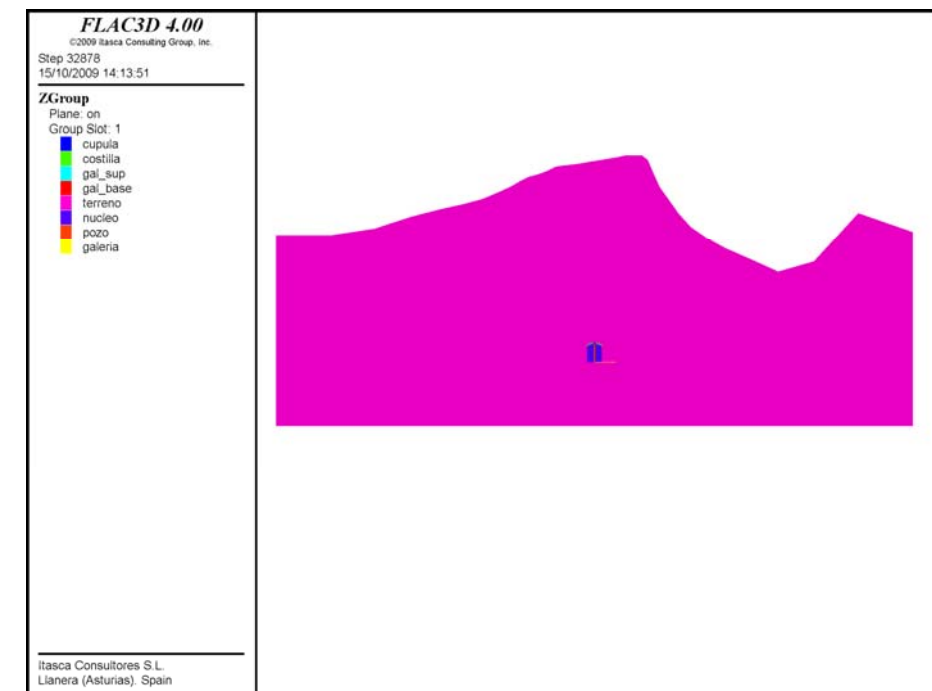


Figure 7.4-7. Transversal profile. Section N-S.

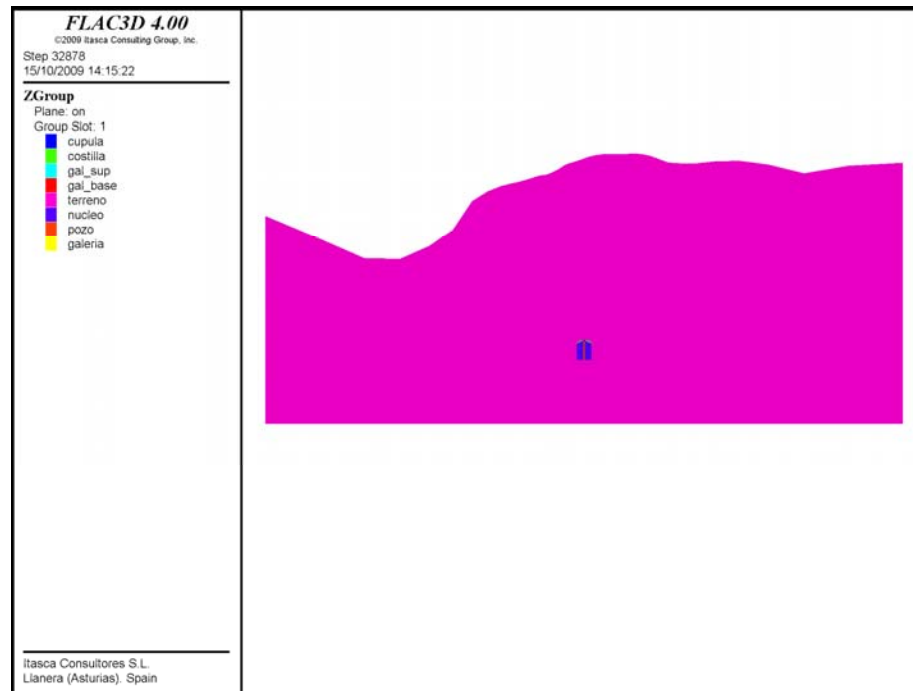


Figure 7.4-8. Transversal profile. Section E-W.

The MEMPHYS type MDC has a circular horizontal cross section, with a diameter in its base of 68 m, and a height of the cylindrical area of 70 m. The vault has a radius of 51.5 m and is 16.3 m high, with a bend in the base of 7.75 m of radius. It is projected the construction of a group of horizontal galleries (with circular shape in plan view) connected with “ribs”, acting as a pre-support of the vault. This geometry has been reproduced in the model. The horizontal galleries have a horse-shoe cross section, 5 m wide and 5.5 m high. The ribs are square sections, 3 m wide. Figure 7.4-9 shows a perspective view of the cavern in the model. Figure 7.4-10 shows a plan view, with the geometry of the horizontal galleries and ribs. Eventually, during construction the geometry of the ribs could be horse-shoe shape and not square as it has been reproduced in this model.

The cavern is designed to be constructed excavating the vault first, and going down then in 3 m high rounds. The waste rock will be extracted through a central shaft which is 4 m diameter, excavated using a “raise boring”, so both the base gallery and the central shaft have been included in the model (in Figure 7.4-11, the vertical shaft can be observed, inside the cylindrical part of the cavern)

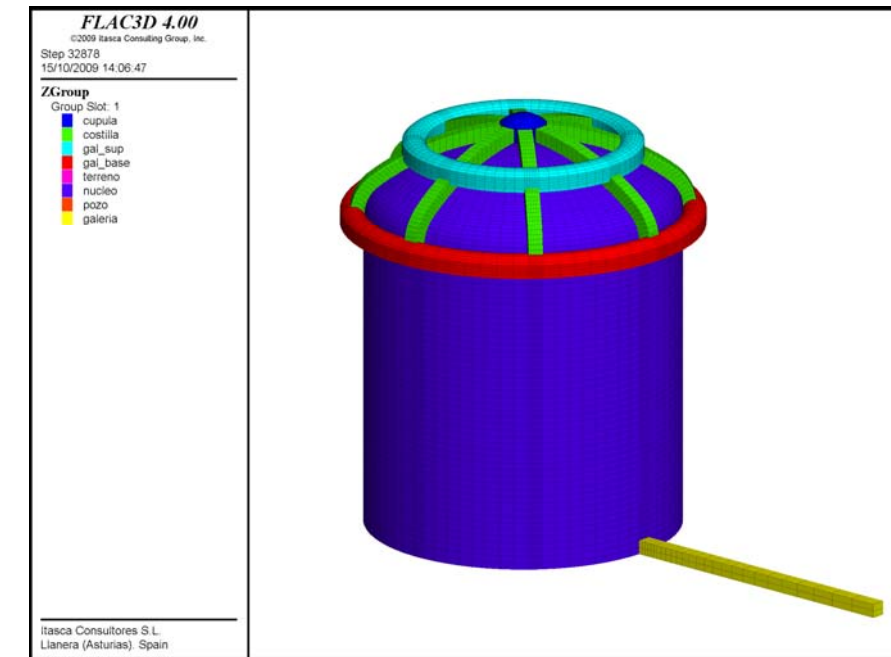


Figure 7.4-9. Cavern geometry.

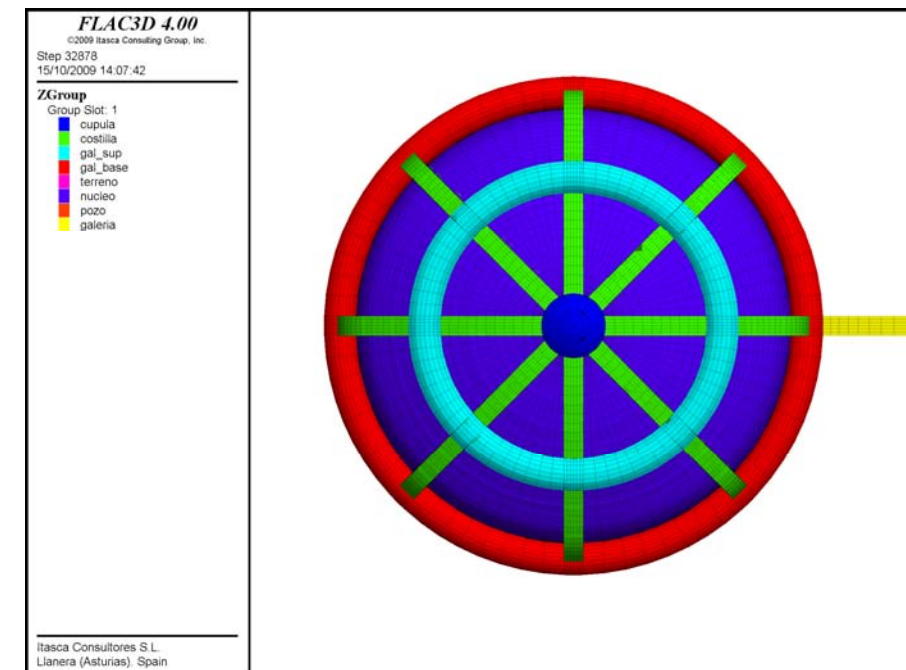


Figure 7.4-10. Detail of the geometry in a plan view.

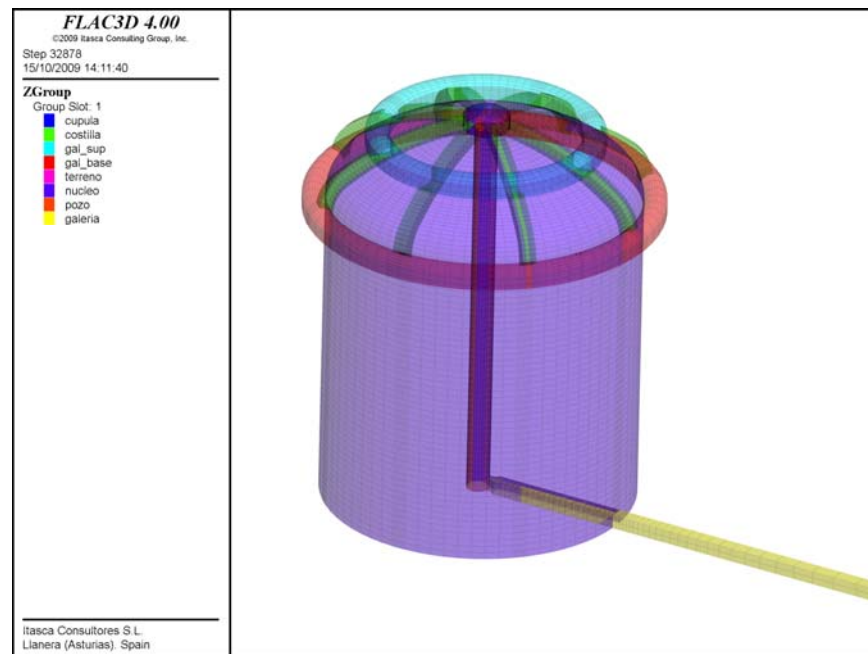


Figure 7.4-11. Geometry of the cavern, with the base gallery and the central shaft for the “raise boring” method.

#### 7.4.3 Geological description and calculation properties

Only one material type has been considered in the model (Shales), to which a Hoek-Brown constitutive model has been assigned, taking in mind the abovementioned rock quality descriptions that were obtained during the construction of the Somport Tunnel. The material properties assigned to the calculation elements are shown in Table 7.4-2. Regarding the coefficient of earth pressure at rest, it has been considered  $K_0 = 1$  before the erosion that could have produced the current topography.

Material	$E$ (GPa)	$\nu$	$\sigma_{ci}$ (MPa)	$m_i$	$D$	$GSI$	$m_b$	$s$	$a$
Shales	4.9	0.3	60	12	0	50	1.677	0.0039	0.506

Table 7.4-2. Calculation properties.

#### 7.4.4 Support elements

In an initial approach, the horizontal galleries and the ribs will be concreted before the excavation of the vault using in situ concrete HM-30. These concrete in galleries and ribs, have been modelled using regular volumetric elements. Two different approaches have been analysed:

- With an elastic constitutive model. The Young modulus has been calculated according to the definition of secant modulus of Spanish concrete standards ( $E_{28} = 8500 \cdot \sqrt[3]{f_{ck}}$ ), that for a concrete HM-30 is obtained a value of  $E=28.5$  GPa. Additionally, a value of  $\nu=0.2$  for the Poisson ratio and a density of  $2.5 \text{ t/m}^3$  has been assigned.
- With a brittle behaviour of the concrete in tension, simulated using a strain-softening model (brittle behavior) in tension, with a peak strength in tension of 3 MPa and no residual tension, and a perfectly-plastic behavior in compression.

The local support of the galleries during the excavation process has not been included in the model, as the objective of this analysis is the global behaviour of the cavern, and not the analysis of local stability.

The other support elements of the cavern, 35 cm of shotcrete HP-30, have been modelled using the FLAC3D structural elements shells (Figure 7.4-12). As the sequential excavation of the cavern has been reproduced, the process of aging of the shotcrete has been considered, simulated by a variation of the Young Modulus with time. The relation between strength and age is pretty standard, defined by the Spanish standards EHE for normal and fast hardening shotcrete. Figure 7.4-13 shows a graphic with these definitions, compared to the results of some tests in shotcrete samples, with a good fit between those and the curve of fast hardening.

On the other hand, the relation between elastic modulus and age is not so clear. According to the data from several tests on shotcrete samples, a simple relation  $E=500 \cdot \text{strength}$  could be assumed (Figure 7.4-14). In the same graphic the relations given by EHE and EH-91 (different Spanish Standards) have been included,

showing a considerable difference between those relations and the results of the tests.

According to this, the model reproduces the aging law given by the Spanish EHE evolution of the strength for fast hardening shotcrete and the relation between this strength and the elastic modulus given by the tests. Along with this moduli law, for a shotcrete of 30 MPa of strength, a Poisson coefficient of 0.2 and a specific weight of 25 kN/m<sup>3</sup> have been assumed.

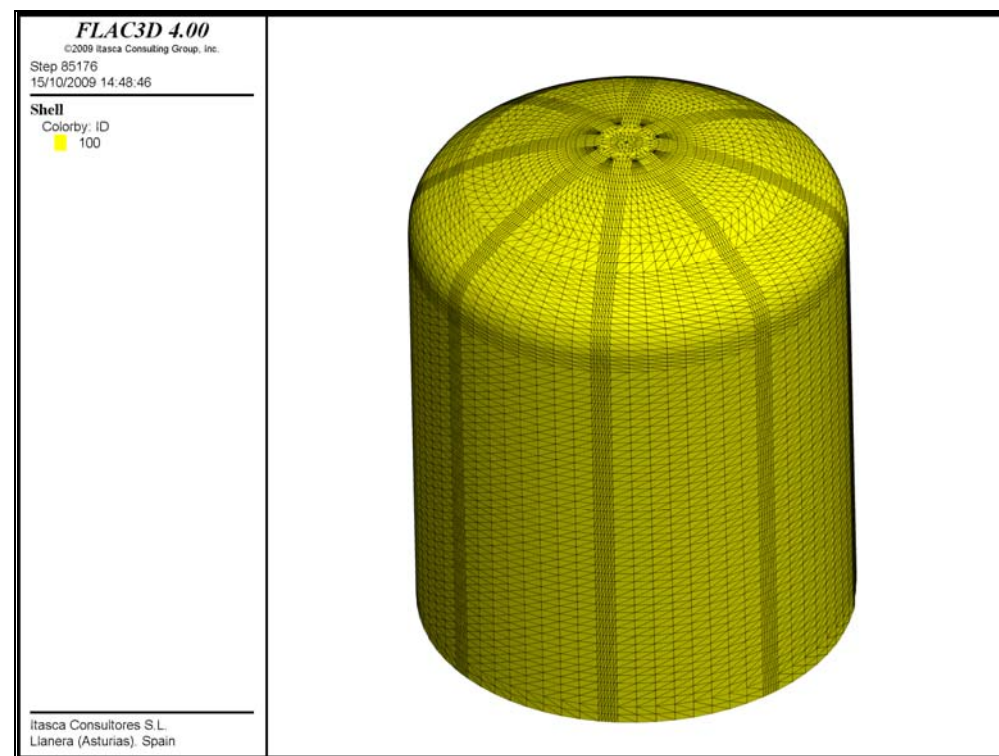


Figure 7.4-12. Shell structural elements to simulate the shotcrete in the cavern.

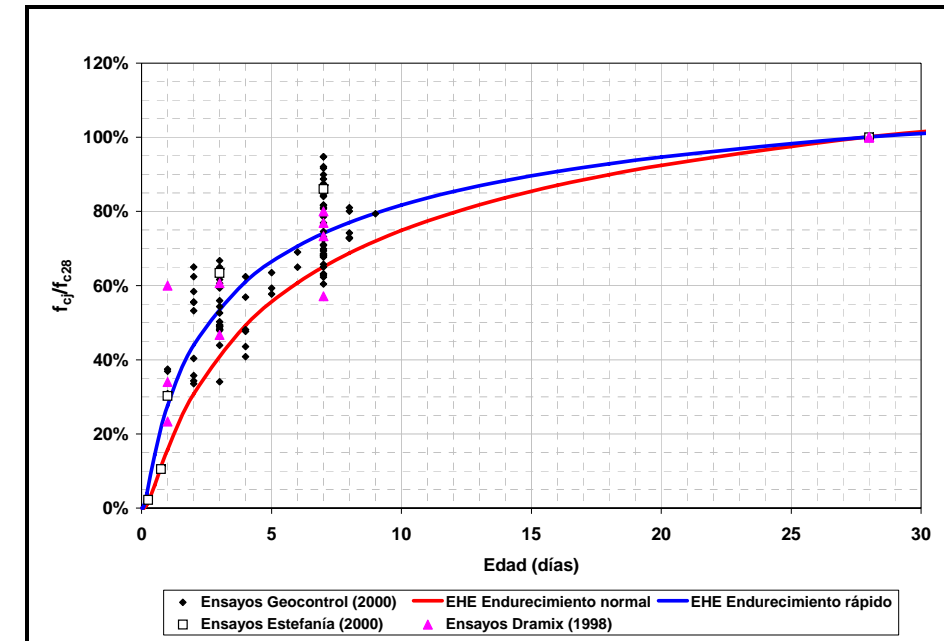


Figure 7.4-13. Shotcrete relative compressive strength vs age.

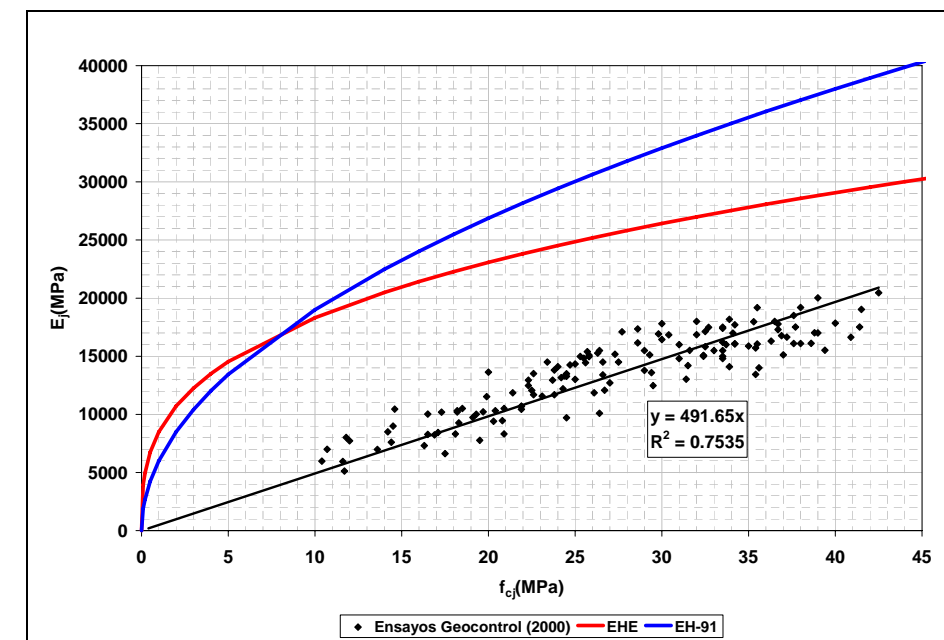


Figure 7.4-14. Young modulus vs compressive strength.



Along with the shotcrete, the cavern will be supported using a mesh of rockbolts and cables, that have been included in the model. The vault is supported using a system of cables 105 Ton and 18 m long, and  $\phi$  32 mm rockbolts, 6 m long, both in a 2x2 m grid, in a staggered pattern.

The cylindrical section of the cavern, will be supported using cables and bolts of the same characteristics and dimensions, in a grid of 3mVx1.33mL, resulting in the same support density (1 cable / 4 m<sup>2</sup>).

Both the cables and rockbolts have been included in the model using cable structural elements, with the properties summarized in table 7.4-3. Figure 7.4-15 shows the distribution of rockbolts and cables in the cavern. Figure 7.4-16 shows a plan view, with the distribution around the cylindrical section of the cavern.

Type	E (GPa)	Area (cm <sup>2</sup> )	Tensile strength (T)	Grout strength (T/m)
Cables (7 strands)	100	9.80	105	20
Rockbolts $\phi$ 32	200	8.04	40	20

Table 7.4-3. Properties assigned to the rockbolts and cables.

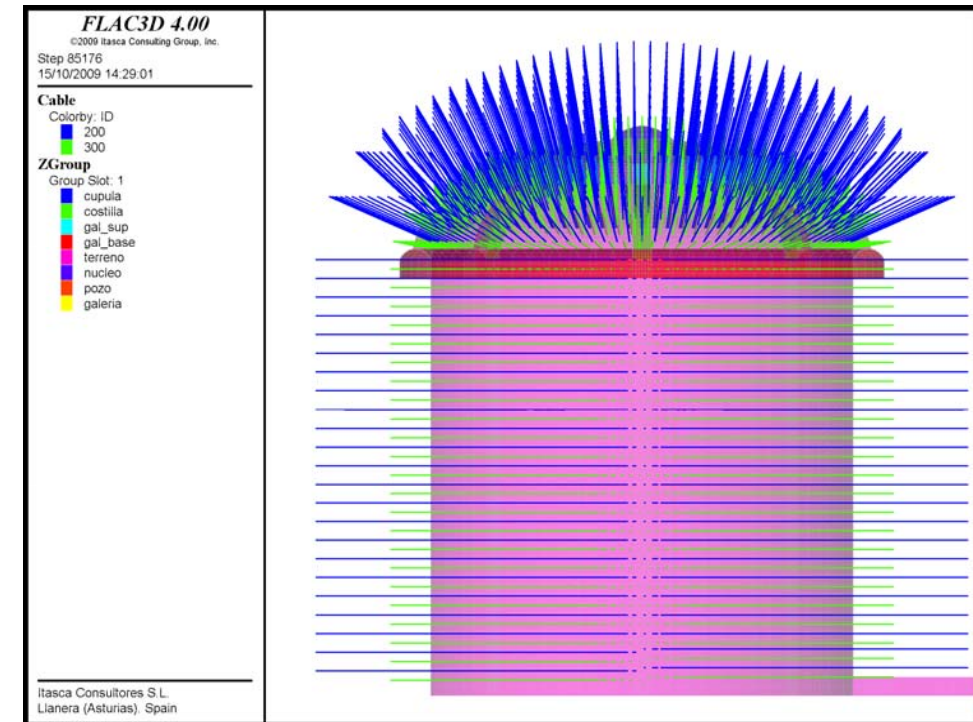


Figure 7.4-15. Cables and rockbolts in the cavern.

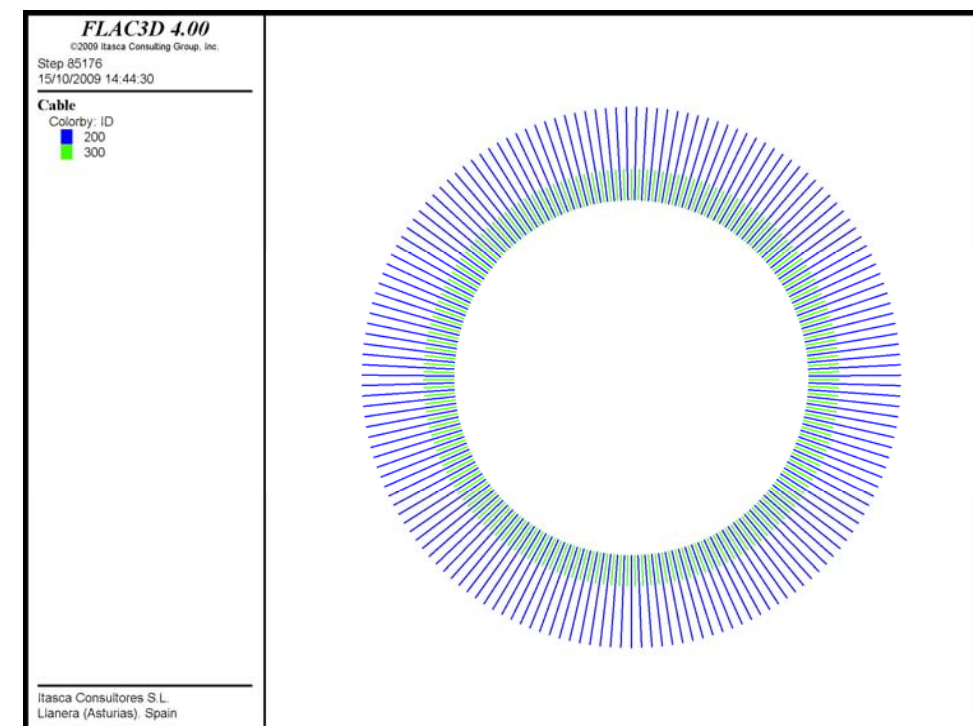


Figure 7.4-16. Cables and rockbolts in the cylindrical section. Plan view.

#### 7.4.5 Excavation sequence

The excavation sequence followed in the numerical model tries to reproduce, as far as possible, the real construction sequence. The excavation sequence modeled is as follows:

1. Establishment in the model of an initial stress state, prior to the excavation of the cavern. Since this initial stress state in equilibrium with the geometry of the mountain is not known, the model has been initialized considering a surface height equal to the maximum elevation of the mountain, constant all along the model, and with a horizontal/vertical stress ratio equal to 1. After allowing the model to reach a mechanical equilibrium, the distribution of initial stresses and the relations horizontal/vertical stress will better approach to the real topography of the problem.
2. Excavation of the base gallery of the vault support.
3. Excavation of the intermediate horizontal gallery of the vault support.
4. Excavation of the upper gallery of the vault support (dome).
5. Excavation of the ribs joining the galleries.
6. Excavation of the base gallery for the raise boring.
7. Excavation of the central shaft for the raise boring.
8. Pour concrete in the galleries and ribs of pre-support of the vault.
9. Excavation of the vault down to level 1082.
10. Support of the vault with 0.35 m of shotcrete HP-30 + rockbolts  $\Phi 32$  6 m long in a 2x2 m grid + cables 18 m long in a 2x2 m grid.

11. Sequential excavation of the rest of the cavern in 3 m high rounds, activating the support elements (0.35 of shotcrete + rockbolts and cables in a 3mVx1.33 mL grid) in the previous round. The sequential excavation consists in the activation of the support elements of one round (in a length equal to the excavation length), and the excavation of the next round. After the successive excavation of each of these rounds, the model is allowed to reach a mechanical equilibrium, before executing a new excavation round.
12. Once the level of 6 m above the raise boring base gallery has been reached, the calculation continues with the excavation of one half of the cavern, out from the gallery area, up to the bottom of the cavern.
13. Excavation of a trench above the gallery, in order to release the rock pillar above it
14. Excavation of the two benches left.

The following figures show different views of the model with the construction sequence reproduced in the calculations.



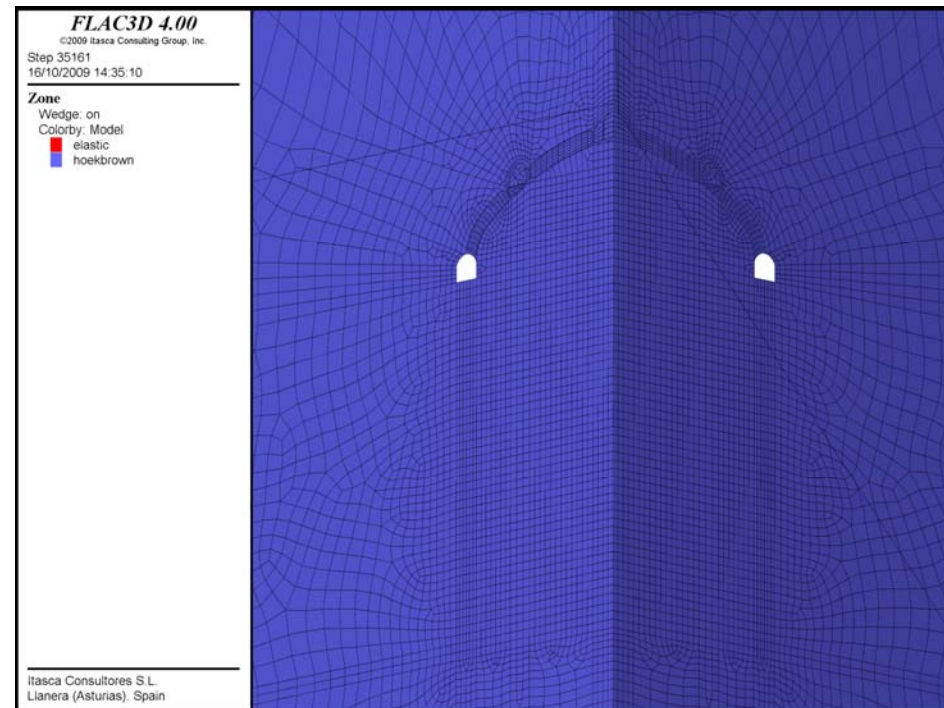


Figure 7.4-17. Phase 2: excavation of the base horizontal gallery.

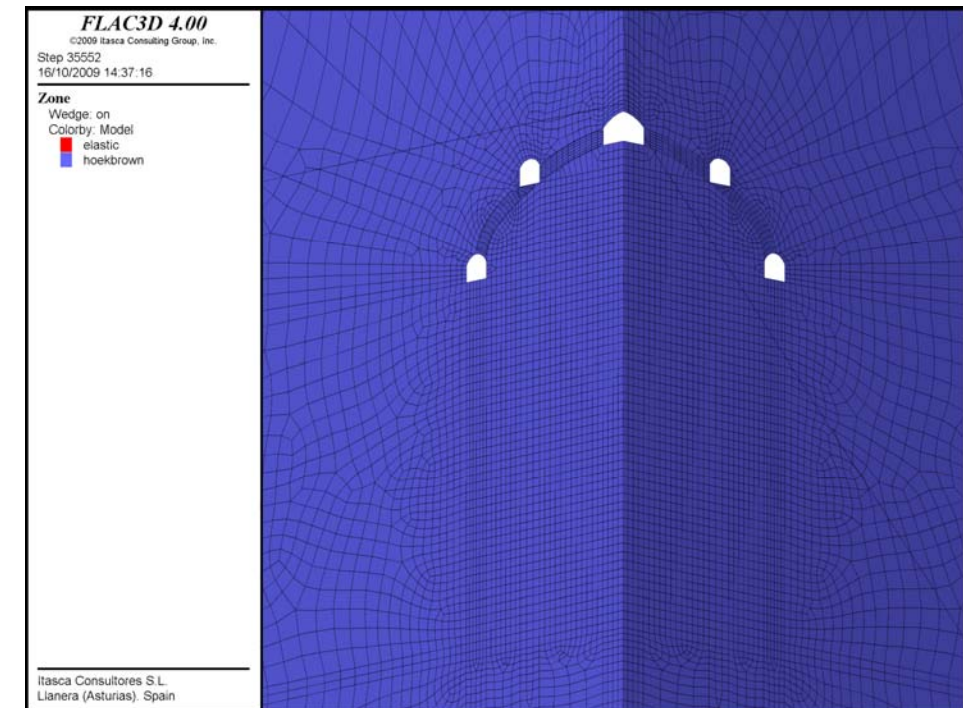


Figure 7.4-19. Phase 4: excavation of the top gallery (dome).

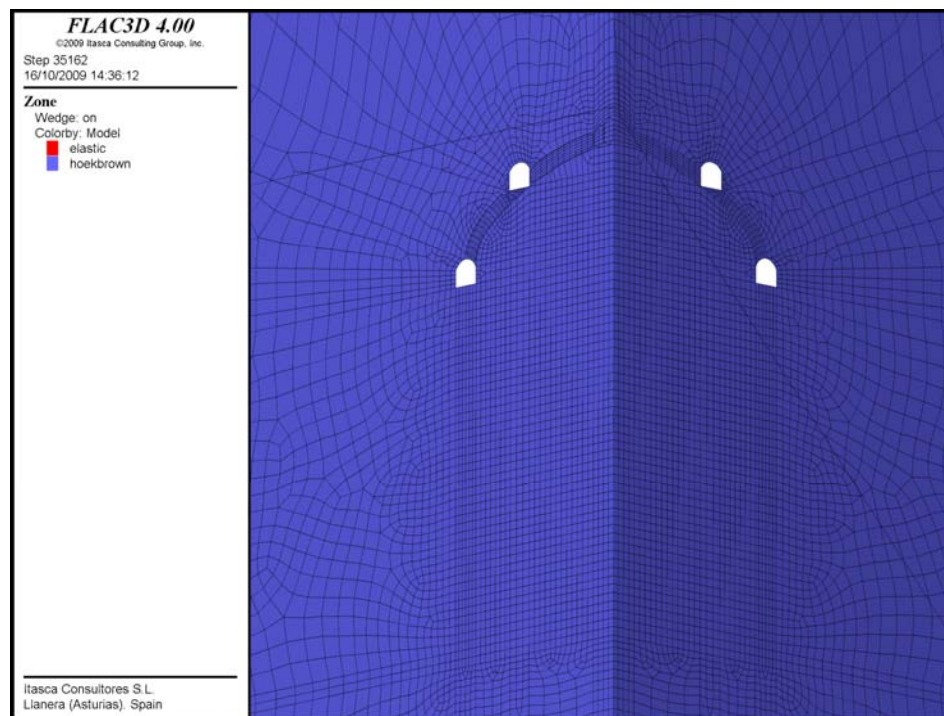


Figure 7.4-18. Phase 3: excavation of the intermediate horizontal gallery.

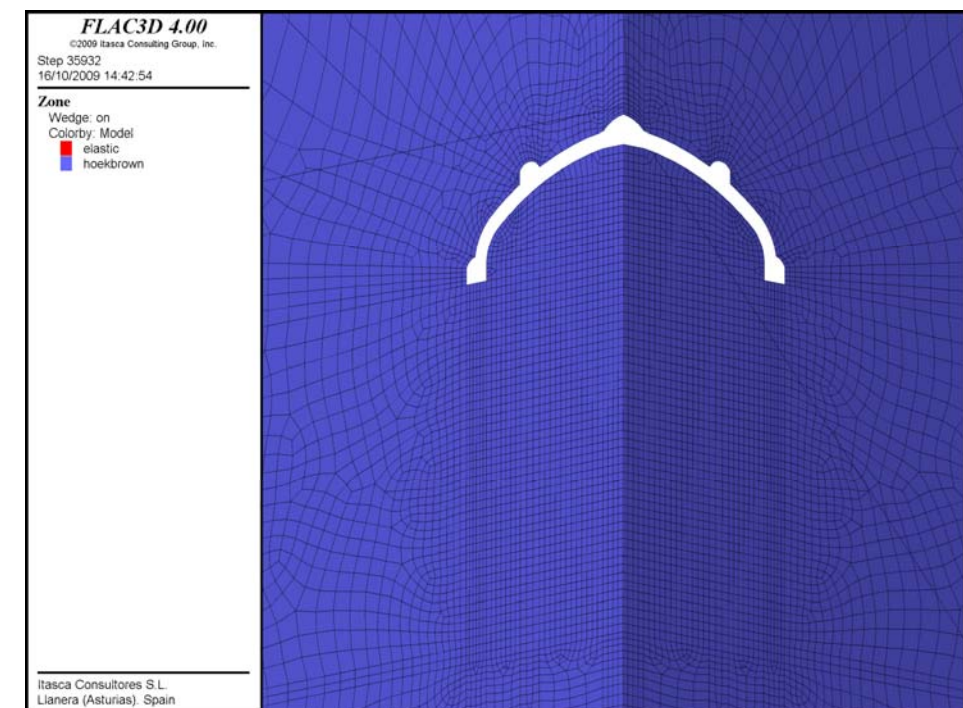


Figure 7.4-20. Phase 5: excavation of the ribs joining the galleries.



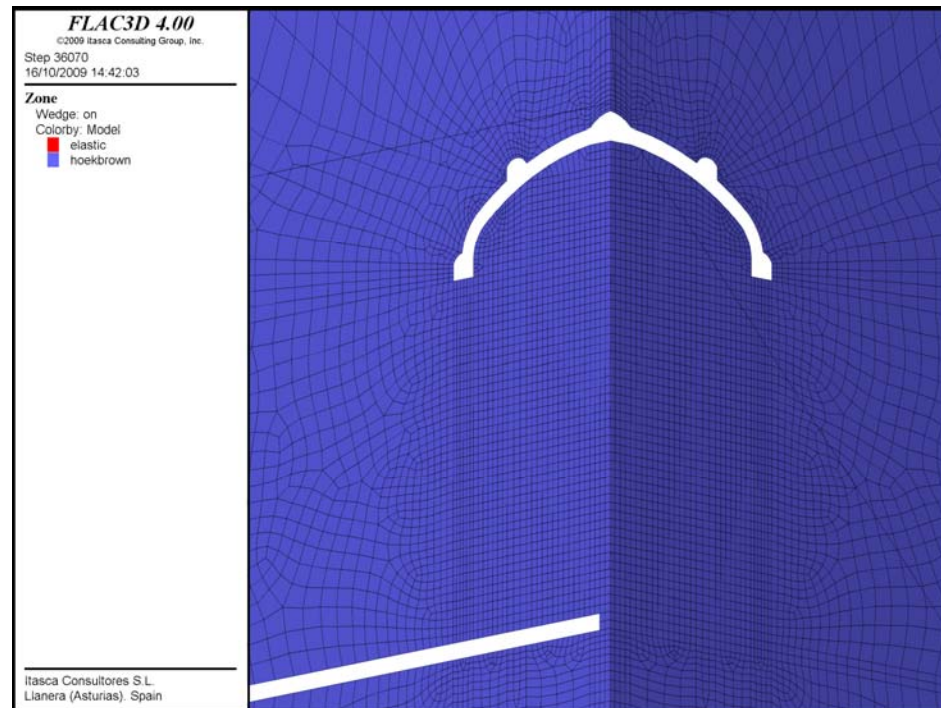


Figure 7.4-21. Phase 6: excavation of the raise boring base gallery.

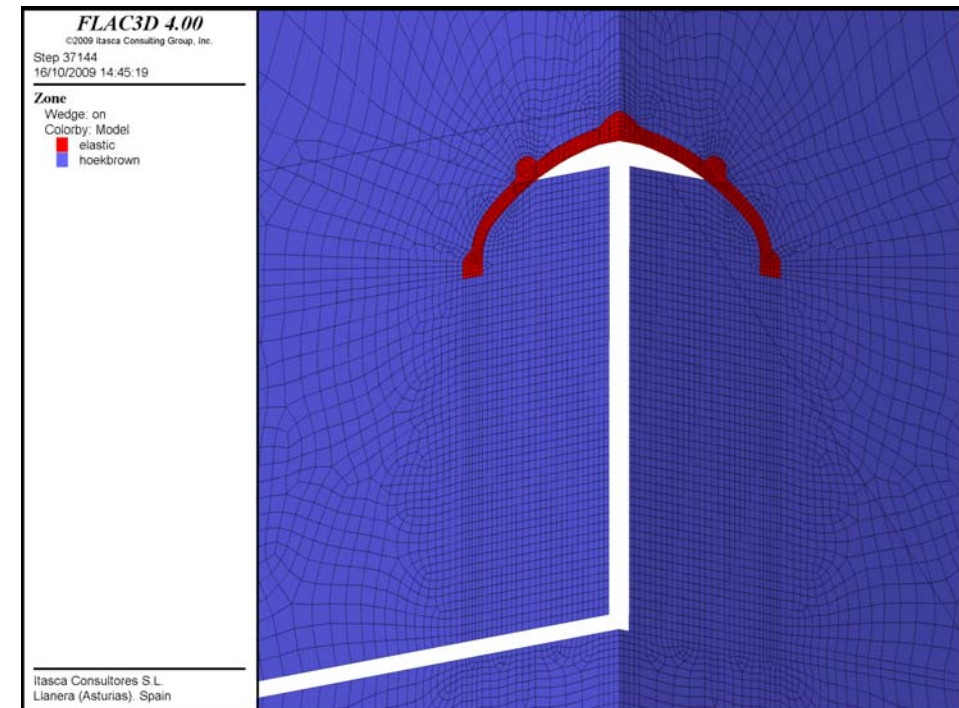


Figure 7.4-23. Phases 8/9: concrete of the pre-support and excavation up to level 1082.

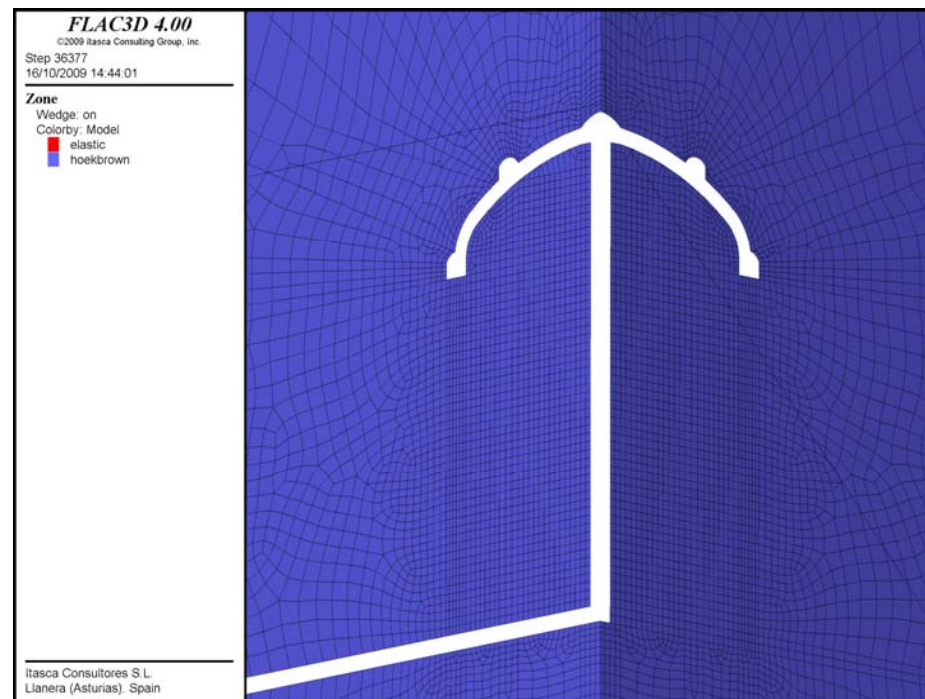


Figure 7.4-22. Phase 7: excavation of the raise boring central shaft.

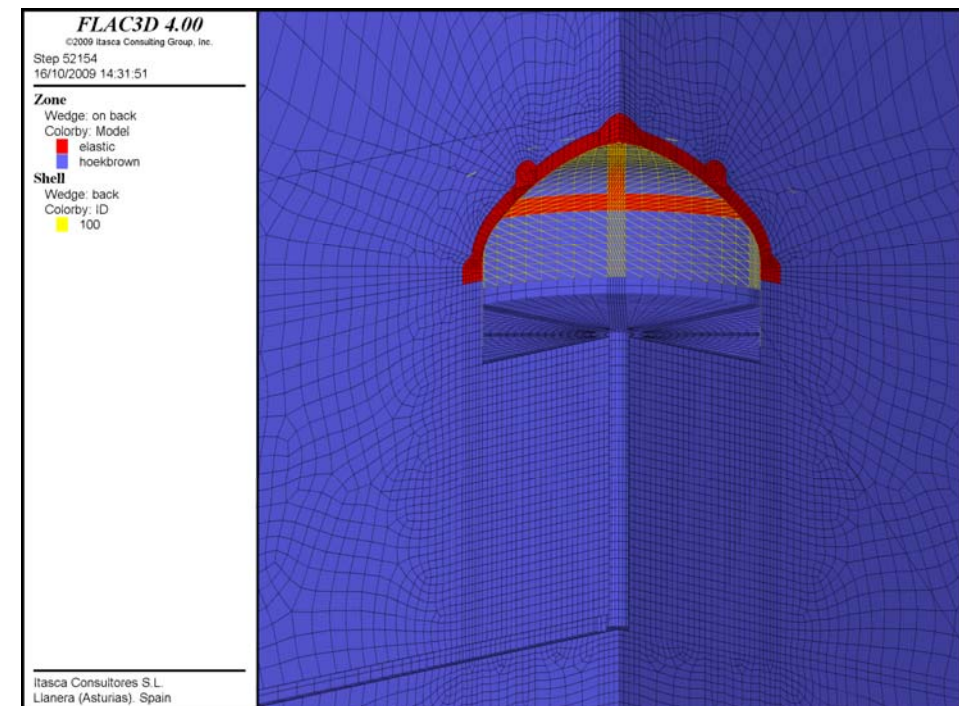


Figure 7.4-24. Intermediate situation in the sequential excavation of the cavern.  
(Note: there are represented  $\frac{3}{4}$  parts of the model, so the red band that appears at middle height is the projection of the horizontal gallery due to the perspective represented)



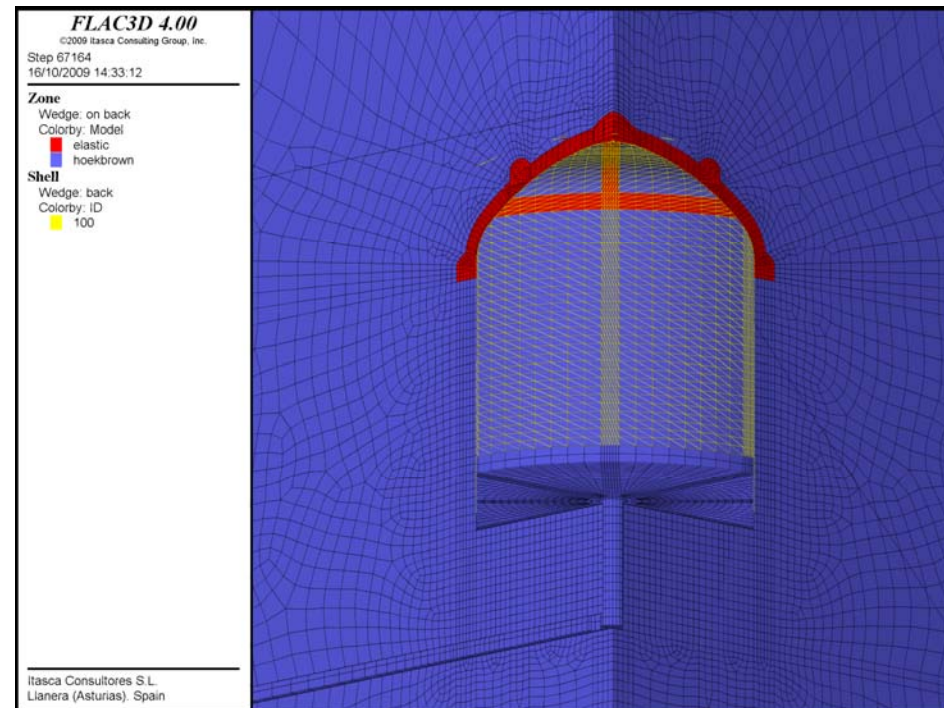


Figure 7.4-25. Intermediate situation in the sequential excavation of the cavern.

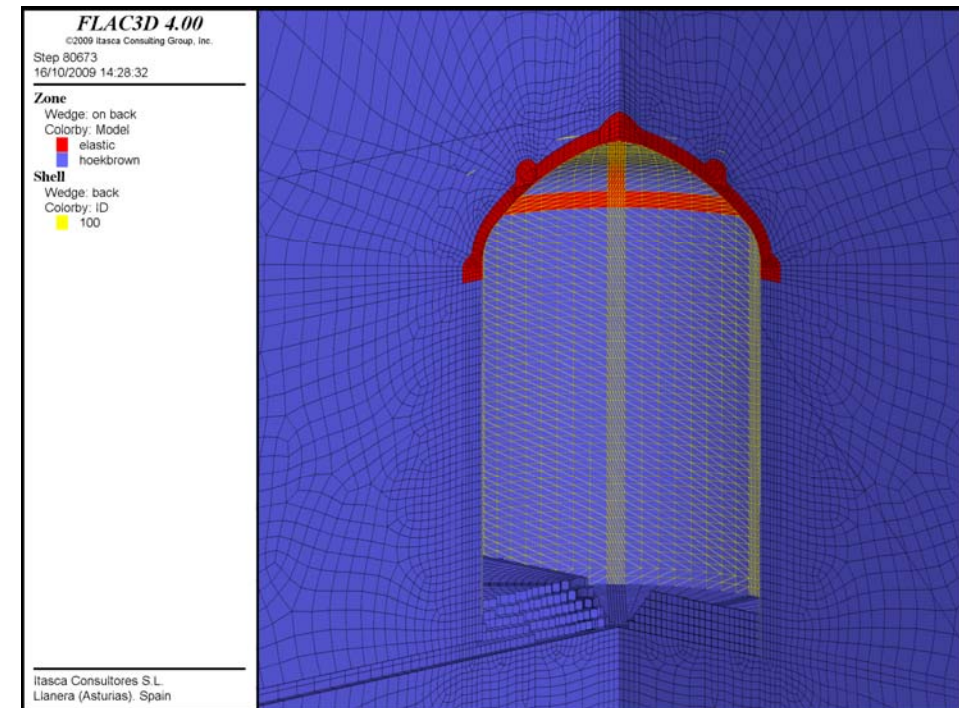


Figure 7.4-27. Excavation of the trench above the gallery.

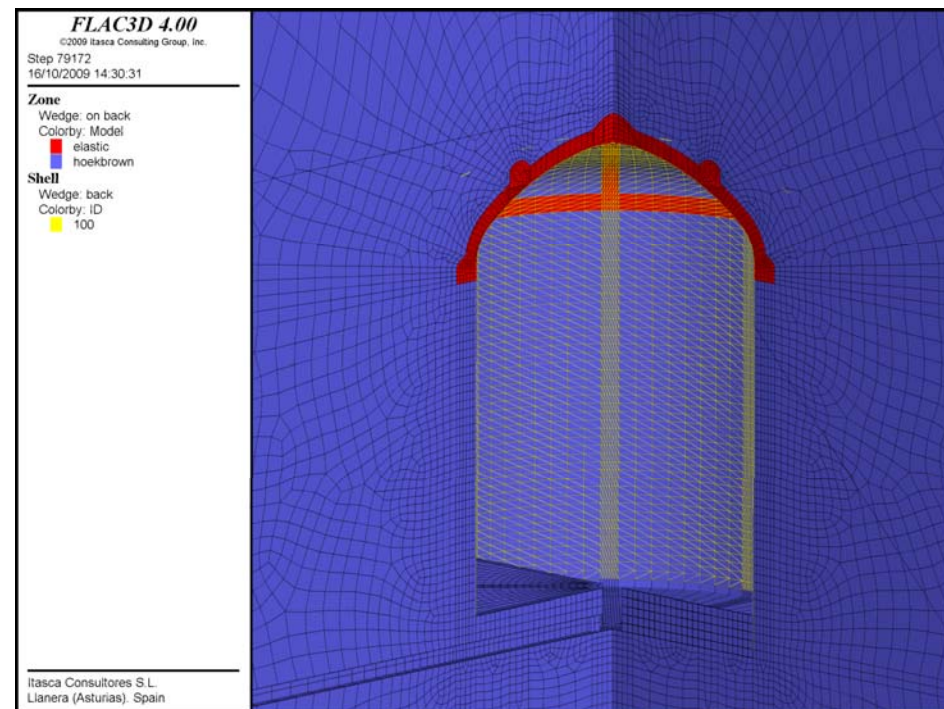


Figure 7.4-26. Excavation up to the bottom of the cavern in the area out from the gallery.

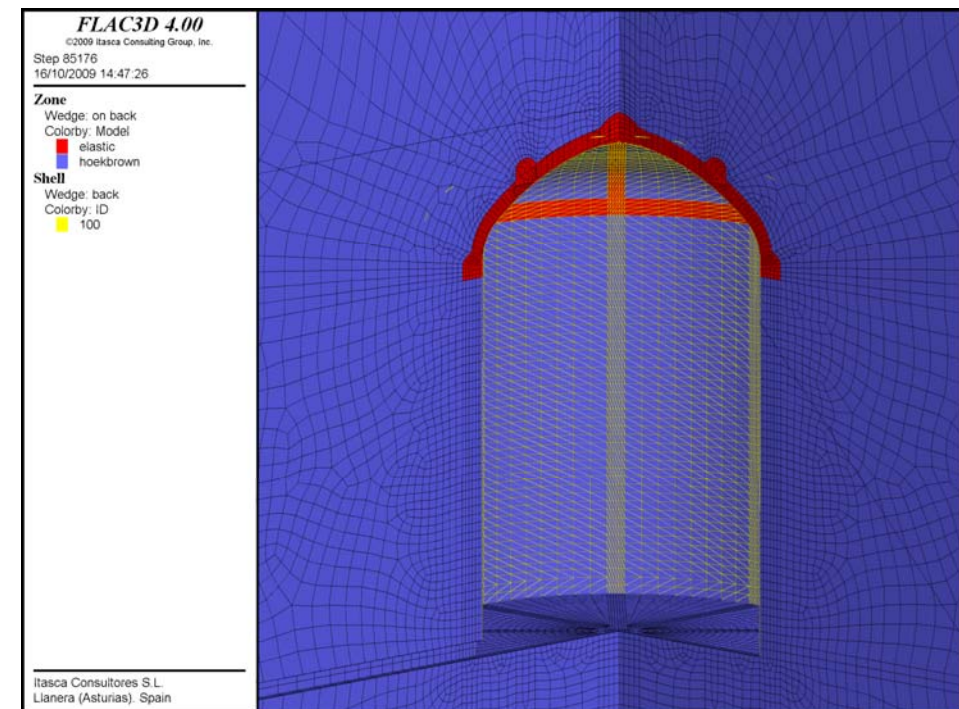


Figure 7.4-28. Final excavation of the cavern (benches).



## 7.4.6 Calculation results

In the next chapters, there is a description of the results obtained at the end of different calculation phases.

### 7.4.6.1 Hypothesis with elastic behaviour of the concrete

#### End of excavation down to level 1082

Figure 7.4-29 shows total vertical displacements at the end of this calculation phase, with a maximum of 7.6 cm above the vault, and a heave of 10.7 in the centre of the excavated area.

Figure 7.4-30 shows the vertical displacements in the concrete filling the galleries and ribs above the vault.

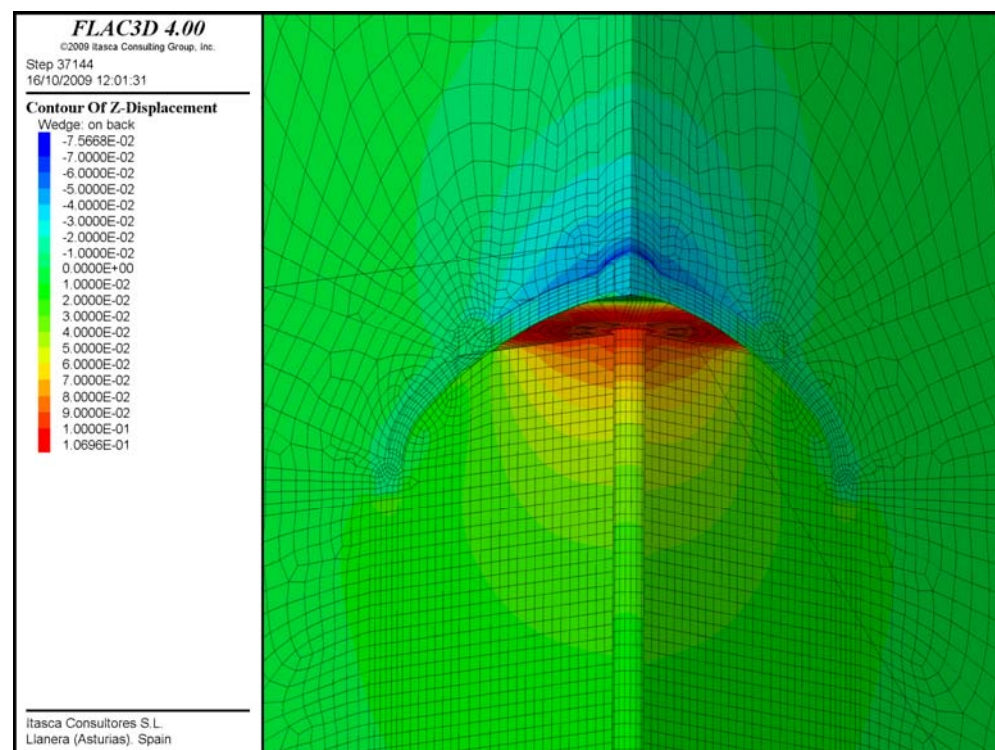


Figure 7.4-29. Total vertical displacements.

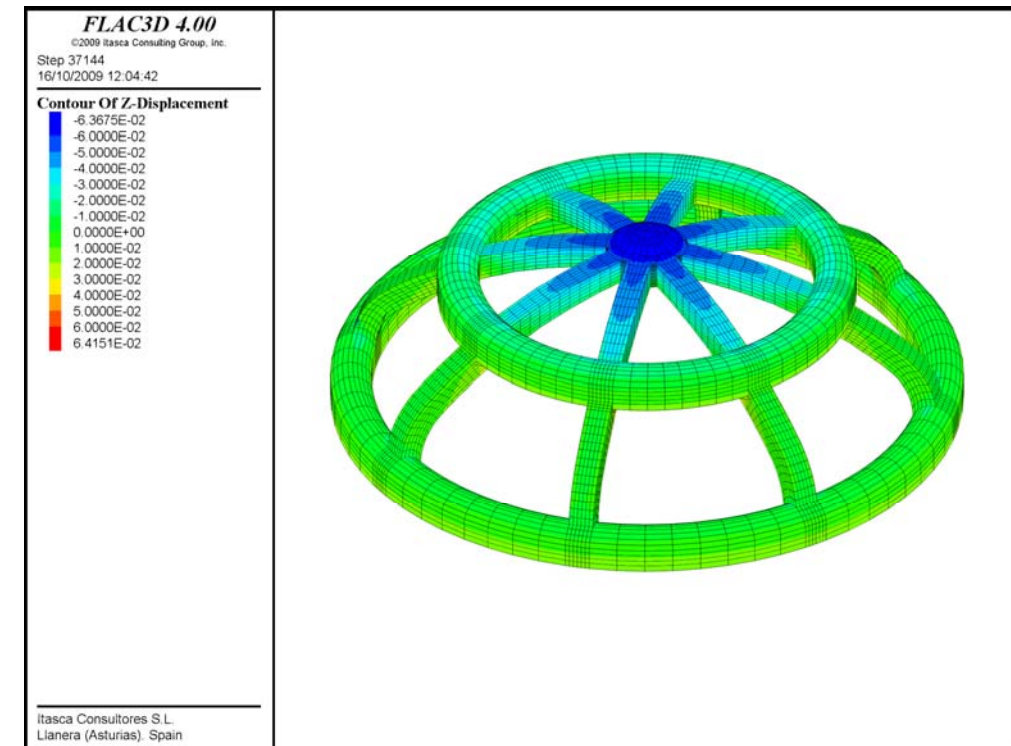


Figure 7.4-30. Vertical displacements in the support concrete.

The plasticity produced is shown in Figure 7.4-31. It is located only around the galleries and the vertical shaft, only in those elements close to the excavation areas (about 2-3 m). There is a deeper plastification area below the excavation, 10 m thick in the centre of the excavation.

Figure 7.4-32 shows the compressive stresses in the concrete of galleries and ribs. High compressive stresses are located in the joints between the ribs and the intermediate gallery, with mean values of about 50 MPa, although specific values up to 90 MPa are calculated in some of these areas.

The same behaviour is obtained for the tension stresses, as it is shown in Figure 7.4-33 (only those values above 3 MPa are represented). In the ribs, values above this magnitude are obtained in general, with maximum peaks up to 36 MPa in some areas.

Those high stress levels are produced because of the geometry of the deformation induced by the excavation: while the horizontal gallery hardly has any vertical displacement in this calculation phase, the top gallery (dome) and the ribs have a vertical displacement of several centimetres. As the joint between them is rigid, there is a high stresses location in the rib-gallery connection.

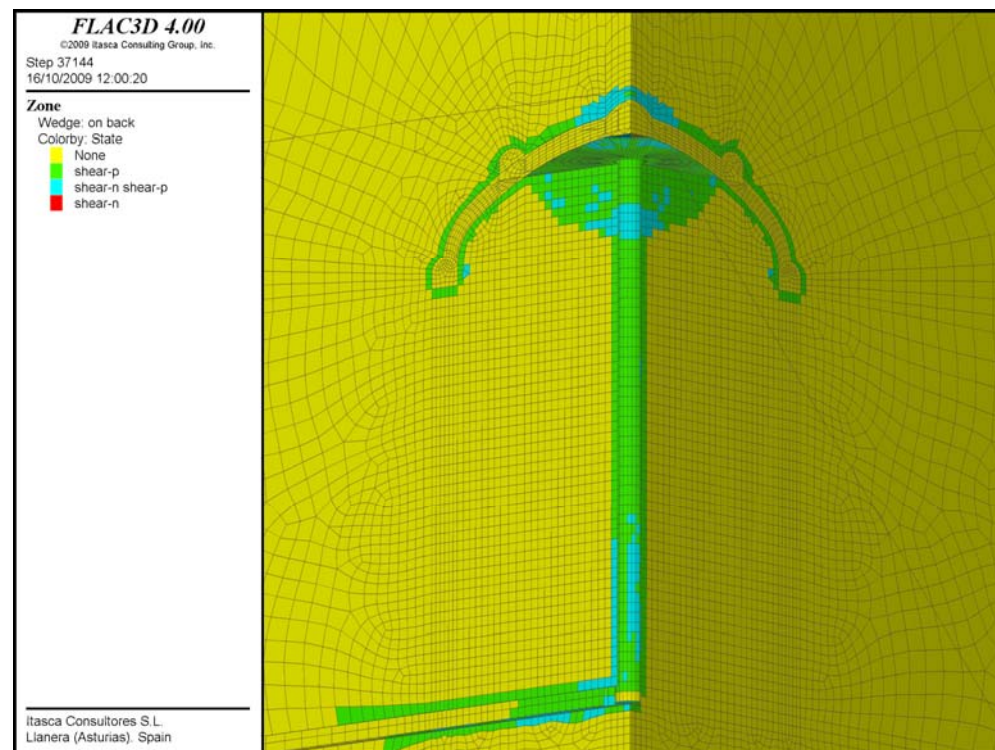


Figure 7.4-31. Plasticity indicators.

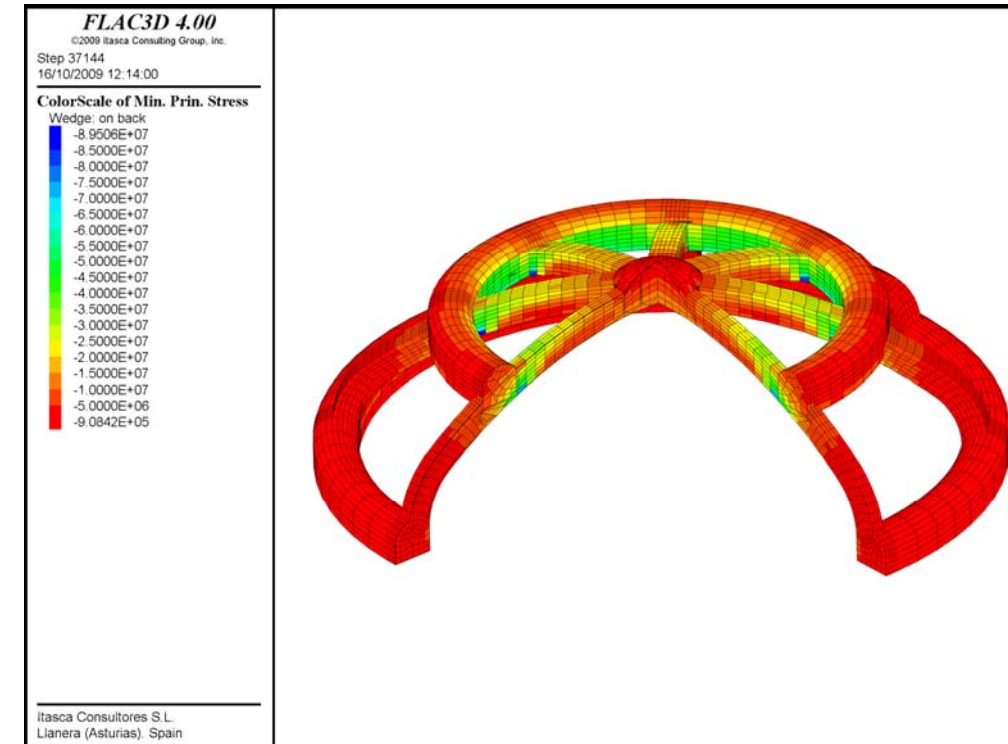


Figure 7.4-32. Compressive stresses in the concrete of the pre-support.

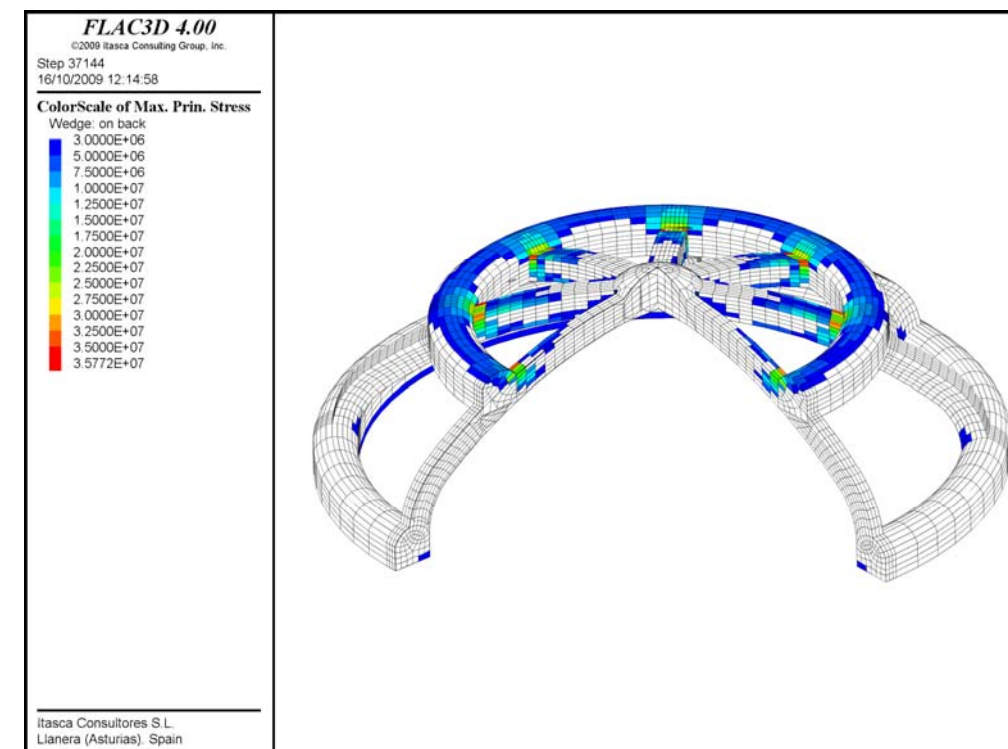


Figure 7.4-33. Tension stresses in the concrete of the pre-support.



### End of excavation of the cavern

Figure 7.4-34 shows total vertical displacements at the end of the excavation of the cavern, with a maximum displacement of 12 cm above the vault, and a heave of 27 cm below the invert.

Figure 7.4-35 shows the vertical displacements in the concrete filling the galleries and ribs above the vault, with a maximum displacement of 9 cm in the top dome.

Displacements in the shotcrete that supports the cavern are shown in Figure 7.4-36, with maximum values of 14 cm (semi-convergence). It can be appreciated in the displacement distribution the sequence followed during the excavation process, in 3 m high rounds.

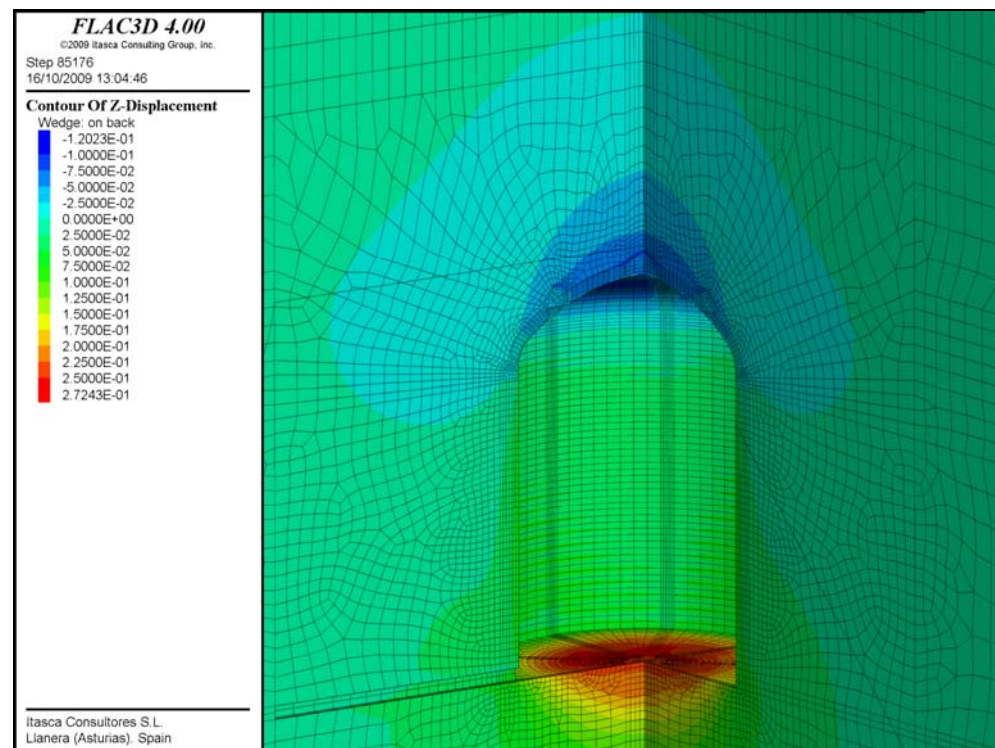


Figure 7.4-34. Total vertical displacements.

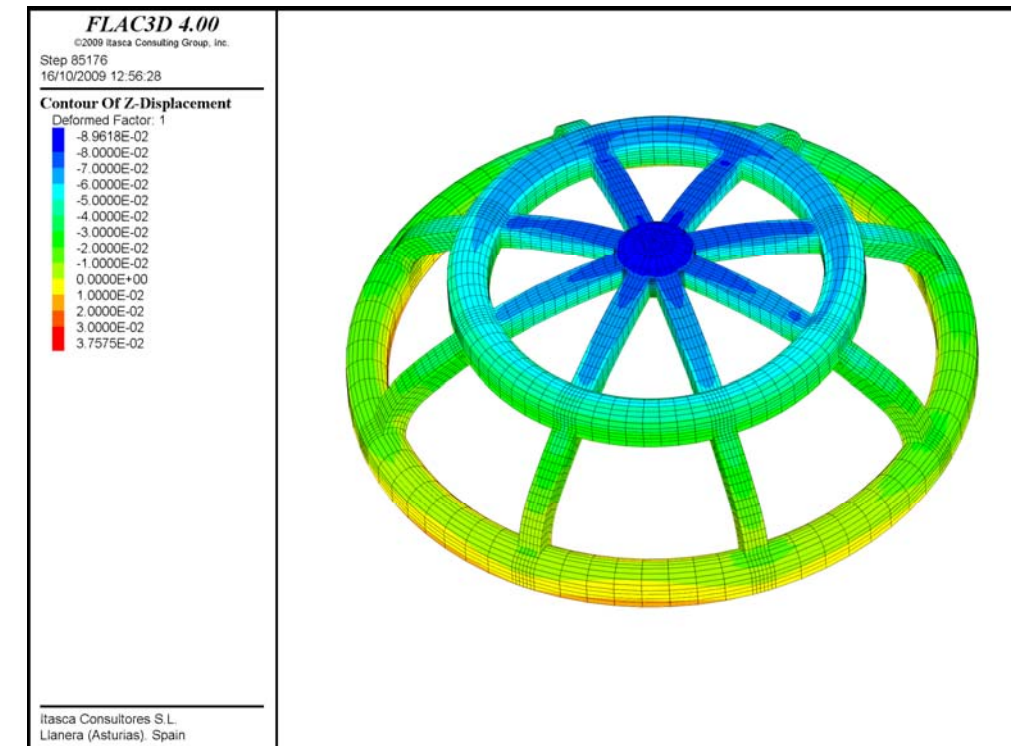


Figure 7.4-35. Vertical displacements in the support concrete.

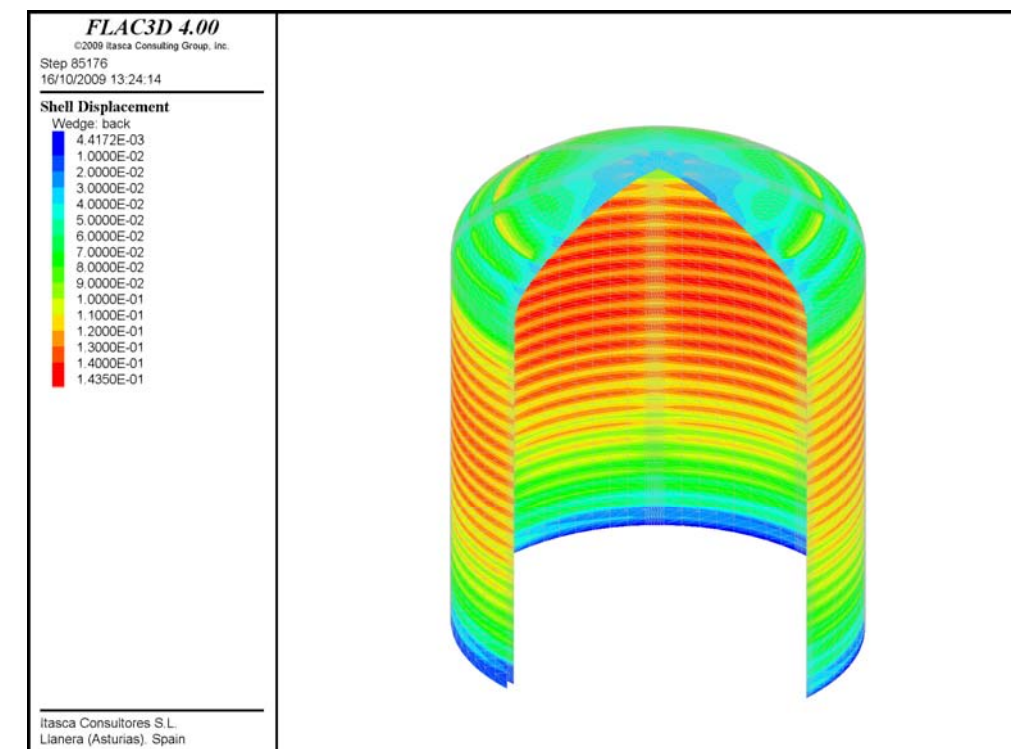


Figure 7.4-36. Vertical displacements in the shotcrete of the cavern.

Figure 7.4-37 shows the plasticity calculated at the end of excavation. The thickness of the plasticity ring around the cylinder is about 13 m in the central area. Below the excavation, the plasticity area is 28 m deep below the centre of the cavern.

Figures 7.4-38 and 7.4-39 show the compressive and tension stresses in the concrete of galleries and ribs. As the excavation of the cavern goes deeper, the higher stresses are located in the joints between ribs and the lower horizontal gallery, and even the areas that had high stresses in the previous phase give now lower values of stresses (specially tensions). The maximum values of compressive stresses in this phase are 137 MPa, located in the joint rib-base gallery, and maximum tension of 30 MPa.

Figure 7.4-40 shows loads in the reinforcement cables, with mean values of 30 Ton, although maximum values up to 54 Ton have been calculated (anyway below their maximum capacity).

Figure 7.4-41 shows the loads obtained in the rockbolts, most of them have reached their maximum capacity (40 Ton) in their initial length (2-3 meters).

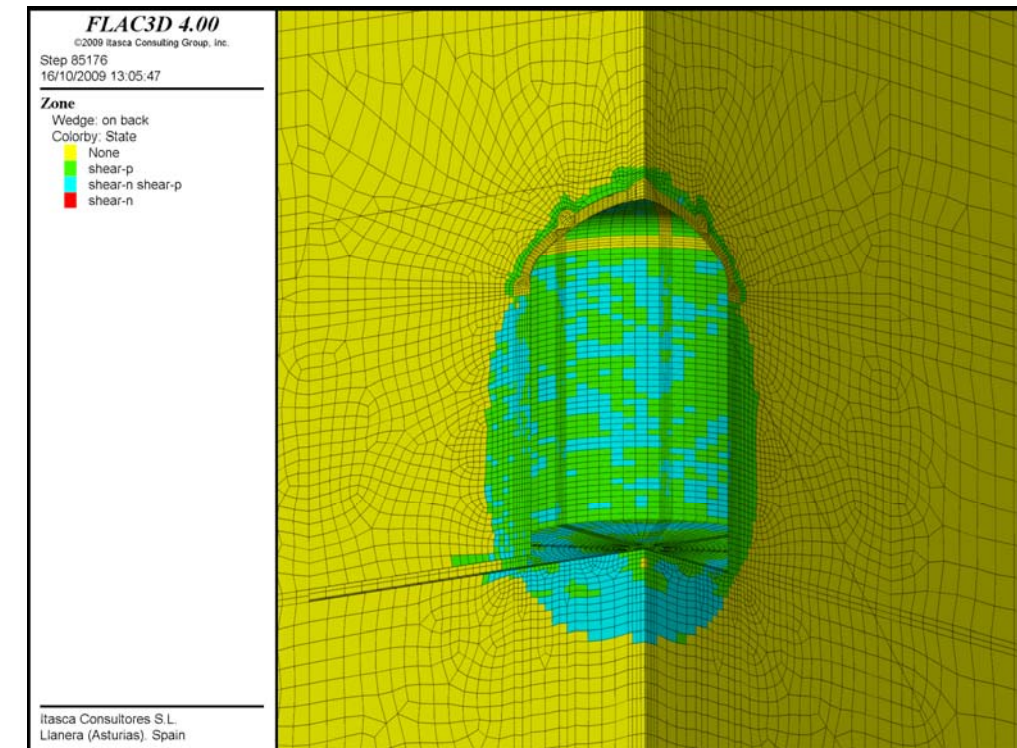


Figure 7.4-37. Plasticity indicators.

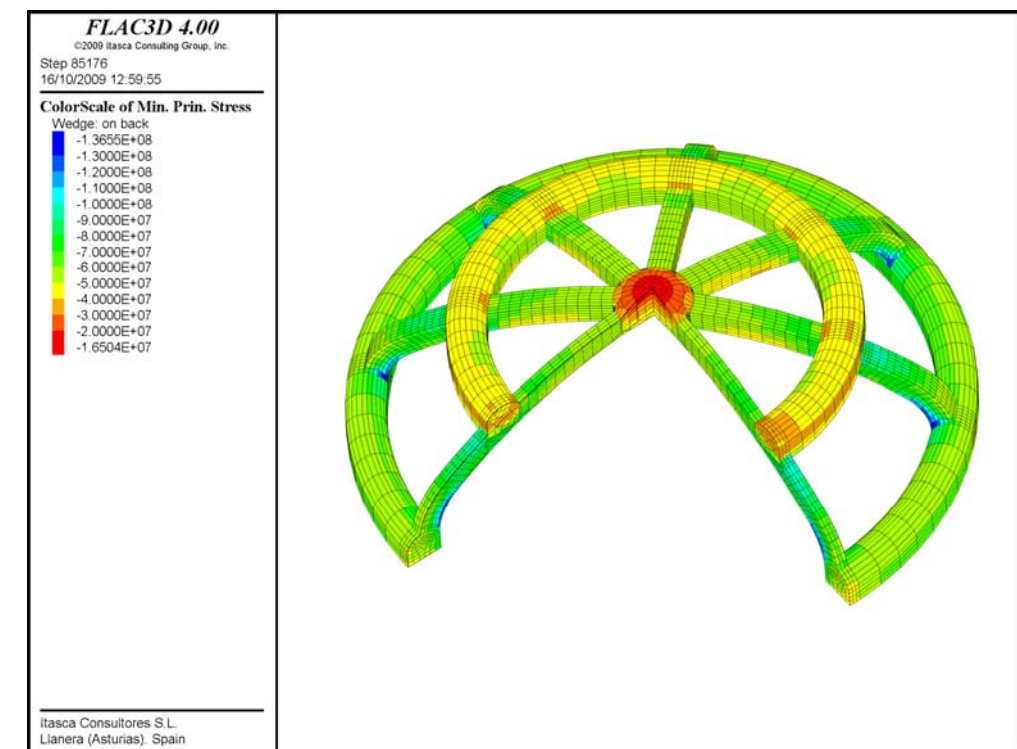


Figure 7.4-38. Compressive stresses in the concrete of the pre-support.



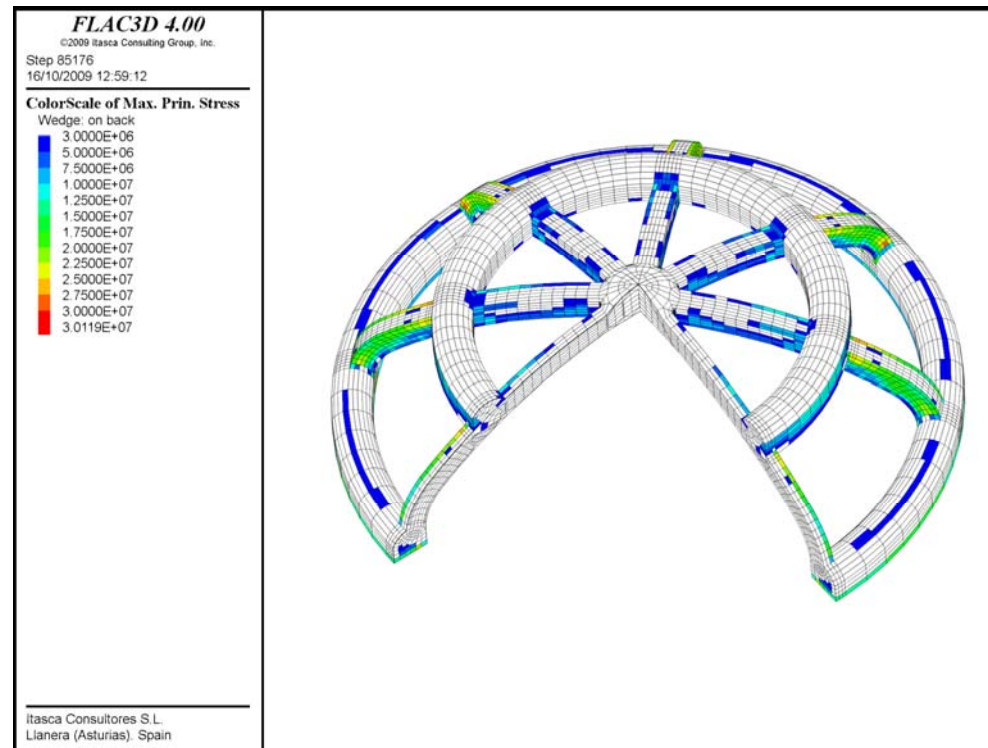


Figure 7.4-39. Tension stresses in the concrete of the pre-support.

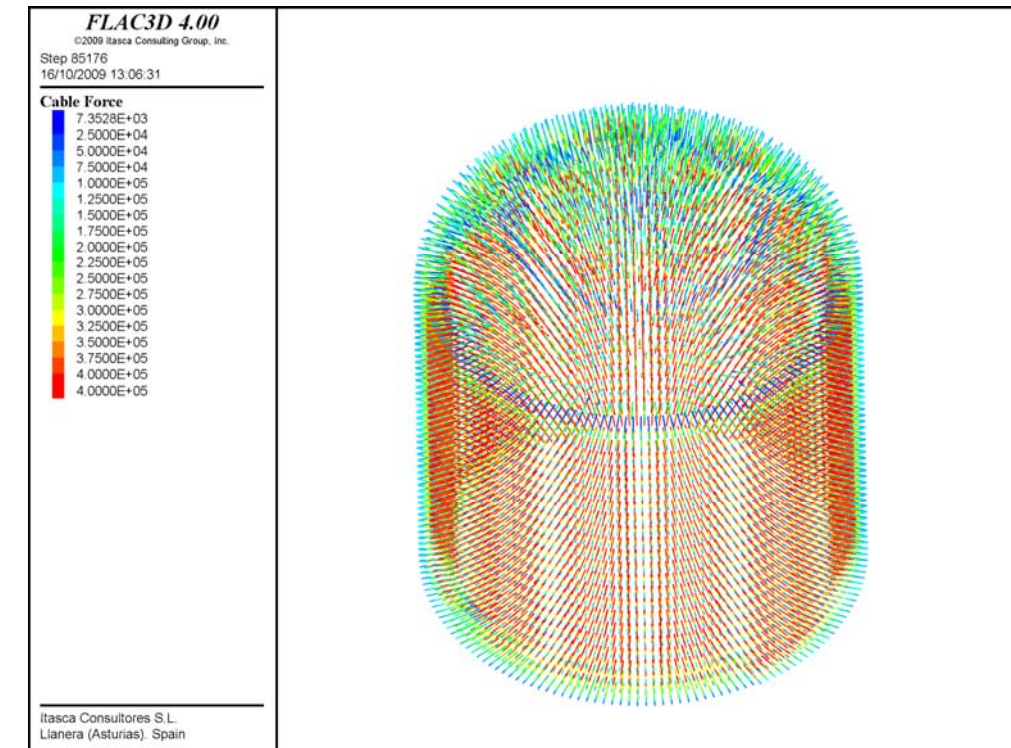


Figure 7.4-41. Loads in the rockbolts.

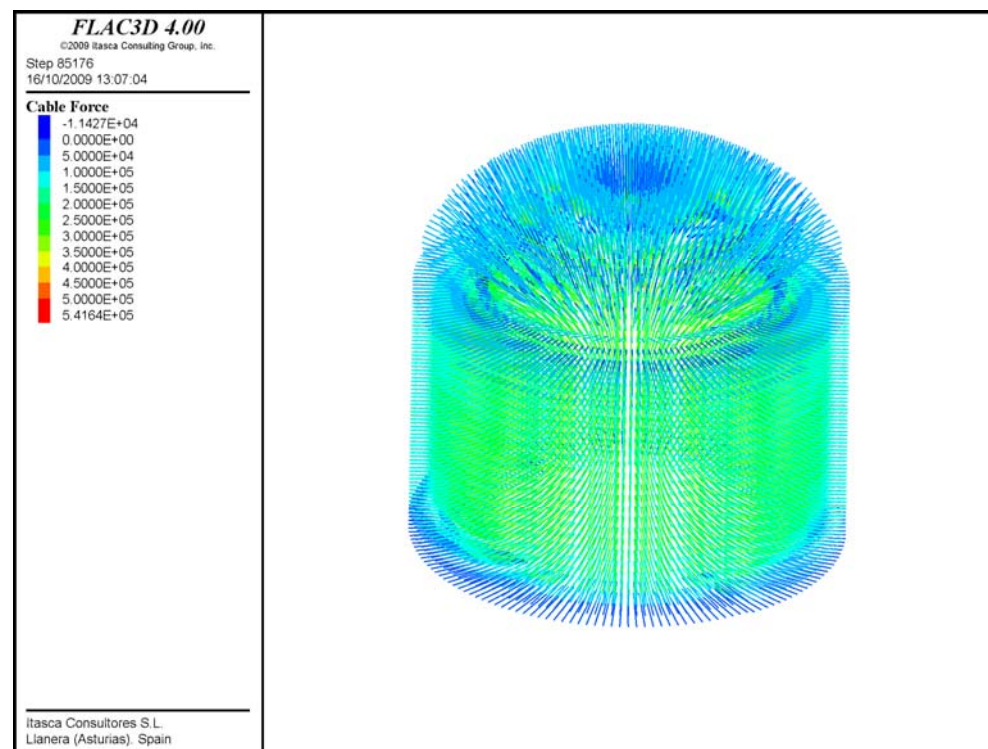


Figure 7.4-40. Loads in the cables.

According to the results obtained, and taking into account the calculation hypothesis considered, it can be concluded that the construction method adopted seems to be valid to guarantee the stability of the cavern. Nevertheless the stresses obtained in the concrete acting as pre-support of the vault are inadmissible, so it could be necessary to redefine the geometry of this support in order to change and improve the distribution of stresses on it.

#### 7.4.6.2 Hypothesis with brittle behaviour of the concrete

##### End of excavation down to level 1082

Figure 7.4-42 shows total vertical displacements at the end of this calculation phase, with a maximum of 10.1 cm above the vault, and a heave of 10.7 in the centre of the excavated area.



Figure 7.4-43 shows the vertical displacements in the concrete filling the galleries and ribs above the vault, with a maximum of 6.94 cm.

Plasticity indicators are shown in Figure 7.4-44. The plasticity produced is located only around the galleries and the vertical shaft, only in those elements close to the excavation areas (about 2-3 m), similar to the results obtained for the elastic model. There is a deeper plastification area below the excavation, 10 m thick in the centre of the excavation.

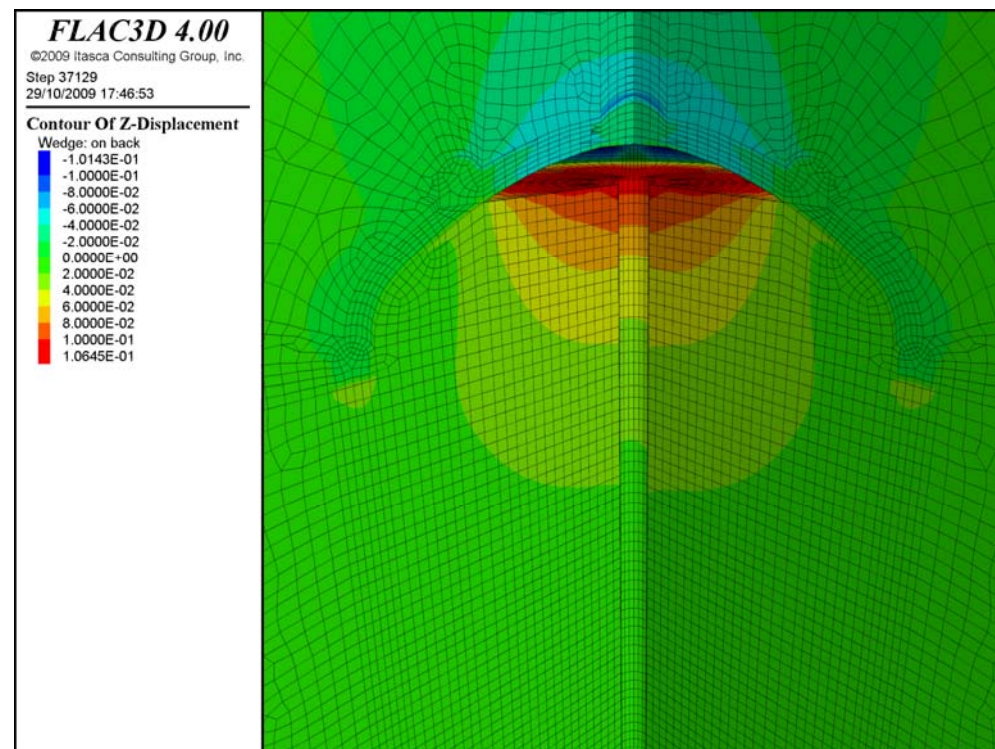


Figure 7.4-42. Total vertical displacements.

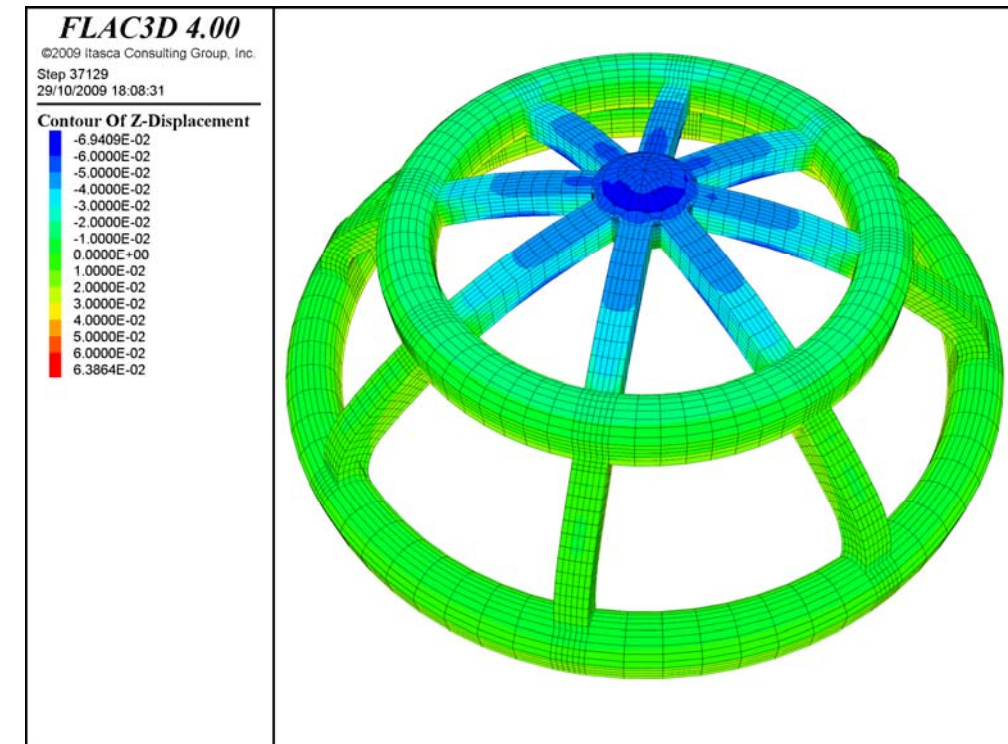


Figure 7.4-43. Vertical displacements in the support concrete.

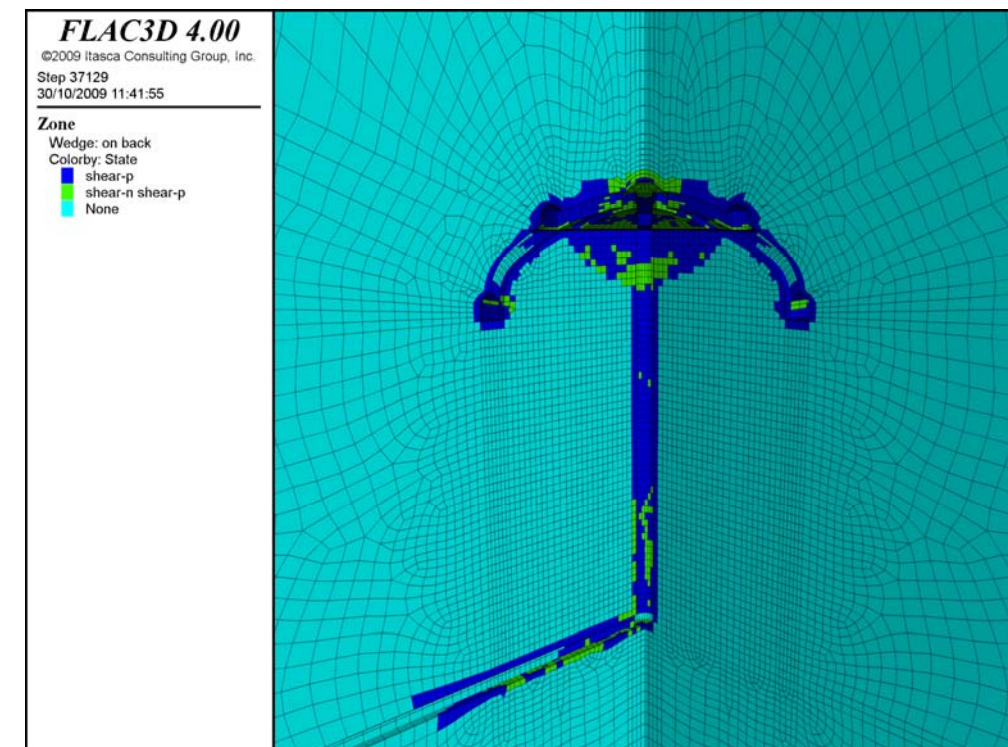


Figure 7.4-44. Plasticity indicators.



Figures 7.4-45 and 7.4-46 show the compressive stresses in the concrete of galleries and ribs. High compressive stresses are now located in the base of the intermediate gallery, with mean values up to 56 MPa. In the upper ribs the compressive stresses are now of about 30 MPa.

Considering this brittle behaviour, the levels of tension are now lower than in the previous hypothesis. The maximum values of 2 MPa are now located in the base horizontal gallery (Figure 7.4-47).

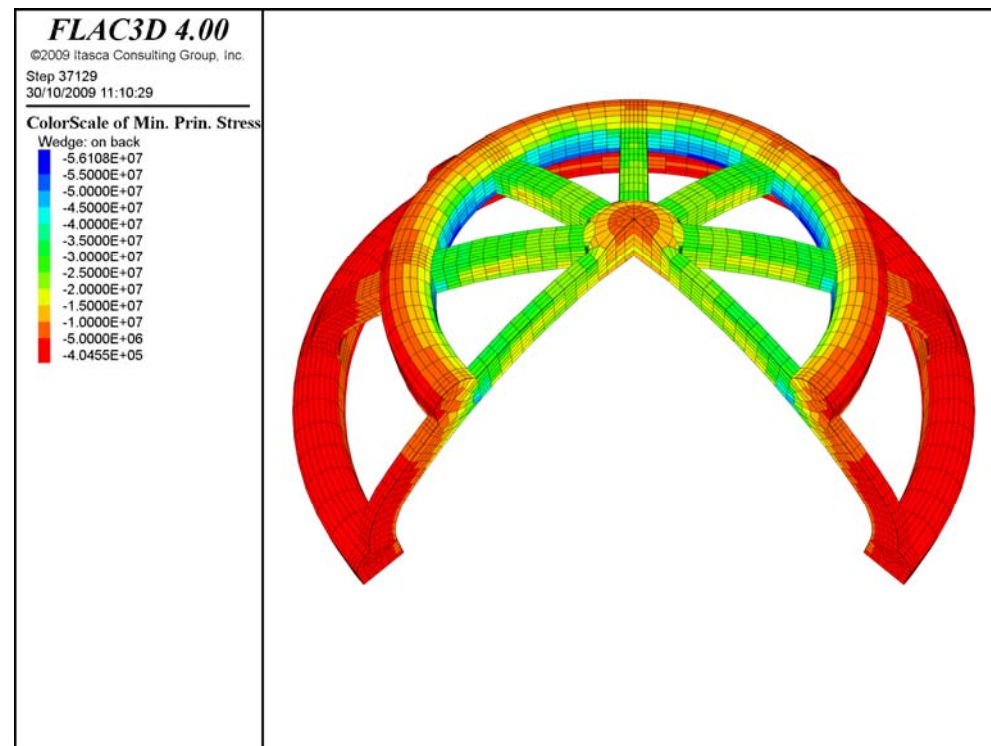


Figure 7.4-45. Compressive stresses in the concrete of the pre-support.

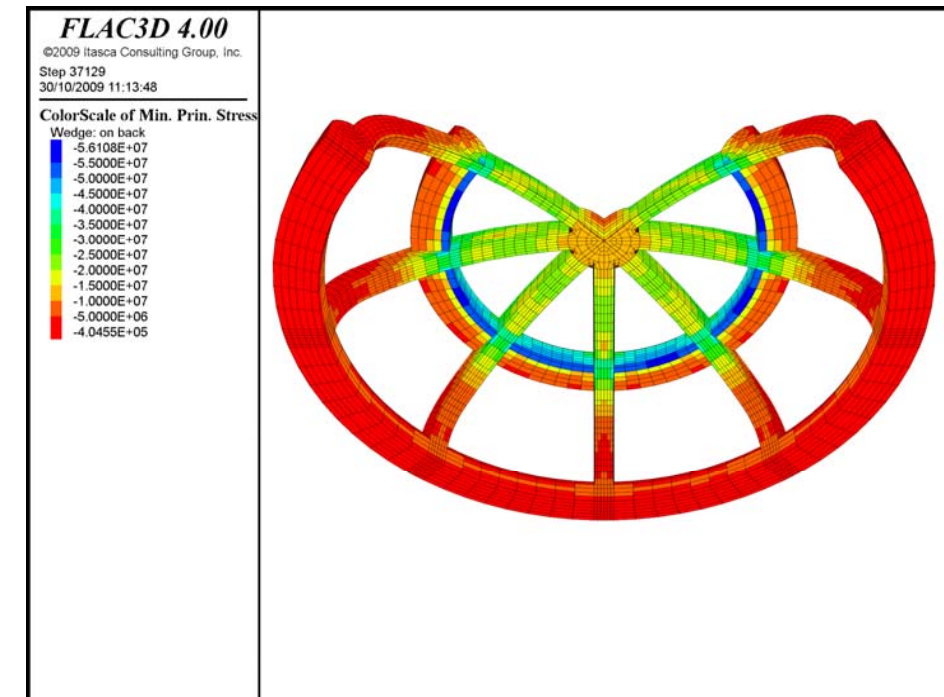


Figure 7.4-46. Compressive stresses in the concrete of the pre-support. Lower view.

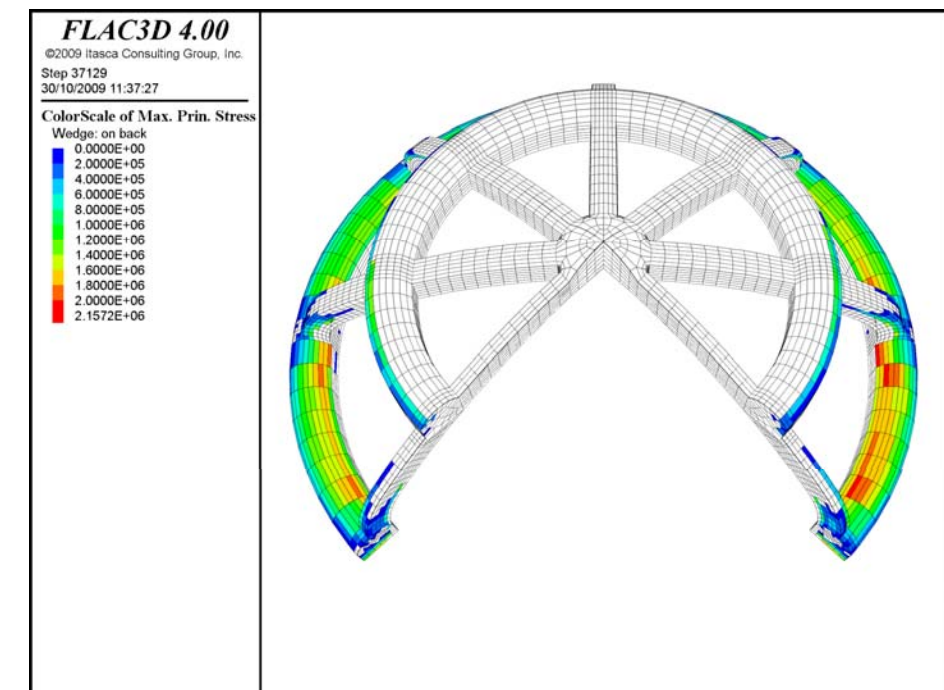


Figure 7.4-47. Tension stresses in the concrete of the pre-support.

Figures 7.4-48 and 7.4-49 show the location of different profiles in the ribs and the horizontal galleries that have been selected to show the stresses distribution in the following figures.

Figure 7.4-50 and 7.4-51 show the minor and major principal stress distribution in the rib, respectively. The values of the mayor principal stress are negative (compressive) so no tensions are calculated in the ribs. The maximum compressive stress is 30 MPa.

Figure 7.4-52 shows the minor principal stress distribution in the horizontal gallery, with a maximum of 56 MPa in the lower left corner.

Figure 7.4-53 shows the major principal stress distribution in the gallery, with a maximum value of 1.8 MPa in the upper right corner, although most of the section is in compression.

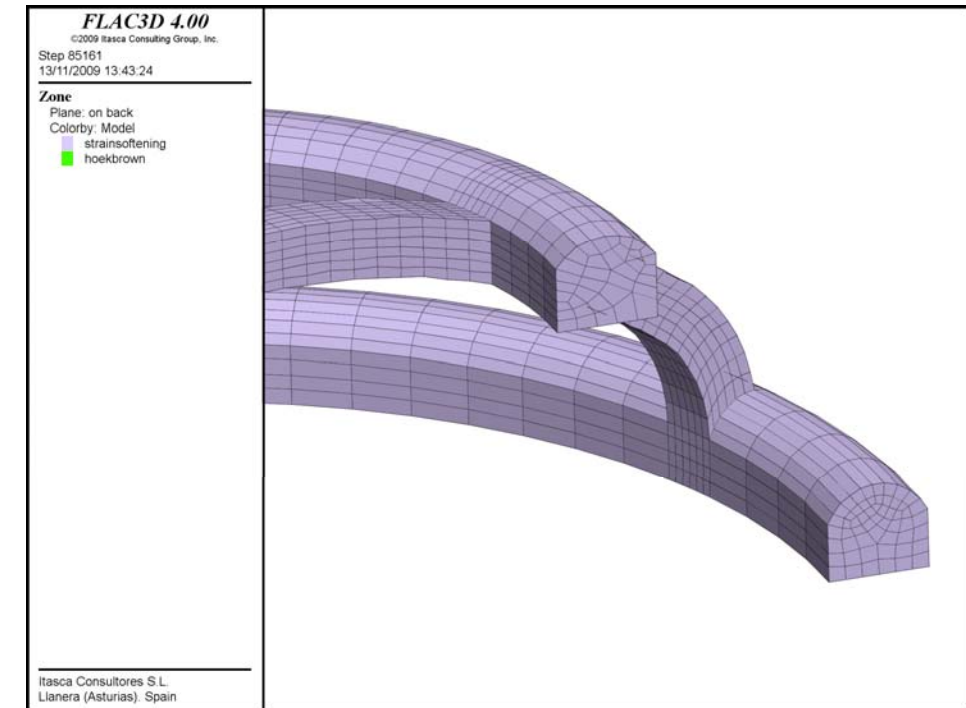


Figure 7.4-49. Location of section in the horizontal galleries.

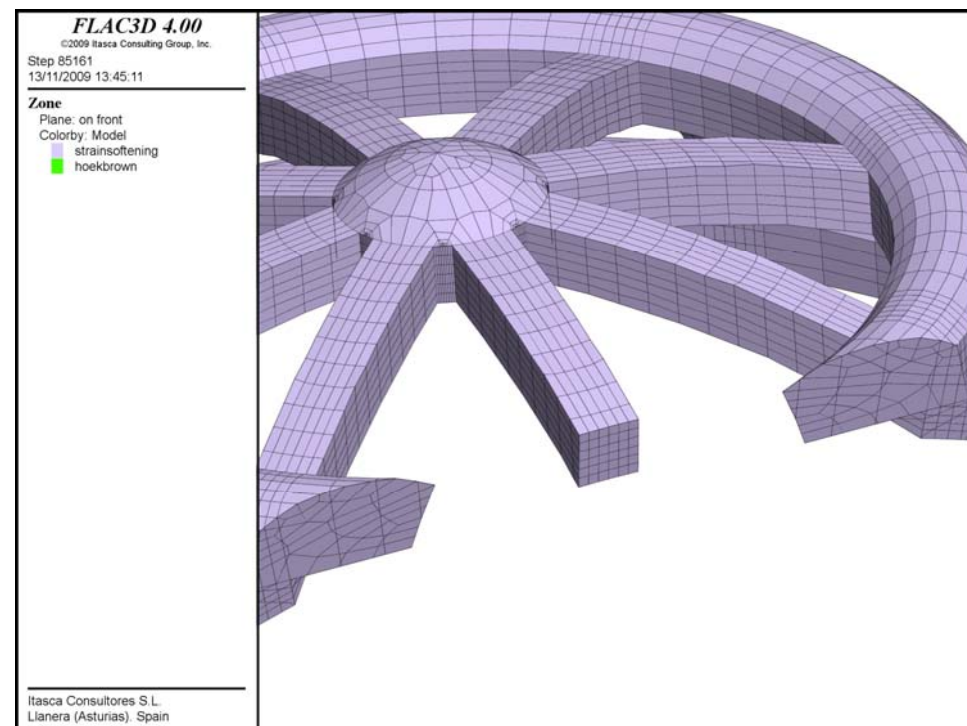


Figure 7.4-48. Location of section in the ribs.

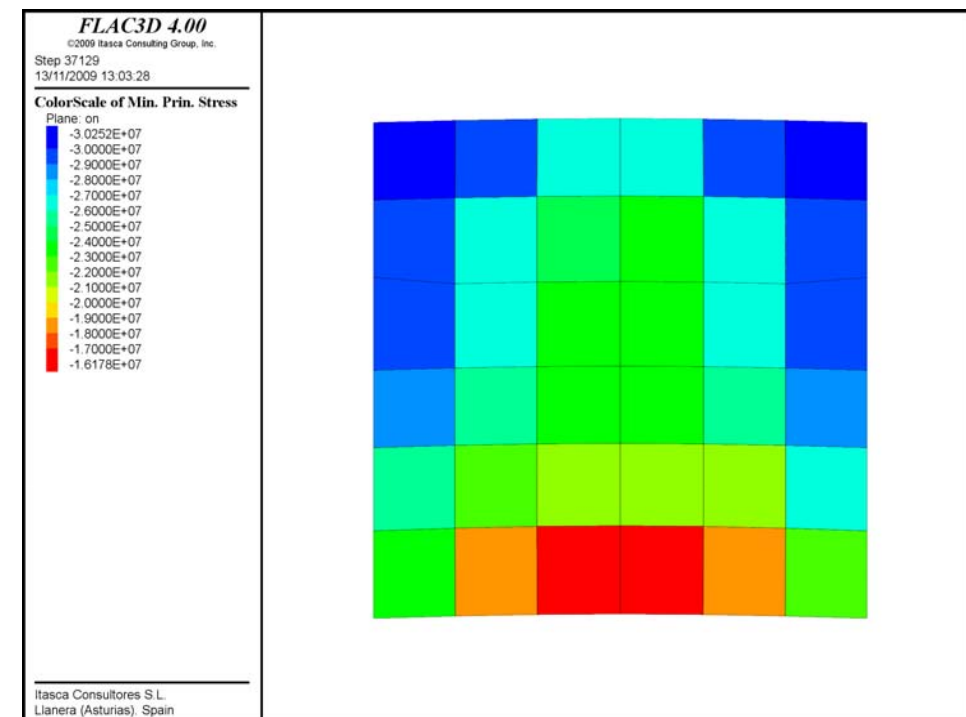


Figure 7.4-50. Minor principal stress in the rib.



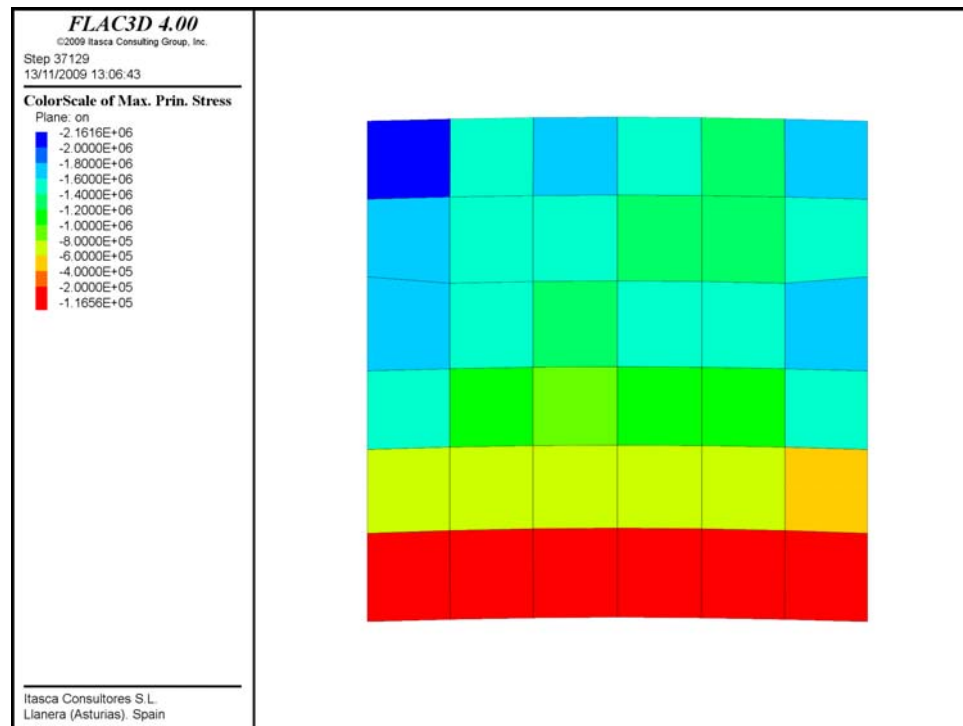


Figure 7.4-51. Major principal stress in the rib.

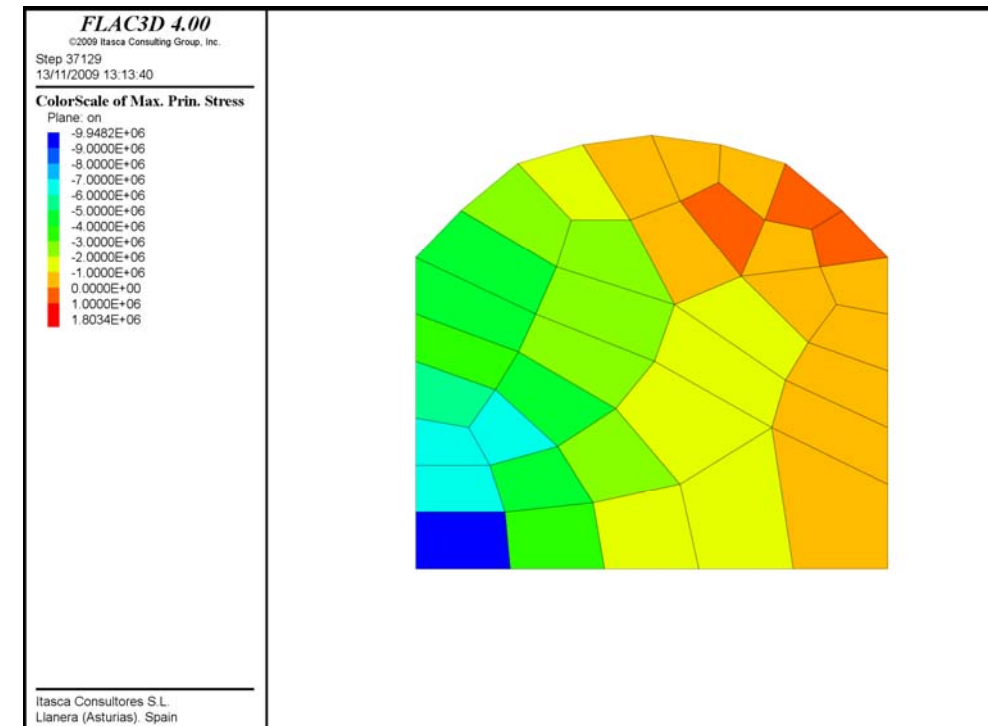


Figure 7.4-53. Major principal stress in the horizontal gallery.

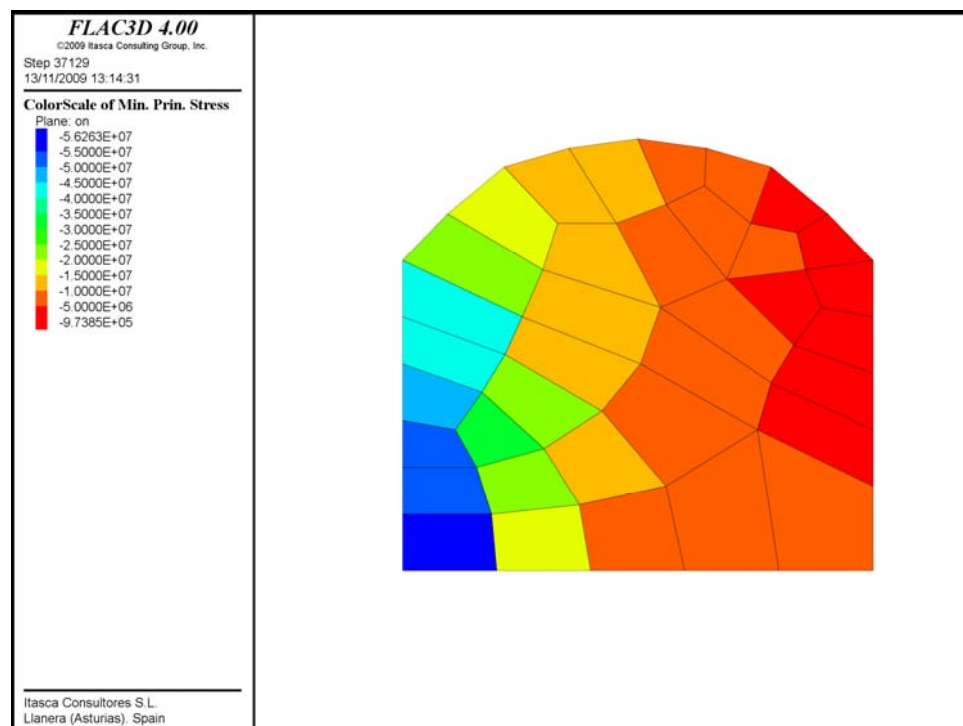


Figure 7.4-52. Minor principal stress in the horizontal gallery.

#### End of excavation of the cavern

Figure 7.4-54 shows total vertical displacements at the end of the excavation of the cavern, with a maximum displacement of 13 cm above the vault, and a heave of 27 cm below the invert.

Figure 7.4-55 shows the vertical displacements in the concrete filling the galleries and ribs above the vault, with a maximum displacement of 11 cm in galleries of the top.

Displacements in the shotcrete that supports the cavern are shown in Figure 7.4-56, with maximum values of 14 cm (semi-convergence). It can be appreciated in the displacement distribution the sequence followed during the excavation process, in rounds 3 m high.

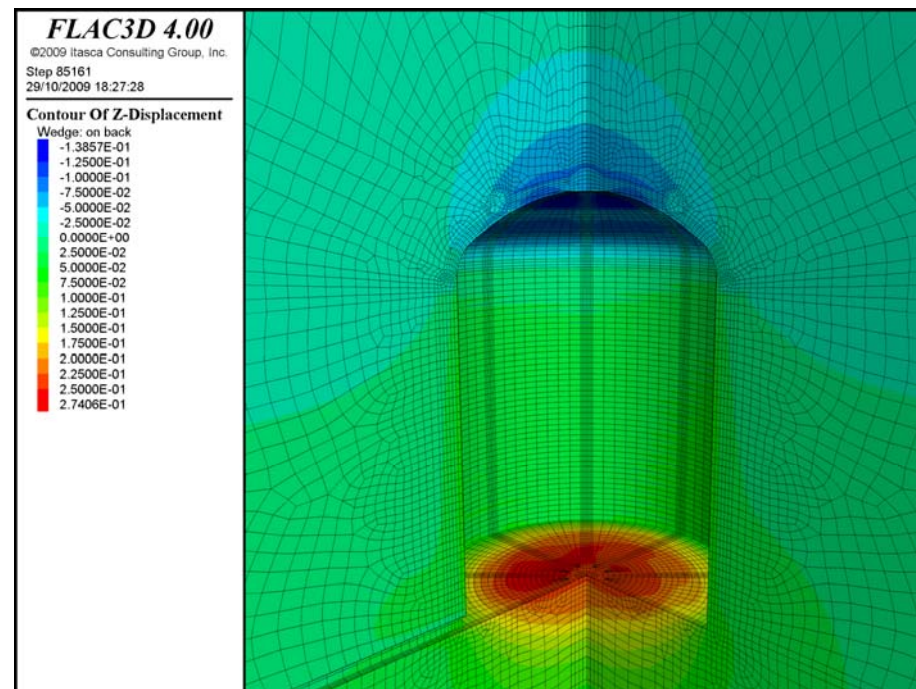


Figure 7.4-54. Total vertical displacements.

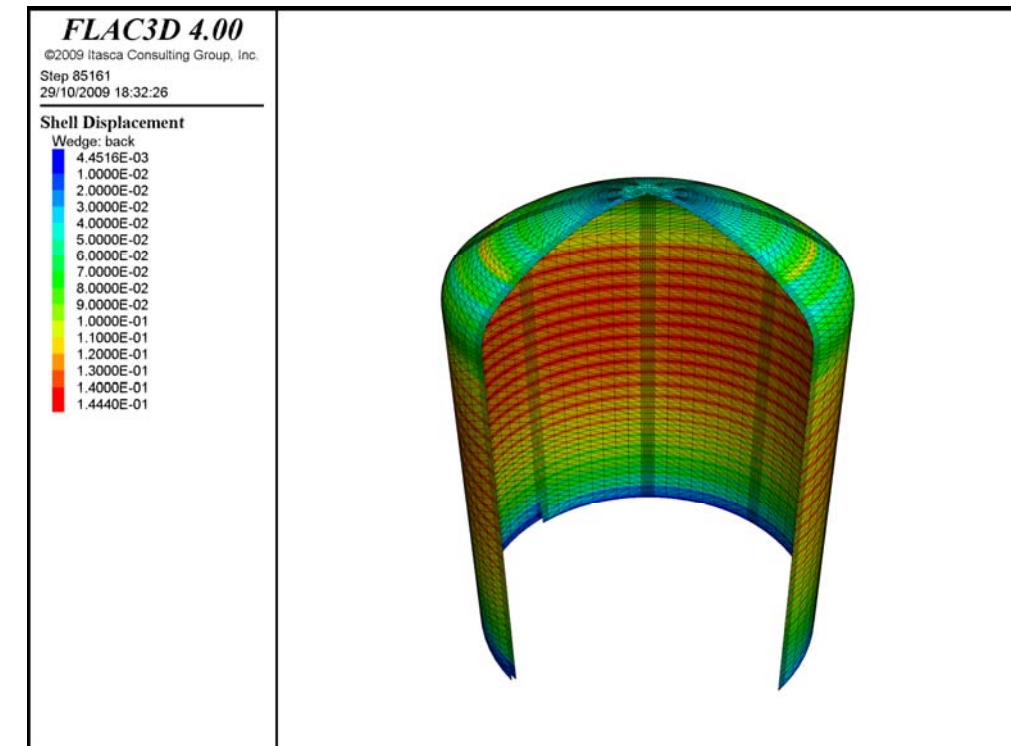


Figure 7.4-56. Vertical displacements in the shotcrete of the cavern.

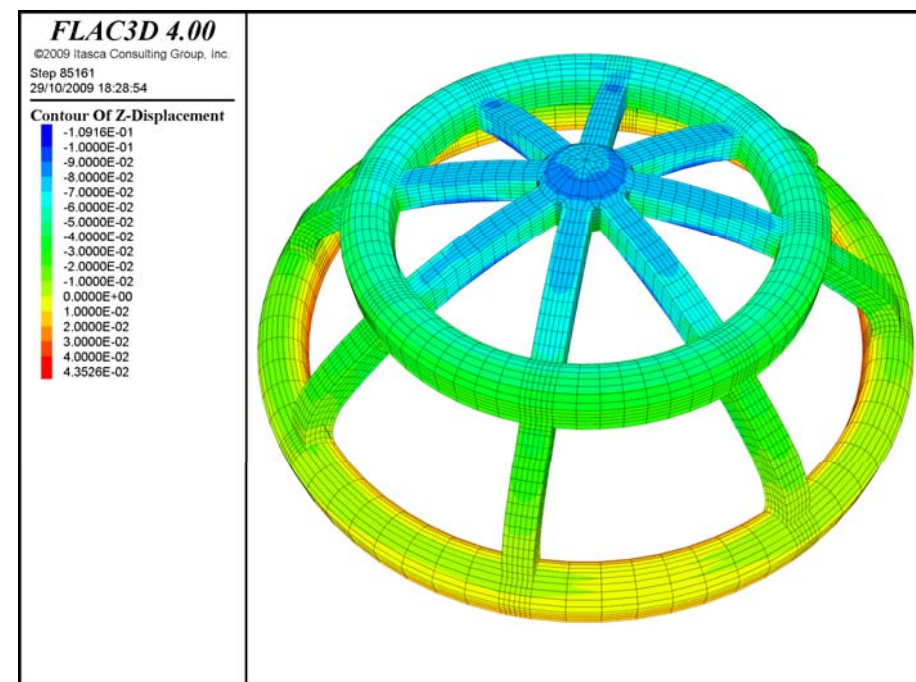


Figure 7.4-55. Vertical displacements in the support concrete.

Figure 7.4-57 shows the plasticity calculated at the end of excavation. The thickness of the plasticity ring around the cylinder is about 13-15 m in the central area. Below the excavation, the plasticity area is 28 m deep below the centre of the cavern. So the distribution is similar to the one obtained in the elastic hypothesis.

Figure 7.4-58 show the compressive stresses in the concrete of galleries and ribs. Most of the section is below 40 MPa, although there are some areas with higher stresses, up to 57 MPa, in the intersection gallery-ribs. Tension stresses distribution is shown in Figure 7.4-59, with maximum values of 1.7 MPa.

Figure 7.4-60 and 7.4-61 show the minor and major principal stress distribution in the rib, respectively (the same sections as shown in previous chapter). Most of the section gives compressive stresses around 35 MPa (varying from 30 to 40 MPa). The values of the major principal stress are negative (compressive) so no tensions are calculated in the ribs.



Figure 7.4-62 shows the minor principal stress distribution in the horizontal galleries, with a maximum value of 47 MPa in the lower gallery, and mean values of about 40 MPa in the upper gallery.

Figure 7.4-63 shows the major principal stress distribution in the galleries, with most of the section in compression, and only 0.4 MPa in the lower right corner of the lower gallery.

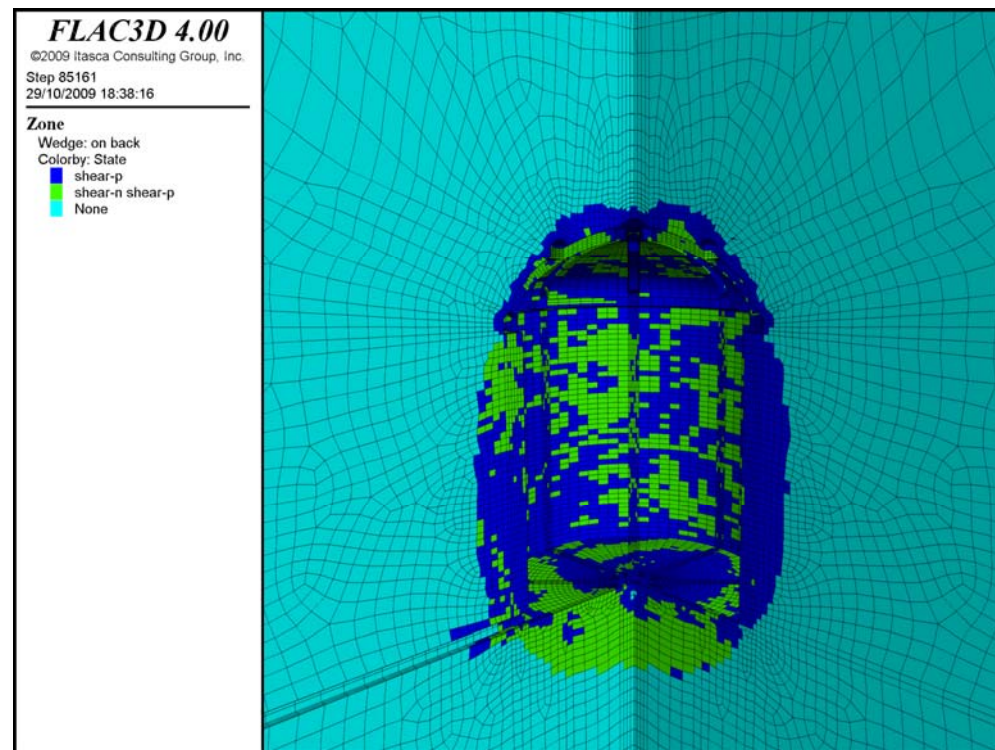


Figure 7.4-57. Plasticity indicators.

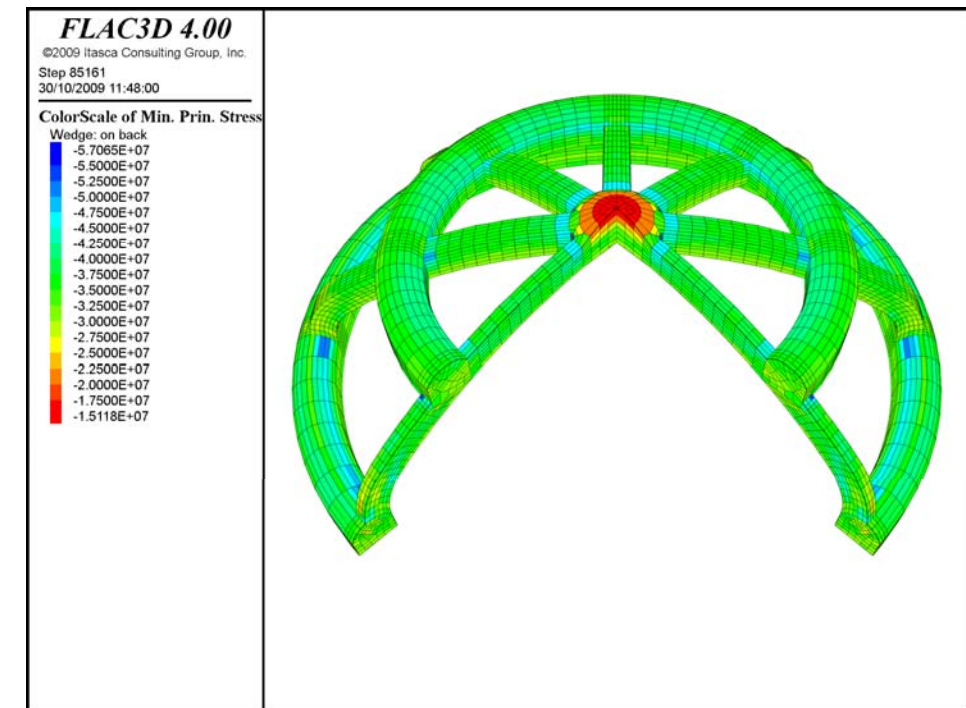


Figure 7.4-58. Compressive stresses in the concrete of the pre-support.

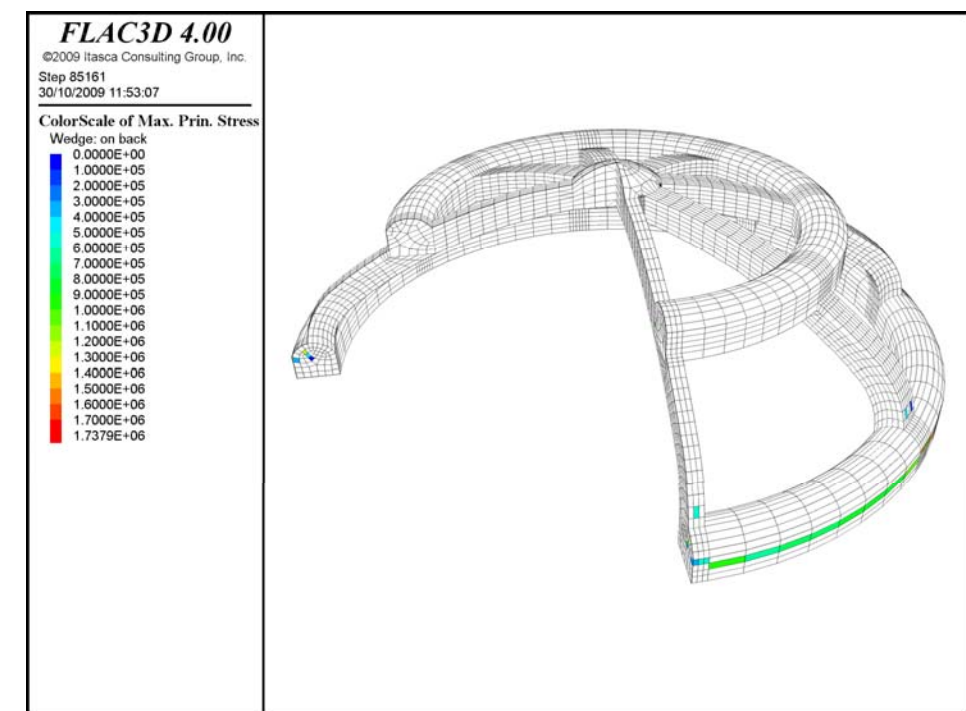


Figure 7.4-59. Tension stresses in the concrete of the pre-support.



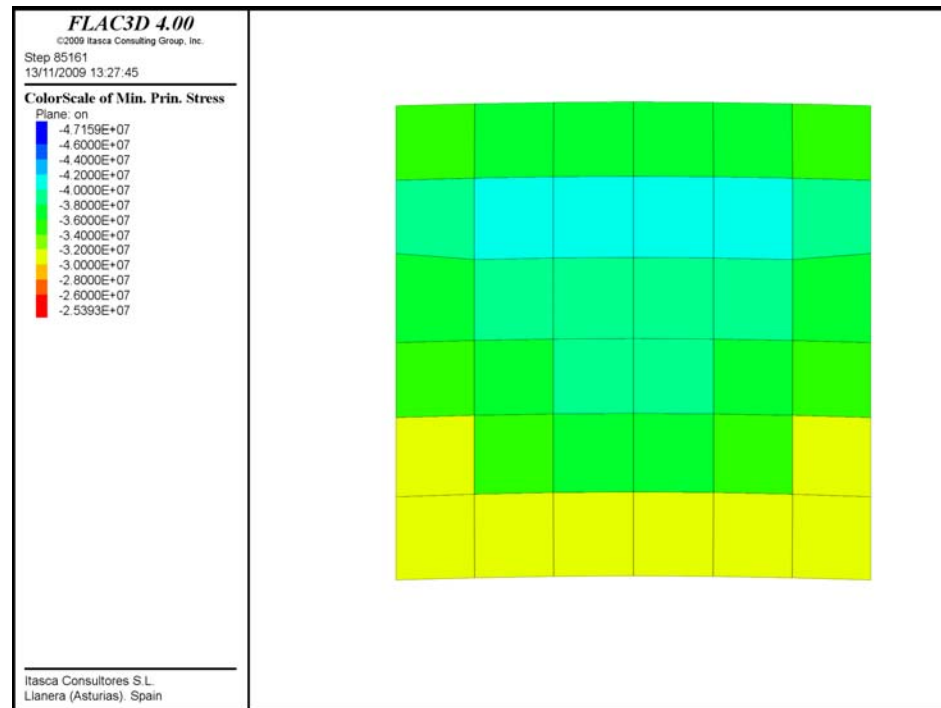


Figure 7.4-60. Minor principal stress in the rib.

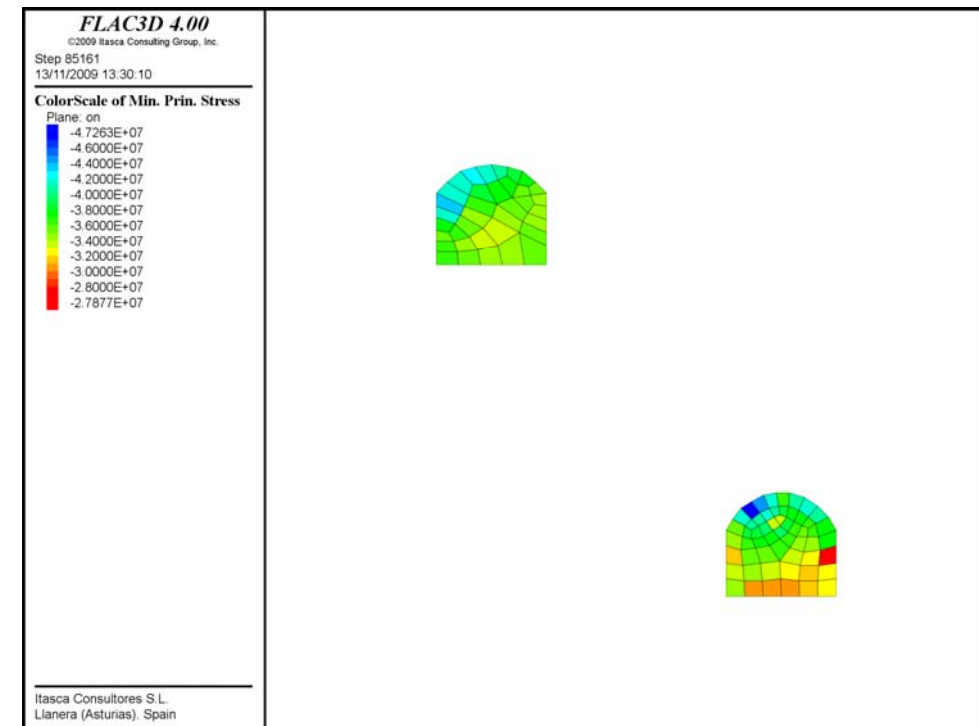


Figure 7.4-62. Minor principal stress in the horizontal gallery.

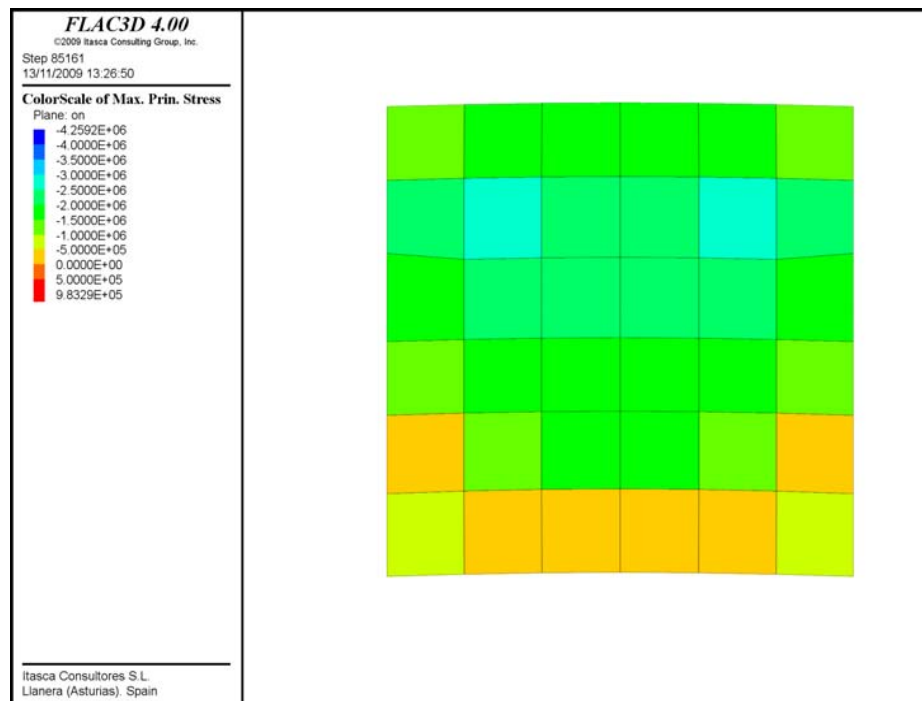


Figure 7.4-61. Major principal stress in the rib.

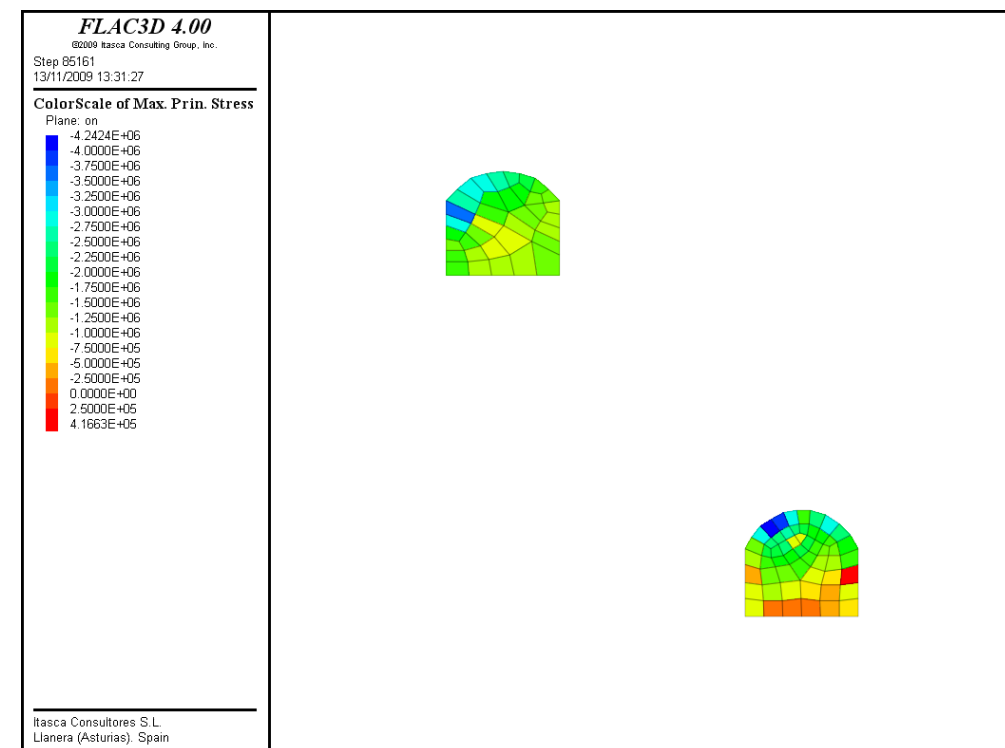


Figure 7.4-63. Major principal stress in the horizontal gallery.

Figure 7.4-65 shows loads in the reinforcement cables, with mean values of 35-40 Ton, although maximum values up to 61 Ton have been calculated (anyway below their maximum capacity).

Figure 7.4-65 shows the loads obtained in the rockbolts, most of them have reached their maximum capacity (40 Ton) in their initial length (2-3 meters).

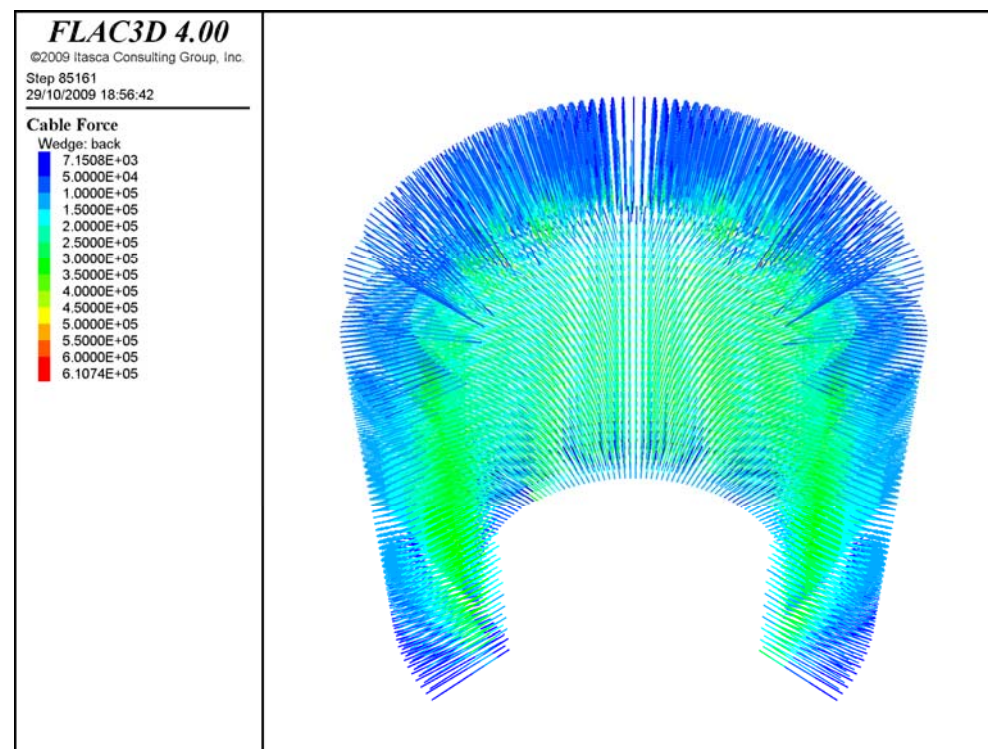


Figure 7.4-64. Loads in the cables.

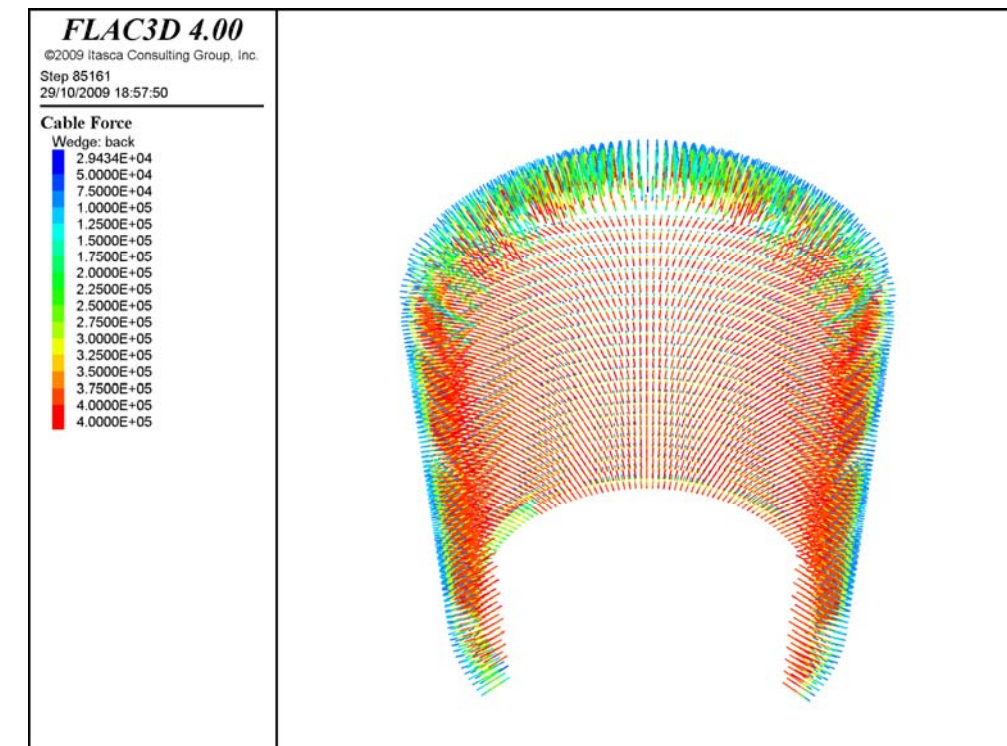


Figure 7.4-65. Loads in the rockbolts.

## 7.5 MEMPHYS SAFETY AND TECHNICAL ASPECTS

### 7.5.1 Ventilation (construction works and final ventilation)

#### 7.5.1.1 Ventilation system during construction works

The ventilation system considered for the site construction will be the necessary to blow fresh air enough against the tunnel face of the auxiliary access gallery during its driving process. Volume has to be enough to provide sufficient fresh air for people working at the front end, and also for removing the smoke of the machinery working and for extracting the dust coming from blasting operations.

A speed of 1 m/s is considered as the working air enough for proper ventilation.

The ventilation system will require axial fans with textile ducts. The number of fans used will increased as the tunnel deepens; however, the maximum number of fans will be three, providing a maximum flow rate of 38 m<sup>3</sup>/s.

The fans are calculated for the pressure drop for a tunnel length of 3 Km (that is, the sum of the access gallery to the upper chamber and the connection galleries), and with a textile duct 2 m diameter.

The three axial fans will be located at the Canfranc portal outside the tunnel and they will be installed in series.

#### 7.5.1.2 Final ventilation system

The final ventilation will have two purposes:

- Human ventilation in the underground system, except for MDC's and AC's, where a specific radon-free ventilation system will be necessary.

- Fire protection ventilation

The ventilation scheme needs a feeding part, where to intake air, and an exit part where the contaminated air can be evacuated.

Ventilation starts at Canfranc portal (1.194.4 a.s.l.) and runs through the access gallery, MDC's and AC's (level 1.073 a.s.l.) and finishes at Rioseta shaft, through a specific ventilation tunnel that starts at the MDC's level and runs with 10% slope (1.182 m. long). The tunnel finishes within a vertical shaft 221 m long, which connects the exit point at surface at level 1.412 a.s.l.

The display that has been chosen for fire protection ventilation is a jet fan system anchored to the vault of the tunnel. These fans will have frequency regulators to change its working speed and will have two ways of working, either for human or for fire protection ventilation.

The speed for human ventilation is calculated with 1 m/s and flow rate will be 38 m<sup>3</sup>/s. In case of fire the jet fans will work at their maximum power. Air speed will be 3 m/s, and flow rate will be 114 m<sup>3</sup>/s.

Fifteen (15) jet fans (45 m<sup>3</sup>/seg each one) will convey smoke through the tunnel to the exit. The distance between the fans will be 200 m.

Every fan is completely reversible, so depending where the fire is it can work in different ways.

In case of fire in the MDC's vault and inside the AC's, a fan will remove the smoke inside these rooms and will evacuate it to the main tunnel, so that the ventilation system can catch and evacuate it to Canfranc portal or to Rioseta shaft, depending on the fire location.



Next figure (that is also annexed in the drawings appendix) provides better understanding to the previously described ventilation scheme. Both human and radon free ventilation is shown.

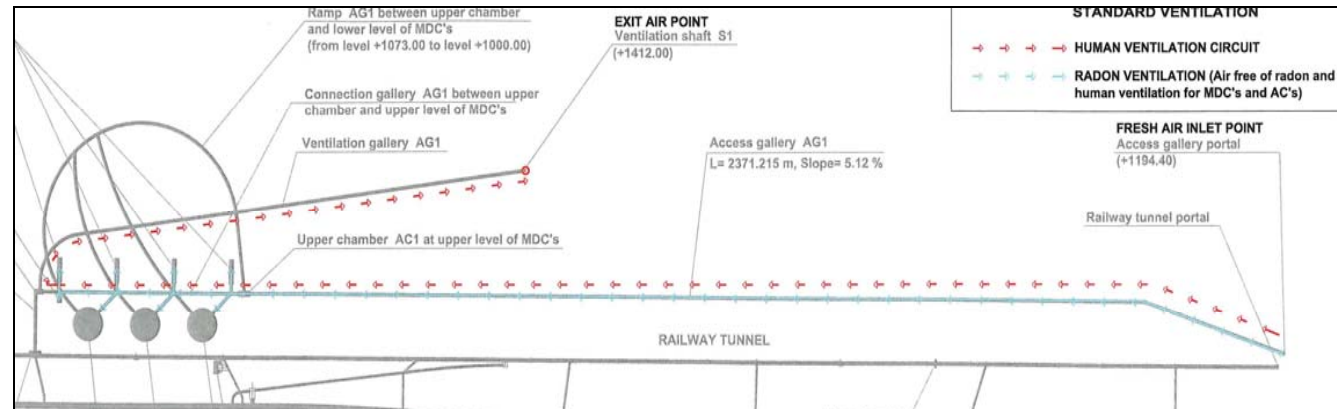


**Figure 7.5-1. Ventilation circuit both for human ventilation (red slotted line), and radon free air (blue line)**

### 7.5.2 Radon free ventilation system

It is likely to have high levels of radon concentration in the tunnel. An independent ventilation will be provided to eliminate this element.

Fresh air will be blown through a duct 2 m diameter to the 3 MDC's, and to the AC1 and the three AC2's.

This ventilation will have two purposes:

- Human ventilation at inside of the MDC's and AC's.
- To have radon free air inside these facilities.

The flow rate considered is 30 m³/s in order to have 1 renovation/hour, that is, the whole air volume is changed each hour.

With this ventilation radon concentration will be reduced below 40 Bq/m³ at the MDC's and at the AC's. A slight overpressure should be created in these rooms with grilles to have proper ventilation.

With the final ventilation (38 m³/s) also 1 renovation/hour is ensured, both for the Connection and Access Tunnels, in order to have the radon concentration below 100 bq/m³.

With radon ventilation working at MDC's and AC's and with the final ventilation working at Interconnection and Access Gallery Tunnels the radon concentration will be reduced to proper values for experiment operation.

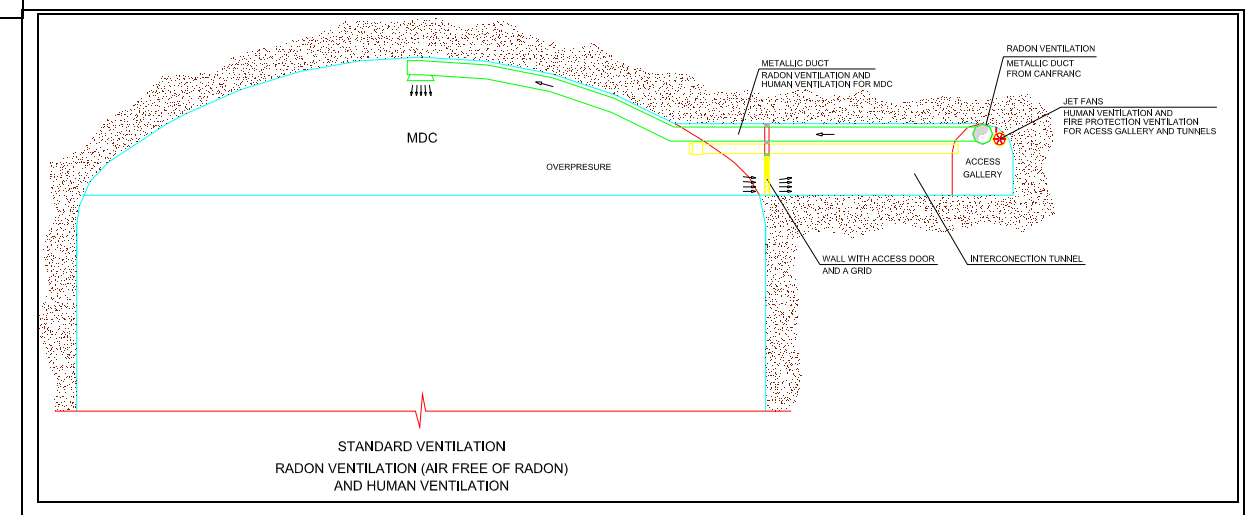


**Figure 7.5-2. Ventilation system scheme, including final ventilation and radon free air supply for MDC's**

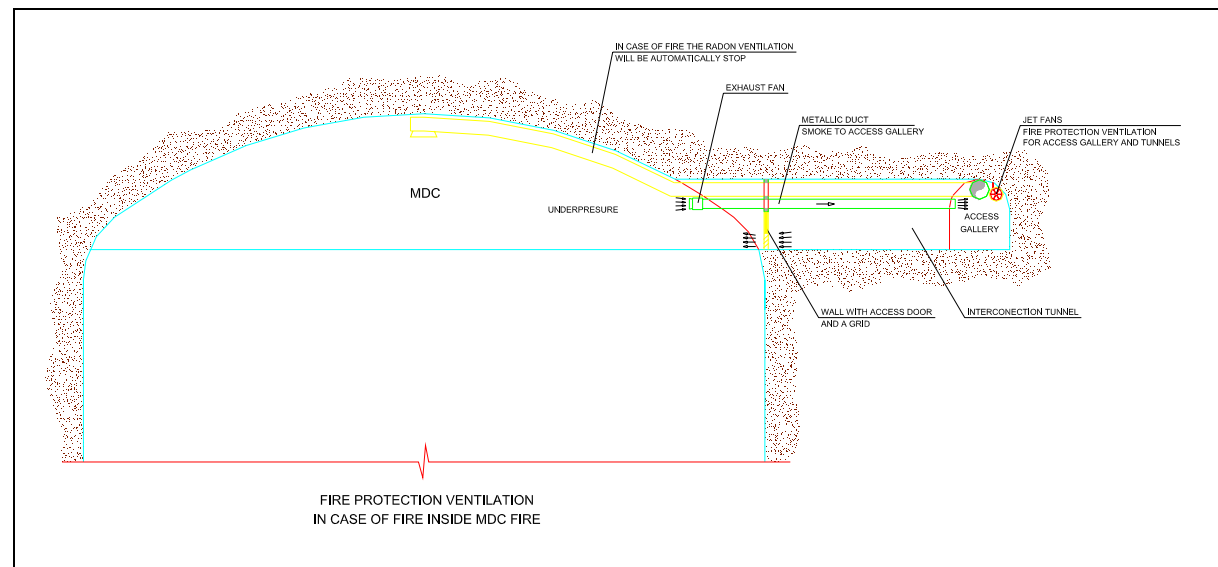


Figure 7.5-3. Fire protection ventilation system scheme for MDC's

### 7.5.3 Cooling and Heating.

Temperature and humidity have been measured inside the road tunnel, nearby to where the experiment will be built and take place. A temperature of 10°C and 80% humidity are the average values of the year, as explained in previous sections of this document.

For the electrical and/or electronic housing at the MDC's air handling units have been foreseen, in order to cool those rooms. Each room will have its proper air handling unit, with a total cooling power of 500 Kw, for each of the electrical/electronic rooms. Air distribution will be ensured by isolated ducts.

The heat coming from the electrical/electronic rooms will be used to heat the MDC's vault, in which expected temperature would be similar to the tunnel case one. In the case that more heat is needed, heating machinery will be used, in order to maintain working temperature at 22°C.

Handling units will be electrical.

Auxiliary Caverns must have a working temperature of 22 °C. In order to maintain the working temperature, electrical air heating units will be used.

### 7.5.4 Handling of dangerous substances

No dangerous substances are to be handled for the MEMPHYS experiment.

### 7.5.5 Fire protection system and evacuation

In case of fire the tunnel has to be prepared so that people working in the experiments can be evacuated and the fire can be easily controlled.

At every location of the tunnel, two exit ways must be ensured, in order to use the free one at each fire event. These exits are:

- The access gallery to the Canfranc portal.
- The communication shaft between the connection tunnel at MDC's level (1.070 m.) and the old railway tunnel.

The connection shaft location can be seen in the layout drawings. Access to the shaft should be designed with two fire protection doors, which will be able to support fires of two hours.

The connection shaft will be equipped with a lift of 8 people capacity that could work even in case of fire. Also emergency stairs are designed for this issue, as fire will not cross inside the shaft in the next two hours after the fire begins.

The tunnels will also be equipped with fire extinguishers, with special concentration at the AC's and MDC's.

Fire water hoses will be provided for the MDC's and the AC's, in order to have water with pressure enough to extinguish potential fire events. An independent pump-

ing water system, located at Canfranc, will supply water to this installation. Fire pumps will be formed by an electrical, a diesel and a jockey pump, so in any case the fire water installation will have power to work, even with no electrical supply.

The exit of the fire pumps will be connected through a carbon steel pipe to a ring net pipes distribution of 5" DIN2440. All the pipes and valves will be designed to work at a nominal pressure of 16 bar. Reduction pressure valves will be installed all along the ring in order to adequate the working pressure.

Two types of fire detection system will be installed: with a wire along the tunnel and with conventional detectors for the AC's rooms and MDC's vaults. Fire detectors will be connected to a cabinet where the alarm can be seen at any time.

In case of fire, ventilation will be provided with jet fans of the final ventilation system with a flow rate of 114 m<sup>3</sup>/s for all the tunnels (Access tunnel and Connection tunnels). Depending on where the fire will be the jet fans will work to evacuate smoke either to Canfranc or to Rioseta.

Figures 7.5-3 and 7.5-4 show different schemes of fire ventilation and evacuation systems.



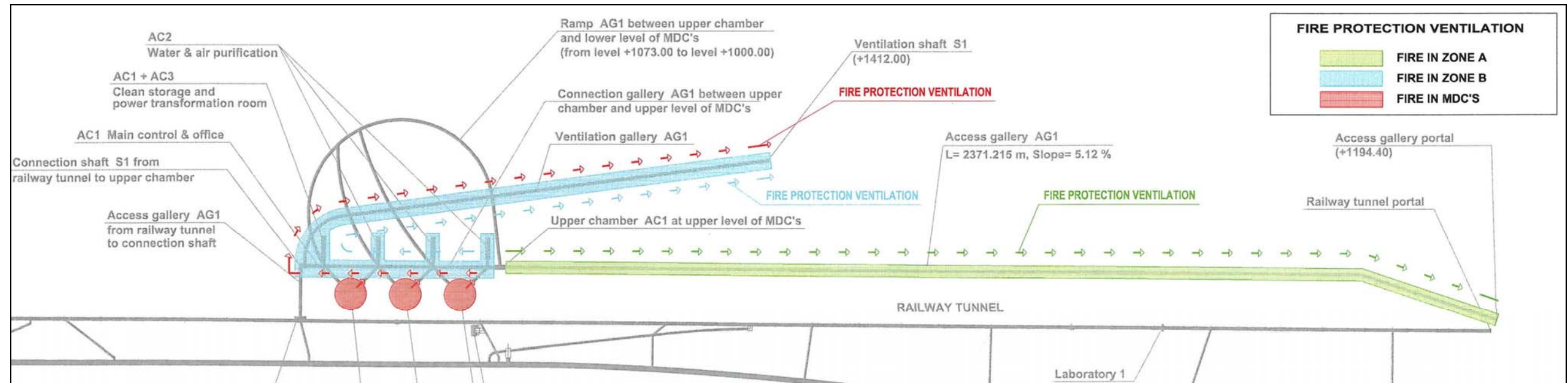


Figure 7.5-4. Fire protection ventilation system.

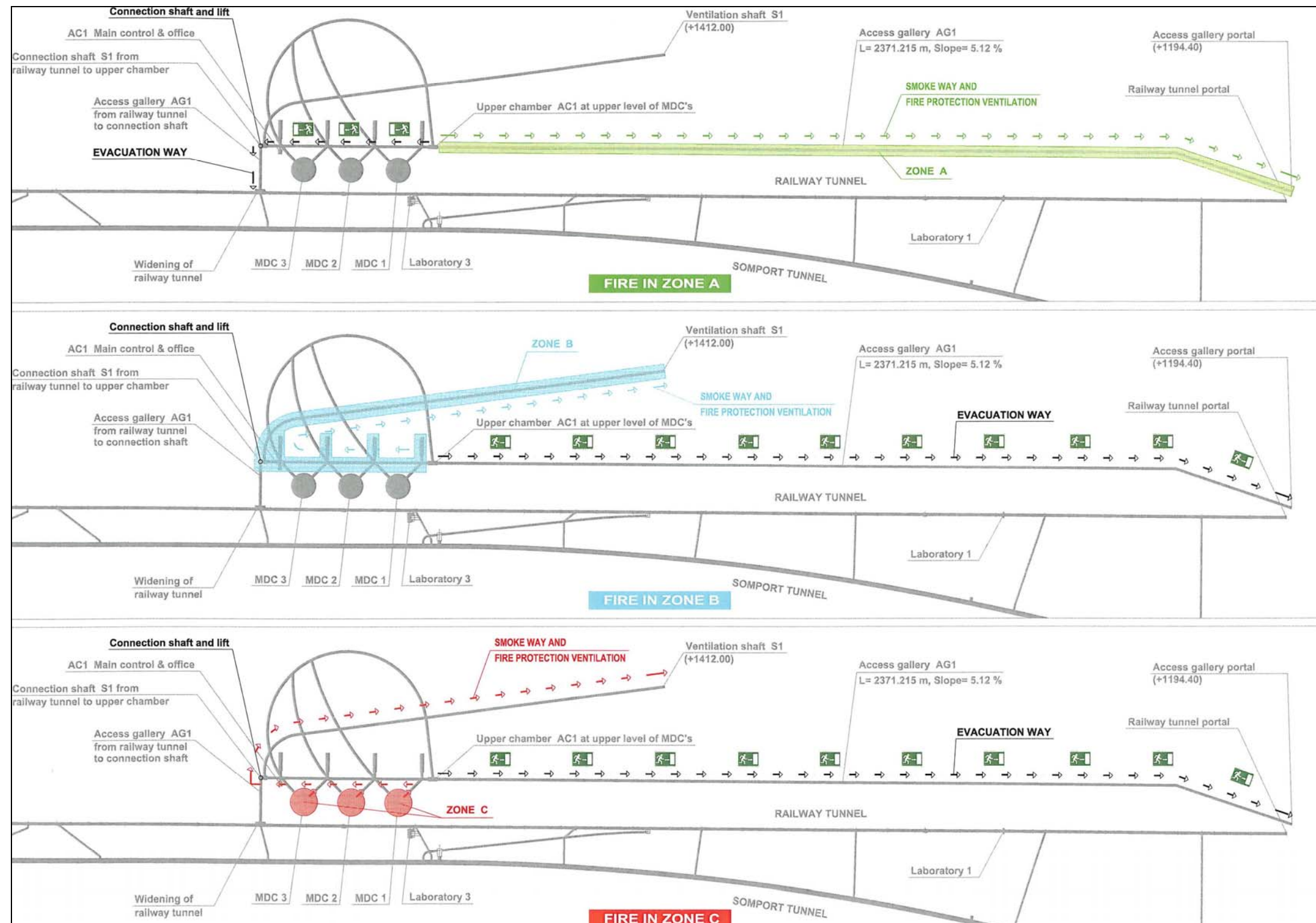


Figure 7.5-5. Evacuation plan and fire protection ventilation system

### 7.5.6 Filling and emptying procedure facilities

Water coming from River Aragón will be used to fill the MDC's. Water resources are already being exploited in some hydroelectrical systems, with small dams along the river. A special concession should be requested from the Local Authority for the Ebro Basin (namely, the Confederación Hidrográfica del Ebro), which is the autonomous body that can authorize water inlets to the experiment.

The filling and emptying system is designed with pumping groups at different levels. The most important feature for this utility is that water has to be moved between different levels, both for the intake and for its evacuation.

A system comprising water pumping stations each 1.175 m. is foreseen. Each station will have an intermediate 10.000 litres tank. They are atmospheric tanks where the water pressure is broken.

The filling flow rate will be 100 m<sup>3</sup>/h. It takes almost 100 days to fill one MDC, so this operation will lead to 300 days for the three tanks. Pressure considered in each pumping station is 4 bar. Every pumping station will be formed by two pumps, working at the same time with the previous data.

The pumping stations will be located at Canfranc (level 1.205), in the tunnel (level 1.138) and the last one at 1.070 m level, where the MDC's are. In order to regulate the pressure in the pipes reduction pressure valves will be installed.

After the last pumping station, the filling pipe will be connected to the purification water system, and after that each MDC will be filled.

The same system will be used for emptying the water circuit. In this case, the first pumping station will be located at 1.000 level, that is, at the level base of the MDC's. Two pumps will be needed, designed for 100 m<sup>3</sup>/h and 8 bar capacity. The same flow rate will be used for emptying and for filling operations.

Two more pumping stations will be located at 1.070 m and 1.138 m levels with the same flow rate and pressure capacity. These two stations will have atmospheric tanks of 10.000 litres to break the pressure.

Some check valves for emptying pipes will be installed, in order to avoid damages to the installation.

In next stages, it ought to be studied if the water coming from the experiment needs to be treated before throwing it to the public sewer line.

Carbon steel pipes 8" ASME Sch. Std. will be used for the filling and emptying system.

### 7.5.7 Liquid handling facilities

#### 7.5.7.1 Drinking water

A water supply capable to get 35 m<sup>3</sup>/h of drinking water will be needed for surface and underground facilities. It can be connected to the water net at Canfranc village.

Drinking water utility will be split in two parts, one for surfaces facilities and other for underground facilities.

A pumping station of 20 m<sup>3</sup>/h and 4 bar, with an intermediate 10.000 litres tank will be provided to attend surface facilities, such as access control, offices, changing room, workshop, kitchen and dining room.

The drinking water system of the underground surfaces will be the same than the one for experiment water filling. Pumping stations each 1.175 m. length will be necessary. Each pumping station will have a 10.000 litres tank. These are atmospheric tanks, where the water pressure is broken.



Filling flow will be 15 m<sup>3</sup>/h and the pressure considered in each pumping station is 4 bar. Every pumping station will be formed by two pumps, working at the same time.

The pumping stations and their location have been previously described when describing filling and emptying system.

The facilities to feed with drinking water will be the access control, the changing room, kitchen and dining room and the warehouse.

Carbon steel pipes 3" DIN2440 will be used to convey the water to the underground facilities.

#### **7.5.7.2 Sewage utility**

The sewage utility for surface facilities will be a standard installation with PVC pipes with 1% of slope to connect to the public sewage line of Canfranc.

For underground facilities it will be used the same system as at surface, but instead of pumping this water to Canfranc, an intermediate pit should be used equipped with a pump working against a 10.000 litres tank. Special lorries will evacuate residual waters when needed. It is foreseen to empty the sewage tank once per month.

#### **7.5.8 Access**

Access to the experiment area will be done from a new tunnel portal, located beside the existing tunnel portal of the railway. Excavations to build the portal should be built in this area. From this portal, the access gallery runs downwards to the MDC's, as explained in different sections of the document.

An alternative pedestrian access is provided by the shaft that connects the existing railway tunnel and the LSC with the MDC's area. This access will be provided with

an elevator for normal operation, and with a staircase for the case of emergency or fire alarm.

Surface installations should provide also access control to underground installations. An independent building, with a security guard in charge of access permits, would be the minimum access requirement to control vehicle access to the tunnels.

#### **7.5.9 Fire event**

See fire protection system at section 7.5.5.

#### **7.5.10 Energy supply**

Electrical utility starts at Canfranc portal place, where an electrical inlet able to feed high voltage power must be connected to the general electrical network.

Two power transformation rooms should be installed, one at the middle of the access gallery (1.138 a.s.l.) and the other at AC1 (1.070 a.s.l.). From these two power transformation rooms, electrical power will be supplied at low voltage for lighting and for MDC equipment, AC's and tunnel.

There will be three power transformers, one for the room which is at the middle of the gallery and two for AC1. All power transformers have 1.600 KVA's.

High voltage power will be distributed through the tunnel with an ironclad cable tray, anchored to the wall of the tunnel. The system designed is through a wire circuit that starts at Canfranc, goes to the power transformation room at the middle of the tunnel and after that to the AC1, finishing the loop ends at Canfranc again.

#### **7.5.11 Bulk transport and stocking**

A huge volume of rock will be carried out the excavations if the Memphys experiment is chosen. It can be resumed in the following parts:

- Rock from MDC's and support system galleries: 1.270.000 m<sup>3</sup>
- Rock from galleries and AC's: 292.000 m<sup>3</sup>
- Ventilation galleries and shafts: 83.000 m<sup>3</sup>

This rock volume is the one to be transferred to dump areas. A factor F=1,40 has been considered to pass from the theoretical volume of excavation to the transported one.

Dump areas can be located at different places; an environmental assessment study should be carried out before deciding where to place muck from underground excavations. Environmental studies to be carried out in further design phases are explained in section 10.

Muck can be carried by dump lorries or by train, if the local Canfranc railway line allows this kind of transportation. In this case, an intermediate dump area nearby the railway line should be created. Since the railway line does not bear heavy traffic, special trains could be prepared for this use.

#### 7.5.12 External installations

Further detailed design should locate external installations once the portal levelled definitive area is designed. This area should house different installations such as power transformation, ventilation units, water intake, parking area and reception and control building. An area of 1.000 to 1.500 m<sup>2</sup> should be reserved for this purpose. The huge railway yard located beside the old Canfranc railway station can be used for external installations, machine shops and warehouses.

## 7.6 MEMPHYS TANK

### 7.6.1 Tank structure

Tank structure is roughly described in paragraph 7.1.2. Super Kamiokande experience will be the base of further design, which is already being carried out by Technodyne.

### 7.6.2 Assembling procedure

No assembling procedure has been designed at this phase. Super Kamiokande experience will be the base of further design.

### 7.6.3 Mechanical and thermal interaction with rock

Assessment about this aspect will be done in future phases.

### 7.6.4 Drainage system

In the case of eventual infiltrations, the MDC's would have a series of drains placed in a radial fashion in order to carry any excess water away from the cavities. The number of drains placed would depend on the conditions encountered during construction. The drainage borings would have a gentle slope (~5%) to allow the water to flow. Figure 7.6-1, shows a sketch of the drainage system for each type of cavern.

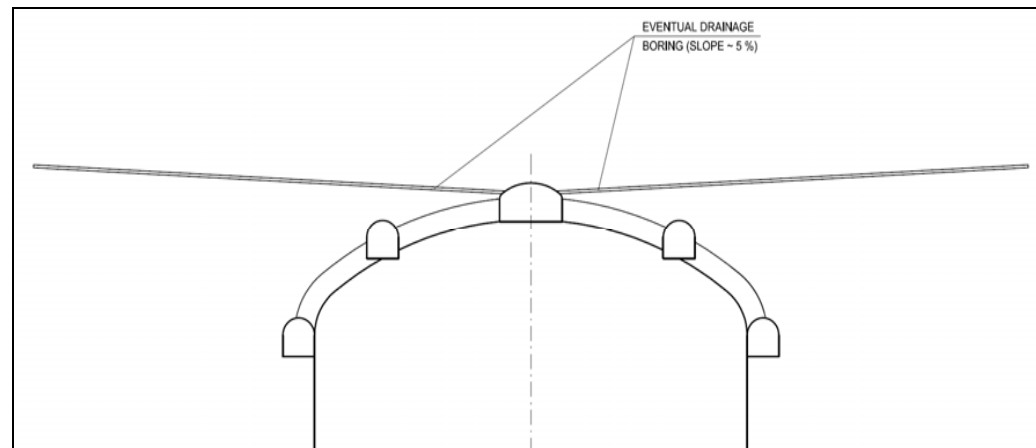


Figure 7.6-1. Eventual drainage curtain in the upper part of the vault.

Other drainage devices, such as drainage vertical curtains, could be displayed if necessary by means of ring galleries and vertical drains. Since Atxerito Formation is very impervious, no significant water inflow should be expected, although further rock investigations should deal with this aspect, comprising the installation of long term measuring devices such as vibrating wire piezometric gauges.

#### 7.6.5 Handling of leakage

Leakage of the tanks should be avoided in order to ensure proper experiment operation. Anyway, if necessary, the drainage pit that is necessary for working purposes can be prepared so as that possible water leakages can be gathered at that point, and measured by means of volumetric control gauges. A ducts network in the external and lower part of the tank must be designed in this case.

A pumping system, elevating water from the bottom to the upper part of the tank will take leakages to the general sewage system.



## 8. LENA EXPERIMENT

### 8.1 MDC'S AND TANK DESCRIPTION

#### 8.1.1 Dimensions

The LENA experiment requires a different cavern; dimensions to be considered are the following ones:

Diameter (cavern)	Target diameter (tank)	Height (cavern)	Height (tank)
34 m	26 m	120 m	≈105 m

The requirements of rock cover are higher in this case. The optimal requirement is to reach 3.500 equivalent m.w.e. The LSC location does not allow this rock cover, unless the cavern is located very deep, in which case difficulties to access from the actual underground facilities would increase. The optimal first design for the Canfranc site leads to locate the MDC in the same site than the northernmost of the three MEMPHYS caverns, so the scheme for access construction galleries and communication with the LSC is be very similar.

#### 8.1.2 Technological specifications

##### 8.1.2.1 Tanks

According to Technodyne conceptual design, the tank needs of two different parts:

- The outer shell of the detector is a stainless-steel tank. According to the initial conceptual design, it seems necessary backfill this tank against the rock, to support liquid pressure once the tank is filled. The outer shell container is in contact with the secondary mass of the experiment, that is, 2

meters a thick water barrier (buffer), which separates the liquid scintillator (LS) from the external tank.

- There is also an inner structure or frame in the tank, to which photomultipliers (PMT's) will be held. This structure allows insulation of the volume of external water from the inner LS. Different levels of water and LS allow for almost compensated pressures at both sides, so the structure should not be a very heavy one.

A complementary isolation must be installed, provided by a nylon membrane, which separates the inner LS to an external LS buffer. Detailed design of this scheme is not yet available.

The upper part of the tank should be occupied by an inert gas, such as nitrogen, which requires of a specific installation.

According to these dimensions, the outer tank would be 34 m diameter.

##### 8.1.2.2 Others

To be specified in further design phases.

#### 8.1.3 General layout

As previously noted, the MDC has been located almost at the same site than the northernmost of the MEMPHYS caverns. With this scheme, the level of the base of the LENA cavern would be 965 a.s.l. The slope of the gallery reaching the upper level of the vault would be 4,90%, and 2.536 m long, attending to the conceptual design. The gallery leads to an upper chamber, as in the MEMPHYS case, from which another horizontal gallery reaches the base of the vault. Portal location is the same than the one considered for the MEMPHYS technology scheme, and the tunnel would run parallel to the railway one.

The underground communication net between LSC and MDC would have a similar scheme than the one of the MEMPHYS case: that is, a shaft provides not only communication between the LSC and the experiment, but exit facilities in the case of emergency. Also an auxiliary construction tunnel from the access gallery to the base of the cylindrical cavern is needed.

A similar ventilation system will be required consisting in a gallery and a vertical shaft ( $\Phi=5,70$  m), with entrance in the Rioseta area.

Attending to geological considerations, the MDC for LENA will be also located in the Atxerito Formation. Primary rock support should deal with this fact. Vault dimensions are smaller, but cavern walls are higher.

Drawings at the end of this document show a comprehensive scheme for this LAGUNA technology infrastructure.

#### 8.1.4 Auxiliary caverns

Auxiliary caverns (AC's) are located around the entrance to the vault, and provide room for the next items:

- Cavern AC1: clean room, liquid and gas handling. Electronics, low background laboratory, main control and offices.
- Cavern AC2: water purification system of the experiment.
- Cavern AC3: power transformation room. Enclosed in AC1 one.

## 8.2 GEOMECHANICAL DESCRIPTION OF THE SITE

A general review on geomechanical characterization has been stated in paragraph 6. Two different rock formations are to be considered for the different experiments.

Regarding to the LENA one, the basic characterization of the Atxerito Formation is resumed in the above mentioned paragraph.

Final parameters used for calculation purposes are the same than the ones that were set out for the Memphys MDC's calculations.

## 8.3 EXCAVATION METHODS FOR THE MDC

### 8.3.1 Introduction

Unlike MEMPHYS, the span of the LENA cavern is within the normal range for underground caverns previously built. Commonly used empirical rules were considered also when pre-designing the support system for the cavern roof. As previously seen the USACE recommendation EM 1110-2-2901, states that for spans between 18 and 30 m the rockbolt length should be a quarter of the span (there is no mention of structures with larger spans than 30 m). This means that for the LENA cavern with a 34 m span the minimum rockbolt length recommended is 8.5 m.

Hoek's recommendations (previously mentioned in the Memphys case) state that the cable length needed to support a cavern should be at least 40% its span, this means 13.6-meter long cables in the case of the LENA cavern. Regarding the minimum length for rockbolts, Hoek recommends bolts longer than 7.1 m (according to the equation:  $L=2+0.15*\text{span}$ ).

Some other considerations, concerning Río Grande and Chuquicamata caverns, have been explained in section 7.3.2. In the end, when selecting the support system there are two major concerns to address:

- The local stability and the relief of tensions close to the walls and vault, and
- The possible failure of a large wedge on the cavern roof

The approach selected to help solving these two issues is based on Dr. Hoek's solution in the Mingtan powerhouse cavern in Taiwan. The powerhouse at Mingtan is 22 m wide, 46 m high, 158 m long and approximately 300 m below surface. The cavern is located in sandstone (strong to very strong), sandstone with siltstone interbeds and siltstones beds (moderately strong and sheared). The powerhouse cavern crosses eight faults or shear zones which made it necessary to provide a pre-treatment to the rock above the cavern roof. This treatment consisted in washing out the clay seams in the faults and reinforcing the rock by means of cables.

The cables were installed from a drainage gallery located about 12 m from the roof of the cavern as illustrated in figure 8.3-1. The un-tensioned and fully-grouted cables were placed before the excavation of the cavern and were expected to suffer tensioning due to the deformation of the rock during excavation. As the ends of the cables were exposed on the cavern roof, they were anchored in place.

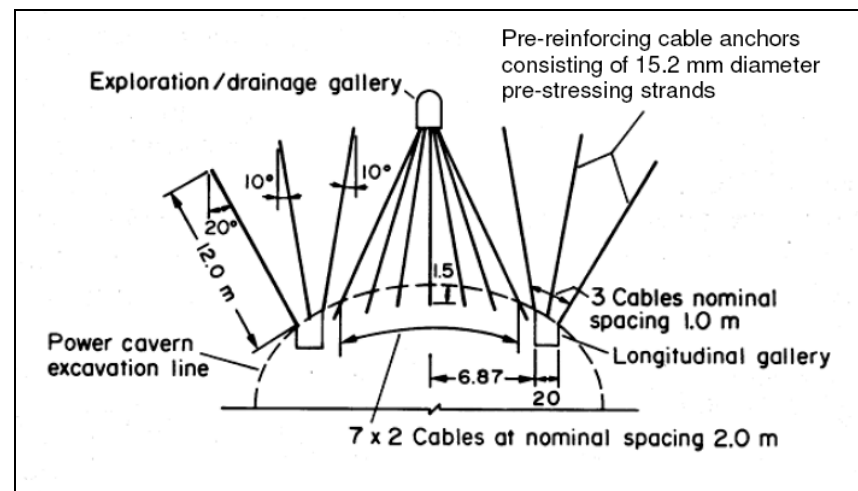


Figure 8.3-1. Pre-reinforcement of the roof of the powerhouse cavern in Mingtan (span = 22 m).

Dr. Hoek's solution of the Mingtan powerhouse addresses both the local stability and the possible failure of a large wedge and appears to be a good approach to emulate in the LENA cavern.

Adapting Dr. Hoek's solution to the cylindrical LENA cavern, a barrel-vault gallery (with section 2.5 m x 3.0 m and 15 m diameter) is excavated 16 meters from the top of the vault as shown in figure 8.3-2. From this gallery, four un-tensioned and grouted cables are installed at each section before the excavation of the cavern roof with a typical separation of 2,95 m on the vault. The total number of cables is 128 units. These cables would also work passively starting to act in tension as the excavation progresses. The ends of the cables are anchored as they are exposed by the excavation.

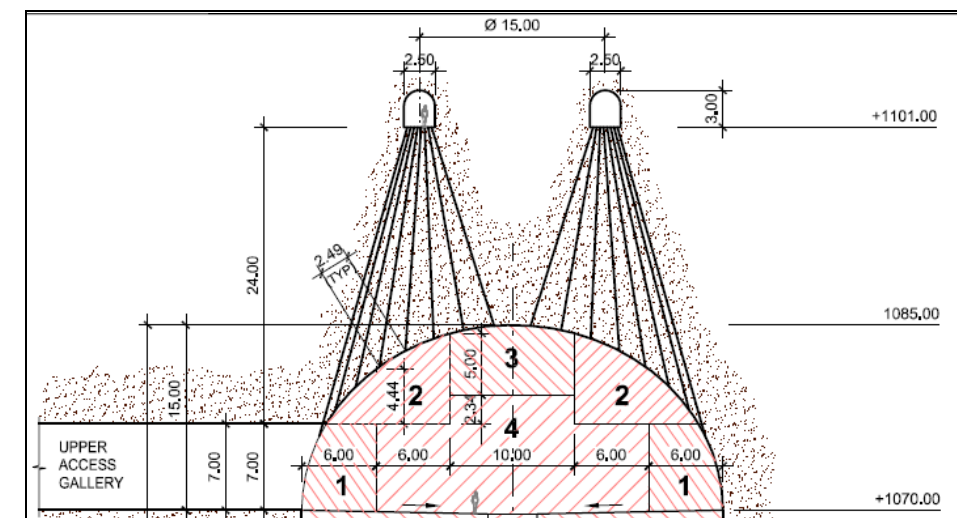


Figure 8.3-2. Pre-reinforcement of the LENA cavern roof

### 8.3.2 Previous stages of excavation and placement of cables

The next paragraphs will cover the excavation sequence and support needed for the construction of the experiment cavern. A circular gallery, located at level 1101, will be built, as previously explained in order to allow cable placement that will act as vault support.

In the case of the LENA MDC, the first phases of the excavation sequence will take place as follows:

- Excavation and support of upper access tunnel at elevation 1073 (H = 7 m)



- Excavation and support of the circular gallery above the cavern roof (3.0 m x 2.5 m) at elevation 1101.
- Drilling and placement of cables.

The upper gallery will be concrete-filled at a later stage.

### 8.3.3 Cavern excavation sequence

Following the pre-reinforcement of the crown, the cavern is excavated following the sequence shown in figure 8.3-3. Explained more in detail, the excavation stages for the LENA cavern are as follows (the stage numbers correspond to the numbering shown on the excavation sequence drawing on figure 8.3-3):

- Stage 1: Excavation and support of the first ring of the dome, at elevation 1070, by the drill-and-blast method
- Stage 2: Excavation and support of the second ring of the dome, by the drill-and-blast method.
- Stage 3: Excavation and support of the third phase at the summit of the dome.

As the excavation progresses, cable bolt heads must be installed at the roof of the vault.

- Stage 4: Excavation of the remaining rock of the vault.

The construction of the lower access tunnel should be completed before starting with the excavation of the cylindrical part of the cavern:

- Stage 5: Excavation and support of lower access tunnel at elevation 965 (H = 7 m) to the centre of the cavern.

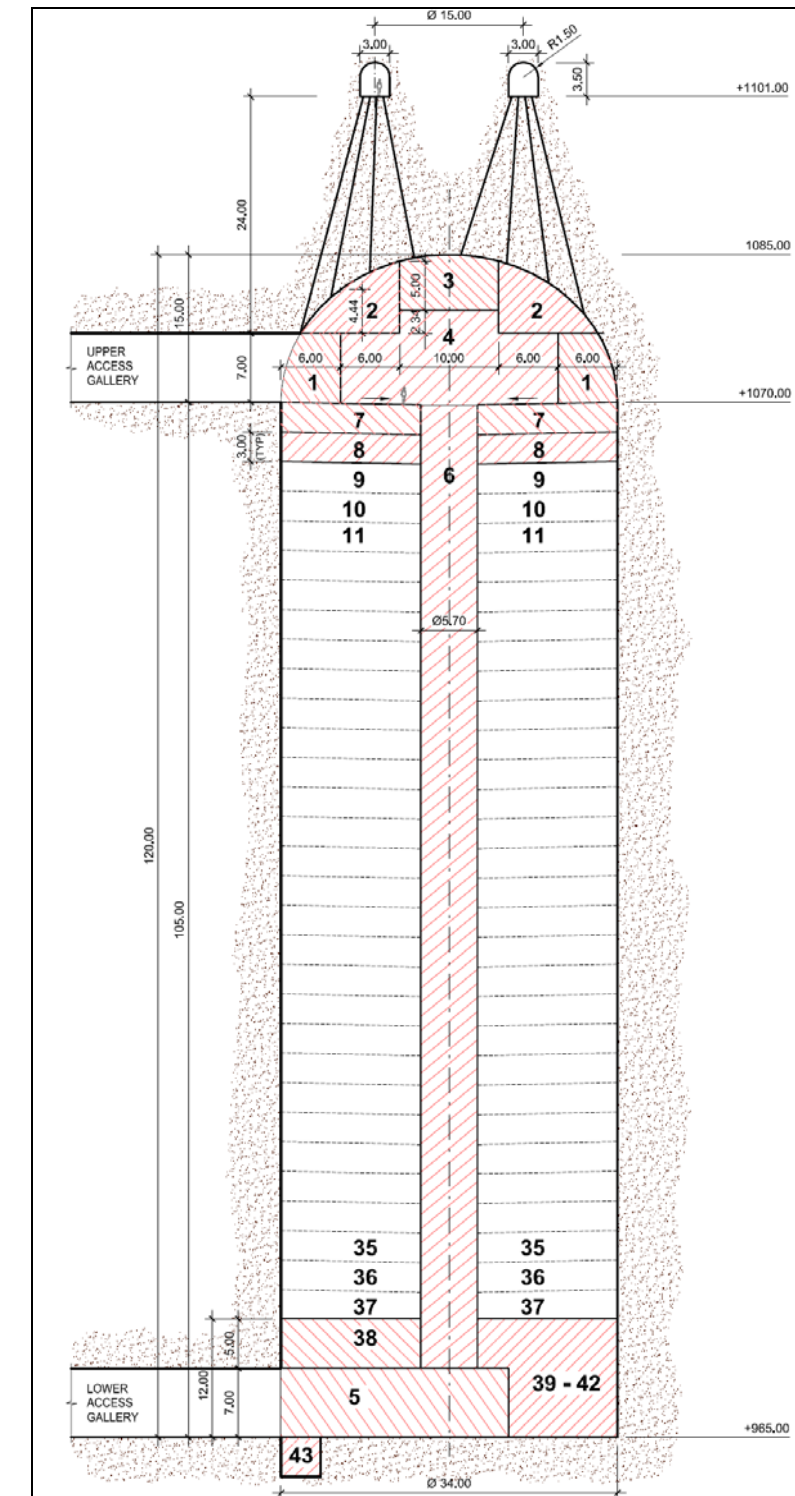


Figure 8.3-3. Excavation sequence for the LENA cavern.

The excavation of the cylindrical section of the cavern will be carried out by raise boring in the next sequence:

Stage 6: Excavation of a shaft ( $\phi$  5.7m) with raise boring:

- Drilling of pilot hole
- Installation of the drill string
- Installation of the reamer head
- Excavation of the shaft from the bottom up
- Mucking out through lower access tunnel

Stages 7 to 37: Excavation of the cavern to elevation 982:

- Excavation in 3 m benches slightly sloped toward the shaft (~ 5%)
- Mucking out through lower access tunnel
- Support of the walls immediately after mucking out

Stage 38: Excavation of the rock on top of the lower access tunnel with the drill-and-blast method

Stages 39 to 42: Excavation of the rock below elevation 1982:

- Excavation of four 3-meter benches
- Mucking out through lower access tunnel
- Support of the walls immediately after mucking out

Stage 43: Excavation of the drainage pit

### 8.3.4 Support system for the LENA cavern

The support system for the dome and the walls of the LENA cavern are presented in this section.

Dome:

Besides being supported by the cables as previously described (and shown in figure 8.3-2), the dome will have cables, rockbolts and shotcrete with the following specifications:

- Cables: 18 m long, 7 strand, cement grouted (grouted bulb length of 6 m), in a 2 m x 2 m pattern
- Rockbolts: 6 m long rebar steel bar,  $\phi$ 38 mm, cement or resin grouted, in a 2 m x 2 m pattern
- Shotcrete: 35-cm thick steel fibre reinforced shotcrete

Walls:

The cavern walls will be supported by cables, rockbolts and shotcrete with the following specifications:

- Cables: 22 m long, 7 strand, cement grouted (grouted bulb length of 6 m, in a  $L_V = 3$  m,  $L_H = 1.33$  m pattern)
- Rockbolts: 6 m long rebar steel bar,  $\phi$ 38 mm, cement or resin grouted, in a  $L_V = 3$  m,  $L_H = 1.33$  m pattern
- Shotcrete: 35-cm thick steel fibre reinforced shotcrete

## 8.4 NUMERICAL MODELLING OF THE MDC

### 8.4.1 Elastic modelling.

An elastic analysis of the problem was made, as in the case of the MEMPHYS experiment caverns. The theoretical background of this simplified model has been already explained.

Rock properties for the LENA cavern are described below:

Material	$E$ (GPa)	$\nu$	$\sigma_{ci}$ (MPa)	$m_i$	$D$	$GSI$	$m_b$	$s$	$a$
Shales	4.9	0.3	60	12	0	50	1.677	0.0039	0.506

Table 8.4-1. Calculation properties

Figure 8.4-1 shows plastic elements around the excavation of the cavern, and local safety factor of these elements. No support was considered.

Plastification reaches 4.5 m at the summit of the vault, 5.6 m at the cavern walls and 9 m in the floor area. A single excavation phase has been also considered. Safety factors range from 0.2 to 1.0 in plastic elements.

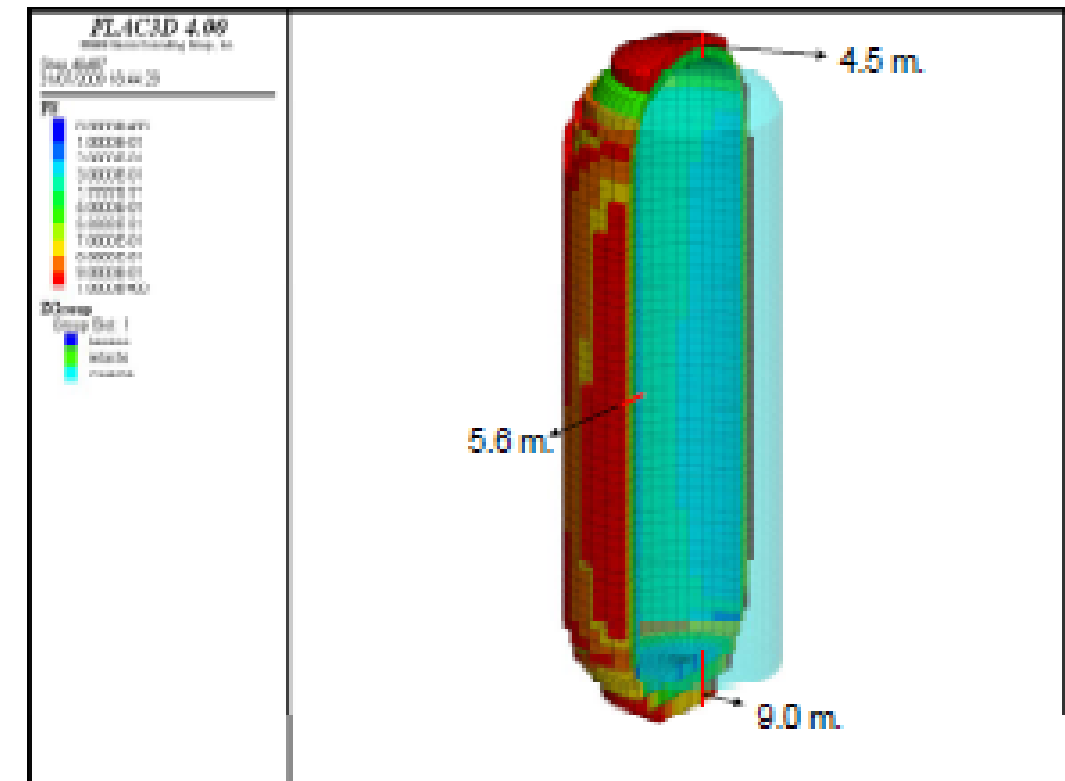


Figure 8.4-1. Plastic elements around the LENA MDC.

No more detailed calculations have been carried out in the LENA case, but this previous numerical modelling allows laying down some interesting conclusions:

- Plastic zones are similar in the vault area and less in the walls than in the case of the Memphis caverns.
- Taking in mind this result, a first approach to the wall support could lead to a similar support device than in the Memphis case, so in this phase of study the elastic model has been considered a satisfactory enough, and further modelling –in the case of a more detailed Lena studies are needed– can confirm the support that has been used for Feasibility phase.



## 8.5 LENA SAFETY AND TECHNICAL ASPECTS

### 8.5.1 Ventilation (construction works and final ventilation)

#### 8.5.1.1 Ventilation system during construction works

The ventilation system considered for the construction process will be the necessary to blow with fresh air against the front end while the tunnel face of the auxiliary access gallery advances. Volume has to be enough to provide sufficient fresh air for people working at the front end, and also for removing the smoke of the machinery working and for extracting the dust coming from blasting operations.

A speed of 1 m/s is considered as the working air enough for proper ventilation.

The ventilation system will require axial fans with textile ducts. The number of fans used will increase as the tunnel deepens; however, the maximum number of fans used will be three, providing a maximum flow rate of 38 m<sup>3</sup>/s.

The fans are calculated for the pressure drop for a tunnel length of 3 Km (that is, the sum of the access gallery to the upper chamber and the connection galleries), and with a textile duct 2 m diameter.

The three axial fans will be located at the Canfranc portal, outside the tunnel and they will be installed in series.

#### 8.5.1.2 Final ventilation system

The final ventilation will have two purposes:

- Human ventilation in the underground system, except for MDC's and AC's, where a specific radon-free ventilation system will be necessary.
- Fire protection ventilation

The ventilation scheme needs an inlet part, where to intake air, and an exit part where the contaminated air can be evacuated.

Ventilation starts at Canfranc portal (1.194.4 a.s.l.) and runs through access galleries, MDC's and AC's (1.070 a.s.l.) and finishes at Rioseta shaft, through a ventilation tunnel that starts at MDC's level with 10% slope (1.182 m. long) that leads to a vertical shaft 224 m deep, that connect the exit point at surface (1.412 a.s.l.).

The display that has been chosen for fire protection ventilation is a jet fan system anchored to the vault of the tunnel. These fans will have frequency regulators to change its working speed and will have two ways of working, either for human or for fire protection ventilation.

The speed for human ventilation is calculated with 1 m/s and flow rate will be 38 m<sup>3</sup>/s. In case of fire the jet fans will work at their maximum power. Air speed will be 3 m/s, and flow rate will be 114 m<sup>3</sup>/s.

Fifteen (15) jet fans (45 m<sup>3</sup>/seg each one) will convey smoke through the tunnel to the exit. The distance between the fans will be 200 m.

Every fan is completely reversible, so depending where the fire is it can work in different ways.

In case of fire in the MDC's vault and inside the AC's, a fan will remove the smoke inside these rooms and will evacuate it to the main tunnel, so that the ventilation system can catch and evacuate it to Canfranc portal or to Rioseta shaft, depending on the fire location.

For better understanding see the next ventilation scheme, where the human ventilation and radon free ventilation are shown.

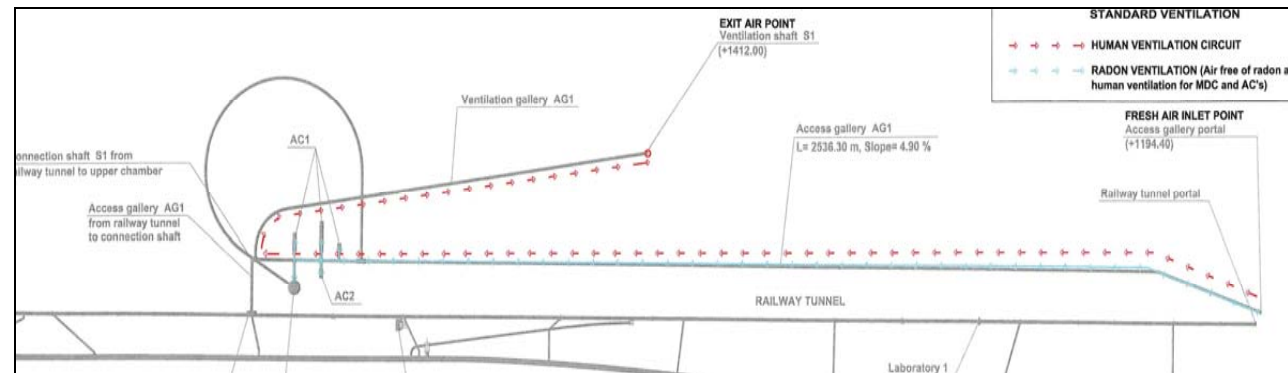


Figure 8.5-1. Ventilation system scheme, including final ventilation (dotted red line) and radon free air supply (clear blue line)

### 8.5.2 Radon free ventilation system

It is likely to have high levels of radon concentration in the tunnel. An independent ventilation will be provided to eliminate this element.

Fresh air will be blown through a duct 2 m diameter to the 3 MDC's, and to the AC1 and the three AC2's.

This ventilation will have two purposes:

- Human ventilation at inside of the MDC's and AC's.
- To have radon free air inside these facilities.

The flow rate considered is 30 m<sup>3</sup>/s in order to have 1 renovation/hour, that is, the whole air volume is changed each hour.

With this ventilation radon concentration will be reduced below 40 Bq/m<sup>3</sup> at the MDC's and at the AC's. A slight overpressure should be created in these rooms with grilles to have proper ventilation.

With the final ventilation (38 m<sup>3</sup>/s) also 1 renovation/hour is ensured, both for the Connection and Access Tunnels, in order to have the radon concentration below 100 bq/m<sup>3</sup>.

With radon ventilation working at MDC's and AC's and with the final ventilation working at Interconnection and Access Tunnels the radon concentration will be reduced to proper values for experiment operation.

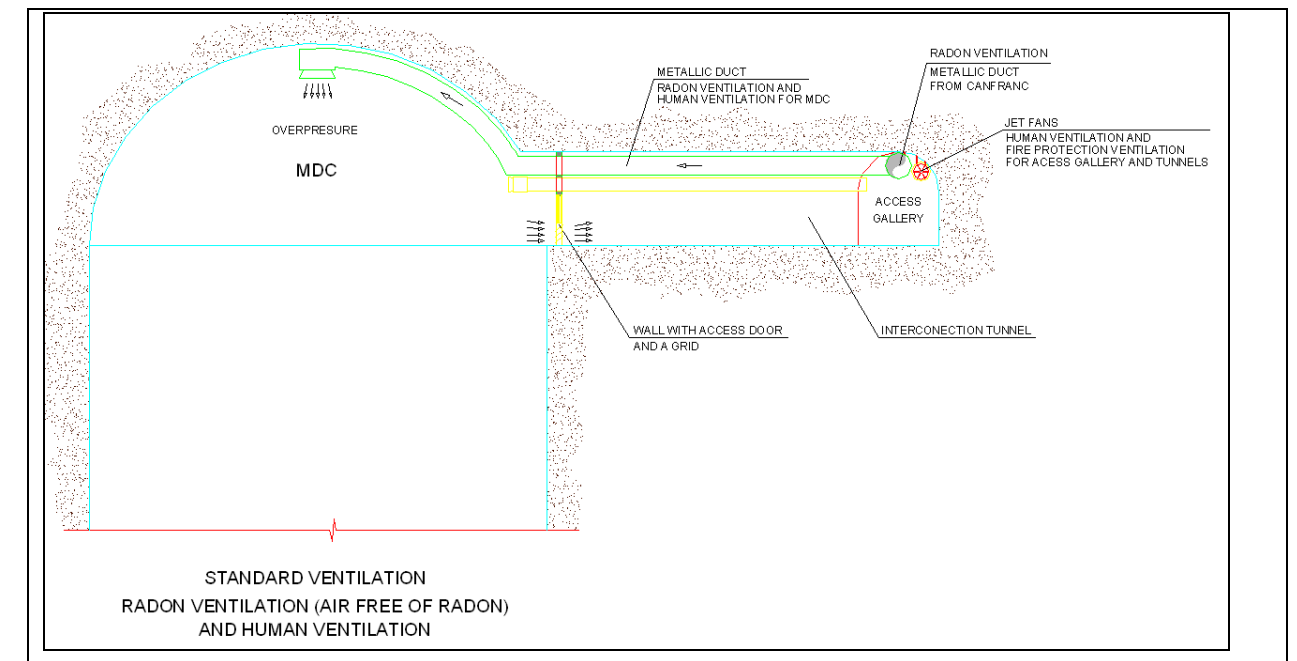


Figure 8.5-2. Ventilation system scheme, including final ventilation and radon free air supply to the MDC.

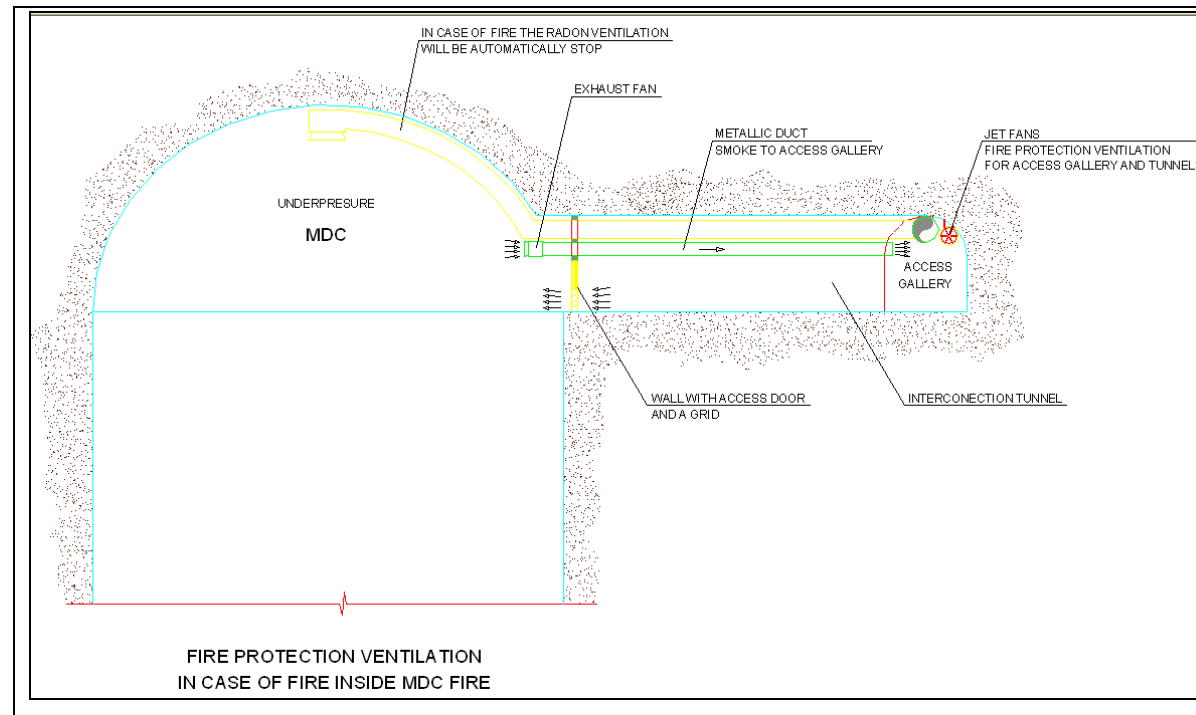


Figure 8.5-3. Fire protection ventilation system scheme for the MDC

### 8.5.3 Cooling and Heating.

Temperature and humidity have been measured inside the tunnel where the experiment will take place. A temperature of 10°C and 80% humidity are the average values of the year.

An air handling unit will be installed for the clean room. This machine will generate heat or cool depending on the needing. The air will be specially filtered to fulfil the requirement of clean rooms, and will be conveyed through metallic ducts with proper isolation.

For the electrical/electronic rooms at the MDC's a similar cooling system is foreseen. Several air handling units will be installed for all the electrical rooms, with a total cooling power of 100 Kw. Air distribution will be ensured by isolated ducts.

The heat coming from the electrical/electronic rooms will be used to heat the MDC's dome. In the case that more heat is needed, heating machinery will be used, in order to maintain working temperature at 22°C.

Handling units will be electrical.

Auxiliary Caverns must have a working temperature of 22 °C. In order to maintain the working temperature, electrical air heating units will be used.

### 8.5.4 Handling of dangerous substances

#### 8.5.4.1 Liquid scintillator

Liquid scintillator as a toxic substance has to be studied in a next stage. Special protocols for liquid management, including transport, storage and racking shall be submitted once its specific characteristics are completely defined.

#### 8.5.4.2 Nitrogen

Nitrogen will be used in order to get an atmosphere free of radon inside the Liquid Scintillator tank.

The tank will be filled with nitrogen gas supplied by lorry. The lorry contains liquid nitrogen, that can be vaporized through an atmosphere vaporizer. This equipment will be located just beside the MDC, in one of the AC's. Its flow capacity will be 100 m<sup>3</sup>/h.

Nitrogen gas is not a dangerous substance itself, because is one of the main components of natural air, but a great concentration of this gas displaces oxygen, so difficulties to breath may appear just in this case. For this reason, an oxygen level control must be installed in the MDC and AC's. This equipment will be installed to the height of knees and will check oxygen concentration. When a substantial re-



duction of oxygen concentration is detected an acoustic and visual alarm has to go off in order to alert people working in the affected areas.

### 8.5.5 Fire protection system and evacuation

In case of fire the tunnel has to be prepared in order that people working in the experiments can be evacuated and the fire can be easily controlled.

At every location of the tunnel, two exit ways must be ensured, in order to use the free one at each fire event. These exits are:

- The access gallery to the Canfranc portal.
- The communication shaft between the connection tunnel at MDC's level (1.070 m.) and the old railway tunnel.

The connection shaft location can be seen in the layout drawings. Access to the shaft should be designed with two fire protection doors, that will be able to support fires of two hours.

The connection shaft will be communicated with a lift of 8 people capacity that can work even in case of fire. Also emergency stairs are designed for this issue, as fire won't cross inside the shaft in the next two hours after the fire begins.

Along the tunnels fire extinguishers will be installed, with special concentration at the AC's and MDC's.

Fire water hoses will be provided for the MDC's and the AC's, in order to have water with pressure enough to extinguish potential fire events. An independent pumping water system, located at Canfranc, will supply this water installation. Fire pumps will be formed by an electrical, a diesel and a jockey pump, so in any case the fire water installation will have power to work, even with no electrical supply.

The exit of the fire pumps will be connected through a carbon steel pipe to a ring net pipes distribution of 5" ASME Sch. Std. All the pipes and valves will be designed to work at a nominal pressure of 16 bar. Reduction pressure valves will be installed all along the ring in order to adequate the working pressure.

Two types of fire detection system will be installed: with a wire along the tunnel and with conventional detectors for the AC's rooms and MDC's vaults. Fire detectors will be connected to a cabinet where the alarm can be seen at any time.

In case of fire, ventilation will be provided with jet fans of the final ventilation system with a flow rate of 114 m<sup>3</sup>/s for all the tunnels (Access tunnel and Connection tunnels). Depending on where the fire will be the jet fans will work to evacuate smoke either to Canfranc or to Rioseta.

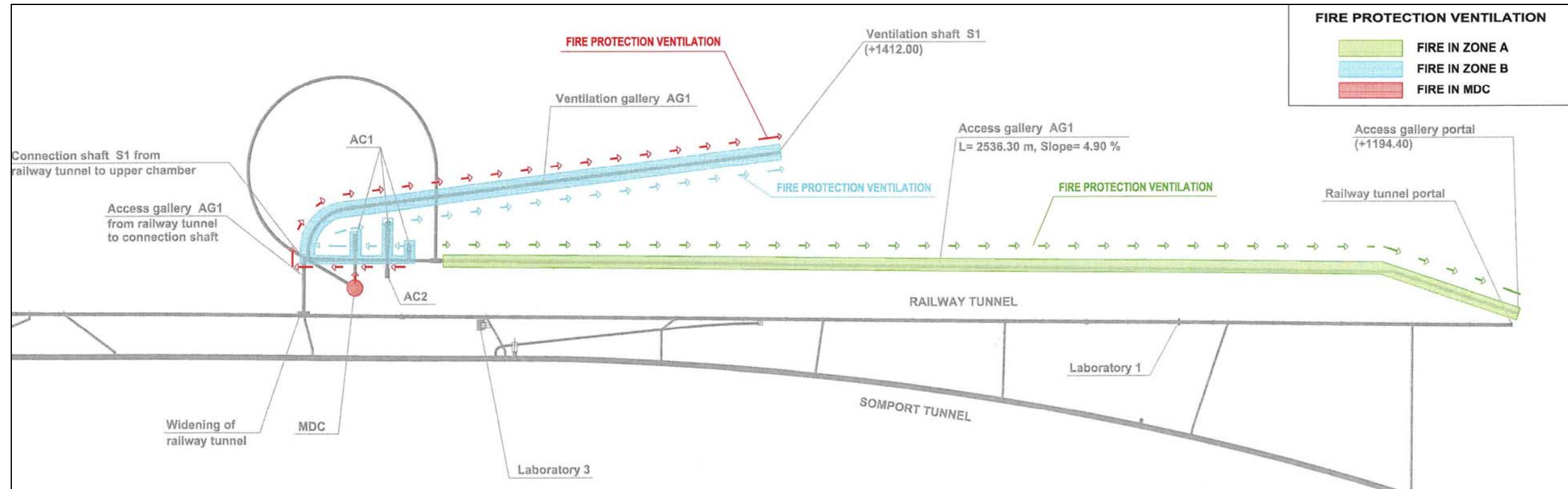


Figure 8.5-4. Fire protection ventilation system.

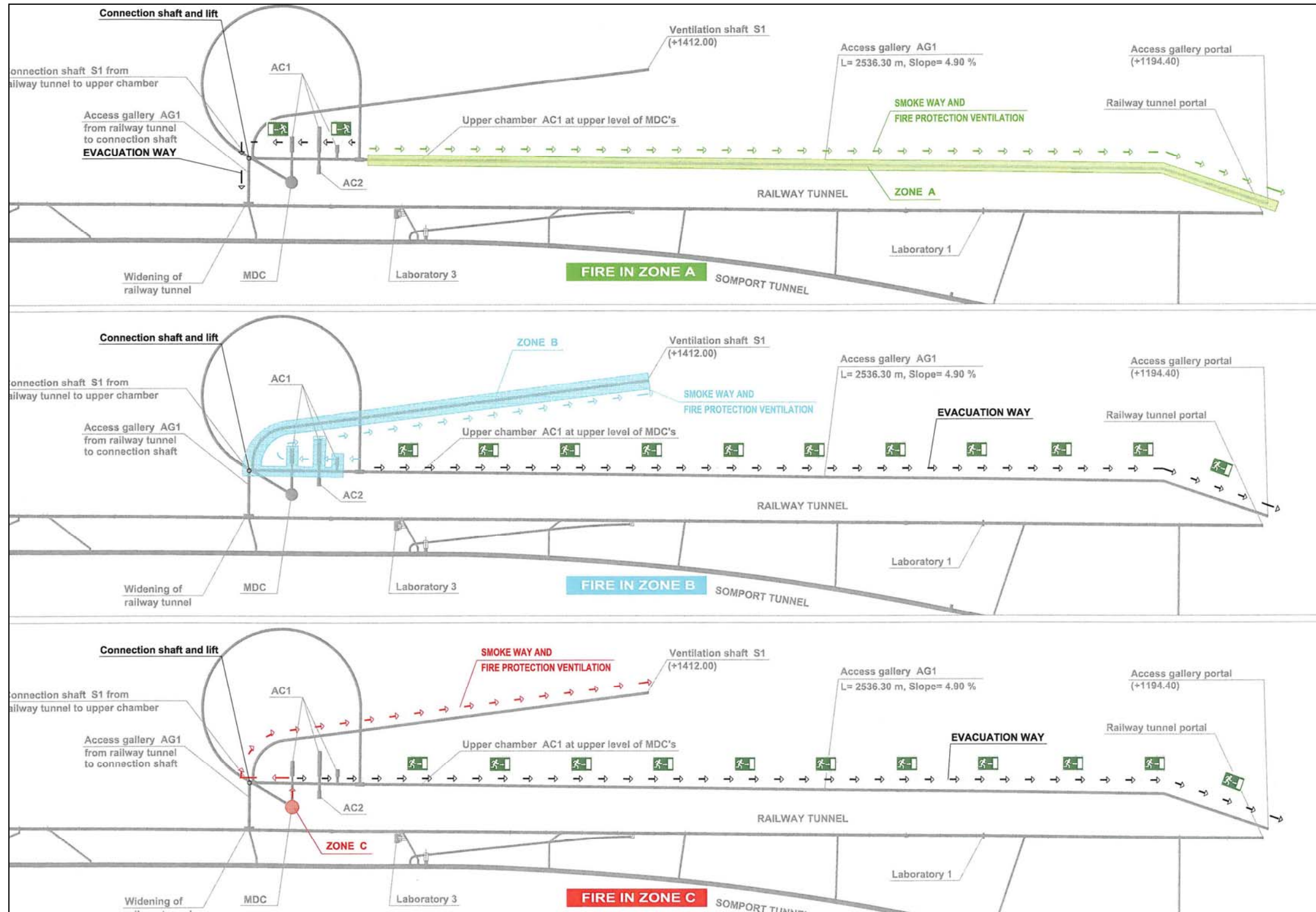


Figure 8.5-5. Evacuation plan and fire protection ventilation system.



### 8.5.6 Filling and emptying procedure facilities

The filling procedure starts with a nitrogen gas filling, in order to ensure there is not any radon element inside the tank. At the first stage the whole tank is filled with this gas.

After that the tank will be filled with common drinking water, coming from Canfranc, as described in the next part of this section. This water must first arrive to the purification system and deionised. With this treatment the tank is filled with deionised water.

While the tank is filled by water, nitrogen gas is taken out, in order to ensure acceptable pressure inside the tank.

Once the deionised water is inside the tank, this liquid is replaced by the liquid scintillator.

As liquid scintillator is a toxic substance no fixed facilities have been designed. The transport of the liquid will be by lorries, reaching the MDC location. An hydraulic pump to fill the purification system will be used.

There will always be nitrogen gas at the top of the tank to maintain the radon concentration in the experiment.

When emptying the tank nitrogen has to be first taken out. After that water will be emptied by pumping stations at several levels; first one at the bottom one (level 965 a.s.l.), second one at MDC level (1070 a.s.l.) and the final one at 1133 level.

Two hydraulic pumps will be installed at each pumping station with the same features. First pumping station features are (20 m<sup>3</sup>/h and 130 bar), second and third pumping station are (20 m<sup>3</sup>/h and 9 bar).

Carbon steel galvanized pipes have been considered following standard ASME Sch. Std and 3 ½" of diameter.

The emptying the scintillator liquid will also be made with lorries equipped with the same pumps than in the filling process.

### 8.5.7 Liquid handling facilities

#### 8.5.7.1 Drinking water

A water supply capable to get 35 m<sup>3</sup>/h of drinking water will be needed for surface and underground facilities. It can be connected to the water net at Canfranc village.

Drinking water utility will be split in two parts, one for surfaces facilities and other for underground facilities.

A pumping station of 20 m<sup>3</sup>/h and 4 bar, with an intermediate 10.000 litres tank will be provided to attend surface facilities, such as access control, offices, changing room, workshop, kitchen and dining room.

The drinking water system of the underground surfaces will be the same than the one for experiment water filling. Pumping stations each 1.175 m. length will be necessary. Each pumping station will have a 10.000 litres tank. These are atmospheric tanks, where the water pressure is broken.

Filling flow will be 15 m<sup>3</sup>/h and the pressure considered in each pumping station is 4 bar. Every pumping station will be formed by two pumps, working at the same time.

The pumping stations and their location have been previously described when describing filling and emptying system.

The facilities to feed with drinking water will be the access control, the changing room, kitchen and dining room and the warehouse.

Carbon steel pipes 3" ASME Sch. Std will be used to convey the water to the underground facilities.

#### 8.5.7.2 Sewage utility

The sewage utility for surface facilities will be a standard installation with PVC pipes with 1% of slope to connect to the public sewage line of Canfranc.

For underground facilities it will be used the same system as at surface, but instead of pumping this water to Canfranc, an intermediate pit should be used equipped with a pump working against a 10.000 litres tank. Special lorries will evacuate residual waters when needed. It is foreseen to empty the sewage tank once per month.

#### 8.5.8 Access

Access to the experiment area will be done from a new tunnel portal, located beside the existing tunnel portal of the railway. Excavations to build the portal should be built in this area. From this portal, the access gallery runs downwards to the MDC, as explained in different sections of the document.

An alternative pedestrian access is provided by the shaft that connects the existing railway tunnel and the LSC with the MDC's area. This access will be provided with an elevator for normal operation, and with a staircase for the case of emergency or fire alarm.

Surface installations should provide also access control to underground installations. An independent building, with a security guard in charge of access permits, would be the minimum access requirement to control vehicle access to the tunnels.

#### 8.5.9 Fire event

See fire protection system in section 8.5.5.

#### 8.5.10 Energy supply

Electrical utility starts at Canfranc portal place, where an electrical inlet able to feed high voltage power must be connected to the general electrical network.

Two power transformation rooms should be installed, one at the middle of the access gallery (1.138 a.s.l.) and the other at AC1 (1.070 a.s.l.). From these two power transformation rooms, electrical power will be supplied at low voltage for lighting and for MDC equipment, AC's and tunnel.

There will be three power transformers, one for the room which is at the middle of the gallery and two for AC1. All power transformers have 1.600 KVA's.

High voltage power will be distributed through the tunnel with an ironclad cable tray, anchored to the wall of the tunnel. The system designed is through a wire circuit that starts at Canfranc, goes to the power transformation room at the middle of the tunnel and after that to the AC1, finishing the loop ends at Canfranc again.

#### 8.5.11 Bulk transport and stocking

The volume of rock to be carried out the excavations if the Lena experiment is chosen is less than in the Memphis case. It can be resumed in the following parts:

- Rock from MDC's and support system galleries: 147.000 m<sup>3</sup>
- Rock from galleries and AC's: 248.000 m<sup>3</sup>
- Ventilation galleries and shafts: 80.000 m<sup>3</sup>

This rock volume is the one to be transferred to dump areas, with similar factor  $F=1,40$  as explained in the Memphis case. In this case the volume perhaps will allow for different locations that can be chosen both nearby Jaca and in different places in the vicinity of the road tunnel. Further environmental assessment studies should be carried out before deciding where to place muck from underground excavations, as explained in section 10.

#### 8.5.12 External installations

Further detailed design should locate external installations once the portal levelled definitive are is designed. This area should house different installations such as power transformation, ventilation units, water intake, parking area and reception and control building. The parking area should reserve place for lorries parking and inspection.

An area of 2.000 to 2.500 m<sup>2</sup> should be reserved for this purpose. The huge railway yard located beside the old Canfranc railway station can be used for external installations, machine shops and warehouses

## 8.6 LENA TANK

### 8.6.1 Tank structure

Tank structure is roughly described in paragraph 8.1.2. Super Kamiokande experience will be the base of further design, that is being carried out by Technodyne.

### 8.6.2 Assembling procedure

No assembling procedure has been designed at this phase. Super Kamiokande experience will be the base of further design.

### 8.6.3 Mechanical and thermal interaction with rock

Assessment about this aspect will be done in future phases.

### 8.6.4 Drainage system

In the case of eventual infiltrations, the MDC would have a series of drains placed in a radial fashion in order to carry any excess water away from the cavities. The number of drains placed would depend on the conditions encountered during construction. The drainage borings would have a gentle slope (~5%) to allow the water to flow. Figure 8.6-1, shows a sketch of the drainage system for the MDC.



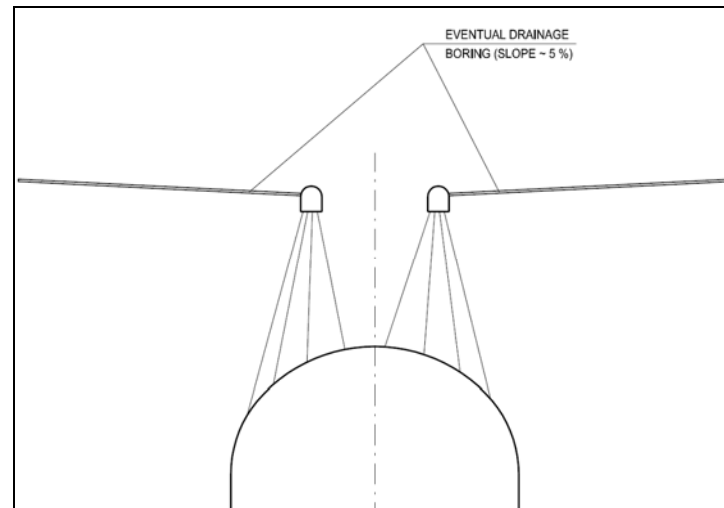


Figure 8.6-1. Eventual drainage curtain in the upper part of the vault.

Other drainage devices, such as drainage vertical curtains, could be displayed if necessary by means of ring galleries and vertical drains if necessary. Since Atxerito Formation is very impervious, no significant water inflow should be expected, although further rock investigations should deal with this aspect.

#### 8.6.5 Handling of leakage

Leakage of the tanks should be avoided in order to ensure proper experiment operation. If necessary, the drainage pit that is necessary for working purposes can be prepared so that eventual water leakage would be gathered at that point, and measured by means of volumetric control gauges. A duct network in the lower part of the tank must be designed in this case.

A pumping system, elevating water from the bottom of the tank to the upper part of the system will take leakages to the general sewage network.

## 9. GLACIER EXPERIMENT

### 9.1 MDC'S AND TANK DESCRIPTION

#### 9.1.1 Dimensions

The GLACIER experiment requires a different cavern; dimensions to be considered are the following ones:

Diameter	Height (cavern)
75 m	40 m

The diameter outgoes any existing dimensions for any kind of underground installation. This experiment requires 600 m.w.e., so this rock coverage can be easily fulfilled in many sections, and the best rock quality can be chosen to locate the cavern. The top level of the cavern has been selected to be below the level of the railway tunnel.

#### 9.1.2 Technological specifications

##### 9.1.2.1 Tanks

According to Technodyne conceptual design, the tank needs of two different parts:

- The outer shell of the detector may be a stainless-steel tank or a concrete wall tank, with a carbon steel lining. The second case is very similar to the LNG containers or tanks, that are usually built to contain 150.000 m<sup>3</sup>. The outer tank should be founded in a concrete slab. It is not necessary backfill this tank against the rock, since the tank could be pressure self supporting if necessary, though in this kind of design the external tank is designed usually to carry vault surcharge and to contain insulation between the outer and the inner lining.

- There is also an inner liner in the tank, which contains argon liquid at a temperature of -185,9 °C. This inner tank is usually built with nickled steel. No PMT's structure is needed for this experiment.
- Due to operational reasons, it is not necessary to built a dome for the tank, such as for LNG tanks. In this case, a bearing structure that provides also insulation can be hanged from the cavern vault.

#### 9.1.2.2 Others

Specifications about liquid argon management and equipment should be defined in further phases.

#### 9.1.3 General layout

Because of the GLACIER experiment dimensions, some previous geological considerations have been taken in mind before locating the cavern: in the Canfranc site, limestone rocks that form El Tobazo mountain are the best quality ones, and the excavation of the Somport road tunnel confirmed this, as it has been mentioned in other paragraphs. A location where the entire vault is excavated in best-quality rock has been chosen, attending to the data collected. In agreement with these, the MDC should be located 600 m North from the actual LSC installation.

Since it is farther away, the access ramp can be built from a new portal, 1.500 m North from the railway existing one. This portal allows a 2.050 m long access gallery, divided into two different sections, with slopes ranging from 6,2 to 0,9%. The first and steeper section runs 1.500 m and connects the portal with a chamber at level +1.206 a.s.l.. From this chamber, an access gallery to the LSC could be easily excavated, communicating both infrastructures. The second section, 550 m long, provides access from the chamber with the base of the vault and slopes gently at only 0,9%.

The cavern would be completely installed in the coralline Tobazo limestones, whose geomechanical quality indexes have been previously described and investigated with specific borehole drilling.

Another auxiliary tunnel would run from the access gallery to the base of the MDC, completing the scheme. Finally, a ventilation auxiliary facility consisting in a gallery and a vertical shaft ( $\Phi=5,70$  m) has been also designed. The scheme of this infrastructure is similar to the one that operates for the road tunnel. The shaft entrance is located in the Riojeta area, and environmental considerations should be taken in mind for this area in future detailed designs.

Comprehensive drawings for this LAGUNA technology infrastructure have been generated.

#### 9.1.4 Auxiliary caverns

Auxiliary caverns (AC's) provide both space for electronic, main control and office facilities, and for storage space. Also a power transformation area will be located in the AC's, which are the following ones:

- Cavern AC1: Electronics, main control and offices. Clean storage space
- Cavern AC3: power transformation room. Enclosed in the AC1 one.

## 9.2 GEOMECHANICAL DESCRIPTION OF THE SITE

A general review on geomechanical characterization has been stated in paragraph 6. Two different rock formations are to be considered for the different experiments. Regarding to the GLACIER one, the basic characterization of the Coralline Limestones is resumed in the above mentioned paragraph.

Final parameters used for calculation purposes are different than the ones that were set out for the Memphis or Lena MDC's calculations. In the case of the Coralline Limestones, two different possible rock qualities have been taken in mind, in order to make comparison of the results if rock quality is lesser than the one found in the road tunnel head excavation.

Geomechanical parameters are shown in section 9.4.1.

### 9.3 EXCAVATION METHODS FOR THE MDC

#### 9.3.1 Introduction

Similar empirical approaches were considered in this case, such as the above mentioned from the USACE (recommendations EM 1110-2-2901), that states that for spans between 18 and 30 m the rockbolt length should be a quarter of the span (there is no mention of structures with larger spans than 30 m). This means that for the GLACIER cavern with a 75 m span the minimum rockbolt length recommended is 18.8 m.

Dr. Evert Hoek's recommendations state that the cable length needed to support a cavern should be at least 40% its span, this means 30-meter long cables in the case of the GLACIER cavern. Regarding the minimum length for rockbolts, Hoek recommends 13-meter long bolts (according to the equation:  $L=2+0.15*\text{span}$ ).

Cables and bolts of such lengths are outside of what is normally available and easily installed. This suggests that the use of cables and rockbolts as the only support for the cavern roof might not be adequate, as seen for the Memphis case.

Considerations about huge roof wedges have been also previously explained. In the end, when selecting the support system there are two major concerns to address:

- The local stability and the relief of tensions close to the walls and vault, and
- The possible failure of a large wedge on the cavern roof

These problems can generally be solved with the use conventional support, such as cables, bolts and shotcrete. However, for the GLACIER experiment the conventional approach is not adequate due to the unprecedented dimensions of the caverns and it is apparent that an additional support system would be necessary to ensure the cavern stability.

This additional support system would be located above the cavern roof and would consist on two horizontal galleries and four diametrical ribs that meet at the top in an upper chamber, as shown in figure 9.3-1. This vault system needs to be in place before starting with the cavern excavation.

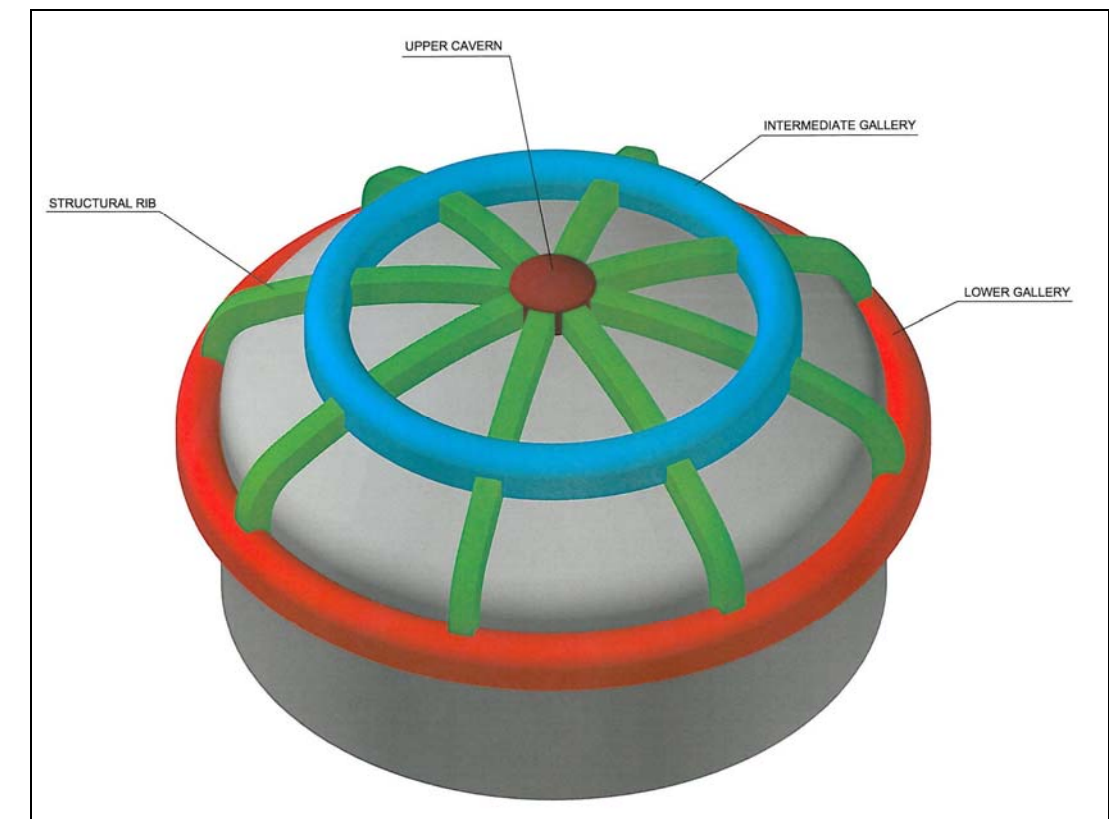


Figure 9.3-1. Perspective view of the vault system.



The excavation sequence of the ribs and galleries shown in figure 9.3-1 is expected to be as follows:

- Excavation and support of upper access tunnel at elevation 1201 (H = 7 m)
- Excavation and support of the lower perimeter gallery (5.0 m x 5.5 m) at elevation 1195.
- Excavation of lower part of structural ribs (2.5 m x 3.0 m) up to elevation 1210.5
- Excavation and support of intermediate gallery (5.0 m x 5.5 m) at elevation 1210.5
- Excavation of the top part of structural ribs (from intermediate gallery to upper cavern)
- Excavation and support of upper cavern (elevation 1215.1)

The galleries and ribs of the vault support structure will be concrete-filled at a later stage; however, based on the results obtained by the numerical modeling run for a similar structure for the MEMPHYS cavern, the concrete filling must be done in stages to avoid overstressing the concrete.

By allowing the rock mass to deform before filling the galleries and ribs with concrete, the stress on the galleries and ribs would be reduced. The concrete-filling sequence will be explained in the next paragraph.

The next paragraphs will cover the excavation sequence and support needed for the construction of the experiment cavern.

### 9.3.2 Cavern excavation sequence

Following the excavation of the galleries and ribs above the crown, the cavern is excavated following the sequence shown in figure 9.3-2. The stage numbers correspond to the numbering shown on the excavation sequence drawing:

Stage 1: Excavation and support of the first ring at elevation 1201, by the drill-and-blast method

Stage 2: Excavation and support of the second ring of the dome, by the drill-and-blast method

After the completion of stages 1 and 2, the following elements of the pre-support system are concrete-filled:

- Upper cavern
- Upper part of ribs (from upper cavern to intermediate gallery)
- Intermediate horizontal gallery

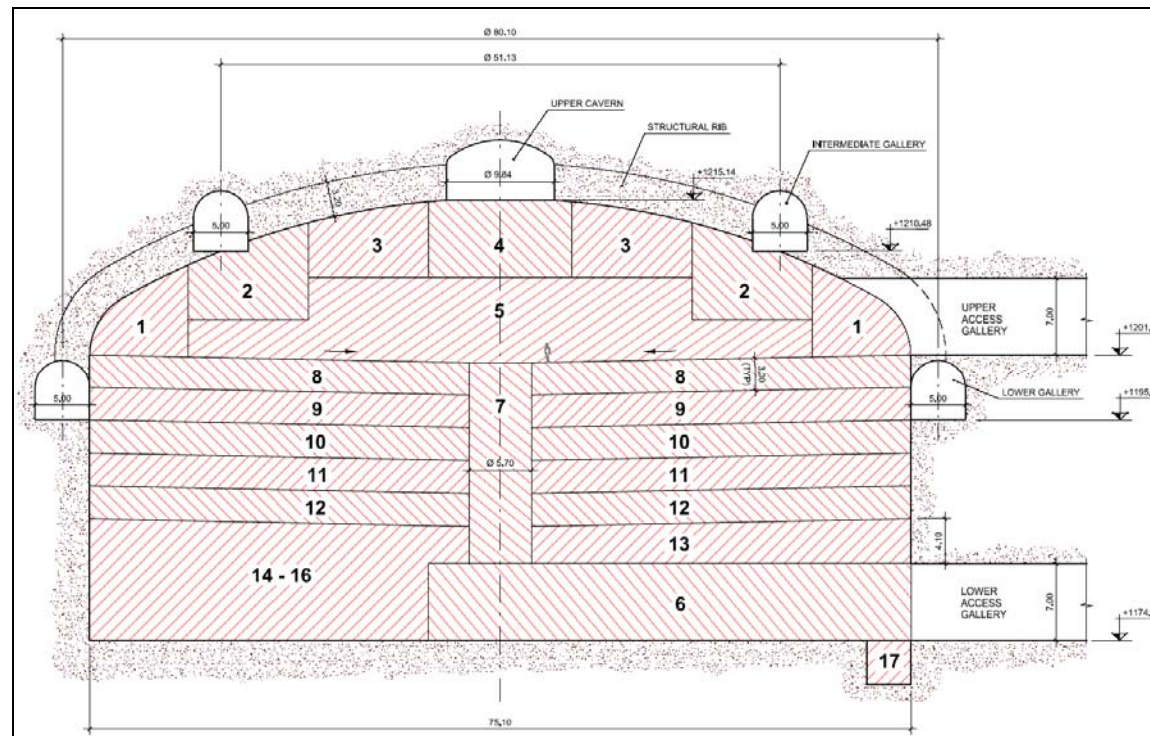


Figure 9.3-2. Excavation sequence for the GLACIER cavern.

Following the partial concrete-filling of the galleries and ribs, the excavation of dome continues:

**Stage 3:** Excavation and support of the third ring by the drill-and-blast method

**Stage 4:** Excavation and support of the top part of the dome by the drill-and-blast method

After stages 3 and 4 are completed, the lower part of ribs (from the intermediate gallery to the lower gallery) and the lower horizontal gallery of the vault system are concrete filled.

The excavation of the dome is completed following the concrete filling of the vault system in the next stage:

**Stage 5:** Removal of the remaining rock on the dome by the drill-and-blast method

The construction of the lower access tunnel should be completed before starting with the excavation of the cylindrical part of the cavern:

**Stage 6:** Excavation and support of lower access tunnel at elevation 1174.9 (H = 7 m) to the centre of the cavern

The excavation of the cylindrical section of the cavern will be carried out by raise boring in the next sequence:

**Stage 7:** Excavation of a shaft ( $\phi$  5.7m) with raise boring:

- Drilling of pilot hole
- Installation of the drill string
- Installation of the reamer head
- Excavation of the shaft from the bottom up
- Mucking out through lower access tunnel

**Stages 8 to 12:** Excavation of the cavern to elevation 1186:

- Excavation in 3 m benches slightly sloped toward the shaft (~ 5%)
- Mucking out through lower access tunnel
- Support of the walls immediately after mucking out

**Stage 13:** Excavation of the rock on top of the lower access tunnel with the drill-and-blast method

Stages 14 to 16: Excavation of the rock below elevation 1186:

- Excavation of two 3,5-meter benches and one 4,1-meter bench
- Mucking out through lower access tunnel
- Support of the walls immediately after mucking out

- Cables: 18 m long, 7 strand, cement grouted (grouted bulb length of 6 m), in a  $L_V = 3$  m,  $L_H = 1.33$  m pattern
- Rockbolts: 6m long, rebar steel bar  $\phi 38$  mm, cement or resin grouted, in a  $L_V = 3$  m,  $L_H = 1.33$  m pattern
- Shotcrete: 35-cm thick steel fibre reinforced shotcrete

Stage 17: Excavation of the drainage pit

### 9.3.3 Support system for the GLACIER caverns

The support system for the dome and the walls of the GLACIER cavern is presented in this section.

#### Dome:

Besides being supported by the vault structure previously described (and shown in figure 9.3-1), the dome will have cables, rockbolts and shotcrete with the following specifications:

- Cables: 18 m long, 7 strand, cement grouted (grouted bulb length of 6 m), in a 2 m x 2 m pattern
- Rockbolts: 6 m long rebar steel bar,  $\phi 38$  mm, cement or resin grouted, in a 2 m x 2 m pattern
- Shotcrete: 35-cm thick steel fibre reinforced shotcrete

#### Walls:

The cavern walls will be supported by cables, rockbolts and shotcrete with the following specifications:



## 9.4 NUMERICAL MODELLING OF THE MDC

### 9.4.1 Elastic modelling.

An elastic analysis of the problem was made, as in the case of the MEMPHYS experiment caverns. The theoretical background of this simplified model has been already explained.

Rock properties for the GLACIER cavern are described below. Since limestones quality is very remarkable, a different alternative lower quality has been also achieved, and two different calculations carried out:

Material	$\sigma_{ci}$ (MPa)	$m_i$	D	GSI	$m_b$	s	a
Limestones	60	12	0	70	4.110	0.0357	0.501
	60	12	0	60	2.876	0.0117	0.503

Table 9.4-1. Calculation properties

Figure 9.4-1 and 9.4-2 shows plastic elements around the excavation of the cavern, and local safety factor of these elements, for both rock qualities. No support was considered. Very small plastic areas were found, due to high rock quality in both cases.

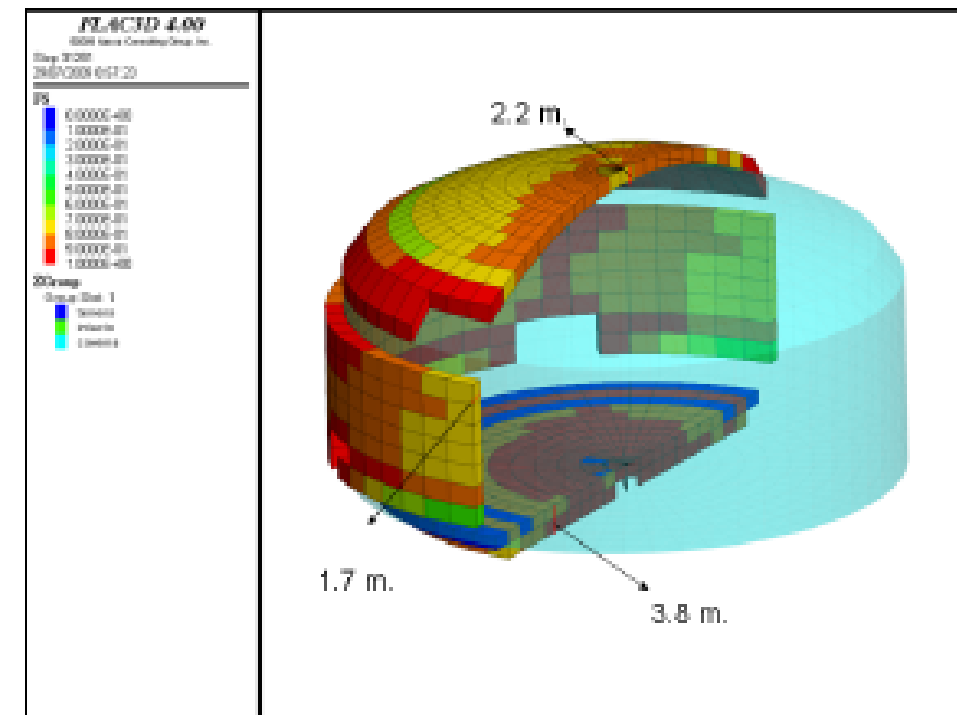


Figure 9.4-1. Plastic elements around the GLACIER MDC. GSI=70.

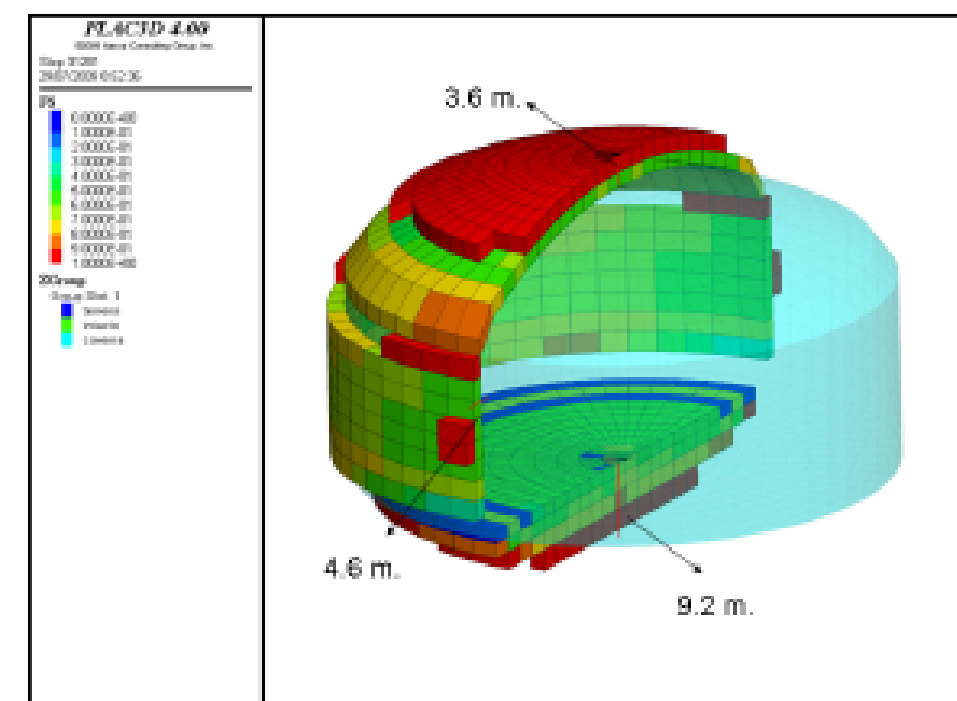


Figure 9.4-2. Plastic elements around the GLACIER MDC. GSI=60.

Plastification ranges from 2.2 to 3.6 m at the summit of the vault, 1.7 to 4.6 m at the cavern walls and 3.8 to 9.2 m in the floor area. A single excavation phase has been also considered. Safety factors range from 0.3 and 0.4 to 1.0 in plastic elements. Obviously, worst values are obtained for lower rock GSI value.

No more detailed calculations have been carried out in the GLACIER case.

The results that have been obtained are encouraging and allow considering the explained support system for this Feasibility Study. Further calculations, made on the base of a detailed subsoil exploration program, will lead to more precise design of rock bolting and anchoring support.

## 9.5 GLACIER SAFETY AND TECHNICAL ASPECTS

### 9.5.1 Ventilation (construction works and final ventilation)

#### 9.5.1.1 Ventilation system during construction works

The ventilation system considered for the site construction will be the necessary to blow with fresh air against the front end while the tunnel face of the auxiliary access gallery advances. Volume has to be enough to provide sufficient fresh air for people working at the front end, and also for removing the smoke of the machinery working and for extracting the dust coming from blasting operations.

A speed of 1 m/s is considered as the working air enough for proper ventilation.

The ventilation system will require axial fans with textile ducts. The number of fans will increase as the tunnel deepens; however, the maximum number of fans used will three, providing a maximum flow rate of 38 m<sup>3</sup>/s.

The fans are calculated for the pressure drop for a tunnel length of 3 Km (that is, the sum of the access gallery to the upper chamber and the connection galleries), and with a textile duct 2 m diameter.

The three axial fans will be located at the Canfranc portal, outside the tunnel and they will be installed in series.

#### 9.5.1.2 Final ventilation system

The final ventilation will have two purposes:

- Human ventilation in the underground system, except for MDC's and AC's, where a specific radon-free ventilation system will be necessary.
- Fire protection ventilation

The ventilation scheme needs an inlet part, where to intake, and an exit part where the contaminated air can be evacuated.

Ventilation starts at Access gallery portal (1.300 a.s.l.) and runs through the access tunnel, MDC and AC (1.201 a.s.l.), finishing at the Rioseta shaft, through a ventilation tunnel that starts at MDC level with 10% slope (1.428 m. long), and leads to the vertical shaft (69 m deep), to connect the exit point at 1.412 a.s.l.

The display that has been chosen for fire protection ventilation is a jet fan system anchored to the vault of the tunnel. These fans will have frequency regulators to change its working speed and will have two ways of working, either for human or for fire protection ventilation.

The speed for human ventilation is calculated with 1 m/s and flow rate will be 38 m<sup>3</sup>/s. In case of fire the jet fans will work at their maximum power. Air speed will be 3 m/s, and flow rate will be 114 m<sup>3</sup>/s.

Fifteen (15) jet fans (45 m<sup>3</sup>/seg each one) will convey smoke through the tunnel to the exit. The distance between the fans will be 200 m.

Every fan is completely reversible, so depending where the fire is it can work in different ways.

In case of fire in the MDC's vault and inside the AC's, a fan will remove the smoke inside these rooms and will evacuate it to the main tunnel, so that the ventilation system can catch and evacuate it to Canfranc portal or to Rioseta shaft, depending on the fire location.

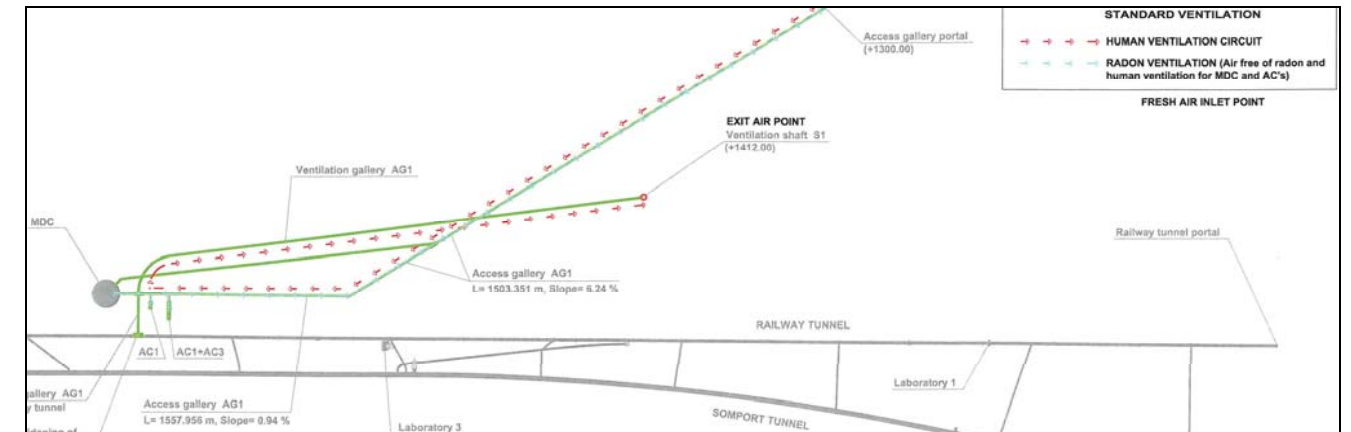


Figure 9.5-1. Ventilation system scheme, including final ventilation and radon free air supply

### 9.5.2 Radon free ventilation system

It is likely to have high levels of radon concentration in the tunnel. An independent ventilation will be provided to eliminate this element.

Fresh air will be blown through a duct 2 m diameter to the 3 MDC's, and to the AC1 and the three AC2's.

This ventilation will have two purposes:

- Human ventilation at inside of the MDC's and AC's.
- To have radon free air inside these facilities.

The flow rate considered is 30 m<sup>3</sup>/s in order to have 1 renovation/hour, that is, the whole air volume is changed each hour.

With this ventilation radon concentration will be reduced below 40 Bq/m<sup>3</sup> at the MDC's and at the AC's. A slight overpressure should be created in these rooms with grilles to have proper ventilation.



With the final ventilation (38 m<sup>3</sup>/s) also 1 renovation/hour is ensured, both for the Connection and Access Tunnels, in order to have the radon concentration below 100 bq/m<sup>3</sup>.

With radon ventilation working at MDC's and AC's and with the final ventilation working at Interconnection and Access Tunnels the radon concentration will be reduced to proper values for experiment operation.

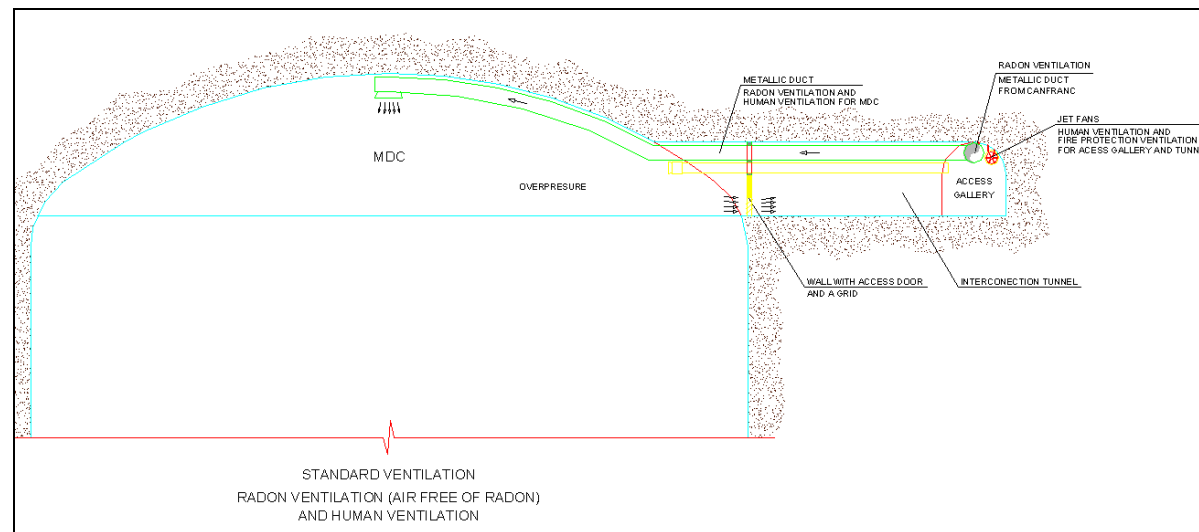


Figure 9.5-2. Ventilation system scheme, including final ventilation and radon free air supply for MDC

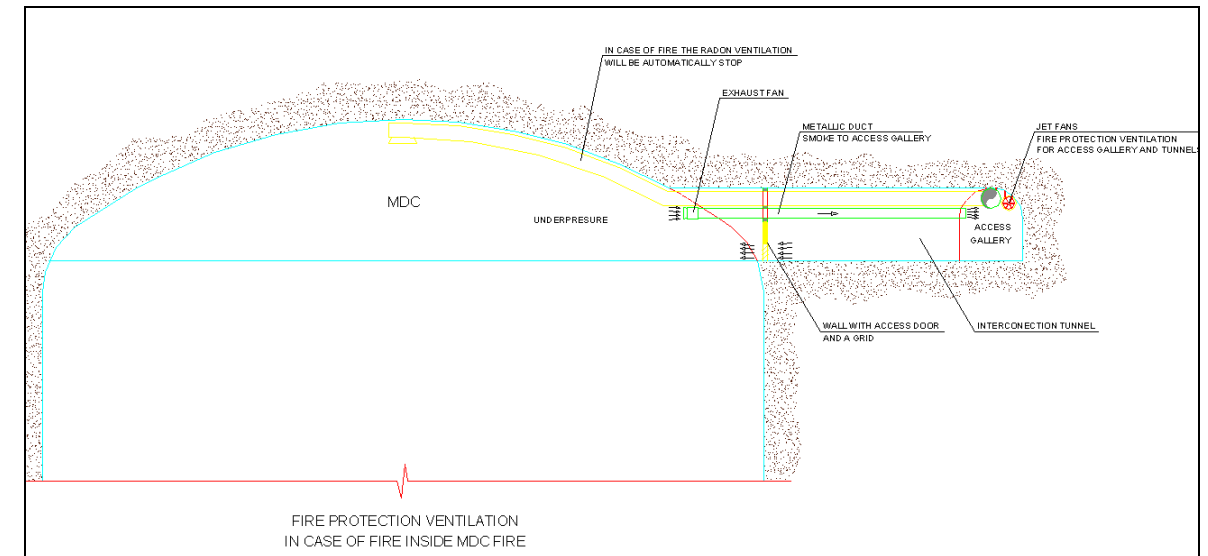


Figure 9.5-3. Fire protection ventilation system scheme for MDC

### 9.5.3 Cooling and Heating.

Temperature and humidity have been measured inside the tunnel where the experiment will take place. A temperature of 10°C and 80% humidity are the average values of the year.

An air handling unit will be installed for the clean room. This machine will generate heat or cool depending on the needing. The air will be specially filtered to fulfil the requirement of clean rooms, and will be conveyed through metallic ducts with proper isolation.

For the electrical/electronic rooms at the MDC's a similar cooling system is foreseen. Several air handling units will be installed in each room, with a total cooling power of 500 Kw. Air distribution will be ensured by isolated ducts.

The heat coming from the electrical/electronic rooms will be used to heat the MDC's dome. In the case that more heat is needed, heating machinery will be used, in order to maintain working temperature at 22°C.

Handling units will be electrical.

Auxiliary Caverns must have a working temperature of 22 °C. In order to maintain the working temperature, electrical air heating units will be used.

#### 9.5.4 Handling of dangerous substances

No dangerous substances are to be handled for the GLACIER experiment. An operation protocol shall be developed in further stages.

#### 9.5.5 Fire protection system and evacuation

In case of fire the tunnel has to be prepared in order that people working in the experiments can be evacuated and the fire can be easily controlled.

At every location of the tunnel, two exit ways must be ensured, in order to use the free one at each fire event. These exits are:

- The access gallery to the Canfranc portal.
- The communication by means of a gallery or connection tunnel at MDC level (1.201 a.s.l.) that provides exit to the old railway tunnel.

The exit gallery location can be seen in the layout drawings. Access to this gallery will need of two fire protection doors, that will be able to support fires of two hours.

Along the tunnels fire extinguishers will be provided, with special concentration at the AC's and MDC's.

Fire water hoses will be provided for the MDC and the AC, in order to have water with pressure enough to extinguish potential fire events. An independent pumping water system, located at road from Canfranc to Candanchu, will supply to this water installation. Fire pumps will be formed by an electrical, a diesel and a jockey

pump, so in any case the fire water installation will have power to work, even with no electrical supply.

The exit of the fire pumps will be connected through a carbon steel pipe to a ring net pipes distribution of 5" ASME Sch. Std. All the pipes and valves will be designed to work at a nominal pressure of 16 bar. Reduction pressure valves will be installed all along the ring in order to adequate the working pressure.

Two types of fire detection system will be installed: with a wire along the tunnel and with conventional detectors for the AC rooms and MDC vaults. Fire detectors will be connected to a cabinet where the alarm can be seen at any time.

In case of fire, ventilation will be provided with jet fans of the final ventilation system with a flow rate of 114 m<sup>3</sup>/s for all the tunnels (Access tunnel and connection tunnels). Depending on where the fire will be the jet fans will work to evacuate smoke either to the access gallery portal of the road from Canfranc to Candanchú or to Rioseta.

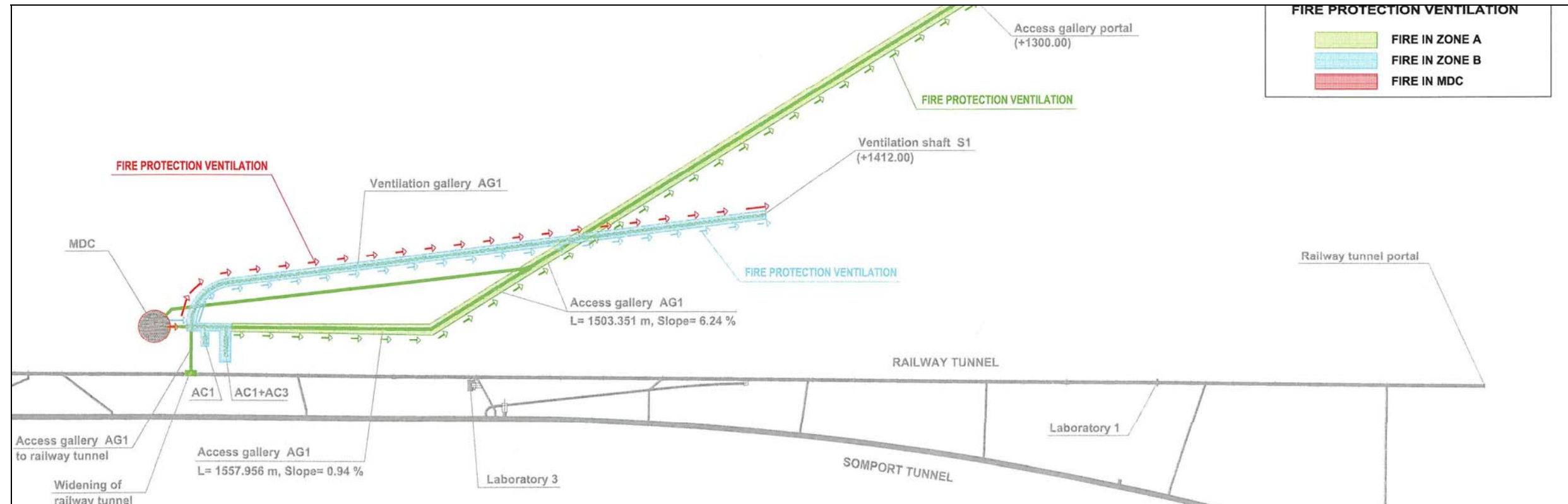


Figure 9.5-4. Fire protection ventilation system.



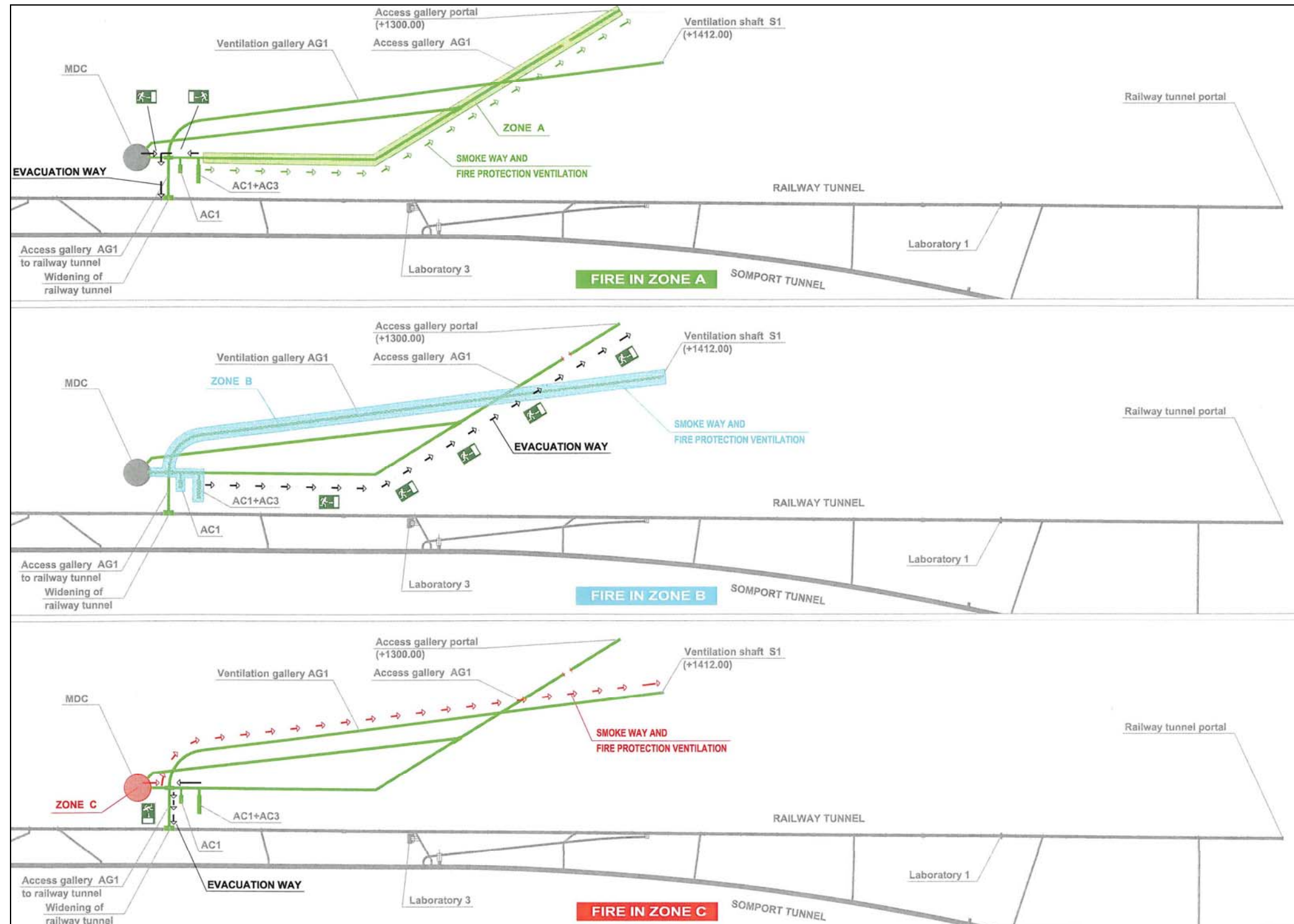


Figure 9.5-5. Evacuation plan and fire protection ventilation system.

### 9.5.6 Filling and emptying procedure facilities

The filling procedure starts with an argon gas filling. That is done in order to ensure there is not any radon element inside the tank. So the complete tank is filled with this gas. An atmospheric vaporizer will be installed to obtain the gas from the liquid buffer of the lorry.

The liquid argon will be delivered by lorry to fill the tank. Lorries must park nearby the MDC place. The filling of the purification system with liquid argon will be done through a special pump that can convey liquid argon (83 °K).

There will always be argon gas at the top of the tank to maintain the radon concentration in the experiment.

Stainless steel pipes have been considered for handling argon gas or liquid. Pipes follow standard ASME Sch. Std.

Emptying of the argon liquid is considered to be done also by lorry, being the same procedure as the filling.

### 9.5.7 Liquid handling facilities

#### 9.5.7.1 Drinking water

A water supply capable to get 35 m<sup>3</sup>/h of drinking water will be needed for surface and underground facilities. It can be connected to the water net at the road from Canfranc village to Candanchú, or provided by a specific inlet coming from the river.

Drinking water utility will be split in two parts, one for surfaces facilities and other for underground facilities.

A pumping station of 20 m<sup>3</sup>/h and 4 bar, with an intermediate 10.000 litres tank will be provided to attend surface facilities, such as access control, offices, changing room, workshop, kitchen and dining room.

The drinking water system of the underground surfaces will be the same than the one for experiment water filling. Pumping stations each 1.175 m. length will be necessary. Each pumping station will have a 10.000 litres tank. These are atmospheric tanks, where the water pressure is broken.

Filling flow will be 15 m<sup>3</sup>/h and the pressure considered in each pumping station is 4 bar. Every pumping station will be formed by two pumps, working at the same time.

The pumping stations and their location have been previously described when describing filling and emptying system.

The facilities to feed with drinking water will be the access control, the changing room, kitchen and dining room and the warehouse.

Carbon steel pipes 3" ASME Sch. Std will be used to convey the water to the underground facilities.

#### 9.5.7.2 Sewage utility

The sewage utility for surface facilities will be a standard installation with PVC pipes with 1% of slope to connect to the public sewage line of Canfranc.

For underground facilities it will be used the same system as at surface, but instead of pumping this water to Canfranc, an intermediate pit should be used equipped with a pump working against a 10.000 litres tank. Special lorries will evacuate residual waters when needed. It is foreseen to empty the sewage tank once per month.

### 9.5.8 Access

Access to the experiment area will be done from a new tunnel portal, in the road from Canfranc to Candanchú ski resort. Excavations to build the portal should be built in this area. From this portal, the access gallery runs downwards to the MDC's, as explained in different sections of the document.

An alternative pedestrian access is provided with the gallery that connects the existing railway tunnel with the MDC's area. This access is horizontal, so it does not need elevator or stairs, such as in the other two experiments, but provides escape facilities in the case of emergency or fire alarm.

Surface installations should provide also access control to underground installations. An independent building, with a security guard in charge of access permits, would be the minimum access requirement to control vehicle access to the tunnels.

### 9.5.9 Fire event

See fire protection system in section 9.5.5.

### 9.5.10 Energy supply

Electrical utility starts at access gallery portal placed beside the road from Canfranc to Candanchú, where permission for a electrical inlet with high voltage power shall be requested in order to supply energy to the different underground and surface utilities.

Two power transformation rooms should be installed, one at the middle of the access gallery) and the other at AC1 (1201 a.s.l). From these two power transformation rooms, electrical power will be supplied at low voltage for lighting and for MDC equipment, AC's and tunnel.

There will be three power transformers, one for the room which is at the middle of the gallery and two for AC1. All power transformers have 1.600 KVA's.

High voltage energy will be distributed through the tunnel with an ironclad cable tray, anchored to the wall of the tunnel. The system designed consists of a wire circuit that starts at the access gallery portal, goes to the power transformation room at the middle of the tunnel and after that to the AC1, finishing the loop ends at the access gallery portal again.

### 9.5.11 Bulk transport and stocking

The volume of rock to be carried out the excavations if the Glacier experiment is chosen is less than in the Memphys case, and slightly more than in the Lena experiment. It can be resumed in the following parts:

- Rock from MDC's and support system galleries: 229.000 m<sup>3</sup>
- Rock from galleries and AC's: 175.000 m<sup>3</sup>
- Ventilation galleries and shafts: 83.000 m<sup>3</sup>

This rock volume is the one to be transferred to dump areas, with similar factor F=1,40 as explained in the Memphys case. In this case the volume perhaps will allow for different locations that can be chosen both nearby Jaca and in different places in the vicinity of the road tunnel, or in the valley. Further environmental assessment studies should be carried out before deciding where to place muck from underground excavations, as explained in section 10.

### 9.5.12 External installations

Further detailed design should locate external installations once the portal levelled definitive are is designed. This area should house different installations such as power transformation, ventilation units, water intake, parking area and reception



and control building. The parking area should reserve place for lorries parking and inspection.

An area of 2.000 to 2.500 m<sup>2</sup> should be reserved for this purpose. The huge railway yard located beside the old Canfranc railway station can be used for external installations, machine shops and warehouses

## 9.6 GLACIER TANK

### 9.6.1 Tank structure

Tank structure is roughly described in paragraph 9.1.2. LNG tanks experience is extensive around the world, and will be the base of further design, that is being carried out by Technodyne.

### 9.6.2 Assembling procedure

No assembling procedure has been designed at this phase. LNG tanks experiences will be the base of further design.

### 9.6.3 Mechanical and thermal interaction with rock

Assessment about this aspect will be done in future phases. This aspect can be of particular importance in the case of liquid argon, and eventual rock burst due to accidental leakage may be a serious hazard in the Glacier case.

### 9.6.4 Drainage system

In the case of eventual infiltrations, the MDC's would have a series of drains placed in a radial fashion in order to carry any excess water away from the cavities. The number of drains placed would depend on the conditions encountered during construction. The drainage borings would have a gentle slope (~5%) to allow the water to flow. Figure 9.6-1, shows a sketch of the drainage system for each type of cavern.

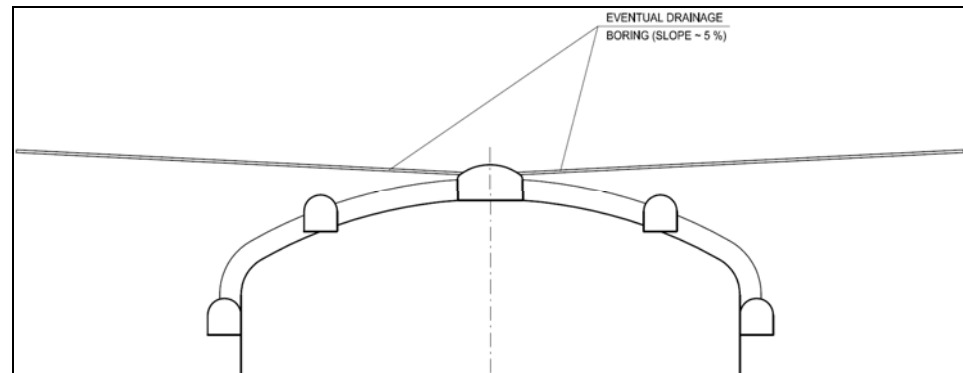


Figure 9.6-1. Eventual drainage curtain in the upper part of the vault.

Other drainage devices, such as drainage vertical curtains, could be displayed if necessary by means of ring galleries and vertical drains if necessary. The Coral-line Limestones can be eventually pervious, but no significant water inflow was measured during the Somport Tunnel construction, since at that depth rock joints are sealed and closed, and no karstic features were recognized when driving the tunnel, apart from minimum leakage. Further rock investigations should deal with this aspect.

#### 9.6.5 Handling of leakage

This section will be considered for further design phases

## 10. ENVIRONMENTAL ASPECTS

### 10.1 INTRODUCTION

In this section, different environmental issues that may affect the LAGUNA project (mainly during the decision making in the design phase and the potential construction phase) will be described.

First of all it must be emphasized that the Project is ongoing the feasibility stage. If the Canfranc location is chosen to implement the LAGUNA Project, further environmental studies will have to be undertaken, and most probably the project will have to follow an environmental impact assessment process. With regard to the environmental issues to be described in this section, they are as follows:

- A compendia of environmental legislation to be taken into account in the LAGUNA Project at the Canfranc site.
- A location analysis in relation with the natural protected areas that could be affected by the project.
- A materials analysis regarding the disposal of the waste material that the construction of the cavern/s will generate.
- Considerations concerning the operation and handling of hazardous substances.
- The environmental impact assessment process in Spain.
- A general index of an environmental monitoring plan.
- Conclusions

## 10.2 COMPENDIA OF ENVIRONMENT LEGISLATION APPLICABLE TO THE AREA OF THE LSC

### 10.2.1 European Regulations

- Council Directive 85/337/EEC of 27 June 1985 on the assessment of the effects of certain public and private projects on the environment.
- Council Directive 97/11/EC of 3 March 1997 amending Directive 85/337/EEC on the assessment of the effects of certain public and private projects on the environment.
- Directive 2001/42/EC of the European Parliament and of the Council of 27 June 2001 on the assessment of the effects of certain plans and programmes on the environment.
- Directive 2000/60/EC of the European Parliament and of the Council of 23 October 2000 establishing a framework for Community action in the field of water policy.
- Council Directive 92/43/EEC of 21 May 1992 on the conservation of natural habitats and of wild fauna and flora.
- Council Directive 79/409/EEC of 2 April 1979 on the conservation of wild birds.
- Council Directive 78/659/EEC of 18 July 1978 on the quality of fresh waters needing protection or improvement in order to support fish life.
- The Convention on the Conservation of Migratory Species of Wild Animals (Bonn Convention).

- The Bern Convention on the Conservation of European Wildlife and Natural Habitats 1979, also known as the Bern Convention (or Berne Convention).
- Commission Regulation (EEC) No 3646/83 of 12 December 1983 amending Council Regulation (EEC) No 3626/82 on the implementation in the Community of the Convention on international trade in endangered species of wild fauna and flora
- Directive 2002/49/EC of the European Parliament and of the Council of 25 June 2002 relating to the assessment and management of environmental noise
- Council Directive 91/156/EEC of 18 March 1991 amending Directive 75/442/EEC on waste.
- Council Directive 91/689/EEC of 12 December 1991 on hazardous waste.
- Council Directive 94/31/EC of 27 June 1994 amending Directive 91/689/EEC on hazardous waste.
- 94/904/EC: Council Decision of 22 December 1994 establishing a list of hazardous waste pursuant to Article 1 (4) of Council Directive 91/689/EEC on hazardous waste.
- Council Directive 96/61/EC of 24 September 1996 concerning integrated pollution prevention and control.
- Council Directive 1999/31/EC of 26 April 1999 on the landfill of waste.

### 10.2.2 National Regulations

Spanish designation has been kept for these regulations, due to their local interest.



- Real Decreto Legislativo 1/2008, de 11 de enero, por el que se aprueba el texto refundido de la Ley de Evaluación de Impacto Ambiental.
- Real Decreto 1131/1988, de 30 de septiembre, por el que se aprueba el Reglamento para la ejecución del Real Decreto Legislativo 1302/1986, de Evaluación de Impacto Ambiental.
- Decreto 148/1990, de 9 de noviembre, de procedimiento para la declaración de impacto ambiental. BOA nº 143. (05-12-90).
- Ley 26/2007, de 23 de octubre, de Responsabilidad Medioambiental
- Real Decreto 2090/2008, de 22 de diciembre, por el que se aprueba el Reglamento de desarrollo parcial de la Ley 26/2007 de Responsabilidad Medioambiental.
- Ley 9/2006, de 28 de abril, sobre la evaluación de los efectos de determinados planes y programas en el medio ambiente.
- Ley 42/2007, de 13 de diciembre, del Patrimonio Natural y de la Biodiversidad.
- Ley 4/1989, de 27 de marzo, de conservación de los Espacios Naturales y de la Flora y Fauna Silvestre.
- Ley 40/1997, de 5 de noviembre, por la que se modifica la Ley 4/1989, de 27 de marzo, de Conservación de los Espacios Naturales Protegidos y de la Flora y Fauna Silvestre.
- Real Decreto 1193/1998, de 12 de junio, por el que se modifica el Real Decreto 1997/1995, de 7 de diciembre, por el que se establecen las medidas para contribuir a garantizar la biodiversidad mediante la conservación de los hábitats naturales (Real Decreto por el que la legislación española transpone la Directiva 92/43/CEE).
- Real Decreto 1421/2006, de 1 de diciembre, por el que se modifica el Real Decreto 1997/1995, de 7 de diciembre, por el que se establecen medidas para contribuir a garantizar la biodiversidad mediante la conservación de los hábitats naturales y de la flora y fauna silvestres.
- Real Decreto 439/1990 de 30 de Marzo, por el que se regula el Catálogo Nacional de especies amenazadas (actualizado por la Orden de 10 de marzo de 2000; Orden MAM/2734/2002; Orden MAM/2784/2004, de 28 de mayo y Orden MAM/2231/2005, de 27 de junio).
- Real Decreto legislativo 1/2001, de 20 de julio, por el que se aprueba el texto refundido de la Ley de Aguas.
- La Ley 3/1995, de 23 de marzo, de Vías Pecuarias
- REAL DECRETO 1481/2001, de 27 de diciembre, por el que se regula la eliminación de residuos mediante depósito en vertedero.
- Ley 10/1998, de 21 de abril, de residuos.
- RD 9/2005, de 14 de enero, por el que se establece la relación de actividades potencialmente contaminantes de suelo y los criterios y estándares para la declaración de suelos contaminados.
- Decreto 2414/1961, de 30 de noviembre, sobre Actividades Molestas, Insalubres, Nocivas y Peligrosas. BOE nº 292. (07-12-61)
- Ley 22/1973, de 21 de julio, de Minas.

- Ley 12/1981, de 24 de diciembre, por la que se establecen normas adicionales de protección de los espacios de interés natural afectados por actividades extractivas.
- Decreto 343/1983, de 15 de julio, sobre las normas de protección del medio ambiente de aplicación a las actividades extractivas.
- Ley 43/2003, de 21 de noviembre, de Montes (BOE, 22 de noviembre de 2003).
- Ley 38/1972, de 22 de diciembre, de Protección del Ambiente Atmosférico. (BOE, de 26 de diciembre de 1972). Decreto 833/1975, de 6 de febrero, que desarrolla la Ley 38/72 (BOE, 22 de abril de 1975). Real Decreto 547/79, por el que se modifica el Decreto 833/1975 (BOE, 23 de marzo de 1979).
- Real Decreto 1613/1985, de 1 de agosto, por el que se modifica parcialmente el Decreto 833/75 y se establecen nuevas normas de calidad del aire en lo referente a contaminación por dióxido de azufre y partículas (BOE, 12 de septiembre de 1985). Real Decreto 1321/1992, de 30 de octubre, por el que se modifica parcialmente el R.D. 1613/85 (BOE, 2 de diciembre de 1992). Corrección de errores (BOE, 3 de febrero de 1993).
- Real Decreto 717/1987, de 27 de mayo, por el que se modifica parcialmente el Decreto 833/75 y se establecen nuevas normas de calidad del aire en lo referente a contaminación por dióxido de nitrógeno y plomo. (BOE, 6 de junio de 1987).
- Real Decreto 1494/1995, de 8 de septiembre, sobre contaminación atmosférica por ozono.
- Real Decreto 1367/2007, de 19 de octubre por el que se desarrolla la Ley 7/2003, de 17 de noviembre, del Ruido, en lo referente a zonificación acústica, objetivos de calidad y emisiones acústicas.
- Ley 37/2003, de 17 de noviembre, del ruido (BOE 18/11/2003).
- Real Decreto 1513/2005, de 16 de diciembre, por el que se desarrolla la Ley 37/2003, de 17 de noviembre, del Ruido, en lo referente a la evaluación y gestión del ruido ambiental (BOE 17/12/2005).
- Real Decreto 1367/2007, de 19 de octubre por el que se desarrolla la Ley 37/2003, de 17 de noviembre, del Ruido, en lo referente a zonificación acústica, objetivos de calidad y emisiones acústicas.
- Real Decreto 212/2002, de 22 de febrero, por el que se regulan las emisiones sonoras en el entorno, debido a determinadas máquinas de uso al aire libre (BOE Núm. 52, de 1 de marzo de 2002).
- Real Decreto 524/2006, de 28 de abril, que modifica el Anexo XI del Real Decreto 212/2002 anterior, que contiene los valores límite.
- Real Decreto 286/2006, de 10 de marzo, sobre la protección de la salud y la seguridad de los trabajadores contra los riesgos relacionados con la exposición al ruido durante el trabajo, (BOE Núm. 60, de 11 de marzo de 2006).
- Ley 34/2007, de 15 de noviembre, de calidad del aire y protección de la atmósfera.
- Real Decreto 105/2008, de 1 de febrero, por el que se regula la producción y gestión de los residuos de construcción y demolición.

- Real Decreto 833/1988, de 20 de julio, por el que se aprueba el Reglamento para la ejecución de la Ley 20/1986 Básica de Residuos Tóxicos y Peligrosos.
- Resolución de 28 de abril de 1995, de la Secretaría de Estado de Medio Ambiente y Vivienda, por la que se dispone la publicación del Acuerdo del Consejo de Ministros de 17 de febrero de 1995, por el que se aprueba el Plan Nacional de Residuos Peligrosos. (BOE nº 114 de 13.05.95).
- Ley 10/1998, de 21 de abril, de Residuos (BOE, 22 de abril de 1.998). Resolución de 17 de noviembre de 1998, de la Dirección General de Calidad y Evaluación Ambiental, por la que se dispone la publicación del catálogo europeo de residuos (CER), aprobado mediante la Decisión 94/3/CE, de la Comisión, de 20 de diciembre de 1993 (BOE, 8 de enero de 1999).

#### 10.2.3 Regional regulations

- Decreto 118/1989, de 19 de septiembre, de procedimiento de Evaluación del Impacto Ambiental BOA nº 103. (02-10-89). (Corrección de errores: BOA nº 113, de 27.10.89).
- Decreto 45/1994, de 4 marzo, de la DGA, de evaluación de impacto ambiental. BOA nº 35. (18-03-94)
- Corrección de errores del Decreto 45/1994, de 4 de marzo, de la Diputación General de Aragón, de evaluación de impacto ambiental.
- Ley 6/1998, de 19 de mayo, de Espacios Naturales Protegidos de Aragón.
- Decreto 45/2003, de 25 de febrero, del Gobierno de Aragón, por el que se establece un régimen de protección para el quebrantahuesos y se aprueba el Plan de Recuperación.

- Orden de 4 de marzo de 2004, del Departamento de Medio Ambiente, por la que se incluyen en el Catálogo de Especies Amenazadas de Aragón determinadas especies, subespecies y poblaciones de flora y fauna y cambian de categoría y se excluyen otras especies ya incluidas en el mismo.
- Decreto 49/1995, de 28 de marzo, de la Diputación general de Aragón, por el que se regula el Catálogo Especies Amenazadas, modificado por el Decreto 181/2005, de 6 de septiembre.
- Ley 15/2006 de Montes de Aragón
- Decreto 58/2004, de 9 de marzo, del Gobierno de Aragón, por el que se aprueba el Catálogo de Montes de Utilidad Pública de la provincia de Zaragoza.
- Ley 3/1999, de 10 de marzo, del Patrimonio Cultural Aragonés.
- Orden de 26 de marzo 2008, del Departamento de Medio Ambiente, por la que se aprueba el Plan General de Pesca de Aragón (PGPA) para el año 2008
- Orden de 16 de agosto de 2005, del Departamento de Medio Ambiente, por la que se determinan las zonas de alto riesgo de incendios forestales y se establece el régimen de tránsito de personas por dichas zonas.
- Orden de 12 de mayo de 2005, del Departamento de Medio Ambiente, por la que se publica el Acuerdo de 26 de abril de 2005, del Gobierno de Aragón, por el que se establece, con carácter transitorio, el procedimiento y contenido de los Planes Integrales.
- Ley 7/2006, de 22 de junio, de protección ambiental de Aragón.



- Corrección de errores de la Ley 7/2006, de 22 de junio, de protección ambiental de Aragón.
- Acuerdo de 11 de enero de 2005, del gobierno de Aragón, por el que se aprueba el Plan de Gestión Integral de los Residuos de la Comunidad Autónoma de Aragón (2005-2008).
- Ley 10/2005, de 11 de noviembre, de vías pecuarias de Aragón.
- Ley 12/1997, de 3 de diciembre, de Parques Culturales de Aragón.

### 10.3 ANALYSIS OF PROTECTED AREAS RELATED TO THE LOCATION

The location analysis in relation with the natural protected areas that could be affected by the LAGUNA experiment, will describe those protected areas in the Canfranc site surroundings. The extent of the protection is different according to the category and law issues. In the LAGUNA Project at Canfranc, the protected areas related in next paragraph may be affected. Plans that accompany this Feasibility Study show the position of tunnels and MDC's in relation with these areas.

#### 10.3.1 Areas protected by European Law

First, it is to be considered, those environmental aspects with specific European legal regulations. They have an EU foundation, and the objective is the protection of the very large number of areas of environmental interest that Europe has, and which are structured, European-wise, in the so-called Natura 2000 network.

- Directive 92/43/EEC of 21 May 1992 on the conservation of natural habitats and of wild fauna and flora.

- Council Directive 79/409/EEC of 2 April 1979 on the conservation of wild birds.

Natura 2000 Network is the centrepiece of EU nature & biodiversity policy. It is an EU-wide network of nature protection areas established under the Directive 92/43 (1992) on the conservation of natural habitats and of wild fauna and flora (so called Habitats Directive) and the Directive 79/409 (1979 on the conservation of wild birds (so called Birds Directive). The aim of the network is to ensure the long-term survival of Europe's most valuable and threatened species and habitats. It is comprised of Special Areas of Conservation (SAC) designated by Member States under the Habitats Directive, and also incorporates Special Protection Areas (SPA) which they designate under Birds Directive. Natura 2000 is not a system of strict nature reserves where all human activities are excluded. Whereas the network will certainly include nature reserves most of the land is likely to continue to be privately owned and the emphasis will be on ensuring that future management is sustainable, ecologically, socially and economically.

The Habitats Directive 92/43/CEE defines as well the so called Sites of Community Importance (SCIs) as those sites that have been adopted by the European Commission but not yet formally designated by the government of each country.

Formally, Directive 92/43/CEE is implemented in Spain thorough the "Law 42/2007, of December 13<sup>th</sup>, of Natural Heritage and Biological Diversity". Due to its recentness most of the foreseen special areas of conservation are at the SCI stage.

No SCI covers the current proposed location of the LAGUNA site at the LSC, nor its auxiliary galleries system.

Nevertheless, the LAGUNA site is underneath a SPA (named "Los Valles"), and although it doesn't strictly affect the SPA, an auxiliary element such as the ventilation gallery and shaft is foreseen to reach the surface in the area of the SPA.

The following SCI's are also close to, but outside of the LSC site and of any reasonable location for LAGUNA and its auxiliary galleries system. See Plans for detailed information.

- SCI ES2410003 "Los Valles"
- SCI ES2410023 "Collarada y Canal de Ip"
- SCI ES2410002 "Pico y turberas de Anayet" (outside map coverage)

As already mentioned, there is one SPA covering the underground part of the existing LSC and the possible location for LAGUNA site. As the LAGUNA Project develops mostly underground facilities, they will not affect directly the SPA. The location of the entrance to the proposed construction tunnel is well outside this SPA. But, a ventilation gallery and shaft, is foreseen to reach the surface in the area of the SPA, specifically in the "Rioseta Campsite". The ventilation system will take advantage of this shaft. See the map "Map of Natural Protected Areas".

- SPA ES0000137 "Los Valles"

There is another SPA close by, but well outside of the LSC and LAGUNA site location.

- SPA ES0000277 "Collarada-Ibón de Ip"

### 10.3.2 Areas protected by Regional Law

At a regional level (that is, the one for the Regional Autonomous Government of Aragón) two issues have been taken into account: Endangered Species and Natural protected areas (at a regional level), so called "Natural Parks".

There is one endangered specie of fauna in the area: the Quebrantahuesos (bearded vulture or lammergeyer, *Gypaetus barbatus*). This bird belongs respec-

tively to the national and regional catalogues of threatened species, under the category of "in extinction danger". For this reason, according to the Regional Decree 45/2003, there is a special protection and a Recovery Plan for the "quebrantahuesos".

The LAGUNA project and its auxiliary galleries system intersects the area of conservation of this species (which occupies almost the whole Pyrenean Range), but as mentioned before, since the Project covers underground facilities, it should not affect the bearded vulture at all, at least during the operation of the project. However, protection measures should be taken during the construction.

Finally there is a regional protected area: The Natural Park "Los valles occidentales". It covers a similar area than the SCI Los Valles. Therefore it is outside and not affected by the LSC and LAGUNA sites. See also the map "Map of Natural Protected Areas".

### 10.3.3 Areas of Recommended Protection

#### 10.3.3.1 European level: Habitats Network

It is regulated in Spain by the Annex I of the Law 42/2007 of natural heritage and biodiversity, which transfers the Council Directive 92/43/EEC of 21 May 1992 on the conservation of natural habitats and of wild fauna and flora.

This law defines natural habitat types of community interest whose conservation requires the designation of special areas of conservation. Some of them have the category of "conservation priority" All these habitats are the basis on which the SACs and SCIs are defined. See map "Habitats' map" (the sign "\*" indicates conservation priority habitat types).

Since the LAGUNA Project comprises underground facilities, no habitat will be affected, except those at the entrance of the gallery system, and the way out to the surface of the ventilation galley and shaft.

There is another protection figure not subject to legal enforcement, but which is recommended to be considered, the so-called IBAs (Important Bird Areas) as defined by the reputed international organization Birdlife International (SEO Birdlife, the Sociedad Española de Ornitología is the Spanish branch). The only relevant IBA is well away from any entrance to the underground complex and therefore the impact of LAGUNA on it is negligible.

#### 10.4 MATERIALS ANALYSIS REGARDING THE DISPOSAL OF THE WASTE MATERIAL

One of the most important environmental aspects to be considered in the LAGUNA project is the production of waste material through the excavations of the MDC's.

The objective is to comply with the national legislation, Royal Decree 105/2008 regarding the production and management of waste (mainly rock) material coming from works and demolitions. The aim of this Decree is to first prevent the production of waste material, second to reuse, third to recycle and finally to put the material in a waste dump.

The LAGUNA project foresees three different alternative experiments; each of these will generate a different earthworks balance. A first approach of waste volumes may be the following one:

LAGUNA Experiment	WASTE MATERIAL (mainly rock) IN M <sup>3</sup>	REUSABLE AS AGGREGATE FOR CONCRETE
MEMPHYS	1.650.000 m <sup>3</sup>	Not considered
LENA	475.000 m <sup>3</sup>	Not considered
GLACIER	490.000 m <sup>3</sup>	75%

The table above shows how important the figures regarding the production of waste material (mainly rock) are. A difference has been emphasised between those MDC's to be excavated in Atixerito Formation and the GLACIER experiment MDC, which would be excavated in high quality limestones: this materials would be reusable as concrete aggregates. The percentage shown in the table has been considered only for informative purposes, since no specific tests have been carried for this characterization.

The regional government of Aragon, in order to solve the problem that waste material implies, and in order to align with national regulations, has recently approved the Integrated Management Plan for Waste in Aragón (Plan GIRA), whose main objective is to maximize the reuse of waste material, to coordinate the different existing works at the same time in a certain area, to plan the needs of material, and to optimize the management of waste material while respecting the environment.

Within this plan, the regional government is creating an "earth exchange" or market (list of reusable construction materials), that is, a list of places that can admit certain left over materials and even transform it, with its admissible volumes, running works than need material supply and so on.

At present, until this plan is not implemented, the procedure to seek a waste dump during construction works, is to ask the Regional Government for authorised landfills or waste dumps, which are economically feasible in terms of distances.

If the location at Canfranc is finally chosen to carry out the LAGUNA Project, the steps to undertake, regarding to the final disposal of material are as follows:

- 1<sup>st</sup>). If the regional government of Aragon has already established the above mentioned earth market, so that the regional Department of Environmental Quality has to be consulted in this matter, they will then direct on where and what to do with the waste material (e.g. take it to another loca-



tion where some construction works have material supply needs, or place it in some particular storage area, etc)

- 2<sup>nd</sup>). If this “bag of earths” does not yet exist, authorised waste dumps should be found out. Take notice that, nowadays, the only authorised waste dump than can accumulate over 300.000 m3 is in the area of Barbastro, quite far from Canfranc (about 130 km), which would make the project unfeasible from an economical standpoint.
- 3<sup>rd</sup>). If none of the two above mentioned alternatives are possible, a location for a new waste dump for rock material should be identified in the surrounding area of the project. It is most likely that an Environmental Impact Assessment (EIA) process will have to be carried out. At the current stage of the project (feasibility study), we can describe the criteria to select a new location. These criteria are:

Exclusion areas: no waste dump will be proposed in areas with:

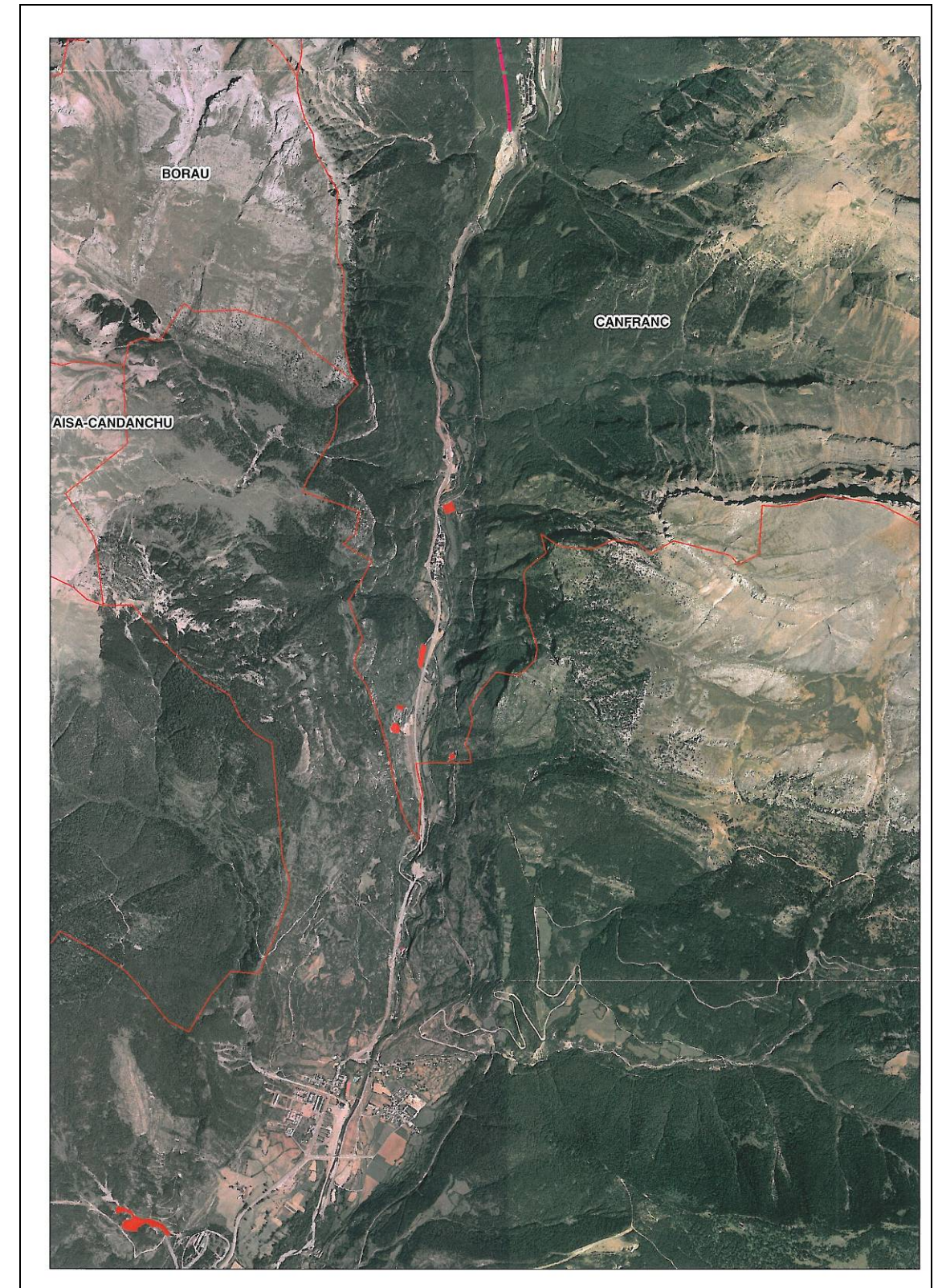
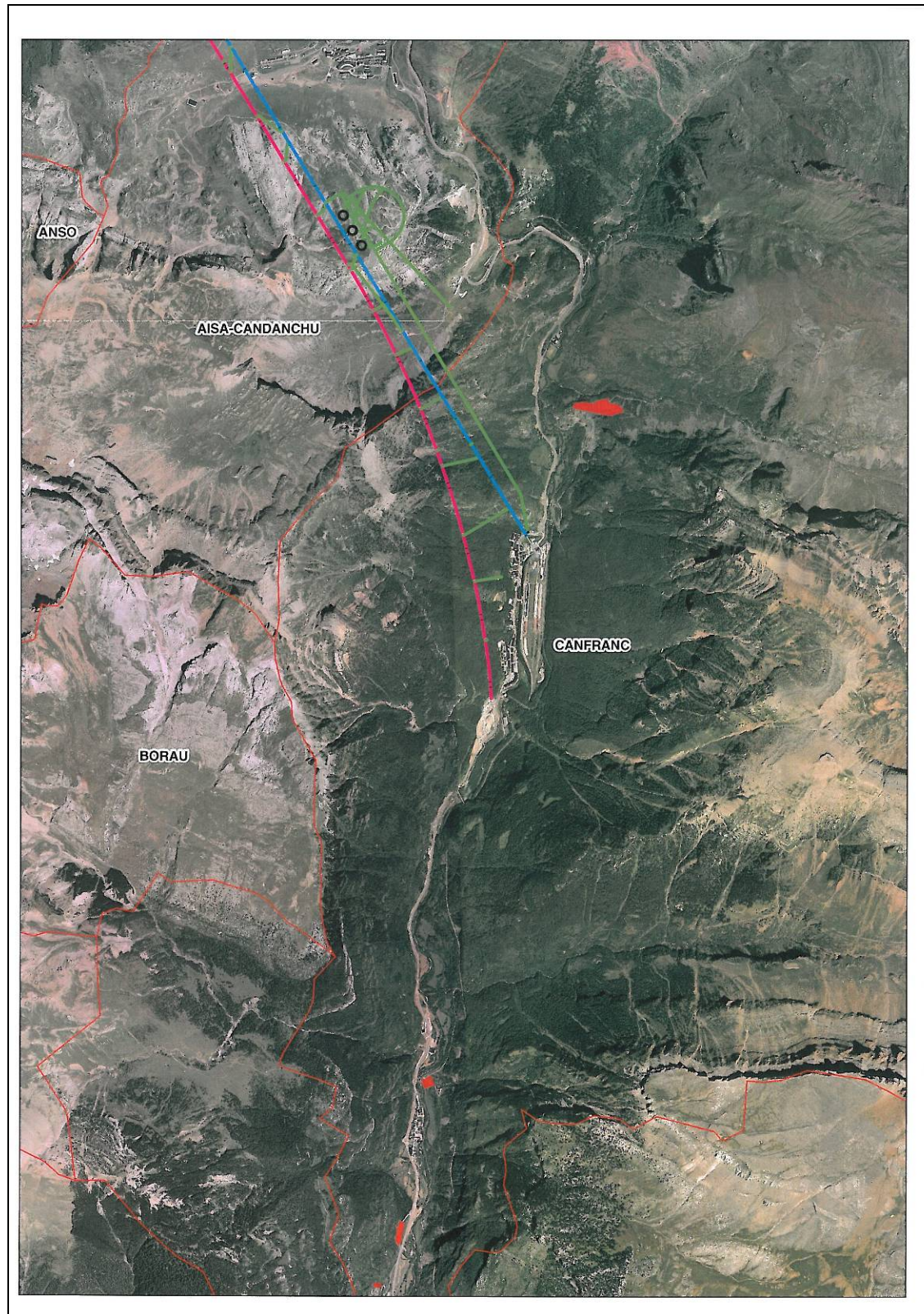
- Environmental protection
- Archaeological fields
- Water courses
- Fauna corridors
- Cattle tracks

Restricted areas: in these areas, environmental value is high and their fragility is intermediate. The waste material disposal can only be temporarily used until before this material is transported to the final disposal location.

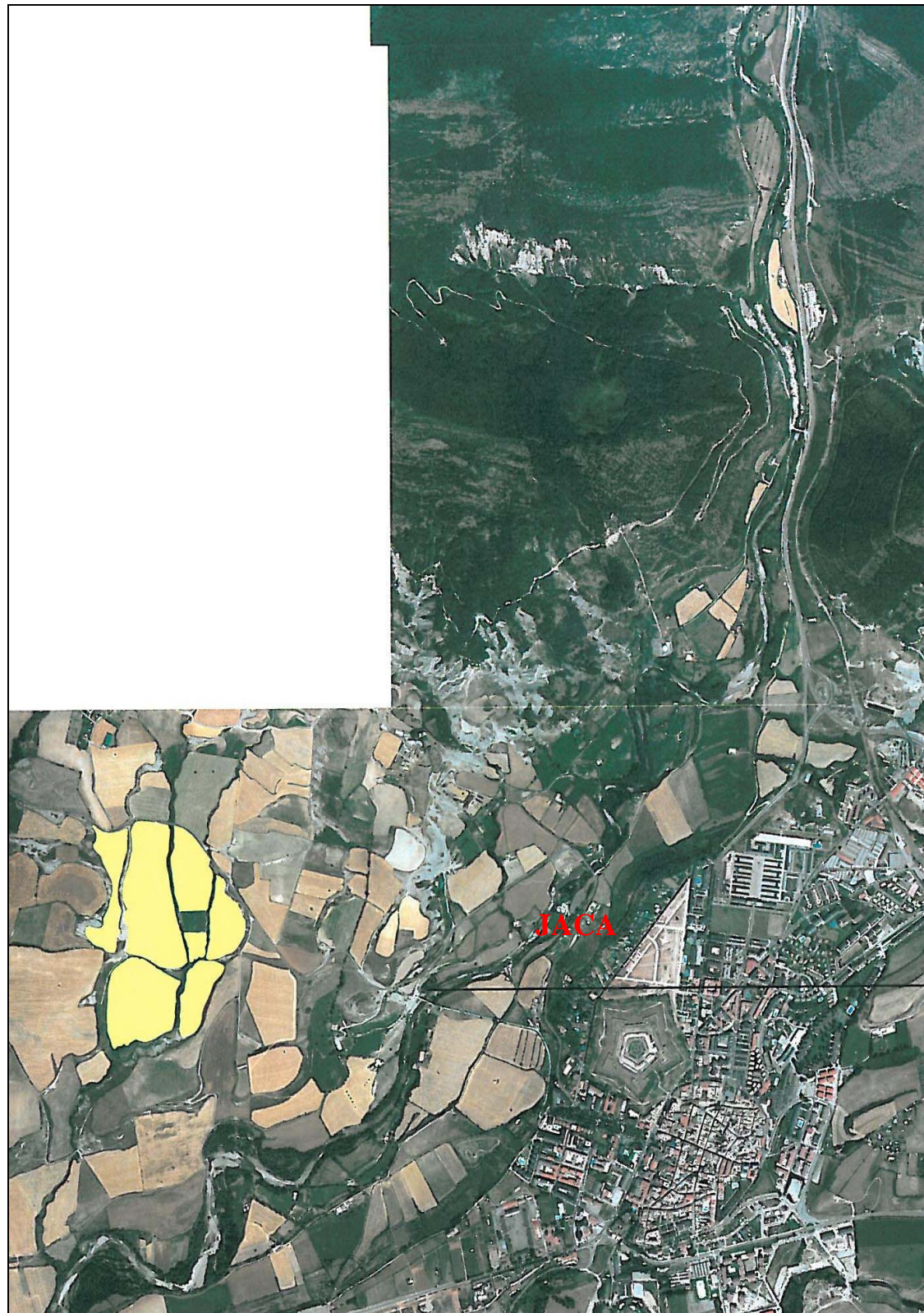
Admissible areas: are those areas with little environmental quality and low fragility, such as abandoned cultivation land, abandoned or almost exhausted quarries, degraded areas by human activity etc.

In the following aerial maps, from North to South, some possible admissible areas are identified (in red, admissible areas where a waste dump can be located). The main areas are located in the surroundings of Jaca, which is the main local municipality. They are 25 kilometers away from the site, so transport to this area will have an extra cost due to this distance.









## 10.5 THE ENVIRONMENTAL IMPACT ASSESSMENT PROCESS IN SPAIN

Among the different possibilities established by the Directive 85/337/EEC of 27 June 1985 on the assessment of the effects of certain public and private projects on the environment, the Spanish legislation has chosen the option of considering EIA as a procedural norm, integrated in the framework of the basic authorizing procedure.

As a procedural norm, a clear distinction is made between Environmental body (responsible for the EIA procedure and the Impact Assessment Declaration) and the Administrative or Authorizing body (responsible for giving the final authorization to the project, taking into consideration the Impact Assessment Declaration).

If the LAGUNA project is finally developed in the Spanish location of Canfranc it's most likely that the project will have to go under an Environmental Impact Assessment procedure (EIA).

To know if a certain project needs to go under a EIA, the State and Autonomous legislation have annexes in which different types of projects are listed. In case of doubt, a consultation to the environmental authority has to be done. In our case, even not knowing which of the three alternative experiments will be finally chosen, there are two aspects that make us think that is most likely that the LAGUNA project will have to go under the EIA as:

- The project may affect some areas included in the Natura 2000 Network
- The construction of any of the three alternative experiments implies the excavation and generation of more than 200.000 m<sup>3</sup> of waste material.

The procedural phases have been grouped as follows:



- A. Initiation and Consultation
- B. Environmental Impact Study
- C. Public Information and Participation
- D. Environmental Impact Declaration (EID) -Environmental Impact Statement-
- E. Project Approval -Authorisation-

An approach to the contents of the Environmental Impact Study might be as follows:

#### Description of the project

- Description of actual project and site description.
- Description of key components, i.e. construction, operations, decommissioning.
- Description of land occupation and natural resources that may be affected.
- For each component list all the sources of environmental disturbance.
- For each component all the inputs and outputs must be listed, e.g., air pollution, noise, hydrology, etc.

#### 2. Alternatives that have been considered

- Examine alternatives that have been considered

#### 3. Description of the environment

- List of all aspects of the environment that may be effected by the development.
- Example: populations, fauna, flora, air, soil, water, humans, landscape, cultural heritage, etc.

This section is best carried out with the help of local experts.

#### 4. Identification and appraisal of the significant impacts on the environment

The word significant is crucial here as the definition can vary. 'Significant' needs to be defined.

- The most frequent method used here is use of the Leopold matrix
- The matrix is a tool used in the systematic examination of potential interactions.
- The impacts can be classified under the following categories: compatible, moderate, severe and critical.

#### 5. Mitigation

This is where EIA is most useful

- Once section 4 has been completed it will be obvious where the impacts will more considerable.
- Using this information, different ways to avoid negative impacts should be developed.
- Protection, mitigation and compensation measures will be defined to be developed in detail within the construction design phase of the project.

## 6. Environmental monitoring Program (\*)

- A program will be defined in order to establish a monitoring system to check the proper execution of the measures under section 4 during the project construction phase.
- The monitoring system will also check the evolution of certain environmental parameters during and after the construction phase.

## 7. Non-technical summary (EIS)

- The EIA will be in the public domain and be used in the decision making process
- It is important that the information is available to the public
- This section is a summary that does not include jargon or complicated diagrams
- It should be understood by the informed lay-person

(\*) Once the procedure is finished, it will necessary to establish monitor mechanisms to guarantee compliance of the environmental conditions which have been imposed. The idea is for the approved activity to be carried out, to observe whether the environmental protection measures included are effective, and to verify the correction of the EIA which was carried out.

## 10.6 ENVIRONMENTAL MONITORING PLAN

A very important document to elaborate in next stages of the project, and that it would be applied in the potential construction phase of the LAGUNA project at Canfranc is the Environmental Monitoring Plan. This Plan can be within the Environmental Impact Study or as an independent document, depending on the obligation or not to develop an Environmental Impact Study.

The Environmental Monitoring Plan details and describes the control and follow-up to be done during construction and operation phases. Its objective is to guaranty the fulfilment of the envisaged measures to prevent, reduce or offset the project effects on environment. Its cost has to be included in the project's budget. An approach of the content f the Environmental Monitoring Plan is as it follows:

1) Introduction

2) General objectives

3) Indicative parameters for monitoring

### 3.1.- General considerations

### 3.2.- Monitoring of predicted impacts

a) Air and noise quality

An example of a follow-up table is described next. There should be as many tables as necessary to monitor road design and construction for every feature considered.

OBJECTIVE: Emissions of pollutants into the atmosphere	
Actions for control	Visual monitoring

OBJETIVE: Emissions of pollutants into the atmosphere	
Location of control	Along the road, construction camps, quarries, access to construction ,etc.
Time of control	Construction phase
Periodicity of control	Weekly
Necessary material for control	None
Parameters of control	Local atmospheric conditions
Limits	Those indicated by law. Alteration of population comfort.
Measures	Increase of regular measures already applied during construction (e.g. construction tracks watering,, control of construction machinery etc.)
Reporting	Register

- b) Soil conservation
- c) Water quality and public health
- d) Flora and fauna
- e) Landscaping
- f) Sanitation and waste disposal
- g) Cultural heritage
- h) Communities and their economic activity
- i) Land acquisition and resettlement

### 3.3.- Follow-up of prevention, mitigation and compensating measures during construction and operational phase.

There should be as many tables as necessary to monitor road design and construction for every feature considered, such as the ones related in the previous paragraph: air and noise quality, soil conservation, water quality and public health, flora and fauna, landscaping, sanitation and waste disposal, cultural heritage, communities and their economic activity, or land acquisition and resettlement.

### 3.4.- Reporting

- a) Previous phase
- b) Construction phase
- c) Operational phase

## 10.7 CONCLUSIONS

Taking into account that this is the Feasibility Study stage, this is a first approach to the main environmental issues, and in subsequent stages deeper studies should be carried out.

The LAGUNA project is to be implemented in an area of high environmental quality, but as we are mainly dealing with underground facilities, not very important impacts are foreseen. Besides, there is no much difference from an environmental viewpoint among the three proposed alternatives regarding the occupation of natural protected areas.

As far as the generation of waste material is concerned, and due to the excavation of the detection caverns, there are big differences among the alternatives. The prediction of earthworks balance for the MEMPHYS experiment is 3,77 times more



than the LENA experiment, and 3,64 times more than in the GLACIER experiment. There is no much difference between the LENA and GLACIER experiments, apart from the possibility of reusing 75% of the material in the GLACIER experiment, since limestone rocks would be excavated at that site.

Depending on the final location of the surplus material an Environmental Impact Assessment process will have to take place.

If the environmental body considers that the LAGUNA Project might affect the Natural 2000 network, an environmental Impact Assessment process will have to take place.

## 11. COST ESTIMATES

Cost estimation for each cavern has been divided into four main sections:

- Main Detector Cavern excavation and support.
- Access galleries, auxiliary caverns and ventilation facilities excavations and support.
- Installations: construction installations, underground installations and surface installations.
- Environmental measures.

Transport of muck to Jaca dump areas has been considered. The distance is 25 km, so rock removal cost must be increased in transport costs.

The costs of cavern design, and professional association fees for Project approval, additional rock exploration, health and safety measures to be taken during the works, and some cavern monitoring have been also taken in mind. The sum of the four main sections and the ones that have been mentioned in this paragraph has been taken as the construction cost.

Finally, Spanish civil works costs are charged with two different percentages: 13% overhead expenses and 6% industrial profit. This goes with the contractor budget. The VA tax is 16%.

No tank assembly costs have been considered at this stage of work, and can be added once the structure is roughly defined. Other particular elements such as PMT's or operational electronics cannot be evaluated in this phase.

## 11.1 MEMPHYS

The three MDC's have been measured when evaluating the cost. The result is separated into three concepts, including surveying of different units, partial costs and final budget:

Unit	Nº	Price definition	Survey
M3	100,001	Vault excavation Excavación en bóveda de caverna Three MDC's	111.999,00
M3	100,002	Main cavern excavation Excavación del cilindro de la caverna en destrozado Three MDC's	757.601,52
MI	100,003	Raise boring excavation for shafts ( $\phi=5,70$ ) Excavación del raise boring ( $\phi=5,70$ ) Three MDC's Ventilation shaft Connection shaft	198,00 220,77 134,69
MI	100,004	Lower and intermediate gallery excavation and support Excavación y sostenimiento de galerías perimetrales Three MDC's lower galleries Three MDC's intermediate galleries	688,01 439,19
MI	100,005	Rib excavation and support Excavación y sostenimiento de costillas Three MDC's	967,80
M3	100,006	Upper cavern excavation and support Excavación y sostenimiento de la caverna superior Three MDC's	915,41
U	100,007	Tunnel portal excavation and support Excavación y sostenimiento de la boquilla Canfranc Site	1,00
MI	100,008	Access gallery AG1 excavation and support (50% Type I, 40% Type II) Excavación y sostenimiento galería AG1 (50%-40%-10%) General Access Connection gallery at level 1073 Ramps between upper chamber and lower level Ventilation gallery Exit to connection shaft Upper access galleries to the three MDC's Access to different AC's	2.349,33 419,50 1.842,48 1.188,12 124,62 165,00 68,00
MI	100,009	Access gallery AG2 excavation and support (50% Type I, 40% Type II) Excavación y sostenimiento galería AG2 (50%-40%-10%) Access to main control and office	7,00
MI	100,010	Auxiliary cavern AC1 excavation and support (70% Type II and 30% Type I) Excavación y sostenimiento caverna AC1 (70%-30%) Clean Storage and Power Transformation cavern Main Control and office cavern Connection chambers	50,00 12,00 50,00
MI	100,011	Auxiliary cavern AC2 excavation and support (70% Type II and 30% Type I) Excavación y sostenimiento caverna AC2 (70%-30%) Water and air purification caverns for three MDC's	150,00
U	100,012	Widening of existing tunnels Obras locales de ensanche del túnel Widening for shaft excavation	1,00

Unit	Nº	Price definition	Survey
m3	200,001	Steel fiber reinforced concrete for vault Gunita en bóveda de caverna Three MDC's	5.606,09
m3	200,002	Steel fiber reinforced concrete for cavern walls Gunita en paredes de caverna Three MDC's	15.701,68
U	200,003	Cable bolt 7 cables L=18 meters for vault support Anclajes en bóveda de caverna Three MDC's	3.398,00
U	200,004	Cable bolt 7 cables L=18 meters for wall support Anclajes en paredes de caverna Three MDC's	10.734,00
U	200,005	Rebar bolt L=6 meters for vault support Bulones en bóveda de caverna Three MDC's	3.398,00
U	200,006	Rebar bolt L=6 meters for cavern support Bulones en bóveda de caverna Three MDC's	10.734,00
M3	200,007	Plain concrete 20 Mpa with steel fiber for MDC's, galleries and AC's Hormigón HM20 c/fibra en losas de túnel o caverna MDC's Access galleries AG1 Access galleries AG2 Ventilation gallery AG1 Auxiliary caverns AC1 Auxiliary caverns AC2	4.358,02 4.472,03 4,20 1.069,31 168,00 225,00
M3	200,008	Plain concrete 30 Mpa with steel fiber for cavern walls and vaults HM30 c/fibra encofrado en bovedas de cavernas auxiliares Cavernas AC1 Cavernas AC2	376,54 1.360,98
M3	200,009	Plain concrete 50 Mpa for support gallery fill Hormigones de relleno de galerías perimetrales y costillas Lower gallery Intermediate gallery Upper cavern Ribs	17.076,38 10.900,81 915,41 9.910,27



Unit	Nº	Price definition	Survey
U	300,001	Drinking water installation for construction	1,00
U	300,002	Fire installations for construction	1,00
U	300,003	Ventilation for construction	1,00
U	300,004	Electric installation for construction	1,00
U	300,101	Water installations for experiment operation	1,00
U	300,102	Drinking water for undergorund facilities	1,00
U	300,103	Sewage utilities for underground installations	1,00
U	300,104	Fire protection for underground caverns and installations	1,00
U	300,105	HVAC installations for underground caverns and installations	1,00
U	300,106	Ventilation installations for underground caverns	1,00
U	300,107	Electrical installations for underground caverns	1,00
U	300,108	Elevator and stairs for emergency shaft	1,00
U	300,201	Drinking water for surface installations	1,00
U	300,202	Sewage utilities for underground installations	1,00
U	300,203	Fire protection surface installations	1,00
U	300,204	HVAC for surface installations	1,00
U	300,205	Electric installations	1,00
U	300,206	Access control building	1,00
M3	400,001	Transport of excavation muck to tunnel portal Transporte a vertedero, medido desde la boca del túnel MDC's excavation 1.217.440,73 Raise boring excavations 19.772,15 Lower and intermediate gallery excavations 39.168,07 Rib excavations 13.874,38 Upper cavern excavations 1.281,58 Access galleries AG1 and AG2 265.465,63 Auxiliary caverns AC1 and AC2 26.714,18 Ventilation gallery AC1 63.441,04	
M3	400,002	Transport of excavation muck to authorized dump area to 25 km	41.178.943,74
Km	400,003	Environmental arrangement of waste and dump areas	1,00
U	400,004	Environmental supervision for civil works	1,00

PRICE Nº	DEFINITION	Unit	Quantity	Unit price	TOTAL (€)
<b>CHAPTER 1.- MDC EXCAVATION</b>					
<b>1.1 MDC EXCAVATION</b>					
100,001	Vault excavation	M3	111.999,00	97,20 €	10.886.302,80 €
100,002	Main cavern excavation	M3	757.601,52	42,30 €	32.046.544,21 €
100,003	Raise boring excavation for shafts (f=5,70)	MI	198,00	3.375,00 €	668.250,00 €
100,004	Lower and intermediate gallery excavation and support	MI	1.127,20	3.870,00 €	4.362.277,33 €
100,005	Rib excavation and support	MI	967,80	6.580,80 €	6.368.898,24 €
100,006	Upper cavern excavation and support	M3	915,41	135,00 €	123.580,56 €
400,001	Transport of excavation muck to tunnel portal	M3	1.291.536,90	1,25 €	1.614.421,12 €
400,002	Transport of excavation muck to authorized dump area to 25 km	M3	32.288.422,40	0,45 €	14.529.790,08 €
<b>PARTIAL</b>					<b>70.600.064,33 €</b>
<b>1,2 MDC SUPPORT</b>					
200,001	Steel fiber reinforced concrete for vault	M3	5.606,09	315,00 €	1.765.919,47 €
200,002	Steel fiber reinforced concrete for cavern walls	M3	15.701,68	300,00 €	4.710.504,02 €
200,003	Cable bolt 7 cables L=18 meters for vault support	U	3.398,00	2.079,00 €	7.064.442,00 €
200,004	Cable bolt 7 cables L=18 meters for wall support	U	10.734,00	1.728,00 €	18.548.352,00 €
200,005	Rebar bolt L=6 meters for vault support	U	3.398,00	162,00 €	550.476,00 €
200,006	Rebar bolt L=6 meters for cavern support	U	10.734,00	135,00 €	1.449.090,00 €
200,007	Plain concrete 20 Mpa with steel fiber for MDC's, galleries and AC's slabs	M3	4.358,02	132,00 €	575.258,29 €
200,009	Plain concrete 50 Mpa for support gallery fill	M3	28.892,60	188,00 €	5.431.808,99 €
<b>PARTIAL</b>					<b>40.095.850,77 €</b>
<b>PARTIAL CHAPTER 1 (euros)</b>					<b>110.695.915,10</b>

PRICE Nº	DEFINITION	Unit	Quantity	Unit price	TOTAL (€)
<b>CHAPTER 2.- ACCESS GALLERIES AND CAVERN EXCAVATIONS AND SUPPORT</b>					
<b>2,1 ACCESS GALLERIES</b>					
100,003	Raise boring excavation for shafts (f=5,70)	MI	134,69	3.375,00 €	454.578,75 €
100,007	Tunnel portal excavation and support	U	1,00	60.000,00 €	60.000,00 €
100,008	Access gallery AG1 excavation and support (50% Type I, 40% Type II and 10% Type III)	MI	4.968,92	4.732,00 €	23.512.941,74 €
100,009	Access gallery AG2 excavation and support (50% Type I, 40% Type II and 10% Type III)	MI	7,00	3.198,00 €	22.386,00 €
200,007	Plain concrete 20 Mpa with steel fiber for MDC's, galleries and AC's slabs	M3	4.476,23	132,00 €	590.862,40 €
400,001	Transport of excavation muck to tunnel portal	M3	265.465,63	1,25 €	331.832,04 €
400,002	Transport of excavation muck to authorized dump area to 25 km	M3	6.636.640,78	0,45 €	2.986.488,35 €
<b>PARTIAL</b>					<b>27.959.089,29</b>
<b>2,2 AUXILIARY CAVERNS</b>					
100,010	Auxiliary cavern AC1 excavation and support (70% Type II and 30% Type III)	MI	112,00	7.558,00 €	846.496,00 €
100,011	Auxiliary cavern AC2 excavation and support (70% Type II and 30% Type III)	MI	150,00	9.471,00 €	1.420.650,00 €
100,012	Widening of existing tunnels	U	1,00	35.000,00 €	35.000,00 €
200,007	Plain concrete 20 Mpa with steel fiber for MDC's, galleries and AC's slabs	M3	393,00	132,00 €	51.876,00 €
200,008	Plain concrete 30 Mpa with steel fiber for cavern walls and vaults	M3	1.737,52	160,00 €	278.002,94 €
400,001	Transport of excavation muck to tunnel portal	M3	26.714,18	1,25 €	33.392,73 €
400,002	Transport of excavation muck to authorized dump area to 25 km	M3	667.854,60	0,45 €	300.534,57 €
<b>PARTIAL</b>					<b>2.965.952,24 €</b>
<b>2,3 VENTILATION GALLERY AND SHAFT</b>					
100,003	Raise boring excavation for shafts (f=5,70)	MI	220,77	3.375,00 €	745.098,75 €
100,008	Access gallery AG1 excavation and support (50% Type I, 40% Type II and 10% Type III)	MI	1188,12	4.732,00 €	5.622.200,07 €
200,007	Plain concrete 20 Mpa with steel fiber for MDC's, galleries and AC's slabs	M3	1069,31	132,00 €	141.149,06 €
400,001	Transport of excavation muck to tunnel portal	M3	63441,04	1,25 €	79.301,30 €
400,002	Transport of excavation muck to authorized dump area to 25 km	M3	1586025,97	0,45 €	713.711,69 €
<b>PARTIAL</b>					<b>7.301.460,87</b>
<b>PARTIAL CHAPTER 2 (euros)</b>					<b>38.226.502,40</b>
<b>TOTAL CHAPTER 1+2 (euros)</b>					<b>148.922.417,50</b>



PRICE Nº	DEFINITION	Unit	Quantity	Unit price	TOTAL (€)
<b>CHAPTER 3.- INSTALLATIONS</b>					
<b>2,1 CONSTRUCTION INSTALLATIONS</b>					
300,001	Drinking water installation for construction	U	1,00	50.000,00 €	50.000,00 €
300,002	Fire installations for construction	U	1,00	20.000,00 €	20.000,00 €
300,003	Ventilation for construction	U	1,00	213.750,00 €	213.750,00 €
300,004	Electric installation for construction	U	1,00	358.000,00 €	358.000,00 €
<b>PARTIAL</b>					<b>641.750,00</b>
<b>2,2 UNDERGROUND INSTALLATIONS</b>					
300,101	Water installations for experiment operation	U	1,00	1.689.000,00 €	1.689.000,00 €
300,102	Drinking water for underground facilities	U	1,00	220.150,00 €	220.150,00 €
300,103	Sewage utilities for underground installations	U	1,00	18.700,00 €	18.700,00 €
300,104	Fire protection for underground caverns and installations	U	1,00	640.920,00 €	640.920,00 €
300,105	HVAC installations for underground caverns and installations	U	1,00	245.650,00 €	245.650,00 €
300,106	Ventilation installations for underground caverns	U	1,00	1.436.000,00 €	1.436.000,00 €
300,107	Electrical installations for underground caverns	U	1,00	5.417.000,00 €	5.417.000,00 €
300,108	Elevator and stairs for emergency shaft	U	1,00	326.000,00 €	326.000,00 €
<b>PARTIAL</b>					<b>9.993.420,00 €</b>
<b>2,3 SURFACE INSTALLATIONS</b>					
300,201	Drinking water for surface installations	U	1,00	27.100,00 €	27.100,00 €
300,202	Sewage utilities for underground installations	U	1,00	14.700,00 €	14.700,00 €
300,203	Fire protection surface installations	U	1,00	14.100,00 €	14.100,00 €
300,204	HVAC for surface installations	U	1,00	5.750,00 €	5.750,00 €
300,205	Electric installations	U	1,00	40.000,00 €	40.000,00 €
300,206	Access control building	U	1,00	150.000,00 €	150.000,00 €
<b>PARTIAL</b>					<b>251.650,00</b>
<b>PARTIAL CHAPTER 3 (euros)</b>					<b>10.886.820,00</b>

PRICE Nº	DEFINITION	Unit	Quantity	Unit price	TOTAL (€)
<b>CHAPTER 4.- ENVIRONMENTAL MANAGEMENT</b>					
<b>4,1 ENVIRONMENTAL MANAGEMENT</b>					
400,003	Environmental arrangement of waste and dump areas	U	1,00	200.000,00 €	200.000,00 €
400,004	Environmental supervision for civil works	U	1,00	500.000,00 €	500.000,00 €
<b>PARTIAL</b>					<b>700.000,00</b>
<b>PARTIAL CHAPTER 4 (euros)</b>					<b>700.000,00</b>

<b>CHAPTER 1.- MDC EXCAVATION</b>	
1.1 MDC EXCAVATION	70.600.064,33 €
1,2 MDC SUPPORT	40.095.850,77 €
<b>PARTIAL CHAPTER 1 (euros)</b>	<b>110.695.915,10 €</b>
<b>CHAPTER 2.- ACCESS GALLERIES AND CAVERN EXCAVATIONS AND SUPPORT</b>	
2,1 ACCESS GALLERIES	27.959.089,29 €
2,2 AUXILIARY CAVERNS	2.965.952,24 €
2,3 VENTILATION GALLERY AND SHAFT	7.301.460,87 €
<b>PARTIAL CHAPTER 2 (euros)</b>	<b>38.226.502,40 €</b>
<b>CHAPTER 3.- INSTALLATIONS</b>	
2,1 CONSTRUCTION INSTALLATIONS	641.750,00 €
2,2 UNDEGROUND INSTALLATIONS	9.993.420,00 €
2,3 SURFACE INSTALLATIONS	251.650,00 €
<b>PARTIAL CHAPTER 3 (euros)</b>	<b>10.886.820,00 €</b>
<b>CHAPTER 4.- ENVIRONMENTAL MANAGEMENT</b>	
4,1 ENVIRONMENTAL MANAGEMENT	700.000,00 €
<b>PARTIAL CHAPTER 4 (euros)</b>	<b>700.000,00 €</b>
<b>CHAPTERS 1 TO 4 (euros)</b>	<b>160.509.237,50 €</b>
<b>HEALTH AND SAFETY</b>	<b>2.407.639,00 €</b>
<b>UNDERGROUND MONITORING</b>	<b>481.528,00 €</b>
<b>FURTHER SUBSOIL EXPLORATION</b>	<b>1.029.354,00 €</b>
<b>DETAILED DESIGN AND PROFESSIONAL ASSOCIATION FEES</b>	<b>2.639.910,76 €</b>
<b>TOTAL CONSTRUCTION COST</b>	<b>167.067.669,26 €</b>
<b>13% OVERHEAD EXPENSES</b>	<b>21.718.797,00 €</b>
<b>6% INDUSTRIAL PROFIT</b>	<b>10.024.060,16 €</b>
<b>TOTAL CONTRACTOR BUDGET</b>	<b>198.810.526,42 €</b>
<b>16% VAT</b>	<b>31.809.684,23 €</b>
<b>TOTAL TENDER COST</b>	<b>230.620.210,65 €</b>



## 11.2 LENA

The result is the one shown in the following table, with similar independent parts:

Unit	Nº	Price definition	Survey
M3	100,001	Vault excavation Excavación en bóveda de caverna MDC	9.050,03
M3	100,002	Main cavern excavation Excavación del cilindro de la caverna en destroza MDC	95.331,63
MI	100,003	Raise boring excavation for shafts ( $\phi=5,70$ ) Excavación del raise boring ( $\phi=5,70$ ) MDC Ventilation shaft Connection shaft	98,00 223,77 137,69
MI	100,004	Upper gallery excavation and support Excavación y sostenimiento de galerías perimetrales MDC upper gallery	47,12
MI	100,005	Rib excavation and support Excavación y sostenimiento de costillas MDC	0,00
M3	100,006	Upper cavern excavation and support Excavación y sostenimiento de la caverna superior MDC	0,00
U	100,007	Tunnel portal excavation and support Excavación y sostenimiento de la boquilla Canfranc Site	1,00
MI	100,008	Access gallery AG1 excavation and support (50% Type I, 40% Type II Excavación y sostenimiento galería AG1 (50%-40%-10%) General Access Connection gallery at level 1070 Ramp between upper chamber and lower level Ventilation gallery Exit to connection shaft Upper access galleries to the MDC Access to different AC's	2.514,34 277,98 1.279,86 1.188,12 126,50 48,00 51,00
MI	100,009	Access gallery AG2 excavation and support (50% Type I, 40% Type II Excavación y sostenimiento galería AG2 (50%-40%-10%) Access to main control and office	17,00
MI	100,010	Auxiliary cavern AC1 excavation and support (70% Type II and 30% Excavación y sostenimiento caverna AC1 (70%-30%) Clean Storage Electronics, low background lab, main control and office cavern Clean room and liquid and gas handling Connection chambers	20,00 42,00 70,00 50,00
MI	100,011	Auxiliary cavern AC2 excavation and support (70% Type II and 30% Excavación y sostenimiento caverna AC2 (70%-30%) Water urification cavern for MDC	21,00
U	100,012	Widening of existing tunnels Obras locales de ensanche del túnel Widening for shaft excavation	1,00

Unit	Nº	Price definition	Survey
m3	200,001	Steel fiber reinforced concrete for vault Gunita en bóveda de caverna MDC	605,31
m3	200,002	Steel fiber reinforced concrete for cavern walls Gunita en paredes de caverna MDC	3.925,42
U	200,003	Cable bolt 7 cables L=18 meters for vault support Anclajes en bóveda de caverna MDC	128,00
U	200,004	Cable bolt 7 cables L=22 meters for wall support Anclajes en paredes de caverna MDC	2.803,00
U	200,005	Rebar bolt L=6 meters for vault support Bulones en bóveda de caverna MDC	432,00
U	200,006	Rebar bolt L=6 meters for wall support Bulones en bóveda de caverna MDC	2.803,00
M3	200,007	Plain concrete 20 Mpa with steel fiber for MDC's, galleries and AC's Hormigón HM20 c/fibra en losas de túnel o caverna MDC's Access galleries AG1 Access galleries AG2 Ventilation gallery AG1 Auxiliary caverns AC1 Auxiliary caverns AC2	363,17 3.867,92 10,20 1.069,31 273,00 31,50
M3	200,008	Plain concrete 30 Mpa with steel fiber for cavern walls and vaults HM30 c/fibra encofrado en bovedas de cavernas auxiliares Cavernas AC1 Cavernas AC2	801,66 190,54
M3	200,009	Plain concrete 50 Mpa for support gallery fill Hormigones de relleno de galerías perimetrales y costillas Lower gallery	1.169,61

Unit	Nº	Price definition	Survey
U	300,001	Drinking water installation for construction	1,00
U	300,002	Fire installations for construction	1,00
U	300,003	Ventilation for construction	1,00
U	300,004	Electric installation for construction	1,00
U	300,101	Water installations for experiment operation	1,00
U	300,102	Drinking water for underground facilities	1,00
U	300,103	Sewage utilities for underground installations	1,00
U	300,104	Fire protection for underground caverns and installations	1,00
U	300,105	HVAC installations for underground caverns and installations	1,00
U	300,106	Ventilation installations for underground caverns	1,00
U	300,107	Electrical installations for underground caverns	1,00
U	300,108	Elevator and stairs for emergency shaft	
U	300,109	Nitrogen installation	1,00
U	300,110	Scintillator installation	1,00
U	300,201	Drinking water for surface installations	1,00
U	300,202	Sewage utilities for underground installations	1,00
U	300,203	Fire protection surface installations	1,00
U	300,204	HVAC for surface installations	1,00
U	300,205	Electric installations	1,00
U	300,206	Access control building	1,00
M3	400,001	Transport of excavation muck to tunnel portal Transporte a vertedero, medido desde la boca del túnel MDC's excavation Raise boring excavations Lower and intermediate gallery excavations Rib excavations Upper cavern excavations Access galleries AG1 and AG2 Auxiliary caverns AC1 and AC2 Ventilation gallery AC1	146.134,32 16.414,03 494,80 0,00 0,00 229.831,46 18.032,20 63.441,04
M3	400,002	Transport of excavation muck to authorized dump area to 25 km	11.858.696,28
Km	400,003	Environmental arrangement of waste and dump areas	1,00
U	400,004	Environmental supervision for civil works	1,00



PRICE Nº	DEFINITION	Unit	Quantity	Unit price	TOTAL (€)
<b>CHAPTER 1.- MDC EXCAVATION</b>					
<b>1.1 MDC EXCAVATION</b>					
100,001	Vault excavation	M3	9.050,03	97,20 €	879.662,92 €
100,002	Main cavern excavation	M3	95.331,63	46,53 €	4.435.780,74 €
100,003	Raise boring excavation for shafts (f=5,70)	MI	98,00	3.375,00 €	330.750,00 €
100,004	Upper gallery excavation and support	MI	47,12	2.322,00 €	109.421,67 €
100,005	Rib excavation and support	MI	0,00	6.580,80 €	- €
100,006	Upper cavern excavation and support	M3	0,00	135,00 €	- €
400,001	Transport of excavation muck to tunnel portal	M3	163.043,16	1,25 €	203.803,95 €
400,002	Transport of excavation muck to authorized dump area to 25 km	M3	4.076.078,98	0,45 €	1.834.235,54 €
<b>PARTIAL</b>					<b>7.793.654,82 €</b>
<b>1,2 MDC SUPPORT</b>					
200,001	Steel fiber reinforced concrete for vault	M3	605,31	315,00 €	190.671,50 €
200,002	Steel fiber reinforced concrete for cavern walls	M3	3.925,42	300,00 €	1.177.626,01 €
200,003	Cable bolt 7 cables L=18 meters for vault support	U	128,00	2.079,00 €	266.112,00 €
200,004	Cable bolt 7 cables L=22 meters for wall support	U	2.803,00	2.112,00 €	5.919.936,00 €
200,005	Rebar bolt L=6 meters for vault support	U	432,00	162,00 €	69.984,00 €
200,006	Rebar bolt L=6 meters for wall support	U	2.803,00	135,00 €	378.405,00 €
200,007	Plain concrete 20 Mpa with steel fiber for MDC's, galleries and AC's slabs	M3	363,17	132,00 €	47.938,19 €
200,009	Plain concrete 50 Mpa for support gallery fill	M3	1.169,61	188,00 €	219.887,61 €
<b>PARTIAL</b>					<b>8.270.560,31 €</b>
<b>PARTIAL CHAPTER 1 (euros)</b>					<b>16.064.215,13</b>

PRICE Nº	DEFINITION	Unit	Quantity	Unit price	TOTAL (€)
<b>CHAPTER 2.- ACCESS GALLERIES AND CAVERN EXCAVATIONS AND SUPPORT</b>					
<b>2,1 ACCESS GALLERIES</b>					
100,003	Raise boring excavation for shafts (f=5,70)	MI	137,69	3.375,00 €	464.703,75 €
100,007	Tunnel portal excavation and support	U	1,00	60.000,00 €	60.000,00 €
100,008	Access gallery AG1 excavation and support (50% Type I, 40% Type II and 10% Type III)	MI	4.297,69	4.732,00 €	20.336.648,01 €
100,009	Access gallery AG2 excavation and support (50% Type I, 40% Type II and 10% Type III)	MI	17,00	3.198,00 €	54.366,00 €
200,007	Plain concrete 20 Mpa with steel fiber for MDC's, galleries and AC's slabs	M3	3.878,12	132,00 €	511.911,44 €
400,001	Transport of excavation muck to tunnel portal	M3	229.831,46	1,25 €	287.289,32 €
400,002	Transport of excavation muck to authorized dump area to 25 km	M3	5.745.786,44	0,45 €	2.585.603,90 €
<b>PARTIAL</b>					<b>24.300.522,42</b>
<b>2,2 AUXILIARY CAVERNS</b>					
100,010	Auxiliary cavern AC1 excavation and support (70% Type II and 30% Type III)	MI	182,00	7.558,00 €	1.375.556,00 €
100,011	Auxiliary cavern AC2 excavation and support (70% Type II and 30% Type III)	MI	21,00	9.471,00 €	198.891,00 €
100,012	Widening of existing tunnels	U	1,00	35.000,00 €	35.000,00 €
200,007	Plain concrete 20 Mpa with steel fiber for MDC's, galleries and AC's slabs	M3	304,50	132,00 €	40.194,00 €
200,008	Plain concrete 30 Mpa with steel fiber for cavern walls and vaults	M3	992,20	160,00 €	158.751,94 €
400,001	Transport of excavation muck to tunnel portal	M3	18.032,20	1,25 €	22.540,25 €
400,002	Transport of excavation muck to authorized dump area to 25 km	M3	450.804,90	0,45 €	202.862,21 €
<b>PARTIAL</b>					<b>2.033.795,39 €</b>
<b>2,3 VENTILATION GALLERY AND SHAFT</b>					
100,003	Raise boring excavation for shafts (f=5,70)	MI	223,77	3.375,00 €	755.223,75 €
100,008	Access gallery AG1 excavation and support (50% Type I, 40% Type II and 10% Type III)	MI	1188,12	4.732,00 €	5.622.200,07 €
200,007	Plain concrete 20 Mpa with steel fiber for MDC's, galleries and AC's slabs	M3	1069,31	132,00 €	141.149,06 €
400,001	Transport of excavation muck to tunnel portal	M3	63441,04	1,25 €	79.301,30 €
400,002	Transport of excavation muck to authorized dump area to 25 km	M3	1586025,97	0,45 €	713.711,69 €
<b>PARTIAL</b>					<b>7.311.585,87</b>
<b>PARTIAL CHAPTER 2 (euros)</b>					<b>33.645.903,68</b>
<b>TOTAL CHAPTER 1+2 (euros)</b>					<b>49.710.118,81</b>

PRICE Nº	DEFINITION	Unit	Quantity	Unit price	TOTAL (€)
<b>CHAPTER 3.- INSTALLATIONS</b>					
<b>2,1 CONSTRUCTION INSTALLATIONS</b>					
300,001	Drinking water installation for construction	U	1,00	50.000,00 €	50.000,00 €
300,002	Fire installations for construction	U	1,00	20.000,00 €	20.000,00 €
300,003	Ventilation for construction	U	1,00	213.750,00 €	213.750,00 €
300,004	Electric installation for construction	U	1,00	358.000,00 €	358.000,00 €
<b>PARTIAL</b>					<b>641.750,00</b>
<b>2,2 UNDERGROUND INSTALLATIONS</b>					
300,101	Water installations for experiment operation	U	1,00	629.950,00 €	629.950,00 €
300,102	Drinking water for underground facilities	U	1,00	220.150,00 €	220.150,00 €
300,103	Sewage utilities for underground installations	U	1,00	18.700,00 €	18.700,00 €
300,104	Fire protection for underground caverns and installations	U	1,00	640.920,00 €	640.920,00 €
300,105	HVAC installations for underground caverns and installations	U	1,00	304.650,00 €	304.650,00 €
300,106	Ventilation installations for underground caverns	U	1,00	1.436.000,00 €	1.436.000,00 €
300,107	Electrical installations for underground caverns	U	1,00	4.750.000,00 €	4.750.000,00 €
300,108	Elevator and stairs for emergency shaft	U	1,00	326.000,00 €	326.000,00 €
300,109	Nitrogen installation	U	1,00	215.000,00 €	215.000,00 €
300,110	Scintillator installation	U	1,00	200.000,00 €	200.000,00 €
<b>PARTIAL</b>					<b>8.741.370,00 €</b>
<b>2,3 SURFACE INSTALLATIONS</b>					
300,201	Drinking water for surface installations	U	1,00	27.100,00 €	27.100,00 €
300,202	Sewage utilities for underground installations	U	1,00	14.700,00 €	14.700,00 €
300,203	Fire protection surface installations	U	1,00	14.100,00 €	14.100,00 €
300,204	HVAC for surface installations	U	1,00	5.750,00 €	5.750,00 €
300,205	Electric installations	U	1,00	40.000,00 €	40.000,00 €
300,206	Access control building	U	1,00	150.000,00 €	150.000,00 €
<b>PARTIAL</b>					<b>251.650,00</b>
<b>PARTIAL CHAPTER 3 (euros)</b>					<b>9.634.770,00</b>



PRICE Nº	DEFINITION	Unit	Quantity	Unit price	TOTAL (€)
<b>CHAPTER 4.- ENVIRONMENTAL MANAGEMENT</b>					
<b>4,1 ENVIRONMENTAL MANAGEMENT</b>					
400,003	Environmental arrangement of waste and dump areas	U	1,00	120.000,00 €	120.000,00 €
400,004	Environmental supervision for civil works	U	1,00	500.000,00 €	500.000,00 €
<b>PARTIAL</b>					<b>620.000,00</b>
<b>PARTIAL CHAPTER 4 (euros)</b>					<b>620.000,00</b>

<b>CHAPTER 1.- MDC EXCAVATION</b>	
1.1 MDC EXCAVATION	7.793.654,82 €
1,2 MDC SUPPORT	8.270.560,31 €
<b>PARTIAL CHAPTER 1 (euros)</b>	<b>16.064.215,13 €</b>
<b>CHAPTER 2.- ACCESS GALLERIES AND CAVERN EXCAVATIONS AND SUPPORT</b>	
2,1 ACCESS GALLERIES	24.300.522,42 €
2,2 AUXILIARY CAVERNS	2.033.795,39 €
2,3 VENTILATION GALLERY AND SHAFT	7.311.585,87 €
<b>PARTIAL CHAPTER 2 (euros)</b>	<b>33.645.903,68 €</b>
<b>CHAPTER 3.- INSTALLATIONS</b>	
2,1 CONSTRUCTION INSTALLATIONS	641.750,00 €
2,2 UNDERGROUND INSTALLATIONS	8.741.370,00 €
2,3 SURFACE INSTALLATIONS	251.650,00 €
<b>PARTIAL CHAPTER 3 (euros)</b>	<b>9.634.770,00 €</b>
<b>CHAPTER 4.- ENVIRONMENTAL MANAGEMENT</b>	
4,1 ENVIRONMENTAL MANAGEMENT	620.000,00 €
<b>PARTIAL CHAPTER 4 (euros)</b>	<b>620.000,00 €</b>
<b>CHAPTERS 1 TO 4 (euros)</b>	<b>59.964.888,81 €</b>
<b>HEALTH AND SAFETY</b>	<b>899.473,00 €</b>
<b>UNDERGROUND MONITORING</b>	<b>239.860,00 €</b>
<b>FURTHER SUBSOIL EXPLORATION</b>	<b>617.612,40 €</b>
<b>DETAILED DESIGN AND PROFESSIONAL ASSOCIATION FEES</b>	<b>1.298.897,78 €</b>
<b>TOTAL CONSTRUCTION COST</b>	<b>63.020.731,99 €</b>
<b>13% OVERHEAD EXPENSES</b>	<b>8.192.695,16 €</b>
<b>6% INDUSTRIAL PROFIT</b>	<b>3.781.243,92 €</b>
<b>TOTAL CONTRACTOR BUDGET</b>	<b>74.994.671,07 €</b>
<b>16% VAT</b>	<b>11.999.147,37 €</b>
<b>TOTAL TENDER COST</b>	<b>86.993.818,44 €</b>

### 11.3 GLACIER

The result is the one shown in the following table, with similar independent parts

Nº	Price definition	Survey
100,001	Vault excavation Excavación en bóveda de caverna MDC	34.611,33
100,002	Main cavern excavation Excavación del cilindro de la caverna en destroza MDC	115.613,96
100,003	Raise boring excavation for shafts ( $\phi=5,70$ ) Excavación del raise boring ( $\phi=5,70$ ) MDC Ventilation shaft Connection shaft	19,10 68,16 0,00
100,004	Intermediate and lower gallery excavation and support Excavación y sostenimiento de galerías perimetrales MDC intermediate gallery MDC lower gallery	160,63 251,64
100,005	Rib excavation and support Excavación y sostenimiento de costillas MDC	331,84
100,006	Upper cavern excavation and support Excavación y sostenimiento de la caverna superior MDC	296,58
100,007	Tunnel portal excavation and support Excavación y sostenimiento de la boquilla Road to Candanchu	1,00
100,008	Access gallery AG1 excavation and support (50% Type I, 40% Type II Excavación y sostenimiento galería AG1 (50%-40%-10%) General Access Connection gallery at level 1201 Ramp between upper chamber and lower level Ventilation gallery Access gallery from railway tunnel to upper chamber Access to different AC's	2.039,26 37,50 875,59 1.435,56 112,88 17,00
100,009	Access gallery AG2 excavation and support (50% Type I, 40% Type II Excavación y sostenimiento galería AG2 (50%-40%-10%) Access to main control and office	17,00
100,010	Auxiliary cavern AC1 excavation and support (70% Type II and 30% Excavación y sostenimiento caverna AC1 (70%-30%) Clean Storage and power transformation Electronics, main control and office cavern Connection chambers	50,00 22,00 50,00
100,011	Auxiliary cavern AC2 excavation and support (70% Type II and 30% Excavación y sostenimiento caverna AC2 (70%-30%) --	0,00
100,012	Widening of existing tunnels Obras locales de ensanche del túnel Widening for shaft excavation	1,00

Nº	Price definition	Survey
200,001	Steel fiber reinforced concrete for vault Gunita en bóveda de caverna MDC	2.204,39
200,002	Steel fiber reinforced concrete for cavern walls Gunita en paredes de caverna MDC	2.155,25
200,003	Cable bolt 7 cables L=18 meters for vault support Anclajes en bóveda de caverna MDC	1.354,00
200,004	Cable bolt 7 cables L=18 meters for wall support Anclajes en paredes de caverna MDC	1.186,00
200,005	Rebar bolt L=6 meters for vault support Bulones en bóveda de caverna MDC	1.354,00
200,006	Rebar bolt L=6 meters for wall support Bulones en bóveda de caverna MDC	1.186,00
200,007	Plain concrete 20 Mpa with steel fiber for MDC's, galleries and AC's Hormigón HM20 c/fibra en losas de túnel o caverna MDC's Access galleries AG1 Access galleries AG2 Ventilation gallery AG1 Auxiliary caverns AC1 Auxiliary caverns AC2	1.771,86 2.774,00 10,20 1.292,01 183,00 0,00
200,008	Plain concrete 30 Mpa with steel fiber for cavern walls and vaults HM30 c/fibra encofrado en bovedas de cavernas auxiliares Cavernas AC1 Cavernas AC2	437,27 0,00
200,009	Plain concrete 50 Mpa for support gallery fill Hormigones de relleno de galerías perimetrales y costillas Lower and intermediate gallery Ribs	10.232,57 3.398,04



Nº	Price definition	Survey
300,001	Drinking water installation for construction	1,00
300,002	Fire installations for construction	1,00
300,003	Ventilation for construction	1,00
300,004	Electric installation for construction	1,00
300,101	Water installations for experiment operation	0,00
300,102	Drinking water for underground facilities	1,00
300,103	Sewage utilities for underground installations	1,00
300,104	Fire protection for underground caverns and installations	1,00
300,105	HVAC installations for underground caverns and installations	1,00
300,106	Ventilation installations for underground caverns	1,00
300,107	Electrical installations for underground caverns	1,00
300,108	Argon installation	1,00
300,201	Drinking water for surface installations	1,00
300,202	Sewage utilities for underground installations	1,00
300,203	Fire protection surface installations	1,00
300,204	HVAC for surface installations	1,00
300,205	Electric installations	1,00
300,206	Access control building	1,00
400,001	Transport of excavation muck to tunnel portal	Transporte a vertedero, medido desde la boca del túnel
		MDC's excavation 210.315,41
		Raise boring excavations 3.117,33
		Lower and intermediate gallery excavations 14.325,60
		Rib excavations 4.757,26
		Upper cavern excavations 415,21
		Access galleries AG1 and AG2 164.930,73
		Auxiliary caverns AC1 and AC2 10.483,70
		Ventilation gallery AC1 76.653,40
400,002	Transport of excavation muck to authorized dump area to 25 km	12.124.966,10
400,003	Environmental arrangement of waste and dump areas	1,00
400,004	Environmental supervision for civil works	1,00

PRICE Nº	DEFINITION	Unit	Quantity	Unit price	TOTAL (€)
<b>CHAPTER 1.- MDC EXCAVATION</b>					
<b>1.1 MDC EXCAVATION</b>					
100,001	Vault excavation	M3	34.611,33	97,20 €	3.364.221,28 €
100,002	Main cavern excavation	M3	115.613,96	46,53 €	5.379.517,56 €
100,003	Raise boring excavation for shafts (f=5,70)	MI	19,10	3.375,00 €	64.462,50 €
100,004	Intermediate and lower gallery excavation and support	MI	412,27	2.322,00 €	957.293,74 €
100,005	Rib excavation and support	MI	331,84	6.580,80 €	2.183.772,67 €
100,006	Upper cavern excavation and support	M3	296,58	135,00 €	40.038,56 €
400,001	Transport of excavation muck to tunnel portal	M3	232.930,81	1,25 €	291.163,51 €
400,002	Transport of excavation muck to authorized dump area to 25 km	M3	5.823.270,23	0,45 €	2.620.471,60 €
<b>PARTIAL</b>					<b>14.900.941,42 €</b>
<b>1,2 MDC SUPPORT</b>					
200,001	Steel fiber reinforced concrete for vault	M3	2.204,39	315,00 €	694.383,71 €
200,002	Steel fiber reinforced concrete for cavern walls	M3	2.155,25	300,00 €	646.576,05 €
200,003	Cable bolt 7 cables L=18 meters for vault support	U	1.354,00	2.079,00 €	2.814.966,00 €
200,004	Cable bolt 7 cables L=18 meters for wall support	U	1.186,00	1.728,00 €	2.049.408,00 €
200,005	Rebar bolt L=6 meters for vault support	U	1.354,00	162,00 €	219.348,00 €
200,006	Rebar bolt L=6 meters for wall support	U	1.186,00	135,00 €	160.110,00 €
200,007	Plain concrete 20 Mpa with steel fiber for MDC's, galleries and AC's slabs	M3	1.771,86	132,00 €	233.885,70 €
200,009	Plain concrete 50 Mpa for support gallery fill	M3	13.630,61	188,00 €	2.562.555,22 €
<b>PARTIAL</b>					<b>9.381.232,69 €</b>
<b>PARTIAL CHAPTER 1 (euros)</b>					<b>24.282.174,11</b>

PRICE Nº	DEFINITION	Unit	Quantity	Unit price	TOTAL (€)
<b>CHAPTER 2.- ACCESS GALLERIES AND CAVERN EXCAVATIONS AND SUPPORT</b>					
<b>2,1 ACCESS GALLERIES</b>					
100,003	Raise boring excavation for shafts (f=5,70)	MI	0,00	3.375,00 €	- €
100,007	Tunnel portal excavation and support	U	1,00	60.000,00 €	60.000,00 €
100,008	Access gallery AG1 excavation and support (50% Type I, 40% Type II and 10% Type III)	MI	3.082,23	4.732,00 €	14.585.089,27 €
100,009	Access gallery AG2 excavation and support (50% Type I, 40% Type II and 10% Type III)	MI	17,00	3.198,00 €	54.366,00 €
200,007	Plain concrete 20 Mpa with steel fiber for MDC's, galleries and AC's slabs	M3	2.784,20	132,00 €	367.514,74 €
400,001	Transport of excavation muck to tunnel portal	M3	164.930,73	1,25 €	206.163,42 €
400,002	Transport of excavation muck to authorized dump area to 25 km	M3	4.123.268,31	0,45 €	1.855.470,74 €
<b>PARTIAL</b>					<b>17.128.604,17</b>
<b>2,2 AUXILIARY CAVERNS</b>					
100,010	Auxiliary cavern AC1 excavation and support (70% Type II and 30% Type III)	MI	122,00	7.558,00 €	922.076,00 €
100,011	Auxiliary cavern AC2 excavation and support (70% Type II and 30% Type III)	MI	0,00	9.471,00 €	- €
100,012	Widening of existing tunnels	U	1,00	35.000,00 €	35.000,00 €
200,007	Plain concrete 20 Mpa with steel fiber for MDC's, galleries and AC's slabs	M3	183,00	132,00 €	24.156,00 €
200,008	Plain concrete 30 Mpa with steel fiber for cavern walls and vaults	M3	437,27	160,00 €	69.963,26 €
400,001	Transport of excavation muck to tunnel portal	M3	10.483,70	1,25 €	13.104,63 €
400,002	Transport of excavation muck to authorized dump area to 25 km	M3	262.092,60	0,45 €	117.941,67 €
<b>PARTIAL</b>					<b>1.182.241,56 €</b>
<b>2,3 VENTILATION GALLERY AND SHAFT</b>					
100,003	Raise boring excavation for shafts (f=5,70)	MI	68,16	3.375,00 €	230.040,00 €
100,008	Access gallery AG1 excavation and support (50% Type I, 40% Type II and 10% Type III)	MI	1435,56	4.732,00 €	6.793.090,90 €
200,007	Plain concrete 20 Mpa with steel fiber for MDC's, galleries and AC's slabs	M3	1292,01	132,00 €	170.545,05 €
400,001	Transport of excavation muck to tunnel portal	M3	76653,40	1,25 €	95.816,75 €
400,002	Transport of excavation muck to authorized dump area to 25 km	M3	1916334,96	0,45 €	862.350,73 €
<b>PARTIAL</b>					<b>8.151.843,43</b>
<b>PARTIAL CHAPTER 2 (euros)</b>					<b>26.462.689,17</b>
<b>TOTAL CHAPTER 1+2 (euros)</b>					<b>50.744.863,28</b>

PRICE Nº	DEFINITION	Unit	Quantity	Unit price	TOTAL (€)
<b>CHAPTER 3.- INSTALLATIONS</b>					
<b>2,1 CONSTRUCTION INSTALLATIONS</b>					
300,001	Drinking water installation for construction	U	1,00	50.000,00 €	50.000,00 €
300,002	Fire installations for construction	U	1,00	20.000,00 €	20.000,00 €
300,003	Ventilation for construction	U	1,00	213.750,00 €	213.750,00 €
300,004	Electric installation for construction	U	1,00	358.000,00 €	358.000,00 €
<b>PARTIAL</b>					<b>641.750,00</b>
<b>2,2 UNDEGROUND INSTALLATIONS</b>					
300,101	Water installations for experiment operation	U	0,00	629.950,00 €	- €
300,102	Drinking water for underground facilities	U	1,00	220.150,00 €	220.150,00 €
300,103	Sewage utilities for underground installations	U	1,00	18.700,00 €	18.700,00 €
300,104	Fire protection for underground caverns and installations	U	1,00	520.000,00 €	520.000,00 €
300,105	HVAC installations for underground caverns and installations	U	1,00	304.650,00 €	304.650,00 €
300,106	Ventilation installations for underground caverns	U	1,00	950.000,00 €	950.000,00 €
300,107	Electrical installations for underground caverns	U	1,00	4.000.000,00 €	4.000.000,00 €
300,108	Argon installation	U	1,00	200.000,00 €	200.000,00 €
<b>PARTIAL</b>					<b>6.213.500,00 €</b>
<b>2,3 SURFACE INSTALLATIONS</b>					
300,201	Drinking water for surface installations	U	1,00	27.100,00 €	27.100,00 €
300,202	Sewage utilities for underground installations	U	1,00	14.700,00 €	14.700,00 €
300,203	Fire protection surface installations	U	1,00	14.100,00 €	14.100,00 €
300,204	HVAC for surface installations	U	1,00	5.750,00 €	5.750,00 €
300,205	Electric installations	U	1,00	40.000,00 €	40.000,00 €
300,206	Access control building	U	1,00	150.000,00 €	150.000,00 €
<b>PARTIAL</b>					<b>251.650,00</b>
<b>PARTIAL CHAPTER 3 (euros)</b>					<b>7.106.900,00</b>



PRICE Nº	DEFINITION	Unit	Quantity	Unit price	TOTAL (€)
<b>CHAPTER 4.- ENVIRONMENTAL MANAGEMENT</b>					
<b>4,1 ENVIRONMENTAL MANAGEMENT</b>					
400,003	Environmental arrangement of waste and dump areas	U	1,00	120.000,00 €	120.000,00 €
400,004	Environmental supervision for civil works	U	1,00	500.000,00 €	500.000,00 €
<b>PARTIAL</b>					<b>620.000,00</b>
<b>PARTIAL CHAPTER 4 (euros)</b>					<b>620.000,00</b>

<b>CHAPTER 1.- MDC EXCAVATION</b>	
1.1 MDC EXCAVATION	14.900.941,42 €
1,2 MDC SUPPORT	9.381.232,69 €
<b>PARTIAL CHAPTER 1 (euros)</b>	<b>24.282.174,11 €</b>
<b>CHAPTER 2.- ACCESS GALLERIES AND CAVERN EXCAVATIONS AND SUPPORT</b>	
2,1 ACCESS GALLERIES	17.128.604,17 €
2,2 AUXILIARY CAVERNS	1.182.241,56 €
2,3 VENTILATION GALLERY AND SHAFT	8.151.843,43 €
<b>PARTIAL CHAPTER 2 (euros)</b>	<b>26.462.689,17 €</b>
<b>CHAPTER 3.- INSTALLATIONS</b>	
2,1 CONSTRUCTION INSTALLATIONS	641.750,00 €
2,2 UNDEGROUND INSTALLATIONS	6.213.500,00 €
2,3 SURFACE INSTALLATIONS	251.650,00 €
<b>PARTIAL CHAPTER 3 (euros)</b>	<b>7.106.900,00 €</b>
<b>CHAPTER 4.- ENVIRONMENTAL MANAGEMENT</b>	
4,1 ENVIRONMENTAL MANAGEMENT	620.000,00 €
<b>PARTIAL CHAPTER 4 (euros)</b>	<b>620.000,00 €</b>
<b>CHAPTERS 1 TO 4 (euros)</b>	<b>58.471.763,28 €</b>
HEALTH AND SAFETY	877.076,00 €
UNDERGROUND MONITORING	233.887,00 €
FURTHER SUBSOIL EXPLORATION	617.612,40 €
DETAILED DESIGN AND PROFESSIONAL ASSOCIATION FEES	1.269.035,27 €
<b>TOTAL CONSTRUCTION COST</b>	<b>61.469.373,95 €</b>
13% OVERHEAD EXPENSES	7.991.018,61 €
6% INDUSTRIAL PROFIT	3.688.162,44 €
<b>TOTAL CONTRACTOR BUDGET</b>	<b>73.148.555,00 €</b>
16% VAT	11.703.768,80 €
<b>TOTAL TENDER COST</b>	<b>84.852.323,80 €</b>

## 12. TECHNICAL TIMESCALE FOR REALIZATION

### 12.1 INTRODUCTION

Estimation of a timescale for each tank has been made with the assessment of technicians involved in ground excavation planning. Mr. Alonso Gullón, Professor of the School of Mines of Madrid has supervised this work.

For each experiment, some assumptions about rock removal rates, gallery excavations, and cavern excavation and support have been made. Weekly work days have been considered to be five, with three daily working shifts, so underground activities can be developed 24 hours-a-day. Although this is usual when underground excavation planning, it may be slightly conservative, since it is not unusual that in Spain alternative working shifts are planned and sometimes works are carried out 6 days-a-week.

Works usually stop only in Christmas time, so 50 weeks-a-year can be considered.

The following underground excavation performances have been considered:

- Gallery support and excavation: 120 to 150 m/month. It depends on gallery sizes and on gallery situation.
- Cavern excavation: the output of vertical excavation of the caverns can be 5.000 m<sup>3</sup> per week. In the case of Lena, a reduced performance of 70% has been considered.
- Vertical shafts: machine assembly takes at least two weeks, once pilot holes have been performed. Usual performances are 8 m/day.

### 12.2 MEMPHYS

The total timescale shows that the completion of the civil works of access galleries and of the three caverns can finish in 84 months. The technical timescale is shown in next pages.

### 12.3 LENA

The total timescale shows that the completion of the civil works of access galleries and MDC can finish in 45 months. The technical timescale is shown in next pages.

### 12.4 GLACIER

The total timescale shows that the completion of the civil works of access galleries and MDC can finish in 47 months. The technical timescale is shown in next pages.





g:\pry209046 laguna canfranc\documentos de trabajo\final report\j0461005-cpg.doc



UNIVERSIDAD AUTÓNOMA  
DE MADRID

## APPENDIX Nº 1: DRAWINGS

## LSC MEMPHYS PLANS

REVISION 12<sup>th</sup> May 2010



## LSC LENA PLANS

REVISION 12<sup>th</sup> May 2010

## LSC GLACIER PLANS

REVISION 12<sup>th</sup> May 2010